Exothermicity and oxidative kinetics of light crude oils for air injection improved oil recovery (IOR) processes

Osindero, Adeyemi O.

Award date:
2000

Awarding institution:
University of Bath

Exothermicity and Oxidative Kinetics of Light Crude Oils for Air Injection Improved Oil Recovery (IOR) Processes

Submitted by Adeyemi O Osindero

For the degree of Ph.D.

Of the University of Bath

2000

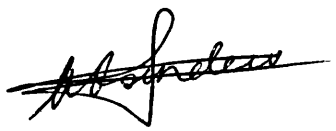

ProQuest LLC
789 East Eisenhower Parkway
P.O. Box 1346
Ann Arbor, MI 48106-1346

This thesis is dedicated to the memory of my brother, Idowu Osindero, and to my parents, Yemi and Doyin Osindero.

ABSTRACT

Improved Oil Recovery (IOR) techniques are necessary to meet the world's growing oil demand. Air injection is a promising IOR technique with the condition that all of the oxygen can be removed by reaction with the crude oil. It is essential that the oxidative kinetics behind these crude oil oxidation reactions are fully understood to facilitate numerical simulations and also to make informed decisions about potential air injection candidates.

A critical review of the oxidative kinetics of both light and heavy oils has been carried out, examining findings from previous investigations. This found a number of areas requiring further investigation. Consequently, a high pressure accelerating rate calorimeter, termed the PHI-TEC II, was used to follow the adiabatic exotherm obtained when oil reacts with air, and when reservoir rock and water are present. The effect of different oil and reservoir parameters on the oxidation was studied. Field implications arise for high water, and/or low oil saturation, as these were found to inhibit reaction, while reservoir rock catalysed the high temperature reaction. Experimental runs were undertaken with SARA (saturate, aromatic, resin, and asphaltene) fractions of certain crude oils which showed the dominant role of the saturates in the low temperature region oil oxidation. Pure light oil components (Decane, hexadecane) were reacted to understand the significance of oil composition on the oxidation behaviour. As these components participated in reactions, they must be included in future reaction kinetic models.

The relationship between the three main parameters affecting crude oil oxidation; oil composition, rock and water have been defined in terms of their exothermicity effects, using ratio analysis. Avenues for additional research to further understand crude oil oxidation behaviour, and obtain detailed kinetic models have been revealed.

ACKNOWLEDGEMENTS

There are so many people who have assisted me in this research, and during my stay at Bath, that I must apologise in advance for any omissions from this page.

Firstly I would like to thank the Engineering and Physical Sciences Council (EPSRC), for funding this project and making it possible. I also wish to thank Amoco, Total and Norsk Hydro for their support

I am sincerely grateful to my two supervisors, who were always generous with their time: Professor Malcolm Greaves and Dr. Richard Rathbone, for their valuable advice and tremendous support throughout my time at Bath.

I am indebted to all the staff of the Chemical Engineering Department for their assistance, especially Sean Chawla-Duggan, Mervyn Newnes, Elaine Odgers and Adrian Tuddenham.

I am deeply grateful to Taiwo Benson, Ibrahim, Jide, Isa, Ahmed, Jon, Brian, Arnaldo, Azleena, Bibi, and many other numerous friends for their unlimited encouragement and comforting words, during times of frustration.

My appreciation also goes to the Kukus for their support and assistance. Most of all, the tolerance, support, and the inspiration of my family (Tolu, Taiwo and Kehinde) was essential to writing this thesis.

TABLE OF CONTENTS

LIST OF TABLES

LIST OF FIGURES

NOMENCLATURE

A	Arrhenius pre-exponential factor
C_0	initial concentration of reactant ($molhr^{-1}$)
C	concentration of reactant, ($molhr^{-1}$)
C_m	instantaneous concentration of fuel ($molhr^{-1}$)
Cp	viscosity (Pas)
c_p	specific heat capacity (J/g K)
E_a	activation Energy (KJ/mol)
k	effective permeability to the displaced fluid (m^2)
K	specific reaction rate constant
L	length (m)
m	reaction order with respect to oxygen
m_c	mass of coke deposited (kg)
m^*	fraction of carbon oxidised to carbon monoxide
M	mobility, effective permeability divided by the viscosity
M or M^*	reacting molecules
n	reaction order with respect to oil concentration
N_c	capillary number
P	pressure (bar)
Po_2	oxygen partial pressure (bar)
q_g	rate of heat generation ($J\ s^{-1}$)
r	pyrolysis rate (% $fuelmin^{-1}$)
R	gas constant (8.314 J $mole^{-1}\ K^{-1}$)

R_c rate of combustion, ($molhr^{-1}cm^{-3}$)

t time (s)

T temperature (K)

T_{ad} adiabatic temperature (K)

T_f maximum temperature reached by the sample (K)

T_s temperature at the start of the reaction (K)

v pore velocity (ms^{-1})

V volume (m^3)

x temperature or pressure for regression analysis (K or bar)

x^* atomic hydrogen-carbon ratio

X composition of oil

y stoichiometric ratio

ΔH heat of combustion ($J\ kg^{-1}$)

Greek Symbols

α' chain branching multiplicity term

ϕ phi-factor

σ interfacial tension between the displaced and the displacing fluid

μ displaced fluid viscosity (Pas)

ρ density (kgm^{-3})

Subscripts

b sample holder, "bomb"

s	sample

Abbreviations

API	American Petroleum Institute
AOR	Air-oil ratio
ARC	Accelerating Rate Calorimeter
BBL	Billion barrels of liquid
BOPD	Barrels of oil per day
BSTB	Billion stock tank barrels of oil
DSC	Differential scanning Calorimetry
DTA	Differential thermal Analysis
DTG	Differential thermogravimetric Analysis
EGA	Evolved gas analysis
EHTO	Energy released during high temperature oxidation
ELTO	Energy released during low temperature oxidation
EOR	Enhanced oil recovery
EPSRC	Engineering and Physical Sciences Research Council
HEL	Hazard Evaluation Laboratory
HTO	High temperature oxidation
IOR	Improved oil recovery
LTO	Low temperature oxidation
MMP	Minimum miscibility pressure
MTO	Medium temperature oxidation
NTC	Negative temperature coefficient

SARA	Saturates, aromatics, resins and asphaltenes
SCF	Standard cubic feet
TG/TGA	Thermogravimetric Analysis

CHAPTER 1:

Introduction

INTRODUCTION

1.1 Background

Money, it is said makes the world go round. In the same vein it can be said that oil equally makes the world go round. For the past 100 years, oil has literally been the fuel upon which the world's tumultuous economic development has been based on. The energy wealth and poverty of nations, measures how much energy countries consume per capita. This is universally used as a primary benchmark of national wealth and development. Oil and gas account for 60 percent of the world's energy needs and with coal making up another 30 percent, hydrocarbons supply over a 90 percent share of the world energy needs (Economides and Oligney, 2000). The oil industry is the biggest and most pervasive in the world and its importance on the world economy and development is far reaching enough to have launched wars between and amidst nations (Yergin, 1992).

Demand for oil tends to fluctuate in an extreme manner depending on geopolitical factors. On the whole though worldwide demand increased at an estimated 1.5 to 2 percent per year during the 1990s. However, the Southeast Asian economic crisis cut this growth to 0.5 percent in 1998, though this started to rise again in 1999 back to the 1-2 percent range. In addition, the amount of oil reserves available worldwide is limited. It is believed that all of the "giant", easily recoverable oilfields have been discovered and the remaining ones will either be deepwater, or small to medium fields. Only a certain percentage of this oil is produceable using "conventional" production techniques. This, as well as the search for more environmentally sound, sustainable methods has lead to the development of improved oil recovery techniques. One fact, which is easily, and often disregarded by the general public and even governments is that there is no realistic substitute for hydrocarbon

fuels, at least in the more immediate future of about 20 to 40 years. Much vaunted renewable energy in the form of solar, wind, geothermal and other methods currently contribute less than 0.5 percent of the world's energy needs, excluding hydroelectric power, according to the Energy Information Administration of the United States, 2000. The opportunity cost of a reduction in crude oil supply therefore would be a global reduction in the standard of living, which makes it imperative that the worlds' growing demand for energy is met.

Production from a reservoir usually begins with primary recovery. This is when the pressure in the reservoir is high enough to cause the oil to flow normally up to the surface without the addition of any other energy. This includes expansion of liquids such as water or gases present in the reservoir, gravitational force, and an expulsive force due to the compaction of poorly consolidated reservoir rocks. After a while though the natural energy in the reservoir is no longer sufficient to produce the reservoir efficiently. The next step usually is the injection of water or gas so as to pressurise the reservoir and displace more oil. This is termed secondary recovery.

Primary recovery can vary from nil in the case of say oil sands to about 50% of the original oil in place in the reservoir, depending on the reservoir characteristics as well as the type of hydrocarbon and the reservoir drive. In the case of a water drive in a light oil reservoir recovery can reach 50%, or more with an efficient gravity drive. Secondary recovery can vary from zero, again in the case of oil sands to a few percent with heavy oils and up to 20-50% for light oil. The implication therefore is that a substantial amount of the original oil in place is left behind using these methods and it is necessary to find ways of recovering more of this remaining oil.

1.2 Enhanced Oil Recovery Methods

Various methods of enhancing oil recovery exist using chemical processes; Surfactant and polymer injection as well as foam injection; miscible displacement injection; water injection; gas and air injection and thermal processes; including steam simulation, steam flooding, hot water injection and in-situ combustion. These have been reviewed by Farouq Ali and Thomas, 1997

The difficulty in moving the residual oil in a reservoir can basically be reduced by one of two ways. One is by improving the mobility ratio, which is a measure of the mobility of the displacing fluid divided by the mobility of the displaced fluid. Mobility is defined as the effective permeability divided by the viscosity. For maximum displacement efficiency, M should be ≤ 1, otherwise more fluid will have to be injected to attain a given residual oil saturation in the pores. This mobility ratio can be made smaller by lowering the viscosity of the oil (especially with heavy oils), increasing the viscosity of the displacing fluid, increasing the effective permeability to oil, or decreasing the effective permeability to the displacing fluid.

The other method of mobilising the oil is by increasing the capillary number, N_c which is defined as shown below

$$N_c = \frac{\mu v}{\sigma} = \frac{k\Delta p}{\sigma L} \qquad \text{Equation 1.1}$$

where μ is the displaced fluid viscosity, v is the pore velocity, σ is the interfacial tension between the displaced and the displacing fluid, k is the effective permeability to the displaced fluid, and $\Delta p/L$ is pressure gradient.

The capillary number can be increased and the residual oil saturation decreased by reducing the oil viscosity, increasing the pressure gradient or by decreasing the interfacial

tension. All of the various forms of EOR aim to achieve greater production using one of these two principles.

The various EOR methods can be broadly classified into thermal and non-thermal methods. The various oil recovery methods starting from primary production are shown in Figure 1.1. The main enhanced oil recovery methods are detailed in Figure 1.2 (Farouq Ali and Thomas, 1996).

Thermal methods include steam injection and in situ heat generation, which can be achieved using in situ combustion or by other means such as electrical injection.

Non-thermal methods include chemical and miscible processes. Chemical methods include polymer, surfactant, caustic, micellar or emulsion floods, and combinations of the above. Other fluids have been field tested including alcohols, ammonia and a host of others and they hold some promise for the future but at present are not commercially used. Miscible methods include high-pressure gas drives, using a hydrocarbon gas, nitrogen or carbon dioxide, as well as liquid hydrocarbons.

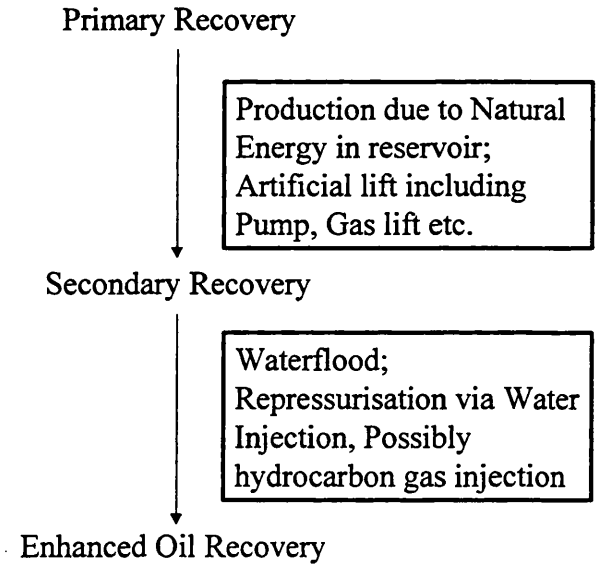

Figure 1.1: Oil Recovery Pathway

Worldwide, thermal recovery, including steam and in-situ combustion is the dominant EOR technique, accounting for about 1.3 million BOPD in 1998. In the U.S.A, about 60 percent of the EOR production is by thermal processes.

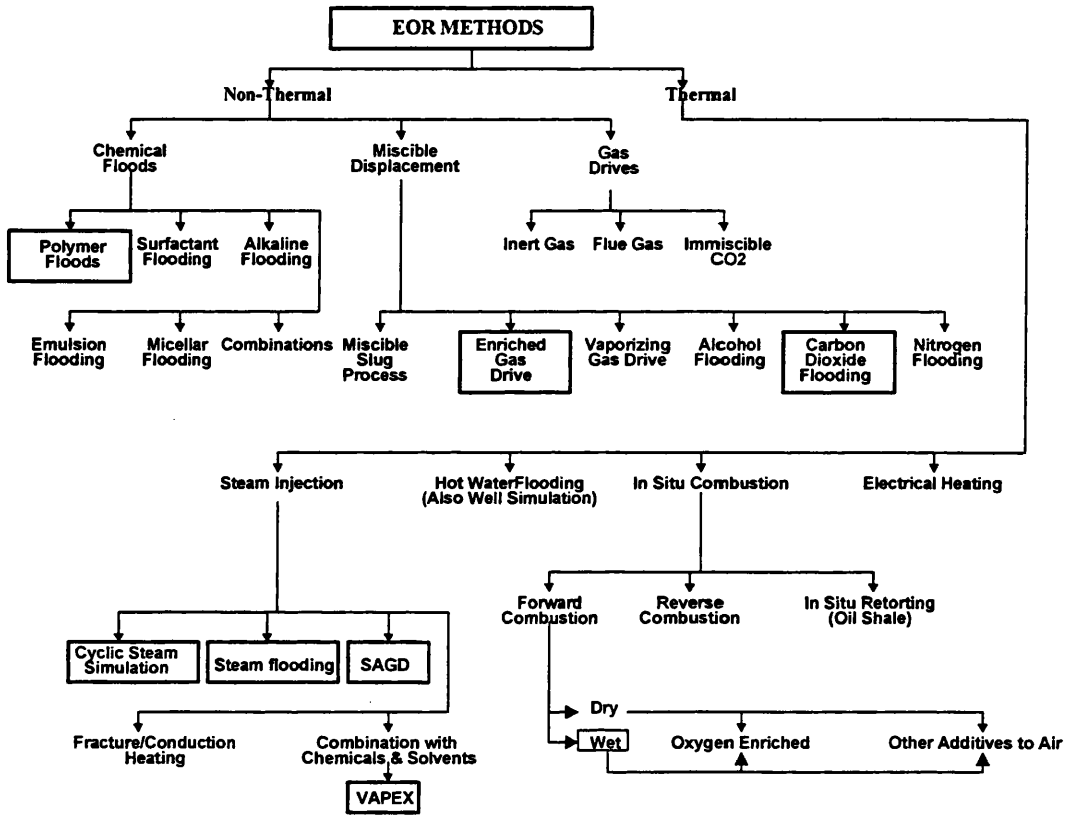

Figure 1.2: Classification of EOR methods, Commercial processes are in blocks (Farouq Ali and Thomas, 1996)

An extensive survey of EOR activity is carried out bi-annually by the Oil and Gas Journal (Moritis, 1998). While EOR production dipped in the early nineties, due to fluctuations in the oil price it has since increased again (Moritis 1994). The countries where substantial EOR activity currently takes place are U.S.A. (all types of EOR), Canada (predominantly thermal methods, CO_2 flooding, bitumen and tar sands mining), Venezuela (steam) and Romania (in situ combustion, including the largest project in the world and

steam). Others are China (steam, microbial, polymer and combustion methods), Colombia (steam), Trinidad (CO_2 immiscible and steam), Turkey (CO_2 immiscible), Libya (miscible hydrocarbon gas), and Indonesia (steam).

Commercially, steam Injection is the principal of these EOR recovery methods, with miscible carbon dioxide flooding a distant second with 179,000 BOPD. Miscible displacement is the dominant recovery method in Canada, with steam injection increasing rapidly with heavy oil developments. CO_2 flooding activity has been continually increasing, while chemical flooding has been on the decline. Worldwide EOR production is over 2.3 million BOPD including heavy oil production out of a total of 70 million BOPD (Moritis, 1998).

1.3 Aims and Objectives

This research was undertaken with a number of objectives in mind. The research aims to identify the reaction regimes and relevant low temperature and high temperature (LTO and HTO) kinetics of a few selected North Sea light crude oils, as well as to fully understand what conditions affect this.

Previous work has shown that air injection into a deep (high pressure) light oil reservoir will initiate reactions with the oil that are LTO (generating in situ nitrogen for immiscible or miscible gas displacement), but HTO reactions (in-situ combustion) will also take place if there is sufficient fuel.

It is imperative to study the oxidative kinetics of crude oils for a number of reasons. A complete understanding of the in situ oxidation processes (both low and high temperature oxidation), is required to facilitate numerical simulation. It is essential to

understand the reaction kinetics of LTO as well as HTO for proper operation of an air injection project.

It is important to identify the effects of different oils and reservoir conditions on the reaction kinetics. Kinetic parameters need to be obtained for use in simulation models, in order to predict air injection performance in new reservoirs, or under new operating conditions. Modelling parameter values are also needed for numerical modelling to calculate the ignition energy requirements of a particular crude oil. These modelling parameters include the Arrhenius activation energy, pre-exponential factor and order of reaction.

It is important eventually, to widen the scope to encompass other crude oils for the purpose of developing a complete 'composite' screening-reaction model. The model will possess a relational database of correlated oil compositional and reservoir rock property data, thereby enabling the prediction as to whether a potential candidate oil reservoir is suitable for air injection. By compositional, this implies a characterisation of crude oil into its precise components and selected pseudo-components.

However since it is impossible to perform an extensive set of measurements on every reservoir of interest, the model would therefore have to relate certain key selected criteria to determine whether a potential reservoir is suitable or not. An oil company would then be able to quickly and efficiently assess the air injection potential of their candidate fields. The work from this research aims to serve as a platform to meeting this need.

A substantial amount of research has been carried out on the oxidation of heavy crude oil in connection with the in-situ combustion process. This work aims to concentrate

on the oxidation of light crude oils, which are expected to follow different reaction pathways from a heavy oil.

Comprehensive study of the oxidation of crude oil due to air injection into crude oil reservoirs involves complex interactions between many processes, including the following, which are generally studied for organic oxidation (Kuo 1986).

1. Thermodynamics
2. Chemical Kinetics
3. Fluid Mechanics
4. Heat and Mass Transfer
5. Turbulence
6. Materials Structure and Behaviour

This research aims to further the boundaries of knowledge specifically in the areas of the thermodynamics and oxidative kinetics of crude oil and materials structure and behaviour, i.e. taking into account the effect of the reservoir rock.

The current project is funded by the Engineering and Physical Sciences Research Council, (EPSRC Grant No. GR/L33191), and is being undertaken in collaboration with the University of Salford. They will use a special DISC reactor to investigate the LTO reaction kinetic studies.

1.4 Screening Model

The overall aim of this research is to further the understanding of the factors behind crude oil oxidation and the inherent effects. A detailed screening capability involving all the parameters affecting the process from laboratory to field case is outside the scope of this work. However an attempt is made to lay out the guidelines and to build a framework

for carrying out this screening evaluation for air injection into a potential reservoir. A summary is then made on the parameters affecting the oxidation kinetics.

1.4.1 *Overall EOR Screening Criteria*

It is important to look at all the key "drivers" behind enhanced oil recovery processes and understand which of them play the biggest role in determining whether or not to use a certain method.

The first step in the screening of reservoirs is to evaluate the oil and reservoir characteristics. These characteristics should then be matched against all available IOR methods including the following:

1. Waterflooding
2. Hydrocarbon gas injection
3. CO_2 Injection
4. Nitrogen Injection
5. Chemical Injection (Surfactants, polymers, etc.)
6. Air Injection; in the event that nitrogen injection is found to be favourable but there is no availability of nitrogen, evaluation of oxidation behaviour can then be carried out to determine air injection potential.

A review of EOR screening methods and the criteria behind them was carried out by Taber et al 1996. Although concentrating mainly on CO_2 flooding, other methods including thermal processes were examined and they pointed out the importance of assessing the improved oil recovery processes early in the life of the reservoir. This can have a major effect on the effectiveness of the recovery method as well as the economics of the project, and should be kept in mind for any reservoir. In practice, improved oil

recovery methods tend to be more of an afterthought rather than an integrated part of the initial reservoir management process. Diaz et al 1996 evaluated screening criteria for CO_2 injection by proposing a hypothetical ideal reservoir and comparing potential reservoirs to this.

Thomas et al 1996 detailed proposed screening criteria for the feasibility of gas injection in mature reservoirs. They reported the main parameters to be those arising from interfacial tension effects, mobility effects and gravity effects as well as wettability. These effects are also important for air injection which is a form of gas injection.

1.4.2 *Basis for Screening Model*

All the various pertinent criteria must be considered and a combination of the most important are used for the evaluation. Some of these factors are discussed below.

Economic Basis

The most important criteria for evaluation of air injection feasibility is economics. One factor which is totally outside the control of the user is the prevailing price of oil, which more than anything else determines the attractiveness of all EOR methods. In situ combustion is traditionally compared with steam-based recovery processes and must be evaluated side by side to determine which is the cheaper option. A past survey by Nodwell et al 1997 reveals that in situ combustion usually has higher front end costs but results in recovery factors up to 60 % higher. By default, air injection processes must be equally economically viable and should come up cheaper than similar steam based processes.

The costs involved in any project are the capital fixed costs and the variable costs. Most air injection projects are carried out on the basis that the facilities for production are in place already, having been built in the primary production phase. Of course this must be

evaluated on a case by case basis but generally this would be expected to bring the fixed cost down substantially to the cost of the compressor.

The variable costs includes a heating cost if any form of artificial ignition or heating is required, but this would generally be expected to start by spontaneous ignition and then be sustained by the exothermic oxidation reaction. The biggest variable cost involved in air injection is the air compression cost. The required air injection rate is a function of the reservoir pressure, heterogeneity of the reservoir, pay thickness of oil in the reservoir and oxidative kinetics of the crude.

Air-oil-ratios of 6000 to 25000 scf/bbl for injection pressures of 200 to 3700 psi have been reported in the literature (Turta 1994). While it might be necessary to operate at a high air-oil-ratio to improve oxidation kinetics, a corollary to this is the higher compression cost. Again, a low air-oil injection ratio could leave the oxidation in the LTO mode. Moore et al 1999 discussed important design considerations for a successful in-situ combustion. One of the most important considerations they noted was that the air injection must be matched to the area being operated, rather than using marginal air capacity. It is therefore helpful to obtain a minimum air-oil-ratio for each field case and operate close to that.

The other question to be answered using an economic basis is which of the available methods would lead to maximum oil recovery from the reservoir, as this would mean maximum revenues.

Technical Feasibility Basis

All of the important parameters affecting the oxidation, including the crude oil kinetic parameters and the reservoir properties must be considered, in the case of air injection conditions that accelerate oxygen utilization. Some of these have been considered

earlier on in Chapter 2 and include the crude oil physical and chemical properties as well as the particular reservoir properties and dynamics.

Turta and Singhal 1998 report some of the important reservoir aspects of air injection as an EOR technique for light oil reservoirs. Some of their findings include the following:

Assessment of the miscibility of the oil with flue gases.This is one of the most important factors for a successful air injection project, which is primarily dependent on the volumetric sweep efficiency.

The oxidation characteristics of the crude oil, including its exothermicity at different temperatures must be understood and can be used to decide whether or not to use air injection. Yannimaras and Tiffin 1995 pointed the importance of continuity in the exothermic profile of the crude oil from the start to end of the exotherm. They postulated that the oxidation would be trapped in the low temperature zone for an oil that did not display this continuity.

The nature of the reservoir and pay zone including porosity, heterogeneity and presence of fractures would affect the success of a project. Low porosity matrix reservoirs are unfavourable for in-situ combustion and air injection due to heat losses in the matrix.

Low reservoir temperatures could reduce the possibility of spontaneous ignition taking place, or it might take a very long time unless artificial ignition is used, which would increase the cost. Other important factors are the formation dip angle as this would affect the gravity drainage of the displacing flue gas.

Environmental and Industry Practicality Basis

This would be based primarily on what the prevailing industry outlook might be at the time of evaluation of the particular IOR method, and some adjustment should be made

for this. Such factors include the effect of legislature, national laws and public bias. An example of how this could have a major effect on the EOR method decision is where a CO_2 injection method is competitive with an air injection method, or even marginally disadvantaged. Due to the public perceptions about the effects of greenhouse gases and global warming, specifically from CO_2, it might be to an oil company's favour to use CO_2 injection as it would appear to be aiding rehabilitation of the environment or reducing a country's CO_2 emissions.

All of the above mentioned criteria must be fulfilled in order to obtain approval for any air injection process in the field.

1.4.3 *Air Injection Selection Criteria*

Investigations have been carried out on the applicability of air injection to various reservoirs. Yannimaras and Tiffin concluded that the most favourable reservoir conditions involved light to medium gravity oil, with gravities greater than 20 API. High reservoir temperatures and good reservoir geometry also promoted the effectiveness of the air injection process.

Previous studies into the feasibility of air injection for field projects have been reported for various fields by Fassihi et al 1996, Watts et al 1997, Clara et al 1998 and Clara et al 1999. These involved an integrated approach including laboratory and field tests, generally including the following steps:

1. Judgement of the applicability of a specific technique given the specific reservoir and oil characteristics
2. Capability to perform tests at conditions covering the possible reservoir permutations, including combustion tube experiments and ARC tests

3. Acquiring of useful and relevant technical parameters from these experiments

4. Building of numerical models to simulate the lab work and predict field behaviour

5. Upon obtaining favourable results from the above, design and commencement of a field pilot test to determine commercial applicability to a particular field

Oxidation Kinetics Screening criteria

This research has been carried out on the oxidation kinetics and exothermicity of crude oils. The screening criteria must accordingly be tailored to rank oils on the basis of the attractiveness of the reaction kinetics based on effects of the different parameters studied. An overview of all the different parameters studied in this research is shown in Figure 1.3

After a succesful evaluation of a candidate oil and reservoir based on the oxidation kinetics screening criteria, the displacement efficiency and fluid flow phenomena of the reservoir must then be taken into account and assessed also, as was discussed in the previous sections.

A method similar to that of Diaz et al 1996 which was used for evaluation of fields for CO_2 injection can be used. A hypothetical best-case scenario crude oil and reservoir is proposed. Comparisons are then made to the ideal situation and based on that ideal situation, each potential oil and reservoir is assigned a technical ranking.

Key technical parameters include the following:

Average residual Oil saturation

Oil API gravity

Minimum miscibility pressure (it is expected this would only be achieved for high pressure light oil reservoirs)

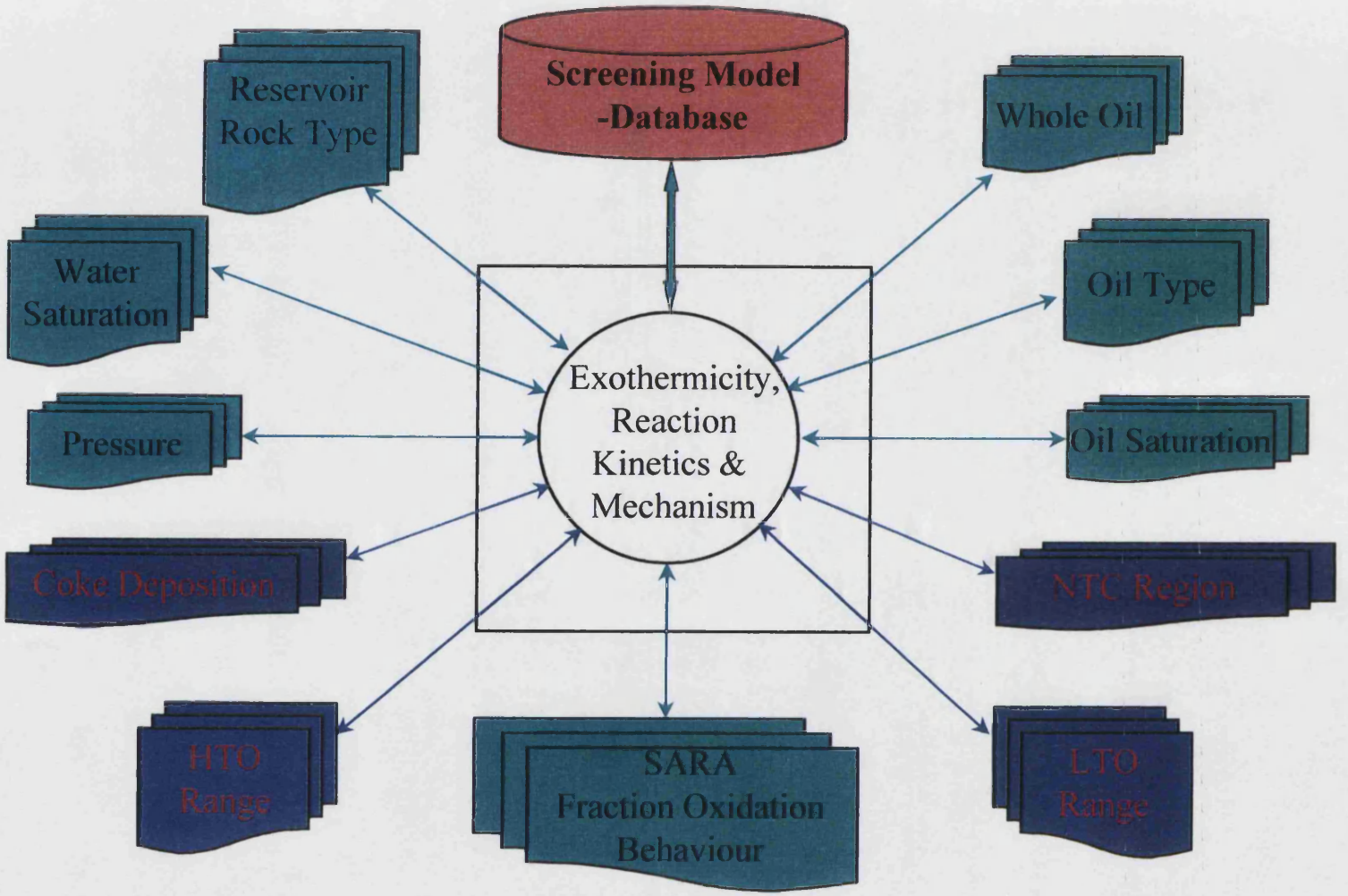

Figure 1.3 Research Overview

1.4.4 *Successful field IOR cases*

Any developed screening model must be tested against successful field IOR cases to determine its effectiveness.

The major field applications of air injection into oil reservoirs have been detailed in Chapter 2. It is important to retroactively evaluate each of these reservoirs using the screening criteria detailed in the model to test the efficiency of the model. This should be carried out to determine if air injection should indeed have been chosen as the IOR method based on the screening model.

1.4.5 *Relational Database*

The oxidation kinetics data obtained from the PHI-TEC II experiments have to be stored and organised in a logical and readily accessible digital format.

Requirements from the relational database

1. Ability to store and organise a large amount of kinetics and exothermicity data
2. Easily accessible and portable data
3. Ability to link with other data analysis tools such as Microsoft excel as required

This can be achieved using a relational database. A relational database is capable of providing data storage in an accessible location. The way data is stored is independent of the relationships between the data and users may then query for kinetic data in the database that match specified criteria, thereby providing an initial screening capability.

To ensure ease of the facility, a Microsoft Windows graphical interface is required. This can be achieved using a two-tier approach ensuring communication between the graphical user interface and the database through a standard structured

query language. Similar databases have been developed and reported by Bastian et al 1997 and Jefferson et al 1997. Commercially available software packages that can achieve this include Microsoft Access, Oracle and SAP amongst others.

1.5 Organisation of Thesis

The organisation of the thesis is explained in this section. The chapters have been arranged to logically present the research and do not follow a chronological fashion.

In the process of understanding the oxidative reaction mechanism of crude oils it was necessary to carry out an extensive literature search the reaction kinetic chemistry behind it. An attempt is made in this thesis to balance the background chemistry with the field application of air injection. While analysing the results and findings from this review an attempt has been made to identify the resulting field implications as that is one of the underlying aims of this work.

Following the background given in Chapter 1, Chapter 2 is a review of the major considerations for air injection suitability studies. These considerations commence with the history and development of air injection as an enhanced oil recovery method and continue with the reaction kinetics of crude oil under oxidation. The importance of the exothermicity to the success of a project is discussed, and salient points are evaluated. The equipment used for this study is described in Chapter 3, together with the experimental methodology. Chapter 4 describes the theoretical development behind the analysis of the experiments and illustrates how the analysis was carried out.

The major factors affecting the oil oxidation as studied in experiments are examined in Chapter 5, while the effect of rock on the oxidation is discussed in Chapter 6. The study of sub-component crude oil fractions is covered in Chapter 7, while

Chapter 8 looks at other relevant aspects of crude oil oxidation. Conclusions and recommendations from the research are detailed in Chapter 10.

An extensive review of existing literature was made and this is presented within each individual chapter where the parameter in question is being discussed, rather than in one single chapter.

CHAPTER 2:

Air Injection Considerations

AIR INJECTION CONSIDERATIONS

2.1 Air Injection into Crude Oil Reservoirs

Air Injection processes can be defined as oil recovery processes that occur naturally when air is injected into an oil reservoir.

The use of Gas Injection as a form of improved oil recovery is a proven method, and is widely used. The IOR potential for gas injection in the United Kingdom's North Sea fields has been estimated at 1.4 BSTB (Gregory, 1994). Hydrocarbon natural gas, which is usually available in the oil reservoirs or from nearby reservoirs has been shown to be a promising injection gas. The additional tertiary reserves producible using gas injection have been estimated to be between 8 and 15 % of the original oil in place depending on the reservoir properties and the injected gas. However if a market exists for the natural gas as well, the availability of natural gas for injection is reduced and other alternatives have to be found. Other possible injection gases include CO_2, N_2 and air.

CO_2 is rather attractive because it possesses a low minimum miscibility pressure and has been applied in numerous field cases. It has several favourable effects such as increased sweep of the reservoir, a decrease in fluid viscosity, an increase in gas-oil ratio, bubble point pressure as well as swelling and formation factors. One example of a reservoir where it was investigated is the Weyburn reservoir in Canada (Srivastava and Huang, 1997). However it is extremely difficult to locate economic supplies of it outside of naturally occurring reservoirs, where it is available at high pressure, especially offshore. The source used in the Weyburn field was from power plants and was only economic with sufficient government subsidies.

The immiscibile performance of N_2 is suitable for efficient oil recovery, but again the problem of availability arises. Evison and Gilchrist, 1992 reviewed the production of nitrogen for use in enhanced oil recovery. While several methods exist for its production such as membrane separation and cryogenic plants, the high cost and usually small size of the production restricts the widespread adoption of nitrogen injection to reservoirs where it is nearby and naturally available.

Air is therefore a much cheaper option and generates CO_2 and N_2 in-situ. The main problem associated with this include those of oxygen breakthrough at the production wells. A means of ensuring complete oxygen utilisation is therefore necessary for field applications of air injection.

During air injection into crude oil leading to combustion, two main reactions are thought to occur. A low temperature oxidation (LTO) reaction extending from the ignition temperature to approximately 350°C, and a high temperature combustion reaction (HTO), which starts after the low temperature oxidation and extends up to 500-600°C. In the case of heavy oils however, this HTO extends to higher temperatures up to 800 ^{0}C. This process has been widely studied as In-Situ Combustion. A number of reviews of the in-situ combustion process have been carried out (White 1985, Moore 1993, Turta 1994) detailing the process.

Air injection has been widely used in the past as a production process for heavy oils, due to the generation of heat via in-situ combustion. This heat reduces the viscosity and enables the recovery of the crude oil.

The parameters affecting the air injection process are a combination of the heat transfer, mass transfer and chemical reaction phenomena occurring during the progression of the oxidation front through the reservoir.

Different zones are created in the reservoir as the oxidation front passes through and are listed below. These zones are shown in Figure 2.1 below.

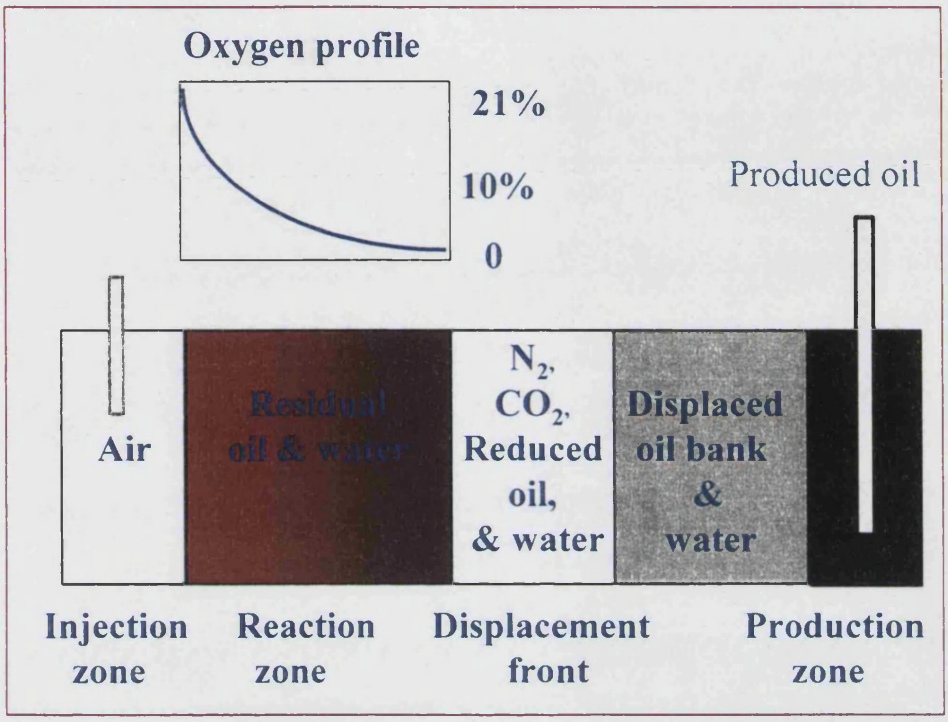

Figure 2.1: Schematic Diagram of Air Injection into Light Oil Reservoirs (Ren et al 1999)

The advantages of air injection have been listed by various investigators including Madaoui and Sakthikumar, 1993, Fassihi et al, 1996, Gilham et al 1997, Ren et al 1999, Clara et al 1999, Greaves et al 2000.

These advantages include most of the classical ones associated with natural gas injection as well as those accruing from the presence of oxygen in the injectant. These are listed as follows:

1. Low initial investment and operating cost
2. Universal accessibility of air over other injection gas options
3. Pressurisation of the reservoir

4. Swelling of the oil by the flue gas

5. Flue gas stripping of the reservoir. The minimum miscibility pressure of nitrogen decreases as the temperature increases. At higher temperatures therefore, there could be high miscibility of the oil with the flue gas, especially if accompanied with combusted light ends due to the oxidation (Rushing et al 1976).

6. Possible increased miscibility due to steam effects (Chekalyuk et al 1979). If supercritical steam conditions are reached, especially at high pressures, miscibility could be achieved

7. Heat losses from the injection well are avoided as the heat is released in situ in the porous media, therefore it is more energy efficient than most of the other processes.

8. Carbon dioxide that is created as well as some flue gas dissolves into the reservoir thereby lowering the oil's viscosity which in turn improves gravity drainage.

9. Possible Solvent Drive from condensation of vaporised light ends.

The biggest limitation to the universal use of air injection is that the reservoir must possess a sufficiently high temperature and reactivity to consume oxygen through oxidation. If the oxygen consumption is not complete, there is the danger of corrosion occurring at the production wells, and even worse, there could be a risk of explosion in the production well. There is also the fear that bacterial growth as well as the creation of emulsions could occur with the accumulation of oxygen in the reservoir. The process of air injection is also more complicated relative to hydrocarbon gas injection.

Air injection displacement may also be more attractive than steam drives under certain conditions (Prats 1986). These conditions include the following:

1. High injection pressures of above 1,500 psi
2. Excessive heat losses from the injection well, usually in reservoirs deeper than 4,000 ft
3. Lack of a supply of freshwater or exorbitant water treatment costs
4. Clay swelling problems due to fresh condensate
5. Undesirable or environmentally unfriendly use of fuel for steam generators
6. Thin or low porosity sands

2.1.1 *Air Injection into Light Oil Reservoirs*

Historically, most of the trials and applications of air injection into reservoirs have been mainly into reservoirs containing medium and heavy crude oils. In situ combustion behaviour in light oils is not as well documented as that for heavy oils. This is perfectly logical as viscous crudes were not recoverable by any other method. Thermal methods can however be applied to light oil reservoirs as well, but the main driving force for oil displacement is the flue gas generated in situ by the oxidation and nitrogen in the air.

The process of air injection into light oils is a complex one and has been studied by several researchers (Yannimaras et al 1991, Kumar et al 1994, Sakthikumar et al 1995, Fassihi et al 1996, Gilham et al 1997, Fraim et al 1997, Kisler and Shallcross, 1997, Ren et al 1999, Greaves et al 2000). Several processes occur when air is injected into a reservoir including some or all of the following:

1. Oxidation of the crude oil and an accompanying heat release.

2. A displacement front composed of nitrogen and flue gas is created which could lead to formation of a miscible gas bank, especially at high reservoir pressures.
3. Due to the presence of water in the formation, steam can be created in-situ and this could favourably influence the oil recovery at high pressures due to increased miscibility.
4. Spontaneous Ignition of the oil.
5. The double displacement process which is a process whereby the gas displacement of a water-invaded oil column recovers additional oil through gravity drainage (Lagenberg et al 1994).

The study of air injection at higher pressures (>1500psi) was undertaken by Yannimaras et al 1991, Tiffin and Yannimaras, 1997. It was found that these processes are more likely to occur significantly at higher reservoir temperatures and pressures. It was noticed that the major effect of pressure is the need to operate at higher air injection rates to sustain the combustion. It is possible that there is insufficient fuel at the combustion front as the pressure increases, since the increased pressure contributes to increasing oil displacement through several mechanisms.

It can be concluded that the biggest limitation to the use of air injection is the possibility of oxygen breakthrough at the production wells. It is essential to consume all of the injected oxygen in oxidation reactions.

2.1.2 *Historical and Field Applications of Air Injection*

The history of air injection into crude oil reservoirs is one that stretches back to the early 1900's when it was used to enhance oil recovery. In 1917 Lewis found that gas analyses from a number of air injection applications showed a deficiency in oxygen

concentration relative to that of nitrogen. He postulated that the excess of nitrogen in the flue gas was probably due to the extraction of oxygen in the air rather than from the picking up of nitrogen. This would probably be due to chemical reaction between the oxygen and the oil, or with other substances underground.

The earliest applications were mainly for the recovery of heavy crude oil with the process of in-situ combustion. Injection of air to burn part of the crude, generating heat and reducing crude viscosity while providing a driving force to displace the oil was recognised as early as 1920 by Wolcott and Howard culminating in patents in 1923. The first large-scale field operation of the underground combustion process was carried out in the USSR in 1934. The largest in situ combustion project is Suplacu de Barcau, Romania, with 9, 000 BOPD (Turta and Singhai, 1998).

Several field applications of air injection exist from the earliest days to the present. A discussion of field projects involving air injection into light deep reservoirs with high pressures and temperatures was done by Yannimaras et al 1991. This discussion included the Moco Fireflood project (1971); the Sloss COFCAW project, Nebraska (1967); the West Heidelberg pressure maintenance Operation, Mississippi (1971); Buffalo light oil field, S. Dakota, (1984). All the fields had high reservoir temperatures and reactivities and self-ignition took place after initiation of air injection. Fassihi et al 1994 reported an incremental oil recovery factor of sixteen percent for the Buffalo Hills project.

West Hackberry

The use of air injection for tertiary light oil recovery at West Hackberry Field in Southwestern Louisiana has also been reported by Fassihi et al 1996 and Gilham et al 1997. The light oil reservoir (30 ^{0}API), with 28% porosity and 300 md permeability had a 19% initial water saturation. Four million standard cubit feet of air is injected into these high-pressure (2500-3300 psi) reservoirs that have been watered out using the double displacement process and also in low-pressure (300-600 psi) reservoirs with large gas caps and thin oil rims. In this field, the oxygen is consumed through spontaneous in-situ combustion in reservoirs with ignition temperatures that range from 79^0 C to 93 ^{0}F, which was estimated from laboratory calorimeter and oxidation tube tests. Spontaneous ignition was believed to have happened, evidenced by a sharp increase in pressure at the air injector after a couple of days of injection had been carried out. Oil production increased significantly from the low-pressure field reservoirs due to air injection. From July 1996 to July 1997, air injection generated 58,500 bbl of incremental oil production in this field. The high-pressure reservoirs are yet to yield an increase in production. Another noteworthy point is that only a minimal amount of carbon dioxide was detected in the produced gas. Majority of the gas had dissolved in the reservoir oil before reaching the production wells. This would improve gravity drainage due to viscosity reduction.

Medicine Pole Hills

Another major field application of Air Injection is that of Medicine Pole Hills in the Williston Basin of North Dakota, reported by Kumar et al 1994. This field had very low primary recovery of about 15 % of the original oil in place (OOIP). The original

reservoir pressure was 4120 psi with an initial reservoir temperature of 110°C. The estimated OOIP is 40 million bbl, with an oil saturation of 63 and 52% at different zones. This light oil field (39 ^{0}API) possessed a low permeability (1 to 30 md) and was part of a carbonate formation. Laboratory testing using the accelerating rate calorimeter (ARC) showed that the crude would vigorously combust at reservoir conditions. An air injection rate of 8 Mscf/STB was used in the field. This project has been quite successful in terms of oil recovery rate, which has doubled. Fassihi et al 1994, report an incremental oil recovery of fourteen percent for the Medicine Poles project. There was also increased natural gas liquids recovery as a result of the stripping of light oil by the in-situ generated flue gas.

Horse Creek

The Horse Creek reservoir, part of the Williston basin, North Dakota has been under Air Injection since May 1996 and has been reported by Germain and Geyelin, 1997, Watts et al 1997 and Clara et al 1998. It is the third air injection project in the Williston Basin, following on the successes of Buffalo Red River unit, South Dakota and Medicine Pole Hills Unit, North Dakota. The Horse Creek field consists of carbonates, predominantly limestones, dolomites and anhydrites and had an estimated oil-in place of 45.7 MMBBLS at 65% oil saturation. The field contains light oil (32.2 ^{0}API) at a reservoir temperature of 92 ^{0}C, with a porosity of 12 to 20 % and a permeability ranging from 1 to 100 mD. Water flooding was ruled out for this field because of the relative permeability of the reservoir, and the inability to form an oil bank, as well as the lack of an abundant supply of water in the area. After evaluating several options, air injection was decided upon. TOTAL carried out laboratory tests and

simulations on the suitability of the reservoir to air injection, including accelerating calorimeter tests, isothermal oxidation and quasi-adiabatic combustion tube tests. The average reservoir pressure increased from 625 psi to an average of 1300 psi. Production increased from 293 BOPD to 400 BOPD nine months after air injection started in May 1996, and then to 700 BOPD by September 1997.

Maureen Field

In the North Sea, in particular the Maureen field a light water flooded reservoir high-pressure air injection has been investigated as a possible improved oil recovery candidate. This field has achieved 53% recovery of the original oil in place but if abandoned will leave 175 MM STB in place as unrecoverable oil. Air injection would have an advantage over miscible hydrocarbon gas flooding. This is due to the effective reservoir volume factor of high-pressure air heated to reservoir temperature. Laboratory investigations by Fraim et al 1997 revealed that only two-thirds of a pore volume of air needs to be injected to sweep the reservoir as opposed to one hydrocarbon pore volume in the case of hydrocarbon gas. However despite the favourable feasibility of the project, it was decided not to go ahead with it due to the organisation's unfamiliarity with operating an air injection project offshore. Most of the fields in the North Sea share similar characteristics with the Maureen field, specifically deep reservoirs (2000-4000 meters), high reservoir pressure (200-400 bar), high reservoir temperature (80-130 ^{0}C) and large well spacing.

Light Oil In Situ Combustion Projects

Combustion projects have been carried out on several light oil fields in the past, and these were mentioned by Tzanco et al 1990. They included the Pontotoc pool of

Southern Oklahoma (18.5 ^{0}API), the May Libby project in India (40 ^{0}API). Other fields were mentioned from Romania (29-31 ^{0}API), and Hungary (39 ^{0}API).

In-situ combustion on Countess B light oil reservoir was reported by Metwally 1989. This light oil field with 28 ^{0}API oil had a reservoir pressure of 9.6 MPa, porosity of 25%, reservoir temperature of 38 ^{0}C and an initial oil saturation of 78%. A combustion temperature of 300-400 ^{0}C was observed, much lower than the typical 500-600 ^{0}C obtained for heavy oil combustion. This was attributed to superwet combustion due to steam.

The H/C ratios obtained were different from those typically obtained from medium and heavy oils.

In conclusion, it can be seen that air injection is slowly becoming accepted as a form of recovery from not only heavy oils but from light oil reservoirs as well. Other air injection field projects are being considered, notably in Indonesia, North Africa and Africa.

2.2 Oxidative Kinetics of crude oil

It is necessary to determine the relevant kinetic aspects of crude oil kinetics including the thermodynamic considerations; the feasibility of the reaction, as well as the energy changes associated with the reaction (enthalpy change). Reaction rates also have to be observed i.e. how fast the reaction is as these affect the spontaneous ignition. The reaction mechanisms must be determined, especially regarding light oil oxidation which could be different from that of heavy oils. Other questions that must be answered include the route the reaction takes as well as a study of the possible mechanisms that

occur; if it involves a series of successive elementary steps or formation of intermediates.

It is imperative to study the oxidative kinetics of crude oils for a number of reasons. It is required for the understanding of the in situ oxidation processes (both low and high temperature oxidation), that occur during air injection to facilitate numerical simulation. It is essential to understand the reaction kinetics of oxidation for proper operation of an air injection project. Kinetic parameters have to be obtained for use in simulation tools so as to be able to predict its performance in new reservoirs or under new operating conditions.

Considerable confusion arises due to the varying terminology used in defining the various reactions and mechanisms that take place during air injection into crude oil reservoirs. An attempt is made below to clarify these, and also to differentiate where possible between processes occurring predominantly in heavy oils and those applicable to light oils.

It is required to explain the various phenomena that have previously been observed in oxidation of crude oil. Previous investigations of the oxidation reactions occurring during air injection show the existence of at least two temperature ranges over which oxygen uptake rates are significant (Tadema, 1959, Alexander et al 1962, Burger and Sahuquet, 1972, Fassihi et al 1984 and Moore et al 1992).

The majority of oxidation tests performed on heavy oils show two distinct local maxima in oxidation rates. Bousaid and Ramey, 1968 detected three major reactions occurring in in-situ combustion. Experiments done on a light crude by Kisler and Shallcross, 1995, also showed three temperature ranges over which maxima occurred in oxidation rates. The two main temperature ranges where energy generation rates were

accelerated are termed the low temperature oxidation and high temperature oxidation or combustion regions, LTO and HTO respectively, with the third, middle region termed the medium temperature oxidation (MTO) region.

For heavy crude oils the range of temperatures associated with LTO is about 150 to 300°C while HTO is in the range of 350 to 800°C. For light crude oils this temperature range reduces somewhat to about 100 to 200°C for LTO and about 250/300 to 600°C for HTO. There are other occurring phenomena that are not fully understood. For instance there could be the occurrence of a slow combustion region as well as a negative temperature coefficient area in a temperature plot of a combustion reaction which occurs between the LTO and HTO regions. This negative temperature coefficient region, recognised by several researchers (Zelenko and Solignac, 1997, Gaffuri et al 1997), is disputed and also termed as a Medium temperature oxidation region (MTO), as it is clearly distinct from the other two regions. It is believed that cracking reactions and fuel deposition occurs in this region.

An analogy has been drawn by Gaffuri et al 1997, between hydrocarbon oxidation in crude oil and the work that has been done (Le Chatelier, 1883, Newitt and Thornes, 1937, Ben-Aim and Lucquin, 1959) on light saturated hydrocarbons specifically C_1-C_{10}. In the gas phase, oxidation of light saturated hydrocarbons consists of the following regions as depicted in the diagram in Figure 2.2 (Gaffuri et al 1997).

This sort of division in reactivity is found under certain conditions in all saturated hydrocarbons, olefins, aldehydes, alcohols, ketones, ethers, etc. Firstly there is a cool flame zone starting at low temperatures which corresponds to the LTO region. The products of this zone are the partial oxidation products of LTO. These products include initial hydrocarbon, alcohols, carbon oxides, water, oxygen, ketones, aldehydes,

ethers, hydroperoxides etc. The LTO of crude oils is a heterogeneous reaction between the gas and liquid phases.

There is also a zone where the rate of reaction decreases as the temperature increases and this is called the negative temperature coefficient zone. This is the region that could lead to a slowing down or total cessation of the oxidation. It has been noted (Moore et al 1999) that at low oxygen fluxes, the negative temperature coefficient region acts as a barrier to achieving a high temperature combustion mode.

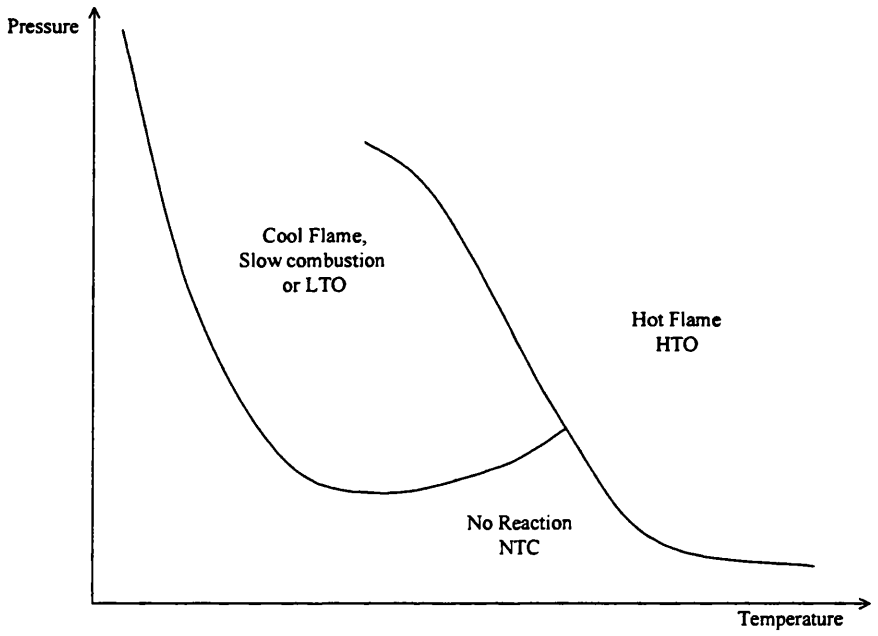

Figure 2.2: Diagram of Hydrocarbon Combustion Regions (Gaffuri et al 1997).

There also exists a normal flame zone, which corresponds to the HTO region of full combustion. It is necessary to reach these temperatures so as to achieve maximum oil recovery, especially with heavy oils. In fact with heavy oils and bitumen, recovery is actually elevated when these regions are reached without the prior formation of an LTO

region. At stoichiometric reactant mixtures the products of these reactions are carbon oxides and water.

One of the biggest problems with obtaining the relevant oxidation kinetics of crude oil arises due to its complexity. Crude oil consists of different types of molecular distributions. It can be characterised by its molecular weight, ranging from C1 molecules to over C200s in the case of heavy oil. It can also be characterised by its molecular type distribution starting with paraffinic hydrocarbons and continuing to single ring aromatic and napthenes to condensed ring molecules. These varying distributions are expected to exhibit varying kinetic behaviour in certain reaction regions. Gas flames of all components essentially have the same kinetics although ignition behaviour may differ. It is impossible to examine every single component and its reaction mechanisms individually therefore a requirement to investigate the mechanisms using both types of characterisations in pseudo component groups. The second group of molecular distribution according to type can be studied using the relevant saturate, aromatic, resin and asphaltene fractions of a particular crude oil.

The reactions involved in all of these zones are huge in number and cannot all be individually described accurately, although computer codes have been written which attempt to model thousands of reactions. It should also be borne in mind that the C-H bonds in hydrocarbons can react successively or simultaneously and there could possibly be an infinite number of these reactions.

Overall Reaction Mechanism

A mechanism for phenomena occurring in the reaction stages of the oxidation is summarised below in Figure 2.3. This procedure was postulated for heavy oil oxidation by Fassihi et al 1984 and is also quoted by a number of researchers including Abu-Khamsin et al 1988, Kisler and Shallcross, 1997.

It includes the distillation, pyrolysis or cracking of the crude oil and combustion which occurs. The first stage involves a distillation of the very light fractions at temperatures up to about 280 °C. The coke which is formed serves as the fuel for the combustion which takes place in the HTO stage. The light fractions are swept off with the displacement gas, and this stage is followed by thermal decomposition, i.e. visbreaking and mild cracking of the resulting medium and heavy fractions. This leads to the loss of small side groups and hydrocarbon atoms from the hydrocarbon groups with the displacement front. The residual oil has a lower hydrogen/carbon ratio, is less branched and undergoes severe cracking to deposit coke on the reservoir matrix.

The factors which affect the oxidation reactions of crude oil have been reviewed by Fassihi et al 1984 and Moore et al 1992. These include the pressure, injection gas flux, oxygen concentration, initial oil saturation, initial water saturation, oxygen partial pressure and reservoir characteristics and surface area.

Kok and Karacan, 1997 identified three regions of reaction occurring during the oxidation of a medium and heavy crude oil with API gravity's of 26.12 and 14.95 respectively.

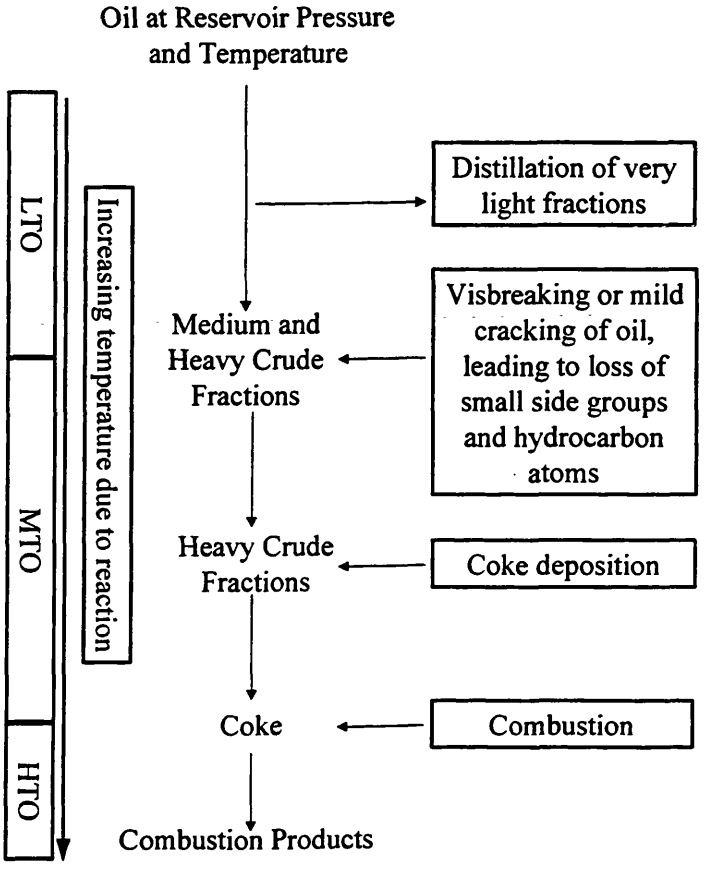

Figure 2.3: Oxidation Reaction Stages of Crude Oil

2.2.1 *Low Temperature Oxidation Kinetics*

Low Temperature Oxidation (LTO) is one of the reaction types that occur during air injection. Generally, LTO consists of the heterogeneous gas-liquid reactions that occur at temperatures in the region of 100-300° C.

Occurrence of LTO in the Field

LTO reactions have been studied quite widely in the past (Dabbous and Fulton, 1972, Lerner et al 1985) especially as regards to heavy oil in situ combustion (Fassihi et al 1990). Its impacts on air injection into light oil reservoirs have not been as widely studied. In air injection projects that go to full combustion, LTO is likely to take place upon air injection prior to ignition, or downstream of a combustion front if oxygen is

available. This could be due to incomplete oxygen consumption in the high temperature combustion zone or air channelling around the front. LTO has happened in in-situ combustion projects where there was insufficient air flux due to low air injection rates. Due to the dominance of these low temperature oxidations, there was no high temperature wave and the oxygen was consumed in LTO reactions spread over a wide region. LTO may occur even at high air injection rates when the heterogeneity is very pronounced. Some air injection processes conducted in micro fractured sandstones containing light oils became LTO dominated due to very high heat losses in regions surrounding the channels through which the combustion front propagated. This occurred in a sandstone reservoir in Dofteana Oligocene and Solont Stanesti, Romania. Oxygen bypass or channelling can be caused the presence of high permeability streaks that enable oxygen to travel so quickly through the high temperature zone that it contacts insufficient fuel for complete utilisation. The other main causes for the occurrence of LTO in heavy oils are low reservoir temperatures and pressures; i.e. the reactivity of the oil is too low to cause ignition or high temperature oxidation.

In light and medium gravity crude oils, operation in the LTO mode is sufficient to obtain additional oil production due to the displacement caused by nitrogen and the flue gas (Ren et al, 1999).

LTO Mechanism

At LTO temperatures below 300°C, most of the oxygen is utilised in hydrogen and hydrocarbon oxidation (addition) reactions rather than in carbon atom oxidation to carbon oxides. LTO reactions are characterised by either no carbon oxides or low levels of carbon oxides in the effluent stream. Burger and Sahuquet, 1972 claimed that LTO in

heavy oils usually results in the formation of oxygenated compounds including carboxylic acid, aldehydes, ketones, alcohols and hydroperoxides.

The reaction mechanism of incorporation of oxygen into the hydrocarbon chains of the crude oil are shown for the production of carboxylic acids, aldehydes, ketones, alcohol or a hydroperoxide in Equations 2.1-2.5 respectively.

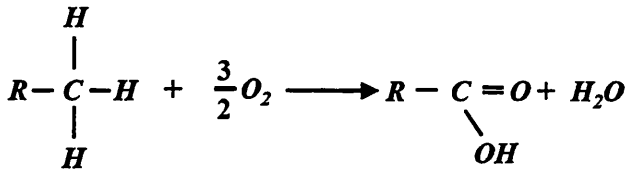

Equation 2.1

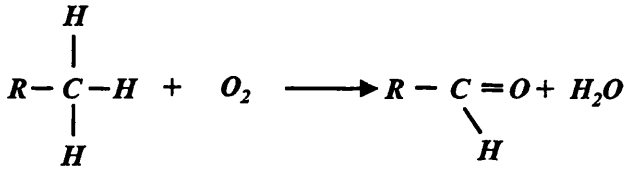

Equation 2.2

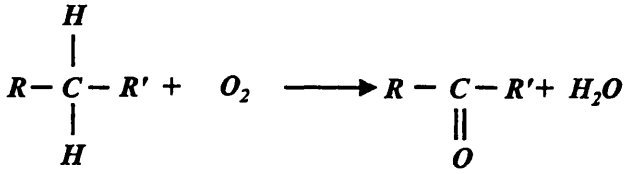

Equation 2.3

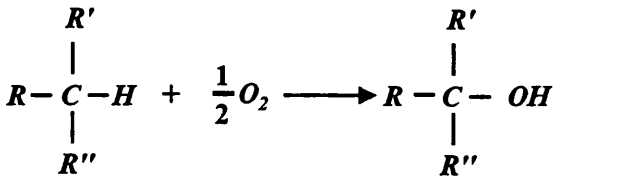

Equation 2.4

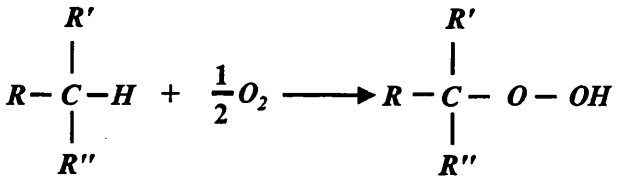

Equation 2.5

Potential disadvantages of LTO in heavy oils are an increase in viscosity of the oil, and a shrinkage of the injected gas due to the uptake of oxygen in the oil. Fassihi et al 1990 carried out experiments on the effect of LTO on the viscosity of oils and found that the rate of viscosity increase was higher for heavier and more asphaltenic oils. This detrimental effect might therefore not be substantial in light oils which have a low viscosity to start with.

It has also been shown by Moore et al 1999 and Ren et al 1999 that bond scission reactions, i.e. combustion reactions actually do take place in the LTO region as well. Significant amounts of hydrocarbons can be consumed if LTO is allowed to operate over a significant period of time.

Possible explanations for the oxidation phenomena have been put forward for heavy oils by Belgrave et al 1990. The heavy oil is divided into two components, maltenes and asphaltenes, in which maltenes has a much higher reactivity to oxygen than asphaltenes. At low temperatures, maltenes, being the more reactive component, preferentially consumes the oxygen thus increasing the asphaltenes content of the oil. Eventually a global reduction in the reactivity of the oil due to the formation of asphaltenes occurs and the negative temperature coefficient region is reached. Higher temperatures are then required for the asphaltenes to react with the oxygen, at which point it then goes in to the HTO zone. It has been proposed by Babu and Cormack, 1984 and Adegbesan 1987 that in heavy oil fractions LTO causes condensations to higher molecular weight material.

Alexander et al 1962 carried out investigations on the deposition of fuel during LTO for a 21.8 °API crude and discovered that the amount of deposit was maximised at 218 °C, and then decreased to zero at 371 °C.

Kok and Karacan, 1991 found that a distillation, visbreaking region where side chains of heavy compounds are split was identified between 25 °C to 377 °C/367 °C for the medium and heavy oil respectively. This included low temperature oxidation (LTO), which was identified as occurring from 300-377 °C and 310-367 °C for the medium and heavy oils.

Kisler and Shallcross, 1997 noted that there was production of carbon oxides during LTO, a phenomena which did not occur with heavy oils they studied during LTO. The LTO was also much stronger in the light oils. Fassihi et al 1997 and Clara et al 1998, observed high levels of CO_2 produced, which is different from the conventional heavy oil low temperature oxidation model. This would seem to confirm the hypothesis that bond-scission reactions do take place in the reservoir even in the LTO phase.

Another field in which LTO reactions have been studied is that of the combustion engine. The oxidation of hydrocarbons has been closely studied here (Gaffuri et al 1997, Jost book, Emanuel et al) and various significant conclusions have been made. In the Low Temperature regime, the oxidation of hydrocarbons is highly complex with different propagation and chain branching reactions. These different reactions and possible reaction configurations are what lead to the variety of phenomena that occur in LTO of crude oil such as slow combustion or the negative temperature coefficient area. An oxidation scheme has been presented to account for LTO in hydrocarbons by Ranzi et al 1995. The primary reactions involved in LTO were classified and large reaction schemes automatically generated. This scheme gets extremely complex with increase in the carbon number of the molecule. It is known from organic chemistry that as the number of isomers of the same homologous molecules and radicals increases, so does the number of reactions. It then becomes

necessary to utilise lumping procedures, both for reactions and components. These lumped mechanisms consist of a limited number of equivalent reactions that are then coupled with a detailed scheme for the oxidation of C_1-C_4 species. The resulting kinetic model of hydrocarbon oxidation involving components from methane to isooctane is constituted of about 150 species involved in 3, 000 reactions. Ranzi et al 1994 found that in the low temperature regime fuel consumption occurs via hydrogen atom abstraction, primarily by $OH^{\cdot}$ and $HO_2^{\cdot}$ and to a lesser extent by $H^{\cdot}$, $CH_3^{\cdot}$ and O_2. This reaction scheme models various experimental data from several different experiments at different conditions in terms of temperatures, pressures, residence times and stoichiometries. It is likely though that more than hydrogen abstraction would be required.

2.2.2 *Thermal Cracking And Fuel Deposition*

Fuel deposition is the process by which fuel from the crude oil is left on the reservoir matrix. The deposition of fuel on the reservoir matrix for subsequent combustion has been widely singled out as the most important factor affecting an In situ combustion process. Discussions have been done on the fuel deposition mechanisms occurring before a full high temperature combustion takes place during In situ combustion of heavy oils (Fassihi et al 1984, Belgrave et al 1990). An attempt is made in this work to differentiate as much as possible between effects arising mainly from thermal cracking (pyrolysis) and oxidation, as many previous investigations show no distinction between the two phenomena.

It is believed that the cracking reactions that occur during an air injection process before high temperature oxidation, or full combustion starts are responsible for

the fuel deposition. The fuel for the HTO process is a coke-like residue that deposits on the sand grain. Lerner et al 1985, postulated that this coke-like residue is formed from the thermal decomposition of the oil molecules; generally small hydrocarbon groups rich in hydrogen are broken off from the parent molecule. The effect of this coking is to reduce the H/C ratio of the fuel left behind for combustion and the vaporisation characteristics of the oil are altered. Cracking or pyrolysis reactions are generally endothermic in nature.

Importance of fuel deposition

The sustainability of HTO during in-situ combustion depends to a large extent on the rate at which the fuel or coke is formed from the original oil and the rate at which this fuel is burned. Fassihi et al 1984 stated that excessive fuel deposition causes a slow rate of advance of the burning front. On the other hand insufficient fuel leads to the heat of combustion being inadequate to raise the temperature of the rock and the contained fluids to a level of self-sustained combustion. It has also been noted (Belgrave et al 1990) that for heavy oil recovery, LTO is an important fuel-forming step before full combustion is initiated.

Fuel Deposition Mechanism

There is a lot of disparity in the literature concerning what processes take place at this stage of the oxidation process and also as to whether or not any form of cracking takes place in light oils.

The mechanism of fuel deposition in heavy oils is subject to two main factors, the vaporisation of light crude oil components and the kinetics of the cracking reaction. These two processes determine how much fuel will be burnt and how much will form coke. If the cracking rate is high, it is likely that most or all of the crude oil in the

cracking zone preceding the combustion zone will be either vaporised or coked and coke will be the sole source of fuel. However if the cracking rate is low, some crude oil will also be burnt in the combustion zone.

Alexander et al 1962 found in their studies on fuel deposition that about 3.3 weight per cent carbon of a 21.8 ^{0}API oil was deposited as a coke like material, and that this deposition occurred in the LTO stage.

Ciajolo and Barbella, 1984 investigated the fuel deposition mechanism under pyrolysis and oxidation of heavy oils and found that a distillation of paraffinic and aromatic phase occurred at lower temperatures. This was followed by a pyrolytic phase at higher temperatures where the polar and asphaltene fractions left a carbon residue.

Nace et al 1971 proposed that coke can be formed from the direct cracking of the gas-oil component and from the intermediate gasoline component.

Abu-Khamsin et al 1988 assumed a chain reaction as follows:

$$crude\ oil \xrightarrow{heat} visbroken\ oil + gas \qquad \text{Equation 2.6}$$

$$visbroken\ oil \xrightarrow{heat} coke + gas \qquad \text{Equation 2.7}$$

A widely accepted mechanism for thermal cracking is that based on the Rice-Kossiakoff theory (Kossiakoff and Rice, 1943), which was developed for paraffins. The free radical mechanisms involved in this theory have been described in detail and proven by numerous experiments. Variations of the mechanism have been used by Lin et al 1987 and Fassihi et al 1990. The chain reaction steps in this cracking mechanism are listed as follows:

1. Isomerisation
2. Decomposition
3. Hydrogen Transfer

4. Condensation

5. Dehydrogenation

6. Polymerisation

The Rice-Kossiakoff model was designed primarily for catalytic cracking, which is based on an ionic cracking model with charged intermediates rather than neutral free radicals. The model requires modification to be used for free-radical cracking. The isomerisation step is not as important because while R+ ions will rearrange, R• radicals or R- ions will not. The cracking reaction has been modelled by Lin et al 1987 and the models show that the first order kinetics generally accepted for cracking of pure components in the literature are generally unsatisfactory for multi-component systems characterised by pseudo-components. Two different models instead are put forward with oil being characterised into pseudo-components and this was found to better model the cracking reactions. In addition it was confirmed that coke is not always the sole source of fuel burned in HTO.

Tzanco et al 1990 carried out combustion studies on Countess B light oil. One of the findings was that the oil does not burn a coke-like fuel, but rather burns an oxidised asphaltene fraction. This would require a different fuel deposition model for light oils if oxidised asphaltene rather than coke is the fuel.

Ranjbar and Pusch, 1991 discovered that the fuel deposition of a crude oil depended on the colloidal composition as well as the heat transfer characteristics of the pyrolysis medium. Ranjbar, 1993 also attributes the fuel deposition solely to pyrolysis or thermal decomposition.

Factors affecting Fuel Deposition

Alexander et al 1962 carried out studies into the factors affecting fuel deposition. They concluded that fuel availability depends on original and residual saturation, air flux, ^{0}API gravity, viscosity, atomic H/C ratio, and Conradson carbon residue. The fuel deposited increased with higher initial oil saturations, oil viscosity and Conradson residue and decreased with increasing atomic H/C ratio and ^{0}API gravity. At the same time it appears rock lithology could be more significant than oil gravity in determining fuel deposition. The issue of whether medium or light oils can undergo the required chemical changes during pyrolysis to from a sufficient quantity of fuel for combustion was raised by Pusch and Ranjbar-Hamghawandi, 1991 after running several oxidation tests.

Several studies (Burger, 1972 and Drici and Vossoughi, 1985, Ranjbar, 1995) identified the importance of the type of rock on the amount of fuel deposited. Ranjbar 1993 studied the relationship between clay content and the amount of fuel formed from light, medium and heavy oils. The results showed a clear dependency of the fuel yield on the clay content in the matrix. This was attributed to the high specific surface area of clay. Vossoughi et al 1985 demonstrated that fuel deposition was not only influenced by clays but was also accelerated by any material with high surface area. Clays are known for the catalytic effect they have on reactions due to their high acid site density and acid strength.

Bousaid and Ramey 1968 found that H/C ratio found that higher viscosity and higher Conradson carbon residue leads to increased fuel deposition.

Bae 1977 found that no general effect on fuel deposition could be ascribed to pressure as different oils had different behaviour.

A study by Kok and Karacan, 1997, identified a medium temperature oxidation (MTO) or fuel deposition region after LTO occurs. This temperature was specified as 377-467 ^{0}C for the medium oil and 367-460 ^{0}C for the heavy oil. These reactions are reported to be homogeneous in the gas phase and involve the oxidation of products of pyrolysis.

There appears to be a very strong correlation between the fuel deposited and the LTO taking place in the oil. Alexander et al 1962 investigated the factors affecting the laydown of fuel for combustion. They made observations on a 28.1 ^{0}API light oil that the amount of fuel available depended on the temperature at which LTO was allowed to occur before HTO was initiated.

Despite the vast amount of literature available regarding fuel deposition, the mechanism by which it occurs still remains one of the biggest unknowns in air injection processes. One of the most important questions arising with respect to light oils is whether fuel is in fact deposited, considering that they contain fairly low amounts of the heavy fuel forming components. A distinction also needs to be made as to whether the fuel deposition is due to pyrolysis or due to a medium temperature oxidation cracking.

2.2.3 *HTO Kinetics*

The high temperature oxidation (HTO) reaction in heavy oils is a heterogeneous gas-solid one where the fuel deposited is combusted. For the case of light oils, it is possible that some liquid combustion occurs as well, involving a break-up of the hydrocarbon chain to form carbon oxides and water. The mechanism for HTO in light oils is not clearly defined in the literature. In heavy crude oils, the operation in the HTO mode is essential to reduce the viscosity of the crude oil. The HTO region is the best

understood of all the kinetic steps that occur during air injection and in situ combustion. When the reaction goes to full completion, it is simply a matter of CO_2, H_2O and CO being produced from the combustion of the fuel laid down in the deposition step as well as the combustion of the crude oil.

Studies on the oxidation of carbon indicate a first order reaction dependency on both carbon concentration and oxygen partial pressure. Fassihi et al 1990, in their model, indicated a first order dependency on oxygen partial pressure but a second order one with respect to carbon concentration.

The HTO combustion reaction can be represented by the following equation, which has been used by Bousaid and Ramey, 1968, Burger and Sahuquet, 1972 and Fassihi et al 1984.

$$R_c = -\frac{dC_m}{dt} = kp_{o_2}{}^m C_m^n \qquad \text{Equation 2.8}$$

Where C_m = instantaneous concentration of fuel, k is the specific reaction rate constant, $P\,o_2$ is the partial pressure of oxygen, while m and n are the reaction orders.

For combustion and kinetic tube experiments Benham and Poettmann, 1958 obtained a stoichiometrical equation for the combustion of the fuel deposited. This equation which was also used by Mamora and Brigham, 1995 is shown below in equation 2.9

$$CH_x + \left(1 - \frac{m^*}{2} + \frac{x}{4}\right)O_2 \rightarrow (1 - m^*)CO_2 + m^*CO + \frac{x}{2}H_2O \qquad \text{Equation 2.9}$$

where x is the atomic hydrogen-carbon (H/C) ratio of the fuel and m^* is the fraction of carbon oxidised to carbon monoxide, termed the m^*-ratio which is shown below.

$$m^{*} = \frac{CO}{(CO + CO_2)} \qquad \text{Equation 2.10}$$

where CO_2 and CO are the mole percent of carbon dioxide and carbon monoxide, respectively, in the produced gas.

Kok and Karacan (1991) observed a main combustion region in the temperature range of 490-580 °C for the medium oil and 460-560 °C for the heavy oil. This region is identified as the HTO reaction where the fuel formed in MTO is oxidised.

The main unknowns therefore in this step of the process are the initial reactants present in the particular crude oil and the extent of the particular reaction. It depends very much on what the final products of the LTO reactions are.

2.3 Exothermicity of crude oil

The exothermicity of the crude oil needs to be fully understood, as it determines how the oxidation reaction releases heat, and it also directly determines the oxidation reaction parameters obtained. This heat could be crucial to the oxidation taking-off upon air injection, and could also determine if an oxidation is extinguished due to heat losses in the reservoir, or not. From these tests various reactivity parameters of any given oil as well as the possibility of spontaneous ignition of the crude oil in the presence of air at reservoir conditions can be determined. These reactivity parameters include the rate of reaction, temperature rise over a given time as well as the continuity of reaction from LTO to HTO. The emphasis in this study is on the exothermicity results obtained from the accelerating calorimeter as these results are adiabatically obtained, rather than being subject to any external influences.

Exothermicity can be measured using the magnitude and rate of heat changes accompanying oxidation reactions.

The exothermicity of a particular oil is affected by the pressure, properties of the matrix, i.e. the composition e.g. clay or limestone; the surface area of the rock. The oxygen content of the air; i.e. using enriched air or not, and the oxygen partial pressure.

A method of studying the exothermicity of crude oil using an adiabatic reaction calorimeter has been developed by Yannimaras and Tiffin, 1995 and has also been reported by Christopher 1995. The experimental results are presented as a plot of the log of the rate of exothermic heat release (°C/min) v temperature. Assuming adiabatic conditions are maintained, the presence of a trace over a temperature interval indicates a region of exothermic reaction, while no reaction is indicated by the absence of experimentally recorded points. This is because once combustion is underway, no heat is allowed to cross the system boundaries as it is adiabatic. This method has been used by Gilham et al 1997, Zelenko and Solignac 1997, Clara et al 1999, with the laboratory results matching field tests.

2.3.1 *Energy released from reaction*

For in-situ combustion i.e. HTO, it is essential to know if the process is self-sustaining in terms of heat production in the reservoir. Therefore the amount of heat produced by the combustion process under conditions similar to reality has to be known. This is essential in assessing the suitability of a reservoir for air injection.

Types of reaction

Chemical reactions can be classified into three types:

1. Endoergic (or endothermic), if the energy absorbed in bond rupture exceeds the energy released by the formation of new bonds, then overall the chemical reaction is observed to be energy absorbing.

2. Exoergic (or exothermic) in the converse cases in which the energy absorbed is less than the energy released.

3. Aergic (or athermic; i.e., without energy change) for rarer cases where the overall absorbed and released energies are equal in magnitude.

In every case, however, energy must be supplied to the reactants in order to initiate the breaking of bonds before other bonds can be formed because a stable bond will not of itself degenerate. In general, therefore, all chemical reactions, even exoergic or aergic, require the introduction of energy in some form from an external source in order to begin. The initiating energy, called the activation energy, is sometimes supplied as heat from another, already initiated exoergic chemical reaction.

It is widely known that oxidation reactions are exothermic in nature. The heat of combustion from HTO reactions has been estimated by Burger and Sahuquet, 1972 to obtain heating values for crude oils.

Bae 1977 studied 15 crude oils, with ^{0}API gravity's ranging from 6 to 38 ^{0}API using TGA/DTA. It was found that the heat generated by LTO was significantly greater than in the HTO phase, although this did not apply to all of the oils tested.

Babu and Cormack, 1983, found that there was more heat evolved per mole of oxygen consumed in the LTO than was produced in the HTO stage. This result was contrary to general belief about heat generation from LTO and HTO which is widely thought to be the more exothermic of the two reactions. In LTO about half the oxygen goes to form water which gives more energy per oxygen than carbon oxides. In HTO less than half the oxygen goes to water, hence the reduction in energy evolution.

Belkarchouche, Price et al, 1988 studied heavy oils using a pressurised DSC and found that the magnitude and rate of heat changes accompanying combustion of oil and

oil core samples increased with increased total pressure and with oxygen partial pressure up to 34 %.

Drici and Vossoughi 1985 observed an increase in the heat given off solid surface was added to the oil, as well as a shift of heat from a high to a low temperature range.

As well as obtaining values for the energy release from the oxidation reaction, it is also useful to understand where the majority of the heat release is taking place. This is indicative of which of the different oxidation reactions is most important for light crude oils. A discussion of the method used in carrying this out is made in later in Chapter 4 and in discussion of each of the individual results

2.3.2 *Spontaneous Ignition*

Ignition is the first step of the in-situ combustion process. It may be obtained by heating the formation around the ignition well with a burner or an electrical heater. Burger, 1976 postulated that this heat required to initiate combustion can also be provided by an exothermic reaction between air and a chemical compound which might be injected to achieve this.

However if the crude oil is sufficiently reactive enough at reservoir conditions, the formation may spontaneously ignite after air has been injected for a period. Schoeppel and Ersoy, 1968 recognised that for this to occur the heat released during LTO oxidation must accumulate and not dissipate to the surroundings.

It has been found (Prats 1982) that when the reservoir temperature rises above 66°C the reservoir oil ignition delay time reduces greatly from a few days to a matter of hours. At even higher temperatures, it should follow that the oil should spontaneously

ignite. The ignition delay may vary from a few days to an indefinite period if the rate of heat dissipation to the surrounding reservoir formation prematurely becomes as high as the rate of heat release.

Spontaneous ignition after the injection of air is favourable to the process as it aids process initiation and usually improves the stability, although Moore et al 1999 have drawn attention to the fact that it isn't favourable for heavy oils. This is due to the fact that it would promote operation in LTO with resultant increase in the oil viscosity. Auto ignition under controlled experimental can be taken as an indication of similar auto ignition in the field. Care should be taken to ensure that the experiment approximates reservoir condition which are nearly adiabatic generally.

The ignition delay corresponds to the initial part of the oxidation process during which a very small fraction of the crude oil is altered. Burger 1976 and Tadema 1970 have used the heat released by the oxidation reaction to estimate the spontaneous ignition time for crude oils. The heat dissipation by conduction and convection was included in a numerical model developed by Burger 1976 to calculate the ignition conditions; ignition delay and position of the ignition zone, as a function of reservoir, oil and gas flow characteristics. It was found that the distance from the well to the ignition zone increases with the airflow rate and with the delay.

Burger et al 1985 defined the ignition delay as the time required for the temperature to exceed 210 ^{0}C around the air injection well. This temperature was chosen as one where the oxidation rate is high enough to sustain the oxidation rate, and was found to be dependent on the reservoir porosity, permeability, oil and water saturation. It also depended on other oil and reservoir properties such as viscosity etc.

The distance at which ignition was found to occur increased with an increase in the flow rate used during the ignition. Using heavy oils, an ignition delay of 10-20 days was seen in oil reservoirs where the reservoir temperature was 50-60 ^{o}C. With a reservoir temperature of more than 70-80 ^{0}C, ignition was seen to occur sometimes within hours. An increase in the injection pressure signifies the start of ignition in the field, although this might not always occur.

The main factors affecting spontaneous ignition have been listed by Rao et al 1997 as the initial reservoir formation temperature, and the reactivity of the crude oil. A laboratory determined reaction rate is necessary to compare with analytical calculations of the ignition time. To adequately model the spontaneous ignition in a field, it is necessary to know the reservoir characteristics and how these affect heat transfer or thermal losses.

2.4 Displacement Efficiency/Miscibility

The main gases present in the flue gas responsible for displacement and which could lead to miscible drive are nitrogen, carbon dioxide, and C_2-C_5 gases. The possibility of miscibility of these various gases and the mixture itself with various crudes is important and should always be investigated for any particular field case. This is due to the favourable effect miscibility has on oil recovery. The barrels of oil recovered per volume of injected gas increases substantially if miscibility of the oil with the flue gas is achieved. Though a detailed study of miscibility effects is outside the scope of this work, a brief review of the salient features is carried out.

Studies of the miscibility of crude oil with nitrogen and other gases have been made previously and several important points need to be considered. These significant points were detailed by Turta and Singhai, 1998.

Depending on the reservoir pressure, nitrogen can be either first contact miscible or multiple contact miscible with the oil. First contact miscibility is usually attained at higher reservoir pressures and is less common. Multiple contact miscibility, which is also known as dynamic miscibility occurs after mass transfer between the oil and gas has taken place during immiscible displacement of the oil by the nitrogen. The presence of the flue gases generated from oxidation in the nitrogen/gas mixture can also greatly aid the process of miscibility being attained.

For a fixed gas composition, the lowest pressure at which the injected gas can develop miscibility with the reservoir crude oil at reservoir temperature is called the minimum miscibility pressure (MMP). Oil displacement tests can and should be carried out in the laboratory to determine the MMP for a particular oil with a fixed flue gas composition. These displacement tubes are made up of very long tubes (15-30 m) with small diameters (about 5-6mm), packed with sand or glass beads and measure the displacement using nitrogen at different pressures. Rising bubble apparatus can also be used to measure the miscibility.

Analytical equations based on laboratory work exist. These can give rough correlations of minimum miscibility pressure for crude oils. These generally show that the minimum miscibility pressure for nitrogen is not very dependent on temperature, while that for carbon dioxide increases with increasing temperature. This effect reduces in the presence of other gases so the miscibility does not increase during the course of the oxidation reaction.

It is worth noting that the minimum miscibility of nitrogen at the sort of temperatures seen in North Sea reservoirs is very high (approximately 400 bar).

It is important, as part of the air injection assessment of a potential reservoir and crude oil, to perform phase equilibrium modelling of the crude oil and the combustion flue gases. This is to investigate the effect the flue gases would have on the oil as it moves through the reservoir and would give useful information on the displacement behaviour.

2.5 Reservoir Aspects of Air Injection

There are various types of reservoirs and it is important to understand how these variations affect the crude oil oxidation. Different characterisations of reservoirs include deep carbonate reservoirs, fractured reservoirs where only vertical flooding is possible, and non-fractured carbonate reservoirs, which include most reported air injection field projects. Chalk reservoirs are generally very tight reservoirs and this would have an impact on the displacement process and possibly on the oxidation.

The reservoir physical properties therefore play a major role in the efficiency or other wise as well as the choice of an IOR process. These properties include porosity, permeability, mineralogy, saturation, pore pressure etc. The specific surface area of the rock, permeability and porosity directly influence the fuel deposition, amongst other parameters.

Heat loss or dissipation through the reservoir is a major cause for spontaneous ignition not occurring upon air injection. This is affected by several reservoir properties including the heat capacity of the rock, heterogeneity, porosity, possibility of

channeling, dispersivity and fingering factors. It is now widely realised that reservoirs are more heterogeneous than was previously thought.

2.5.1 *Heterogeneity or non-uniformity of the reservoir*

The existence of serious heterogeneity in a reservoir almost always leads to the failure of a sustainable combustion front due to oxygen channelling and the proliferation of LTO as was noted by Turta and Singhai, 1998. LTO may occur even at high air injection rates when the heterogeneity is very pronounced.

The type of reservoir in which the oil is found also affects the way the air injection process could develop. Some air injection processes conducted in micro fractured sandstones containing light oils became LTO dominated due to very high heat losses in regions surrounding the channels through which the combustion front propagated. This occurred in a sandstone reservoir in Dofteana Oligocene and Solont Stanesti, Romania. Another test of air injection in a fractured reservoir was carried out in the extensively fractured CAPA Madison reservoir, North Dakota, and has been reported by Erickson et al 1993. After a year this project had to be terminated due to a high air/oil ratio.

A direct consequence of reservoir heterogeneity is the complexity of reservoir recovery processes. These effects range from migration of gas cap in reservoirs with discontinuous shales, overpressured zones and the tracking of injected water, steam or temperature during recovery in reservoirs with large spatial variations of permeability.

In previous field applications of air injection reported by Gilham et al 1997, early nitrogen breakthrough has been caused by a combination of high permeability layer, faulting and a low bed dip.

2.5.2 *Other important reservoir parameters*

Other important reservoir characterisation factors include the reservoir porosity, permeability, grain size and surface area of the matrix. Turta and Singhal, 1998 pointed out that in-situ combustion is not feasible in low porosity matrix reservoirs due to heat losses within the matrix.

Turta and Singhal, 1998 reviewed the engineering aspects of air injection into light oil reservoirs, where they differentiated air injection processes as those occurring naturally as opposed to in-situ combustion where ignition is required. The different types of processes that could possibly occur were listed as follows:

1. Immiscible air flooding with intensive oxidation
2. Immiscible air flooding without intensive oxidation
3. Miscible air flooding with intensive oxidation
4. Miscible air flooding without intensive oxidation

The possibility of any of these different processes occurring is therefore dependent on various factors including the pressure of the reservoir and the reactivity of the oil. These would affect the miscibility and hence increased miscibility and the intensity of the oxidation process respectively. As the stoichometric volume of air injected is roughly the same as that of the gases produced, the oxidation reactions do not have a negative impact on the pressure maintenance in the reservoir, which depends on the volume of injected air.

2.6 Development of Reaction Kinetics Model

Several attempts have been made in obtaining a kinetic model that accurately captures the various oxidation processes that take place upon air injection.

A common problem is the difficulty in fitting a one-step reaction model to the kinetic data obtained from experimental kinetic investigations. Kok and Okandan 1997 obtained weighted mean activation energies using the weight lost in a TG/DTG analysis and the activation energy corresponding to each area of Arrhenius linearity.

A number of detailed studies of oxidation kinetics have been carried out, especially considering common organic chemicals. Wilk et al 1987, Behar and Vadenbroucke 1996, D'Anna and Violi 1998 amongst others carried out experimental studies of alkane and aromatic oxidation respectively. It was found that alkanes form alkenes as intermediates, which then compete with the parent fuel for radicals and oxygen, leading to secondary reaction mechanisms. Propene for example is a primary hydrocarbon intermediate in the oxidation of propane, n-butane, as well as other higher alkanes which due to its double bond provides additional free-radical pathways and complicates the reaction mechanism. Considering that alkanes are just one class of organics present in crude oil with hundreds of others, the number of different pathways and possible permutations of oxidation reactions is therefore astounding. As a result, it is impossible to include all the elementary reactions, which actually do or could take place. It is therefore necessary to have a reaction model involving broadly characterised groups of oil components. Attempts to carry this out have been reported by several investigators including Ungerer et al 1988, Belgrave et al 1990, Hutchence and Freitag 1991.

The reaction model must incorporate some of the broader features and effects of various parameters affecting the oxidation of crude oils, where these have been shown to possess significant dominance. Lower temperature reactions would primarily involve free-radical formation and addition. At higher temperatures there is sufficient energy to

break primary C—C and C—H bonds, therefore abstraction and direct decomposition reactions dominate the reaction.

For numerical modeling, a reaction scheme that predicts the NTC zone is superior to one that does not.

Lin et al, 1984, 1987 used distillation cut fractions of crude oil in their kinetic model. While the oxidative reaction properties of one single distillation cuts are too varied to obtain reasonable results, these distillation cuts are necessary for modelling of pyrolysis that occurs during air injection. Lin et al 1987, in their model developed global reaction models suitable for thermal free-radical type cracking as well as catalytic carbonium-ion type cracking reactions.

Abu-Khamsin et al developed models for the crude oil cracking reactions based on this above mechanism. Henderson and Weber, 1965 studied these reactions in crude oils and bitumen using a batch reactor. It is important to note that a highly paraffinic oil was found the least susceptible to visbreaking. This is important because light oils tend to have a high paraffinic content.

Vossoughi and Saim, 1992 developed kinetic models breaking the oxidation reactions into five groups of reactions. The stages, which were based on TGA and DSC tests on a heavy oil, are listed below with the temperature ranges over which they found the reactions to be occurring.

1. Distillation (25-425 C)

The distillation model was based on temperature, pressure and composition dependent vapour liquid equilibrium coefficients, i.e. y = K (T, P, X). It would be expected that at the higher pressures seen in light oil reservoirs, the distillation effect would be less than for low pressure reservoirs.

4. Light Oil combustion (200-312 C)

5. Heavy Oil combustion (200-425 C)

6. Heavy Oil cracking (312-425 C)

This would be far less important for light oils as the percentage of heavier ends is low to non-existent.

7. Coke Combustion (312-600 C)

The kinetic reaction rates for all the other stages listed above were implicitly derived from the TGA curves obtained in the experiment and were therefore not general equations. These cut-off temperature ranges were also somewhat arbitrarily chosen by interpolation on the TGA curve.

The reaction regions with the biggest uncertainty are the LTO reaction and the coke deposition process.

The reaction between organic compounds and oxygen has been studied for decades, especially in the study of combustion engines, and several of these mechanism can be found in the literature (Minkoff and Tipper, 1962, Glassman, 1977). The mechanism for LTO reactions in crude oil would logically follow these albeit at different conditions. Despite the numerous publications on the subject, the detailed mechanisms of many of the oxidations are still uncertain, primarily because of the large number of products formed. It is generally agreed though that they are almost invariably chain reactions involving atoms and free radicals.

A screening method for light oils was developed by Yannimaras and Tiffin, 1995, which used accelerating calorimetry to check for continuous exothermicity. It was found that about twenty per cent of light oils would propagate full combustion. This

suggested that majority of light oils would undergo only low temperature oxidation and illustrates the importance of understanding the reaction mechanisms in this region.

LTO promotes the formation of free radicals in the crude oil, as the addition of oxygen into the oil molecules leads to oxygenated molecules, which easily give off free radicals.

The reaction products from the LTO of propane were studied by Wilks et al 1987. It was found that similar to crude oil, carbon monoxide, carbon dioxide, ethene, methane, formaldehyde and acetaldehyde were the major products. For mixtures rich in fuel content (propane-air ratios of 2/3), methanol was present in significant amounts, up to 1 percent, whereas at lean conditions there was no methanol present.

Ren et al 2000 report a step model for the LTO process involving oxidation where the oil consumes oxygen and generates oxygenated compounds, and decomposition which produces carbon oxides.

Fassihi et al 1984 listed two possible mechanisms to account for fuel deposition which are shown below.

$$(C_xH_y) \rightarrow xC \downarrow + \frac{y}{2} H_2 \qquad \text{Equation 2.11}$$

$$(C_xH_y) \rightarrow C_nH_m \downarrow + C_{x-n}H_{y-n} \qquad \text{Equation 2.12}$$

The first mechanism would imply the production of free hydrogen. As hydrogen has not been detected from light oil reservoir production wells, this is unlikely to be the predominant mechanism for coke deposition for light oil HTO.

While an understanding of the underlying theory is essential, there are a number of steps that need to be carried out in the development of a reaction model from experimental data.

An analysis of the vapour and liquid phases after reaction is essential for the development of the reaction model. The actual amounts are not important, rather the molar ratios of the chemical species in the vapour and liquid products should identified and applied as an added constraint to the model.

The pressure and adiabatic temperature rise in the experiment must be matched to that predicted via the model.

The ratios between the Arrhenius kinetic parameters for different parameters could be useful in numerical modelling where an adjustment for a particular parameter is required in the simulation.

Multi step reaction models would probably better model the reaction, although the trade-off would be the computing power available. In order to get a rough idea of what the intermediate steps involve, it would require samples being taken from the calorimeter at different reaction times so as to identify the intermediates and products formed. In conjunction with the ARC studies, other kinetic methods need to be used with analysis of the reacting components in order to have a full reaction model.

For heavy oils, the kinetic model is widely accepted to be one where cracking occurs, producing lighter oil components and coke. The processes occurring under air injection into light oil reservoirs are somewhat different from those that take place with heavy oils.

CHAPTER 3:

Experimental Techniques and Equipment

EXPERIMENTAL TECHNIQUES AND EQUIPMENT

3.1 Adiabatic Calorimeter

The process of choosing the right piece of equipment for the objectives in mind was a careful and selective one. The first action was a listing of the exact requirements from the experimental system.

3.1.1 *Calorimeter Requirements*

In order to accurately simulate a deep light oil reservoir, the experimental equipment had to meet a number of criteria. These requirements included:

1. Pressure range of 0 to ~ 40 MPa: The calorimeter had to be able to attain high pressures, and an upper pressure limit of 400 bar was chosen. The majority of the calorimeters available as well as and most of the other thermal analysis techniques available at present are incapable of operating at these high pressures.
2. Adiabatic Conditions: Whereas most reactors are isothermal in nature, due to its large size, a reservoir is considered an adiabatic reactor. An adiabatic environment is one in which enthalpy is neither lost from or given to a sample. In reactions which cause an enthalpy rise in the sample; i.e. an exothermic one; this heat will be contained within the material and it's temperature will rise. In an oil reservoir, due to the large volumes involved, adiabatic or close to adiabatic conditions will be obtained. The potential heat loss to the environment is also quite low, ensuring adiabatic conditions. The importance of these conditions being maintained in the experimental apparatus can not be

understated. The surrounding theories governing the calculation of the oxidation kinetics of the oil are only valid if the sample or sample-container system is held in a strictly adiabatic environment. The majority of the investigations into oxidation kinetics of crude oil have been performed under non-adiabatic conditions.

3. Investigation of a Consolidated Medium: Another requirement from the equipment was the possibility of using a consolidated medium in which the reservoir porosity, permeability and other rock properties are correctly represented. This was with the intention of eventually carrying out experiments using consolidated reservoir core. This required a sufficiently large sample holder large enough to hold the reservoir core.

3.1.2 *Equipment Selection*

The calorimeter selected, termed the PHI-TEC II, is an adiabatic calorimeter supplied by Hazard Evaluation Laboratories (HEL). A number of other calorimetry options existed including established accelerating rate calorimeters from other manufacturers. The PHI-TEC II meets the criteria detailed above with certain modifications to handle high pressures and was therefore chosen as the instrument due to the pressure flexibility. The PHI-TEC has the added advantage over established accelerating calorimeters of being able to track much faster exotherm rates, enabling more accurate reaction kinetic parameters being obtained.

3.1.3 *Features of PHI-TEC II High Pressure (HP)*

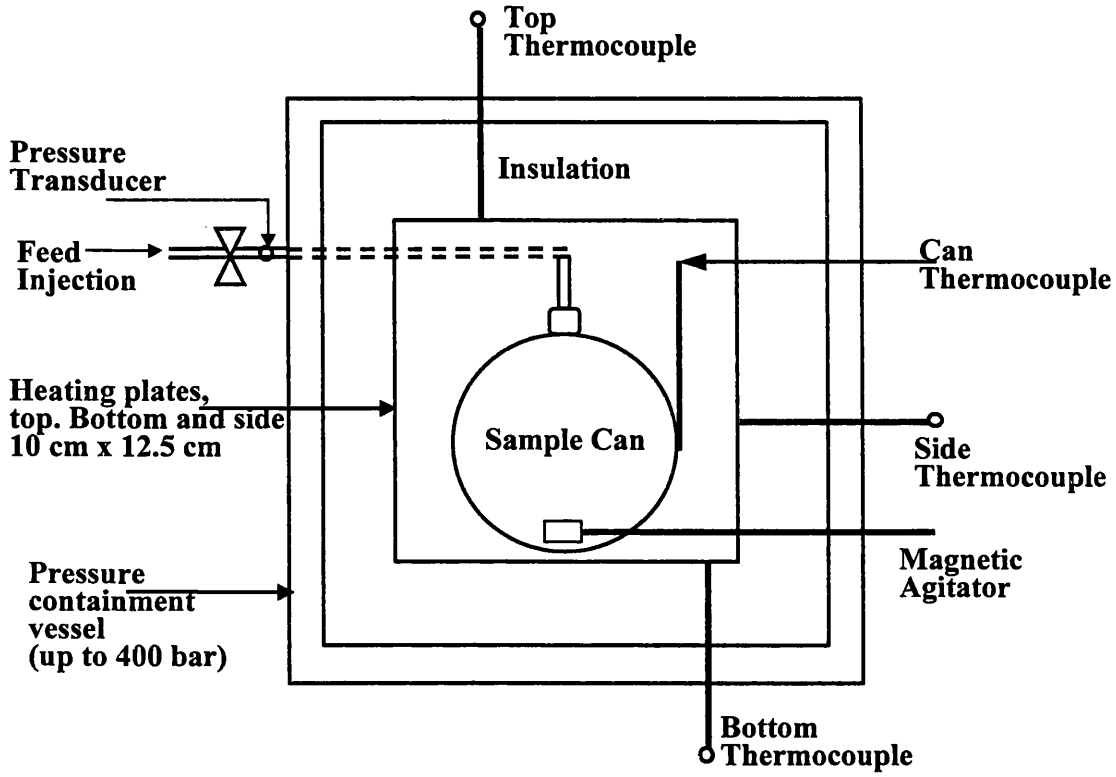

Figure 3.1: Diagrammatic Representation of the PHI-TEC II

Three zone heaters at the top, bottom and side of the bomb track the sample to ensure adiabatic conditions. These heaters are independently monitored and powered. The heater control uses proportional, integral and differential modes. The test cell used for the experiments is a 6ml bomb. A magnetic agitator is present at the bottom of the PHI-TEC to ensure adequate stirring of the contents when required.

3.1.4 *Operating Procedure of the PHI-TEC II*

An experimental plan is used to control the operation of the experiment, and requires a set-up as follows (HEL, 1997):

1. Specifying an initial temperature for the test. The guard heaters will reach this initial temperature and remain there.

2. Setting a temperature increment with which to heat the sample if an exotherm is not detected.
3. A settle period in which the sample is allowed to reach steady state.
4. The maximum temperature to search and to track any exotherm is specified.
5. The minimum rate of change of temperature (i.e. self-heat rate) below which reaction is determined to have stopped.

Running the plan after inputting the above details will result in a heat-wait search experiment. The sample and guard heaters will heat the bomb to the specified start temperature, wait for the contents to settle and then search for an exotherm. In the event that an exotherm is detected, it will be tracked up to its termination point or to the maximum track temperature specified. If an exotherm is not detected, the bomb is heated again by the increment specified and the heat-wait search procedure is repeated. This process continues until the maximum search temperature specified is reached.

A typical heat-wait search procedure is shown in Figure 3.2.

A software program termed PHI is used to control the hardware and access the experimental data. This software is used for setting up and running experiments, with the above operating procedures recorded using the PHI software.

This software is also used to calibrate sensors using additional temperature and pressure calibration instruments. It is used to set the safety limits on all the hardware and also to tune the PID control loops. The safety limits used in the experiments were specified based on the hardware limits, i.e. 350 bar and 480 ^{0}C for pressure and temperature respectively.

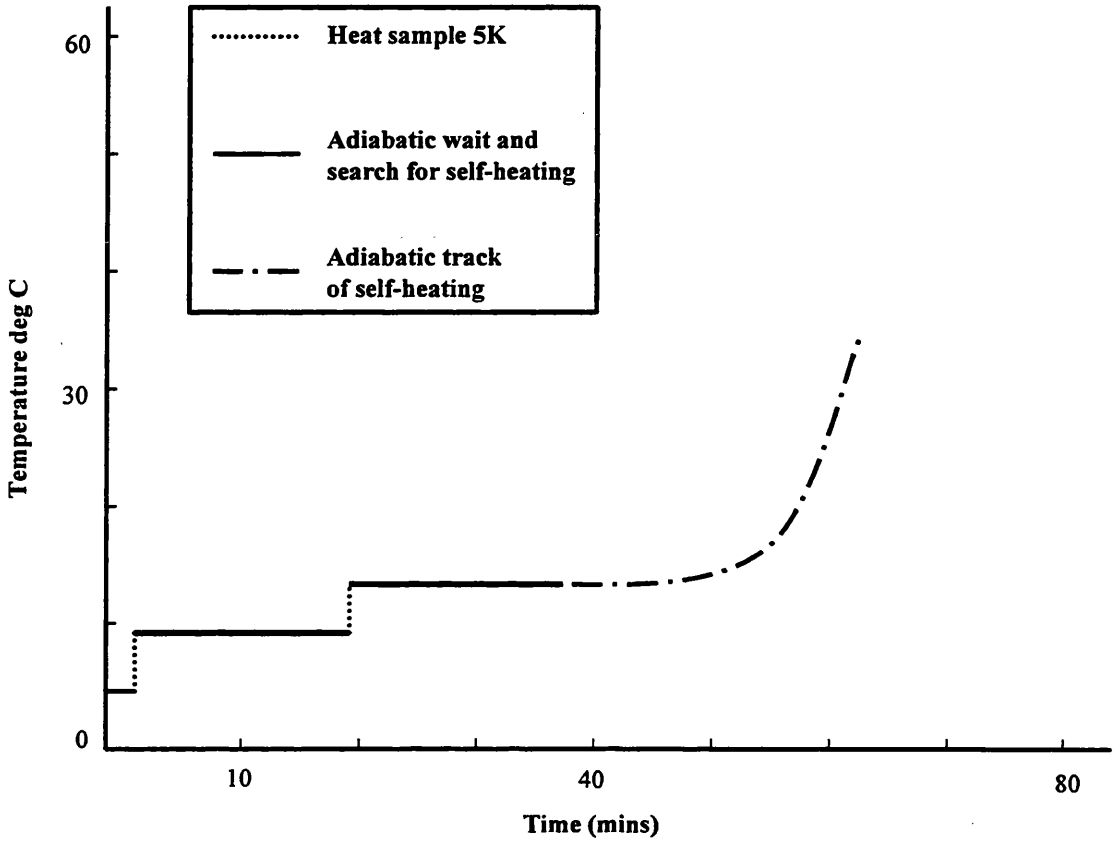

Figure 3.2: Typical PHI-TEC II Heat-Wait-Search

3.1.5 *Experimental Procedure*

After the experimental plan is set up, samples are prepared for the experiments. The bomb preparation involves injection of crude oil or the oil fraction into the bomb together with any other rock material if appropriate. The following experimental procedure is then used:

1. Wrap the sample thermocouple around the bomb. The thermocouple wire is taped to the bomb with aluminium foil. This improves the sensitivity of the thermocouple to the changes in the sample temperature and ensures the bomb and not the immediate surrounding air temperature is measured.
2. Wrap the sample heater around the around the bomb.

3. Place the bomb in the guard heater assembly and connect the feed line to the inside of the pressure vessel wall. When connecting the feed line, one must ensure that the connection inside the vessel wall does not move. This is to prevent gas leaks due to stress in the pipe when the air is injected.
4. Connect the sample thermocouple and sample heater leads and then push these back into the recess to protect them from the high temperatures during the experiment.
5. Place a disk of kaowool over the guard heater assembly to provide good insulation.
6. Replace the lid of the pressure vessel and bolt in place.
7. Connect the top heater thermocouple and heater cables.
8. Open the air supply line valve and allow the air to be injected until the required pressure reading is reached.
9. Shut off the air supply when this reading is reached. Allow the pressure to reach steady state before turning on the experiment. If the vessel pressure reading is fluctuating while waiting for steady state, it implies there is a gas leak in one of the lines, and leak testing is done. This could require having to start the set up over again.

The experiments normally operate for a period of 24 hours, however some experiments continued for up to 72 hours.

3.1.6 *Calibration of the PHI-TEC II*

While the PHI-TEC II approaches closely adiabatic conditions, deviation from a fully adiabatic state arises from two sources:

1. The thermal inertia of the system or heat lost into the sample test cell or "bomb", which leads to thermal dilution. This is because the sample and the bomb are

held together in an adiabatic environment. The thermal dilution of the system can be compensated for using a thermal dilution or phi (ϕ) factor.

2. The heat losses from the container itself to the environment. This is a measure of the operational adiabatic accuracy of the equipment itself and can lead to substantial errors.

In order to improve the operational adiabatic accuracy of the PHI-TEC II, a heat loss compensation is added to the experiments. This compensates for the heat loss to the environment and minimises the errors due to this. This is another feature of the PHI-TEC II which is absent in several other commercially available calorimeters.

The calculation of the heat loss compensation is by calibration of the PHI-TEC II under the proposed experimental conditions (0-500° C and 0-400 bar). This involves a set up of the apparatus as is described earlier:

1. Wrap the sample thermocouple around the "bomb" test cell.
2. Wrap the sample heater around the bomb.
3. Place the bomb in the guard heater assembly and connect the feed line to the inside of the pressure vessel wall.
4. Connect the sample thermocouple and sample heater leads and then push these back into the recess to protect them from the high temperatures during the experiment.
5. Place a disk of kaowool over the guard heater assembly to provide good insulation.
6. The experimental calibration is then run.

The calibration test uses a similar procedure to the 'heat-wait-search' test, only the search period on this occasion searches for the stability of the sample temperature rather than for exothermicity.

Different shaped and sized test cells have different heat losses and experiments with rock or other materials require another heat loss compensation.

The temperature and pressure instruments were periodically re-calibrated to limit the error arising from instrument drift over time, although some electronic drifting was unavoidable.

The performance of the PHI-TEC II heaters and can temperature thermocouple is periodically sanity checked to ensure it follows the set point it should. An enlarged sample of this over the highest temperature change period is shown below in Figure 3.3. It can be seen that the heaters closely follow the set-point temperature (upper lines).

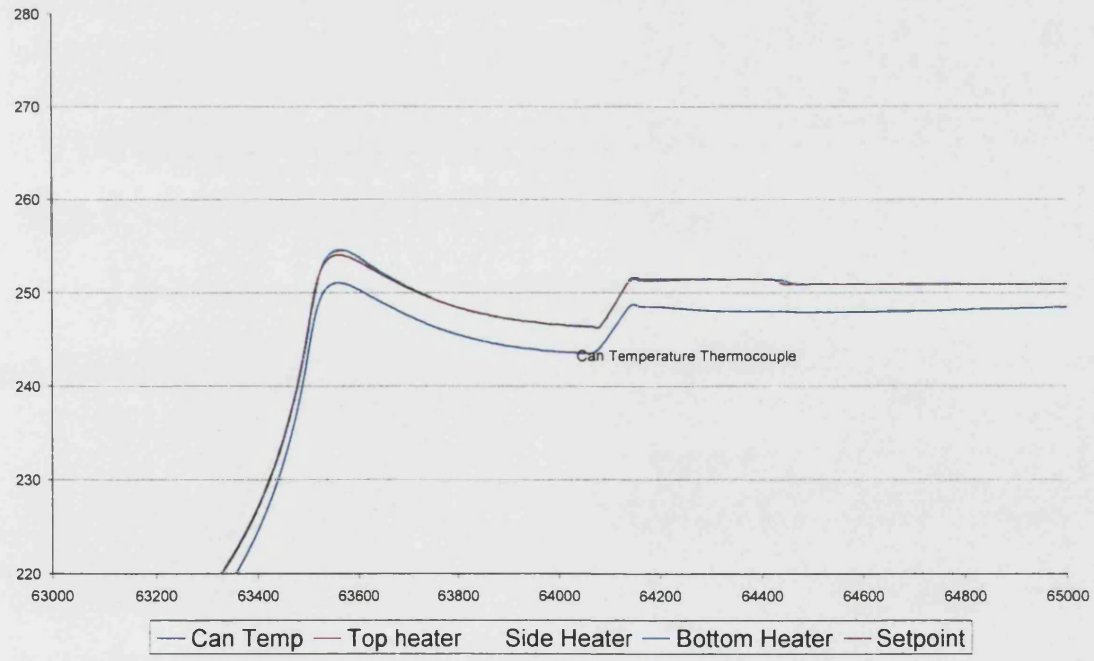

Figure 3.3 Differential between the PHI-TEC heater and thermocouple

3.2 Research Experimental Methodology

Experiments were performed in different stages and designed in such a way as to be able to study the effects of various parameters on the oxidation kinetics and exothermicity. The range of experimental stages is described in this section.

Four North Sea Oils were used for the majority of the experiments and the properties of these are given in Table 3.1.

Table 3.1: Crude Oil and Reservoir Properties

	Oil A	Oil B	Oil C	Oil D
API gravity	36	37	37	39
Viscosity (cp, at reservoir cond.)	0.71	0.27	0.27	0.40
Reservoir Temperature (°C)	118	111	116	121
Reservoir pressure (bar)	218	446	442	172
Permeability (Ave) (md)	150	50-150	250	50
Porosity	0.22	0.23	0.24	0.22

Certain experiments were carried out with some other oils and these crude oils are listed below:

1. Oil Au; Australian Oil of 41 API
2. Oil M; Medium Heavy Maya Oil of South American origin and 20.8 API
3. Oil W; Heavy Wolf Lake Oil of Canadian origin and 10.8 API.

To ensure familiarisation with the equipment, a number of experimental runs are made, after which an experimental standard was designed. This standard was designed with oxygen in excess overall, implying low initial amounts of oil in the bomb. As the volume of the bomb is 6 ml, 0.25 ml was chosen to give a volumetric ratio of 4% oil at

atmospheric pressure. The amount of air in the bomb would increase accordingly with an increase in the pressure.

As the pressure increases over the course of the experiment, the final pressure had to be taken into account as well so as not to exceed the pressure limit of the equipment. 50 bar was chosen as a safe standard starting pressure, as it still allowed investigations at higher pressures when required.

For experiments with rock and water, the amount of rock for the standard experiment is chosen based on the amount of oil used in experiments, and 0.5g of rock was used. As the density of the standard rock used (rock D) is very close to 1, this gave a value of 0.5 ml volume and about 50 % saturation.

Reproducibility of the experiments was considered to be one of the major concerns and a number of experiments were repeated to investigate this, specifically experiment B5, B3 and B4 have the same experimental conditions. The self-heat rate results for experiment B3 and B5, which are shown below in Figure 3.3 show the reproducibility of the PHI-TEC results.

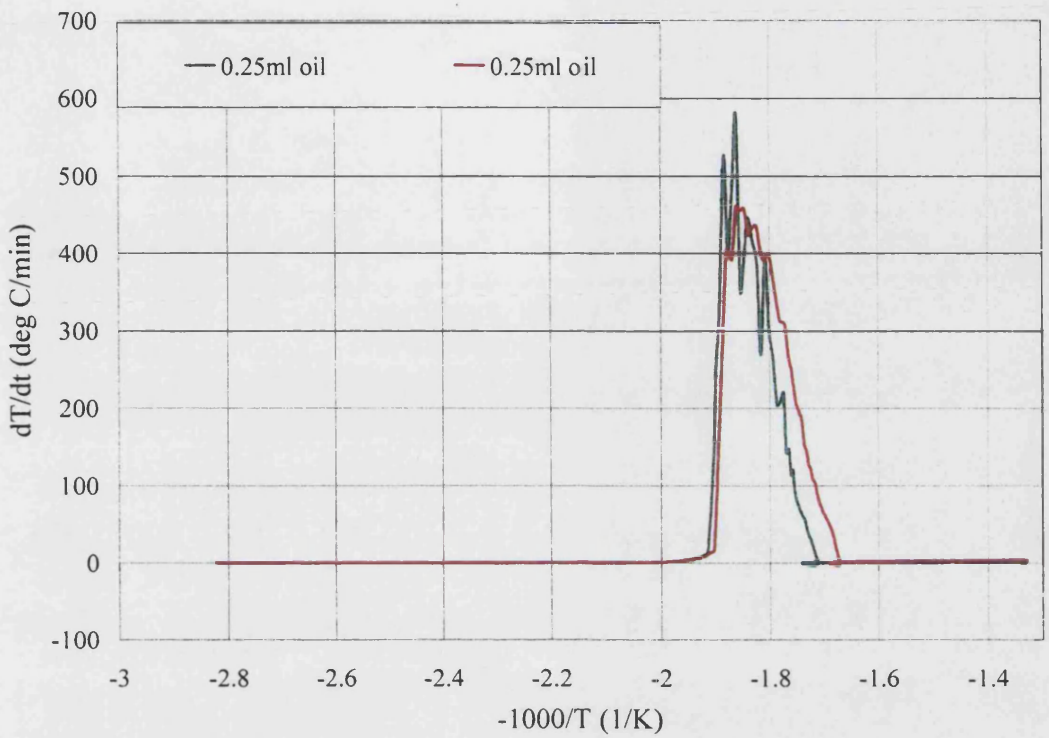

Figure 3.4 Reproducibility of PHI-TEC II Data

As has been discussed earlier in this chapter, the amount of heat lost to the environment by the equipment is accounted for by adding a heat compensation to each of the experiments. This heat compensation was measured and changed at periodic intervals to take into account of instrument drift, changes to the apparatus itself and other sources of error. However, this lead to some reproducibility errors and it was found that experiments carried out with different heat compensation values could lead to slightly different results, as was witnessed by experiments B5 and B0. B0 had the same experimental conditions as B5 but does not show exactly the same reproducibility as experiments B3 and B4, having a lower initiation temperature. This could be due to different heat loss compensation values being used or instrument drift.

3.2.1 *Whole crude oil alone, different reaction conditions*

Table 3.2: Experiments with Oil at Different Reaction Conditions

Experiment	Oil	Pressure (bar)	Amt. of oil (ml)	Experiment	Oil	Pressure (bar)	Amt. of oil (ml)
A0	A	50	0.25	Au1	Au	50	0.25
A1	A	100	0.25	B0	B	50	0.25
A2	A	50	1	B1	B	100	0.25
A5	A	50	0.25	B2	B	50	0.5
C0	C	50	0.25	B3	B	50	0.25
D1	D	30	0.25	B4	B	50	0.25
D3	D	50	0.25	B5	B	50	0.25
D2	D	100	0.25	B7	B	50	1

3.2.2 *Addition of Rock and Water at different reaction conditions*

The effect of different reservoir rocks and water on the oil oxidation was measured by adding reservoir rock from two North Sea reservoir, termed rock D and A, industrial grade sand (silica), clay, chalk and varying amounts of water. The industrial grade sand (Buckland sand) consisted of 97-99% silica, and traces of Iron, titanium, chromium, and other metals with a very fine particle size of W150, and a clay content of 0%. These different experimental configurations are presented in Table 3.3.

Parameters that have been varied include the amount of rock (0.5g-2.0g) and water (0.1 ml-0.5 ml) varied in a 6 ml test cell so as to map the effects of having various oil and water saturation's in the rock. The effect of reservoir rock and water on these oxidation reaction parameters is outlined via this process. The parameters varied

included the amount of oil in the test bomb (0.25 ml –1 ml in a 6 ml test can) and the initial pressure at which the experiments are carried out (30, 50 and 100 bar) using the different oils. The importance of the different types of reservoir rock is reflected in the experimental matrix design and the effect of the reservoir rock on the kinetics is investigated.

Table 3.3: Experiments with Different Types of Rock and Water

Experiment	Oil	Pressure (bar)	Type of rock	Amt. of oil (ml)	Amt. of rock (g)	Amt. of water (ml)
Ar1	A	50	D	0.25	0.5	0.1
Br1	B	50	D	0.25	0.5	0.1
Br2	B	50	D	0.25	2.0	0.1
Br3	B	100	D	0.25	0.5	0.1
Bw	B	50	D	0.25	None	0.1
Bw1	B	50	D	0.25	0.5	0.5
Cr1	C	50	D	0.25	0.5	0.1
Dr1	D	50	D	0.25	0.5	0.1
Dr2	D	50	D	0.25	0.5	None
Dr3	D	50	D	0.25	2.0	0.1
Dr4	D	50	D	1.0	0.5	0.1
Dr5	D	0	D	0.25	0.5	0.1
Dr_c2	D	50	clay	0.25	0.5	0.1
Dr_ch1	D	50	chalk	0.25	0.5	0.1
Dr_p1	D	50	A	0.25	0.5	0.1

Dr_s1	D	50	Buckland sand	0.25	0.5	0.1
Drw	D	50	D	0.25	0.5	1
Mr1	M	50	D	0.25	0.5	0.1

3.2.3 *Pure Component experiments*

Certain single oil components were run in the bomb also using 0.5g rock D, 0.1ml water and 0.25ml of the component at 50 bar.

Table 3.4: Experiments with Pure Components

Experiment	Oil
C10	n-Decane
C16	n-Hexadecane

3.2.4 *Pyrolysis experiments*

Two experiments were run using nitrogen instead of air to investigate and quantify the pyrolytic effect.

Table 3.5: Experiments with Nitrogen

Experiment	Oil	Pressure (bar)	Type of rock	Amt. of oil (ml)	Amt. of rock (g)	Amt. of water (ml)
Dn0	D	50	D	0.25	None	None
Drn1	D	50	D	0.25	0.5	0.1

3.2.5 *SARA Fraction experiments*

Separation of crude oil into its SARA Fractions

As has been stated earlier in this report, crude oil possesses a huge number of individual components and it is near impossible to investigate the oxidative properties of each component. Separation of the whole crude oil into fractions which react in a more similar fashion are therefore very useful in defining the behaviour of the crude oil.

SARA fractions are defined as saturates, aromatics, resins and asphaltenes. These fractions of crude oil exhibit the same sort of behaviour as they possess similar polar compounds. They are obtained by separating crude oil into fractions according to their solubility in solvents of different polarity and their affinity for absorption on a solid granular packing (natural clays, silica gel and alumina have all been used). Standard ASTM procedures are used.

Asphaltenes are separated first by collecting the precipitate formed by adding a specified quantity of a paraffinic solvent, usually either n-pentane or n-heptane (Hutchence and Freitag, 1991). The portion that remains dissolved, the maltenes, is then separated by elution through the solid packing by solvents with increasing polarity. The saturates can be eluted with hexane, the aromatics with 1% diethylether in hexane, and the resins or polars can be eluted with acetone and methanol in equal volumes. This part of the experimental work was done by Salford University and the SARAs supplied in glass vials.

Saturates are the fraction of the crude oil which is not adsorbed on calcined F-20 alumina adsorbent after the n-hexane effluent is passed through the column and collected.

Aromatics are the fraction of the crude oil that is adsorbed on the calcined F-20 alumina in the presence of n-hexane, and desorbed by toluene, after removal of the saturates. This fraction is distinguished by the presence of one or several benzene rings.

Resins are the fraction of the crude desorbed from F-20 alumina adsorbent after removal of saturates and aromatics, using dichloromethane and methanol. They are less aromatic than asphaltenes but could contain heteroatoms such as S, N, O and metals.

Asphaltenes are the colloid disperse components of coal and oil which are soluble in aromatic hydrocarbons and carbon disulphide but insoluble in n-pentane and n-heptane. Asphaltenes are the fraction of the crude oil which is insoluble in C_5-C_7 paraffins. They consist essentially of polycyclic aromatic, aliphatic chains and napthenic rings. They could also contain heteroatoms as described for the resins. Asphaltene fractions are among the heaviest fractions of crude oil, and are also designated crude oil residues.

The saturate fractions are obtained in a solvent form and therefore can be easily injected into the bomb for the experiments. However, the aromatic and resin fractions are in a gel-like state and require dissolution in order to get them into the bomb. The solvent used to dissolve the fractions was dichloromethane. The weights and volumes of the SARA fractions are not known, therefore the weights are calculated by subtracting the weight of an empty cell from the weight of the cells with the SARA fractions. The procedure for preparing the aromatic and resin fraction samples is more complex and is shown as follows:

1. Fill all cells to the 8ml mark (volume of individual cells) with dichloromethane to dissolve the gel-like samples. One can determine the volume of the specific SARA fraction as the amount of dichloromethane added is known.
2. Leave the samples for 24 hours to ensure that the gel-like SARA fractions fully dissolve in the dichloromethane solvent.
3. Insert 0.5g of reservoir rock into the bomb.

4. Inject the calculated volume of the desired SARA fraction into the bomb using a fine syringe.

5. Place the bomb containing the sample into an oven at a temperature of 50°C for a 24-hour period. A temperature of 50°C is well below the boiling points of the hydrocarbons in the sample and greater than that of dichloromethane, which is 39°C. This ensures that the dichloromethane will evaporate off leaving the original SARA fraction.

6. After 24 hours remove the bomb from the oven and inject 0.1ml of water into the bomb.

The saturate fractions are taken directly from the glass cell and injected into the bomb either alone or with 0.5g of rock and 0.1ml of water, as required.

The amount of samples used for the experiments with the whole oils was 0.3g. Therefore as the experimental results for the SARA fractions are to be compared with those of the original oils, 0.25ml of saturates was injected into the bomb for the experiment. The values obtained for the densities of the aromatic and resin fractions were 0.933 and 1.0 respectively. As the density of the saturate fractions is less than that of aromatic fractions, 0.25ml is a good approximation. The calculation for the amount of aromatics and resins added was not so simple as dichloromethane had been added to the samples. A typical calculation procedure is shown below.

The initial step was to calculate the density of each SARA fraction. Therefore, the weight and volume of aromatics and resins was required.

Weight of glass cell containing SARA fraction – Weight of glass cell = Weight of SARA fraction

Aromatic weight: 11.0g – 9.6g = 1.4g Resin weight: 9.9g – 9.6g = 0.3g

Total volume of glass cell – Volume of solvent added = Volume of SARA fraction

Aromatic volume: 8ml – 6.5ml = 1.5ml Resin weight: 8ml – 7.7ml = 0.3ml

density = Mass/Volume,

Density of aromatic fractions = 0.9333 Density of resin fractions = 1.0

The amount of the aromatic and resin samples to be added to the bomb could now be calculated

$$Volume = \frac{Mass}{Density} \times \frac{Total\ volume\ of\ cell}{Volume\ of\ SARA\ fraction} \qquad \text{Equation 3.1}$$

i.e. For Aromatics $V = \frac{0.3}{0.933} \times \frac{8}{1.5} = 1.71ml$

For Resins $V = \frac{0.3}{1} \times \frac{8}{0.3} = 8ml$

The percentages of each SARA fraction present in each of the whole oils is shown below in Table 3.6.

Table 3.6: Oil SARA Fraction Analysis (Analysis performed by H. Al-Saffar, Salford University)

Oil	Saturates, %	Aromatics, %	Resins, %	Asphaltenes, %
A	69.18	18.26	12.56	0.0
B	61.13	23.76	15.11	0.0
C	76.58	12.56	10.86	0.0
D	71.31	12.70	15.99	0.0
Australian	64.94	18.01	17.05	0.0
Maya	33.88	31.51	26.39	8.22

Wolf Lake	25.18	37.40	27.33	10.09

The behaviour of the different SARA fractions of the oils was studied by carrying out a range of experiments, as shown in Table 3.7. This involved experiments at 50 bar using 0.3 g of the SARA component. Table 3.6 shows that the most significant constituent of the light oils is the saturate fraction. There is a concentration on saturate experiments to reflect this importance.

3.2.6 *Effect of different Parameters*

The research methodology was to investigate the effect of different parameters on the exothermicity. A comparative basis is used to study these effects, i.e. two experiments are run with one factor varying between them. Experiments with highly divergent values of the parameter being studied are compared to observe the effect of the differing factor on the resultant exothermicities.

One caveat to be kept in mind is that some of the experiments did not undergo reaction exotherms at certain temperatures, indicative of reduced reactivity at that temperature. To ensure consistency in the results the exothermicity ratios of these experiments are compared over similar temperature intervals, as the self-heat rate is a function of the temperature. This difference would arise mainly in the induction regions as the experiments could initiate reaction at different temperatures. Small temperature differences can be ignored but care must be taken where wide variations arise. This could be indicative of a reduction in reactivity due to the added parameter. Due to reproducibility errors arising due to instrument drift and other sources of error the comparison of experiments was limited as much as possible to experiments carried out with the same heat compensation values.

The different parameters studied and the experiments compared are shown in Table 3.1 and also discussed in subsequent chapters.

Table 3.7: Experiments with SARA fractions

Experiment	SARA Fraction	Type of Oil	Type of rock	Amt. of rock (g)	Amt. of water (ml)
As1	Saturates	A	None	None	None
Bs3	Saturates	B	None	None	None
Cs0a	Saturates	C	None	None	None
Ds0	Saturates	D	None	None	None
Wls0	Saturates	W	None	None	None
Asr1	Saturates	A	D	0.5	0.1
Bsr1	Saturates	B	D	0.5	0.1
Dsr1	Saturates	D	D	0.5	0.1
Aar1	Aromatics	A	D	0.5	0.1
Bar2	Aromatics	B	D	0.5	0.1
Wlar1	Aromatics	W	D	0.5	0.1
Brr1	Resins	B	D	0.5	0.1
Wlrr1	Resins	W	D	0.5	0.1
Aasr1	Asphaltenes	A	D	0.5	0.1
Masr1	Asphaltenes	M	D	0.5	0.1
Wlasr1	Asphaltenes	W	D	0.5	0.1

3.3 Oil Analysis

At the end of the experiments, the residual material in the bomb is evacuated by solution in solvents and kept for analysis. Toluene, which is a commonly used solvent for all types of crude oils, was used to dissolve the crude oil.

The original intention was to carry out analysis of this residual oil as well as the produced gas in the bomb after experiments. However due to difficulties in optimising the analytical technique using gas chromatography, this was not done. Samples of the residual oil have been kept in storage and would be available for further analysis if required.

3.4 Reservoir Rock Analysis

In the experiments carried out with different reservoir rocks, the residual solid material was evacuated from the bomb and a post-mortem was carried out on it. The liquid crude oil is dissolved and removed from the bomb using toluene as described above. The removal is done using a thin syringe needle, which stops the rock from passing through, and several flushes are carried out to make sure no crude oil remains.

Toluene dissolves saturates, aromatics, resins and asphaltenes and any leftover toluene-insoluble hydrocarbon material is likely to be coke formed during the reactions. This therefore gives a reasonably accurate method for determining the coke deposited during the experiments. The left over rock is then removed and left to dry. After drying the rock is weighed in a crucible which is then placed overnight in a furnace at 800 ^{0}C. The remaining rock is then weighed and a difference in the weight gives the amount of solid "coke" deposited, which would presumably be oxidised to carbon oxides and steam at these temperatures.

CHAPTER 4:

Theoretical Development and Data Analysis

THEORETICAL DEVELOPMENT AND DATA ANALYSIS

4.1 Methods of Kinetic Analysis

Kinetic reactions have been studied using a variety of methods. Various thermal analysis methods exist which subject a very small sample of crude oil to variations of temperature with time. These methods have been reviewed by Kok and Pamir, 1995. They generally use instruments which operate by imposing a constant heat flux to a sample and to a reference and collect data on the positive deviation in heat flow from the crude oil sample compared with the reference.

Thermogravimetric (TGA) or differential thermogravimetric (DTG) methods follow the change in weight of the sample as a function of temperature or time. Differential thermal analysis (DTA) analysis similarly measures the temperature difference between a substance and a reference material while the subject is heated at a programmed rate.

Differential Scanning Calorimetry (DSC) follows the evolution of heat in a sample and a reference material as they are heated. The heat value of the crude and activation energies of different reactions are calculated.

In all the above methods continuous analysis of the effluent is made, from which atomic H/C ratios as well as $CO/CO + CO_2$ ratios are obtained. The ratios are analysed to give an idea of the kinetics.

Another method used is effluent or evolved gas analysis (EGA) technique. This method involves heating a mixture of sand, oil and water with the temperature increased at a constant rate. An oxidising gas is constantly passed through the mixture as it is

heated and the effluent gas is analysed continuously for oxygen and carbon oxides content.

Tadema, 1959 and Yoshiki and Phillips, 1985 used differential thermal analysis (DTA) and TGA methods at high temperatures and pressures and it was concluded that LTO and HTO rates increased with pressure as did their exothermicities. The effect of pressure was also studied by Bae 1977 using these techniques on fifteen oils and it was found that the results were oil specific, but in general pressure increase causes the LTO heat generation to increase.

TGA methods have been used on heavy oils and cores by Jha and Verkoczy, 1986, from which they estimated kinetic data for occurring oxidation phenomena. Kinetic and thermochemical data for thermolysis, low-temperature oxidation, cracking, coking, and combustion reaction in cores and oils were obtained. Verkoczy and Freitag, 1997 used TGA as well as reactor autoclaves to study the oxidation behaviour of SARA fractions of crude oil

DSC and TGA were applied to crude oil combustion in the presence and absence of metal oxides by Drici and Vossoughi, 1985. The heating rate used was 10 $Cmin^{-1}$, with air flowrates of 120 cc min^{-1}. It was found that in the presence of a large surface area such as silica, the surface reactions are predominant and unaffected by the small amount of metal oxide present. DSC and TGA techniques were also used to test the feasibility of the in-situ combustion process by Kharrat and Vossoughi, 1985 who calculated the minimum amount of oil necessary to sustain combustion.

High pressure DSC was applied by Racz et al in studies of crude oil oxidation and the effect of sand particle size, pressure, oxygen partial pressure, carbon dioxide addition and different metal oxides on LTO. This method using a high pressure DISC

technique capable of attaining pressures of 400 bar was also applied by Hughes et al 1998. The effect of oxygen partial pressure was also investigated using DSC by Nickle et al 1987 and it was detected that increasing the partial pressure sharpens the LTO and HTO peaks and shifts them to lower temperatures. The exothermicity of oil and oil core samples was investigated using high-pressure DSC by Belkarchouche et al 1988. They observed that the overall exothermicity of combustion increases with increasing total pressure, and an increase in the matrix surface area causes the LTO region to become predominant. It was also noticed that the addition of clay causes both the LTO and HTO peaks to coalesce with a large increase in the exothermicity.

Kok and Karacan, 1997 used TG/DTG and DSC methods to study oxidation behaviour of two crude oils and their SARA fractions. The heating rate used was 10 °C/min with a constant air flow rate of 50 ml/min.

Kisler and Shallcross, 1997 used an Effluent gas analysis (EGA) method to study the oxidation behaviour of a light and heavy oil at relatively low pressures. This technique was also used by Al-Saffar, 1999 to study the reaction kinetics of light crude oils. The oxygen flux was 11 ml/min (0.95 m^3/m^2.hr) and consolidated reservoir core was used, heating the sample up to 480 ^{0}C @ 3 ^{0}C /min.

Ranjbar and Pusch, 1991 performed pyrolysis experiments on crude oils using DTA. The phenomena of pyrolysis is integral and complementary to oxidation and must also be understood for a particular crude.

The most widely used tool for studying the in-situ combustion process has been the combustion tube. This set up closely represents processes occurring in a reservoir. Its main disadvantage for kinetic measurements is that the reactor is integral (Greaves and Dudley, 1990), therefore measurements made over the whole tube can not give

individual reaction rates. Another drawback is the high fluxes used are not representative of points in the reservoir, being much higher than would be obtained except next to the air injector. It is a useful tool for evaluating fuel content and air requirements as long as the porous medium and crude are representative of the reservoir but does not give adequate kinetic parameters.

Various forms of other reactors have been adapted to study the crude oil oxidation process. In the study of organic fuels including aviation fuels, the liquid phase oxidation of paraffins and other organics have been studied with isothermal flowing test rigs using passivated heat-exchanger tubing over the temperature ranges required. Mamora and Brigham, 1995 reported the use of a kinetic tube reactor to obtain data. Fassihi et al, 1990 studied LTO of viscous crude oils using a small packed bed reactor where the produced gases where continuously analysed to distinguish the reactions taking place. Ren et al 1999 investigated the kinetics of light oil oxidation using a small batch reactor (100 ml capacity), at higher pressures which was also reported by Greaves et al 1999. This reactor measured the pressure drop in the reaction as a function of time. Clara et al 1999 reported the use of an adiabatic disk reactor which was capable of utilising consolidated rock in oxidation experiments.

Limitations of TGA/DTA and DSC tools

Nickle et al 1987 performed a detailed study into the shortcomings in the use of TGA/DSC techniques in the evaluation of crude oil combustion. This included a review of the applications of these techniques for studying crude oil oxidation in the literature.

One of their major findings was that the results obtained using these techniques were a function of the heating rate selected. They selected a heating rate of 0.2 to 20 ^{0}C

/min and found different fuel lay down, heat evolution and peak temperatures from the combustion.

A number of the experiments carried out in the literature have used different rates. Verkoczy and Freitag, 1997 and others used a heating rate of 10 ^{0}C /min, while Al-Saffar et al 1999 and used 3 ^{0}C /min. In the event that the reaction mechanism is dependent on the heating rate, the reaction data obtained would vary for each case. Fassihi and Brigham, 1980 found that the rate of heat rise in a combustion tube affected the fuel deposition. Yoshiki and Phillips, 1985 also found in their DTA experiments that the heating rate used had a major impact on the type and extent of oxidation taking place, with the disappearance of LTO at higher heating rates. As the heating rate used in experiments is totally subjective and chosen at the researchers discretion, it could create problems in comparing results across different experiments.

Majority of the investigations carried out using TGA, DTA and DSC techniques have been done at lower pressures. Lukyaa et al 1994 report the development of a high pressure differential scanning calorimeter capable of operation up to 7 MPa (1000 psi) to overcome this drawback and to study the oxidation at higher pressures.

It was noted by Moore et al 1998 that ramped temperature oxidation tests such as TGA, DTA and DSC do not reflect the quantitative behaviour observed during one-dimensional in situ combustion tube tests. This is because of the high degree of pre-oxidation experienced by the oil during the portion of the ramped temperature oxidation test when the core temperature is increased due to the external application of the heater. This is not a significant problem with calorimetric instruments as the crude oil is brought to the reservoir temperature very rapidly before oxidation can start. Greaves

and Dudley, 1990 pointed out that TGA methods fail to adequately model the residence-time distribution of a packed bed as is seen in a reservoir.

As any experimental data is obtained with a view to using in field air injection projects, it is important to carry out the experiments in situations which simulate the conditions of the reservoir, especially in terms of the air flux. Certain crucial points should however be borne in mind which affect this decision.

1. As has been pointed out by past investigators (Zelenko 1999) apart from the region immediately downstream of the injection wellbore, most points in the reservoir will not see high flowrates of air and it is important to understand the oxidation behaviour under these conditions.
2. In order to study the kinetics of an oxidation process, it is essential that the reaction should be studied in the kinetic region, where the reaction is not being controlled by the rate of diffusion of oxygen into the liquid. In the case of many of the experimental setups used to study the oxidation, it is very probable that the reaction is being diffusion controlled rather than kinetically controlled. It is more accurate to compare the effect of different factors and parameters on the oxidation behaviour with the true kinetics.

4.1.1 *Calorimetry Studies of Reaction Kinetics*

As has been shown earlier, a large amount of research has been carried out on the oxidation kinetics of crude oil. From basic chemistry, it is known that chemical reactions are accompanied by a change in the reacting system enthalpy. This has lead to the rise of the calorimeter as a useful technique for studying chemical reaction kinetics, as this is a premier tool for the measurement of heat changes.

Crude oil is a multi-component system with hundreds of different constituents and it is difficult to study the overall reaction. The calorimeter is suited to handling this overall reaction without having to break the oil down into its individual components.

Adiabatic techniques such as accelerating rate calorimetry, adiabatic dewar calorimetry and adiabatic calorimetry are used extensively to determine the thermokinetic properties of an exothermic reaction. The broad objective of adiabatic techniques is to determine the rate of temperature and pressure rise as a function of temperature for an exothermic reaction under conditions where heat losses to the surroundings are eliminated. A number of important assumptions have to be made in order to derive the thermokinetic parameters of an exothermic reaction from experimental data on the rate of self-heating under adiabatic conditions. These assumptions are:

1. The reaction mechanism is assumed to be independent of temperature so that the temperature and concentration dependencies can be treated separately.
2. The total heat generated is evaluated directly from the adiabatic temperature rise assuming constant heat capacity.
3. At any stage in the reaction, the heat generated is assumed to correspond to changes in concentration such that the rate of change of concentration and the rate of heat generation are directly proportional to the rate of temperature rise under adiabatic conditions. In addition the extent of reaction is equal to the temperature increase expressed as a fraction of the total adiabatic temperature rise.
4. The temperature dependence of the reaction rate constant is assumed to follow the Arrhenius equation.

5. The dependence of reaction rate on concentration is represented by a single order of reaction with fractional values used so that complex mechanisms can be represented by simple overall kinetic expressions.

6. These assumptions are necessary particularly in systems where only limited data are available on physical and chemical properties of the reaction system. As long as the experimental data can be fitted to a one reaction model (Columbia Scientific Industries, 1987), an adiabatic calorimeter can be used to determine the Arrhenius kinetic data as well as the starting temperature and exothermicity of the crude oil.

Drawbacks and Advantages of accelerating rate calorimetry

The chief advantage of accelerating rate calorimetry over other forms of thermal analysis equipment is the fact that it allows the reaction to proceed adiabatically. The crude reacts at its own exothermic rate rather than any artificially imposed heating rate which could affect the reaction mechanism or blur the exothermic effects taking place.

It is capable of operation at high pressures, closer to that of a real light oil reservoir than the other thermal analysis methods.

The experimental data obtained from an accelerating rate calorimeter is dominated by the temperature dependency, rather than the concentration dependence of the reaction rate. The parameters obtained are derived under an assumption of a constant heat capacity for the crude oil system as the temperature increases. This is generally not the case and investigations have been performed by Snee et al 1992 into the effect this could have on the accuracy of results obtained. They found that the effect on the accuracy of the thermokinetic results obtained is not significant.

Different calorimeters have been used to obtain kinetic data on crude oil oxidation. Reports have been made (Yannimaras and Tiffin1995) of the use of an accelerating rate calorimeter to screen crude oils for their In situ combustion potential. Germain and Geyelin used an ARC to test the suitability of Horse Creek crude oil to air injection, but did not detail their findings.

Kumar et al 1995 used an ARC to study 39 ^{0}API oil from the Medicine Pole Hills project. Adiabatic testing was carried out from reservoir temperature (111 ^{0}C) to 500 ^{0}C. The major exotherm was seen from 150 ^{0}C to 368 ^{0}C. The exotherm then continued at lower levels to 425 ^{0}C, where no further exothermic activity was detected. Kinetic parameters were obtained, with the first reaction having an Arrhenius activation energy of 30 kcal/gmol and the second having an activation energy of 70 kcal/gmol. The oil also showed good continuity from the LTO to HTO zones.

Watts et al 1997 reported results from and ARC study on Horse Creek oil. They found an LTO reaction initiating at 137 ^{0}C and continuing until 157 ^{0}C. A second reaction started again at 207 ^{0}C and continuing until 227 ^{0}C. This was described as the reaction which would produce significant quantities of carbon oxides.

Zelenko and Solignac, 1997 used an ARC test on 28 and 21 ^{0}API oil. They used a temperature interval of 5K and a search time of fifteen minutes, searching up to a temperature of 377 ^{0}C. It was noticed that oxidation reactions were stopped around 197 and 217 ^{0}C respectively. These reactions started again at a temperature of 227 and 247 ^{0}C respectively.

As has been mentioned earlier in this chapter, other kinetic instruments including DTA, DSC and TGA are limited to low and medium pressures.

Appropriate experimental modelling of the reservoir in the calorimeter is required to obtain accurate results.

One of the limitations of ARC for reaction kinetic studies arises from the assumptions made. A reaction model should include one of 2 parameters, rate of oxygen consumption or rate of formation of gaseous oxygenated products. Either of these are measured by proxy via heat release but neglects the intermediates formed in the reaction.

4.2 Analysis of PHI-TEC II Data

Equation 2.8 from Chapter 2 is frequently used to describe the combustion of crude oil.

$$R_c = -\frac{dC_m}{dt} = k{p_{o_2}}^m C_m^n \qquad \text{Equation 2.8}$$

A simplified representation of the temperature and concentration dependencies is adopted in order to determine the thermokinetic parameters of an exothermic reaction from calorimetric data. Assuming a simple nth order reaction for the fuel and a zero order dependency on oxygen (i.e. oxygen in excess):

$$R_c = -\frac{dC_m}{dt} = k_T C_m^n \qquad \text{Equation 4.1}$$

The rate constant, k_T, can follow one of various temperature dependency theories. The general model for the rate constant is shown below:

$$k_T = \alpha T^{\beta}.\exp(-E/RT) \qquad \text{Equation 4.2}$$

where in the Arrhenius theory $\beta = 0$

in the collision theory $\beta = 0.5$

in the Absolute Rate theory $\beta = 1$

4.2.1 *Arrhenius Kinetic Theory*

At the very foundation of this analysis is the Arrhenius theory of kinetics and fundamental thermodynamic laws.

Although Bae, 1977 questioned the use of an Arrhenius-type kinetic equation for the oxidation of crude oil, due to the complexity of the reaction, it has been used by several investigators to model the reaction kinetics of crude oil oxidation. These investigators include Fassihi 1984, Greaves et al 2000.

Arrhenius law is detailed in several classical works (Kuo, 1986) and can be shown as below:

$$k = A\exp\left(-\frac{E_a}{R_u T}\right) \qquad \text{Equation 4.3}$$

where k is the proportionality constant called the specific reaction rate constant. For a given chemical reaction, k is independent of the concentrations and depends only on the temperature.

The factor $\exp^{-Ea/RT}$ (f) is known as the Boltzmann expression for the fraction of systems having energy more than the value E_a. It may be identified as the fraction of the reactant molecules undergoing collision at a given instant that are activated complexes. An activated complex is a transition state of the configuration of the reacting molecules which have more than the activation energy. The activation energy, E_a is the difference in energy between the activated complex and the reactants. Only a small fraction of molecules have enough energy to surmount the energy barrier between reactants and products. The greater the activation energy, the smaller the fraction, f and the slower the

reaction; so reactions with large activation energies are slower at a given temperature than ones with small activation energies and as T increases, the rate of the reaction increases.. The higher the temperature, the larger the fraction and the faster the reaction. As the activation energy increases,

A includes the effect of the collision terms, the steric factor associated with the orientation of the colliding molecules, and the number of collisions per unit time, which has a mild temperature dependence. This equation is applied to reactions of all orders.

For reactions which follow Arrhenius law, the kinetic data plotted on a graph of lnk versus T^{-1} follows a straight line as shown below.

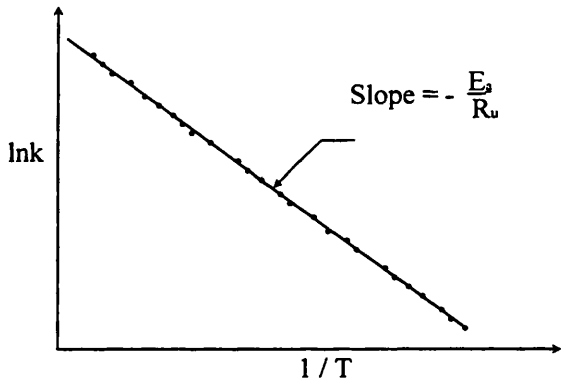

Figure 4.1: Temperature Dependence of the Specific Reaction Rate Constant, k

The equation for lnk, as shown in Fig 4.1 below can be derived from the natural logarithm of the Arrhenius Equation 4.3, which gives

$$\ln k = \ln A - \frac{E_a}{R_u T} \qquad \text{Equation 4.4}$$

A, the pre-exponential factor has the same units as the rate constant, while E_a, the activation energy has the same units as *RT*. Typical values lie in the range of 50-200

$Kjmol^{-1}$. The lower the activation energy the lower the barrier to be overcome, so the reaction proceeds.

It has to be noted that the specific reaction rate constant depends on both temperature and temperature range (Jordan, 1981). The Arrhenius equation cannot describe the combustion process over a wide temperature range. A set of reactions which matches the test data at low temperatures may provide erroneous results at high temperature. However another set of reactions may match the experimental results well. This is illustrated below in Figure 4.2.

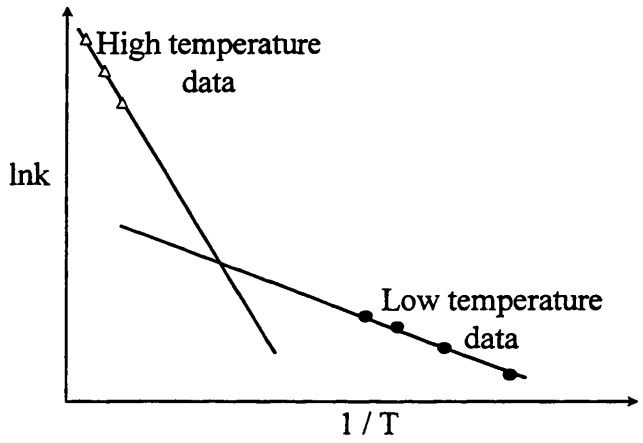

Figure 4.2: Dependence of the Specific Reaction Rate on Temperature Range (Jordan, 1981)

It is therefore important to ensure the kinetic constants obtained are valid for each temperature range under consideration.

Under closely adiabatic conditions the basic kinetic rate equation 4.1 can be re-written as shown below:

$$\frac{dp}{dt} \equiv \frac{dT}{dt} \equiv -\frac{dC}{dt} = A.e^{-E/RT}C^n \qquad \text{Equation 4.5}$$

Therefore, thermodynamically, the relationship between the initial concentration, C_0, and the concentration at any time, C may, in an adiabatic state, be related to temperatures. The assumption here is that the amount of concentration of reactant left is proportional to the amount of heat still to be produced, and temperature changes are directly proportional to changes in concentration and the extent of reaction.

$$C \propto T_f - T \qquad \text{Equation 4.6}$$

Where T_f is the final temperature, and T is the temperature

$$C_0 \propto \Delta T_{ad} \qquad \text{Equation 4.7}$$

where ΔT_{ad} is the instrument temperature rise in a fully adiabatic system, therefore

$$\frac{C}{C_O} = \frac{T_f - T}{\Delta T_{ad}} \qquad \text{Equation 4.8}$$

The temperature rise in a fully adiabatic system relates directly to the heat of reaction.

$$\Delta T_{ad} \propto \Delta H \qquad \text{Equation 4.9}$$

The heat of reaction in a fully adiabatic system assuming constant heat capacity is given below

$$\Delta H = \Delta T_{ad} Cp \qquad \text{Equation 4.10}$$

where Cp is the heat capacity, although in actuality it is the Cv, the average specific heat over the course of reaction at constant volume not constant pressure.

Differentiating the concentration/temperature relationship with respect to temperature

$$\frac{dC}{dt} = \frac{-C_O}{\Delta T_{ad}} \qquad \text{Equation 4.11}$$

From calculus,

$$\frac{dT}{dt} = \frac{dT}{dC}\frac{dC}{dt} \qquad \text{Equation 4.12}$$

and

$$\frac{dT}{dt} = \left(\frac{dC}{dt}\right)^{-1} \qquad \text{Equation 4.13}$$

Therefore

$$\frac{dT}{dt} = \left(\frac{-C_O}{\Delta T_{ad}}\right)^{-1} k_T C^n \qquad \text{Equation 4.14}$$

Rearranging the above;

$$\frac{dT}{dt} = \frac{\Delta T_{ad} k_T C^n}{C_O} \qquad \text{Equation 4.15}$$

Substituting k_T to give the rate at any temperature

$$\left(\frac{dT}{dt}\right)_T = \frac{\Delta T_{ad}}{C_O}\left(\frac{T_f - T}{\Delta T_{ad}}\right)^n {C_O}^n A.e^{-E/RT} \qquad \text{Equation 4.16}$$

This can be arranged to give the following equation

$$\left(\frac{dT}{dt}\right)_T = \left(\frac{T_f - T}{\Delta T_{ad}}\right)^n {C_O}^{n-1} \Delta T_{ad} A.e^{-E/RT} \qquad \text{Equation 4.17}$$

However the self-heat rate close to or at the onset of the reaction simplifies to the equation below

$$\left(\frac{dT}{dt}\right)_O = C_O{}^{n-1}\Delta T_{ad} A e^{-E/RT_O} \qquad \text{Equation 4.18}$$

The above two equations are used to determine the activation energy and order of any given reaction.

When Cp is assumed constant, ΔH, can be evaluated directly from the adiabatic data using the expression:

$$\Delta H = -\Delta T_{ad}.\ C_p.\Phi \qquad \text{Equation 4.19}$$

If the enthalpy change is proportional to the change in conversion, the rate of heat generation due to a simple exothermic reaction is given by:

$$q_g = -\Delta H.m_s.\ C_0{}^{n-1} A.\exp(-E/RT) \qquad \text{Equation 4.20}$$

and the corresponding rate of self-heating of a sample in a thermally isolated container is:

$$\frac{dT}{dt} = \frac{\Delta H.A.C_O{}^{n-1}}{C_p.\Phi}.\exp(-E/RT) \qquad \text{Equation 4.21}$$

where the thermal dilution factor, Φ is given by the following equation:

$$\Phi = \frac{M_b Cp_b + M_s Cp_s}{M_s Cp_s} \qquad \text{Equation 4.22}$$

Where C_{ps} = sample specific heat M_s = sample mass

C_{pb} = bomb specific heat M_b = bomb mass

This thermal dilution or phi factor takes account of the distribution of heat between the sample and the sample container. As a heat compensation is added to the system during the course of reaction (detailed in chapter 3), it should not be necessary

to compensate for the thermal dilution to the sample container or bomb during slow reactions. However in periods where the exothermic reaction is very fast, to accurately calculate the heat given off by the reaction, the phi factor should be factored into the calculation.

The main data from the PHI-TEC II experiments therefore is the adiabatic temperature rise which is defined as the log of the rate of exothermic heat release (^{o}C/min) vs temperature.

It is possible to see the complexity of reactions from the plot of the self-heat rate versus temperature. A single Arrhenius reaction gives a self-heat plot similar to that shown below:

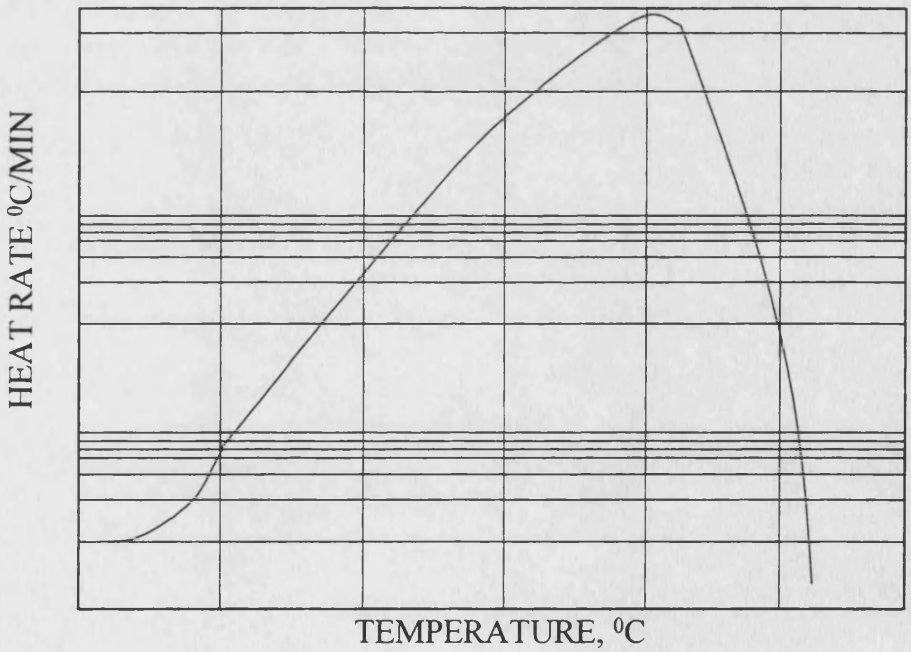

Figure 4.3: Self-Heat Rate vs. Temperature; Simple Reaction

More complex reaction mechanisms give different shapes to that shown above. Two reactions in series give a self-heat plot similar to that in Figure 4.4. In the case of an autocatalytic initiation, there is a very steep initial rise in the rate and the plot is similar to that shown below. Care should be taken with this because it could also be caused by other reasons apart from autocatalysis. These include an endotherm occurring prior to exotherm, loss of inhibitor or a build up of accelerator. Two parallel reactions give a plot similar to that shown in Figure 4.5.

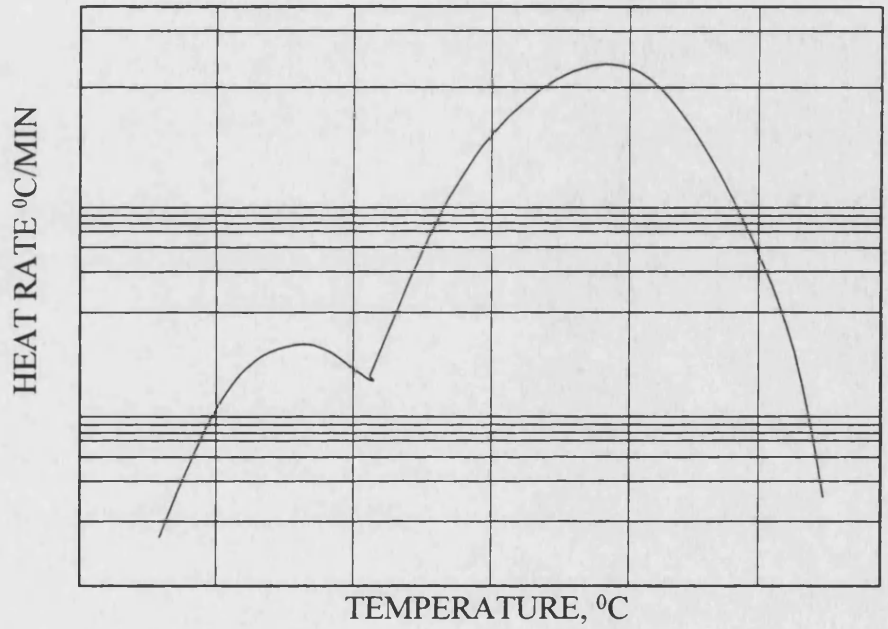

Figure 4.4: Self-Heat Rate vs Temperature; Two Reactions in Series

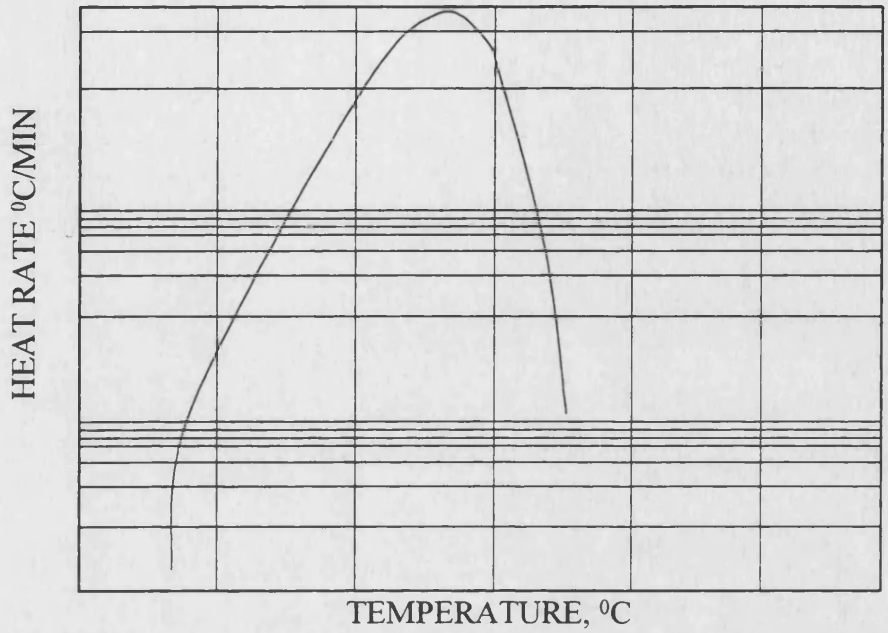

Figure 4.5: Self-Heat Rate vs Temperature; Autocatalytic Reaction

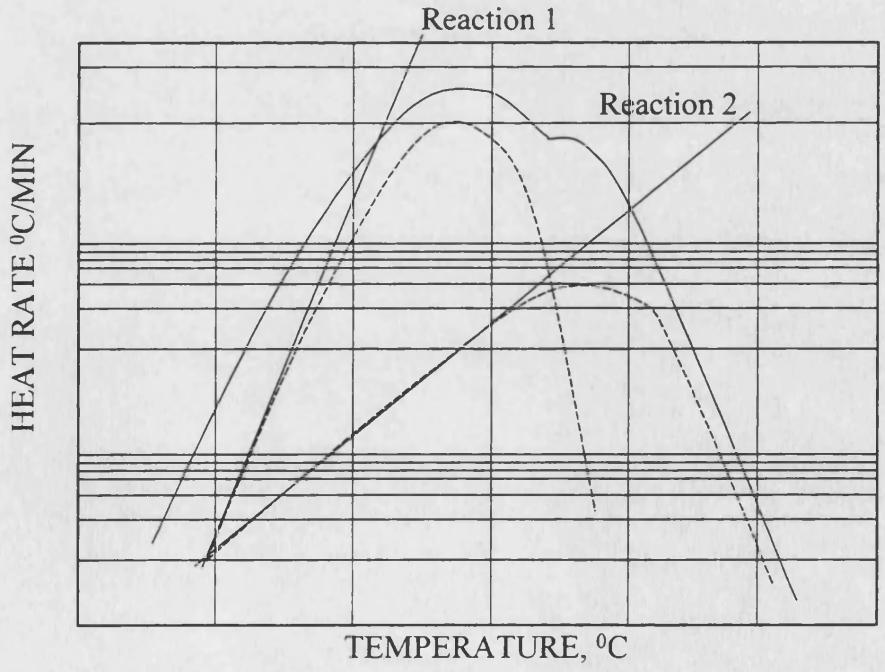

Figure 4.6: Self-Heat Rate vs Temperature; Two Reactions in Parallel

4.2.2 *WINCALC Software*

The PHI-TEC II possesses a suite of software which control the experimental set-up and recording. This was detailed earlier in chapter 3. There is also another software which aids in the analysis of the experimental data obtained. This is termed the WINCALC software.

The adiabatic experimental data obtained is reformatted using the WINCALC software. The point at which the exotherm starts is marked on the graph after zooming in to see the exact point at which the exotherm starts.

The starting temperature of the exotherm is noted and this temperature is inputted into the wincalc reformatting program.

The data is reduced over the entire period of the exothermic reaction and kinetic parameters are obtained. The data is then reduced to the relevant regions where reaction is seen to have occurred by following the following procedure.

1. The temperature at which the low temperature reaction is seen to switch into a different mode is also noted and is inputted into the reformatting program. The data is reduced over the LTO period and kinetic parameters are obtained.
2. The behaviour over the MTO/NTC region is noted and this can be compared with other results.
3. The temperature at which the high temperature reaction resumes as well as the terminating temperature is noted and inputted into the reformatting program. The data is reduced over the HTO period and kinetic parameters are obtained

Time, temperature and pressure data is extracted from the experimental data and the rates of change of temperature and pressure is calculated by regression on

successive batches of raw data. For each batch of n values of time, temperature and pressure, a least squares fit gives:

$$\frac{dx}{dt} = \frac{\sum x_i t_i - (\sum x_i \sum t_i \sum t_i)/n}{\sum t_i^2 - ((\sum t_i)^2)/n} \qquad \text{Equation 4.23}$$

$$x_{mean} = \sum x_i - \frac{dx}{dt}\sum t_i + \frac{dx}{dt} t_{mean} \qquad \text{Equation 4.24}$$

where x = temperature or pressure

x_{mean} = mean temperature or pressure during the interval

t_{mean} = time corresponding to the midpoint of the batch.

The size of the batch data used to calculate the temperature and pressure gradients; i.e. the smoothing interval and the time step between successive data points in the reduced output may be changed. The smoothing interval varies with the calculated change of temperature or pressure. At the beginning of the exotherm, when dT/dt is small and not changing rapidly, the smoothing interval and time step should be large to ensure that accurate values for dT/dt and dP/dt are obtained. As the temperature and/or pressure accelerate the smoothing interval and time step should be gradually reduced until the smoothing interval is only a few points and the time step approaches the interval between raw data points. It should be checked that a representative summary of the original data has been achieved in the smoothing process. Comparing a plot of T v t for the reduced data with a similar plot for the original data does this.

The data obtained from the reformatting and regression of the original data include the self heat rate of the reaction, dT/dt (^{0}C/sec), dP/dt (bar/sec), lnP,(with P in Pascal's) and lnk, where k is a pseudo rate constant obtained from the following equation:

$$k = \frac{dT/dt}{(T_f - T_s)((T_f - T)/(T_f - T_s))^n} \qquad \text{Equation 4.25}$$

where T_f = maximum temperature reached by the sample

T_s = temperature at the start of the reaction

n = supposed order of the reaction

From the slope of lnk v temperature, which should be a straight line, the remaining kinetic parameters are obtained. The slope of the plot equates to the activation energy of the reaction, E divided by the gas constant R, and the intercept is related to the logarithm of the pre-exponential term, A, in the Arrhenius equation.

4.2.3 *Determination of Reaction order*

The order of the exothermic reaction is verified by plotting lnk against –1000/T and checking if the curve is linear.

From equation 4.17

$$\left(\frac{dT}{dt}\right)_T = \left(\frac{T_f - T}{\Delta T_{ad}}\right)^n C_O{}^{n-1} \Delta T_{ad} A.e^{-E/RT} \qquad \text{Equation 4.26}$$

which may be rewritten as shown below

$$\left(\frac{dT}{dt}\right)_T = \left(\frac{T_f - T}{\Delta T_{ad}}\right)^n C_O{}^{n-1} \Delta T_{ad} k \qquad \text{Equation 4.27}$$

The initial step is to assume a zero order reaction, and defining a pseudo zero-order rate constant, k^* defined below as

$$k^* = kC^{n-1} \qquad \text{Equation 4.28}$$

then

$$\left(\frac{dT}{dt}\right)_T = \left(\frac{T_f - T}{\Delta T_{ad}}\right)^n \Delta T_{ad} k^* \qquad \text{Equation 4.29}$$

Rearranging,

$$k^* = \frac{\left(\frac{dT}{dt}\right)_T}{\left(\frac{T_f - T}{\Delta T_{ad}}\right)^n \Delta T_{ad}} \qquad \text{Equation 4.30}$$

and

$$k^* = kC_O{}^{n-1} = C_O{}^{n-1} Ae^{-E/RT} \qquad \text{Equation 4.31}$$

Taking logs

$$\ln k^* = \left(AC_O{}^{n-1}\right) - \frac{E}{R}\frac{1}{T} \qquad \text{Equation 4.32}$$

A correct value of n should give a straight line when a plot of k against 1/T is made, and therefore this equation can be used to check for the reaction order. Incorrect values of n will produce curves when the plot is made. From the slope of the line the activation energy is obtained and the activation energy is the intercept of the line, as is detailed earlier in this chapter.

Comparing the different reaction orders used shows that the choice of reaction order does not substantially alter the other obtained kinetic parameters. A reaction order of one is therefore assumed for the subsequent kinetic analysis. As the analysis of the effect of different factors is made on a comparative basis any errors arising from an incorrect reaction order should be insignificant. A search of the literature also reveals that most studies have taken the reaction order to be one previously.

4.2.4 *Exceptions to Arrhenius Kinetic Theory*

Apart from the assumptions that have to be made to use Arrhenius kinetic model, there are two classes of reactions for which Arrhenius equation does not hold. These involve the following situations, reported by Benson 1960, Williams 1965 and Glassman 1977:

1. Low-activation energy free radical reactions: In these reactions, temperature dependence in the pre-exponential term assumes greater importance and the so-called absolute theory of reaction appears to provide better correlation of kinetic data with temperature. In this theory, first proposed by Benson 1960, the reactants are in equilibrium with an activated complex which forms.
2. Radical Recombination: When simple radicals recombine to form a single product, energy must be removed from the product upon its formation in order to stabilise it. A third body is necessary to remove this energy. The pressure dependence of third-body recombination reactions can be quite pronounced, hence the specific reaction rate does not follow Arrhenius equation.

4.3 Reaction Kinetics Model

An attempt is made to fit a reaction mechanism to the results obtained. This is illustrated using a sample experiment as shown below.

4.3.1 *Branched chain reactions*

Elementary reactions are called chain initiating or chain terminating reactions according to how they produce or destroy free radicals. With regard to the ratio of the number of free radicals in the product to that in the reactant, elementary reactions are

called chain propagating (or chain carrying) reactions if the ratio is equal to 1, and chain branching reactions if their ratio is greater than 1.

In general (Glassman 1977), branched chain reactions and explosions can be studied by considering the following chemical kinetics:

$$M \xrightarrow{k_1} R \qquad \text{Chain-initiating}$$

$$R + M \xrightarrow{k_2} \alpha' R + M^* \qquad \text{Chain-branching, } \alpha > 1$$

$$\left.\begin{array}{l} R + M \xrightarrow{k_3} P \\ R \xrightarrow{k_4} M(on\ wall) \\ R \xrightarrow{k_5} nonreactive\ species \end{array}\right\} \qquad \text{Chain-terminating}$$

Where M and M^* are reacting molecules, P stands for products formed, and R represents chain carrying radicals. The last group of equations includes one showing the termination of the radical on the wall of the vessel. This termination effect is accelerated for metallic surfaces and is one of the limitations of the ARC; i.e. the metallic bomb would play some role in the oxidation reactions.

Applying the steady state assumption that the mean concentrations of the free radicals remain nearly constant, the rate equation is:

$$\frac{dC_R}{dt} = 0 = k_1 C_M + (\alpha' - 1) k_2 C_R C_M - k_3 C_R C_M - k_4 C_R - k_5 C_R \qquad \text{Equation 4.33}$$

Solving for C_R gives

$$C_R = \frac{k_1 C_M}{k_3 C_M + k_4 + k_5 - (\alpha' - 1) k_2 C_M} \qquad \text{Equation 4.34}$$

The rate of change of the product concentration is given as

$$\frac{dC_P}{dt} = k_3 C_R C_M = \frac{k_1 k_3 C_M^2}{k_3 C_M + k_4 + k_5 - k_2 (\alpha' - 1) C_M} \qquad \text{Equation 4.35}$$

The quantity $k_2(\alpha'-1)C_M$ is positive; as its value increases it tends to decrease the denominator in equation (4.35). The critical value of α' is given as

$$\alpha'_{critical} = 1 + \frac{k_3 C_M + k_4 + k_5}{k_2 C_M} \qquad \text{Equation 4.36}$$

and we have

$\alpha' \geq \alpha'_{critical}$ $\Rightarrow$ chain branching explosion

$\alpha' < \alpha'_{critical} \Rightarrow$ no explosion, slow reaction

In the LTO zone therefore, the reaction is governed by the previous chain reactions. After the autocatalytic induction then occurs, the kinetics changes and the HTO zone is governed by a different set of kinetics.

Rate data for the reactions of methyl radicals have been obtained by a method of comparative reactions (Benson, 1960). These results can be compared with those obtained for the various regions of the oxidation.

Activation Energies of 8 – 14 Kcal/mole for various methyl radicals

Activation Energies of 15 – 27 Kcal/mole for heavier organics including some dimerization reactions.

Greaves et al 2000 report activation ranges for LTO reactions at temperatures of 90-140 ^{0}C from 55.4 to 62.7 KJ/mol.

4.3.2 *Kinetics of Low temperature Oxidation*

Radicals and their behaviour in oxidation of organics are well documented (Benson, 1960, Stirling, 1965, Kuo 1986). Radicals are defined as atoms or molecules containing one or more unpaired electrons and are the most active species in a reaction process.

C-H bonds are susceptible to attack by molecular oxygen, initial products being of the type ROOH. These reactions are catalysed by the hydroperoxide products themselves, making it an autocatalytic reaction.

The following simple mechanism is commonly used to represent the process and has been found to cover most observations:

Initiation

The first step is the initiation, where the crude oil oxidation is initiated by the reaction between the native hydrocarbons and the dissolved oxygen to form free radicals. This reaction explains the induction period seen in the experiments and generally in hydrocarbon combustion.

$$O_2 + RH \rightarrow R\bullet + HO_2\bullet \qquad \text{Equation 4.37}$$

where RH is the alkyl fuel and $R^{\bullet}$ is a hydrocarbon fragment

Propagation

The second step is the propagation, where the hydrocarbon free radical propagates the reaction by the formation of intermediates such as aldehydes or peroxides. In the peroxide case, hydrocarbon radicals react with an oxygen molecule to

yield peroxide radicals, which then produce hydroperoxides and a free radical $R\bullet$ that continues the chain. This method of propagation is particularly easy because formation of hydroperoxides only requires the rupture of one bond in the oxygen molecule. Several studies on the liquid-phase oxidation of certain olefinic, alkylaromatic and hydroaromatic compounds at low temperatures have also shown the formation of hydroperoxides as the only products (Emanuel et al 1967). However, oxidation of alkanes and aromatic hydrocarbons produce the variety of products discussed earlier, although hydroperoxides may still be the main primary products.

$$R^{\bullet} + O_2 \rightarrow ROO^{\bullet} \qquad \text{Equation 4.38}$$

$$ROO^{\bullet} + RH \rightarrow ROOH + R^{\bullet} \qquad \text{Equation 4.39}$$

where $ROO^{\bullet}$ is the peroxide radical and $ROOH$ is the hydroperoxide radical.

The main method of forming radicals when the oxidation is underway is by the attack of radicals such as $H\bullet$, $CH_3\bullet$, $OH\bullet$, $HO_2\bullet$, $RO\bullet$ and $RO_2\bullet$ on the fuel particles, examples of which are shown below.

$$HO_2{}^{\bullet} + RH \rightarrow H_2O_2 + R^{\bullet} \qquad \text{Equation 4.40}$$

$$OH^{\bullet} + RH \rightarrow H_2O + R^{\bullet} \qquad \text{Equation 4.41}$$

$$RO^{\bullet} + RH \rightarrow ROH + R^{\bullet} \qquad \text{Equation 4.42}$$

At about 100^0 C, the temperature decomposition of hydroperoxides becomes significant. Peroxides are unstable and their presence usually implies degenerate branching reactions, which initiate subsequent reactions. This is shown below:

$$ROOH \rightarrow RO^{\bullet} + OH^{\bullet} \qquad \text{Equation 4.43}$$

$$2ROOH \rightarrow RO\bullet + H_2O + ROO\bullet \qquad \text{Equation 4.44}$$

Initiation of chains by the radicals derived from the hydroperoxide decomposition is responsible for the autocatalysis.

New chain radicals $RO^{\bullet}$ and $OH^{\bullet}$ are formed, which go on to react with native hydrocarbons to produce additional primary radicals.

Termination

The third and final step in the chain radical equations is the termination stage, where the free radicals $R^{\bullet}$ and $RO_2^{\bullet}$ result in the formation of hydrocarbons of greater molecular weight than the native hydrocarbon. The following termination reactions occur producing non-radical products such as polymers and oxygenated hydrocarbons (Equation 2.1 – 2.5) containing groups such as ketones, acids and alcohols.

$$R^{\bullet} + R^{\bullet} \rightarrow RR \qquad \text{Equation 4.45}$$

$$ROO^{\bullet} + R^{\bullet} \rightarrow ROOR \qquad \text{Equation 4.46}$$

$$ROO^{\bullet} + ROO^{\bullet} \rightarrow ROOR + O_2 \qquad \text{Equation 4.47}$$

As some light oil reservoirs have been seen to produce CO_2, CO and H_2O during the LTO process, without entering the HTO/ISC process, some alternative mechanisms must be occurring. Some previous studies have postulated that coke-like deposits must be formed during LTO which occur by polymerisation reactions (Moore et al 1998). Also the production of CO is caused by the decomposition of oxygenated hydrocarbons, which is then oxidised to produce CO_2 and H_2O.Babu and Cormack, 1984 confirmed that the LTO process increases the asphaltenes content of crude oil and decreases the aromatics and resins content.

Research into the low temperature oxidation of propene by Wilk et al 1987 showed a similarity with the LTO of the crude oils studied. The curves of temperature and pressure displayed a characteristic S-shape, including a well-defined induction period followed by a rapid pressure rise. The induction period is the time required to build-up the radicals for the faster reactions to consume in reaction, and in the case of propene oxidation, corresponded to the time required for significant fuel consumption to occur. The time of maximum reaction rate as measured by temperature and pressure rise was the same as that measured by fuel consumption. Increasing the initial temperature also had the effect of reducing the induction period or increasing the maximum overall rate.

4.3.3 *Example of Reaction Kinetics Analysis: Experiment Dr_s1*

An example of the one of the experiments is shown to demonstrate the analytic procedure followed for each of them.

0.25 ml Oil D @ 50 bar, 0.5g pure silica, 0.1 ml water, Dr_s1

0.25 ml of oil D is reacted at 50 bar with 0.5g pure silica as well as 0.1 ml water. The resulting adiabatic temperature and pressure profile over time is shown below in Figure 4.7. A LTO reaction exotherm starts at a temperature of 71 ° C and continues until it reaches a temperature of 185 ° C, where the reaction undergoes autocatalytic reaction. The exotherm progresses until a temperature of 251 ° C, at which point it drops to a temperature of 244 ° C before it starts rising again. It then increases at a slower rate in the HTO mode until a temperature of 480 ° C, which is the temperature

limit for the equipment, and is halted. The data is analysed and a plot of the exothermic self-heat rate is made which is shown in Figure 4.8.

The data is analysed to fit an Arrhenius type reaction model using the analytical relationships detailed earlier in this chapter. The reaction rate constant is obtained from the self-heat rate data using equation 4.25 and is shown in Figure 4.9. A logarithmic scale representation of the same self-heat rate for experiment Ds_r1 is shown in Figure 4.10. Figures 4.9 and 4.10 are notable for their similarity. This arises as the reaction rate constant is directly calculated from the self-heat rate values as shown earlier.

Characteristics of the Reaction Rate Constant plot

It is obvious from Figure 4.9 that the plot of reaction rate constant is not a single straight line. An inspection of the plot reveals that the reaction can be split into different regions, indicating changes in the reaction mechanism over the course of temperature increase. The plot also confirms that chain branching reactions involving free radicals are occurring as described earlier.

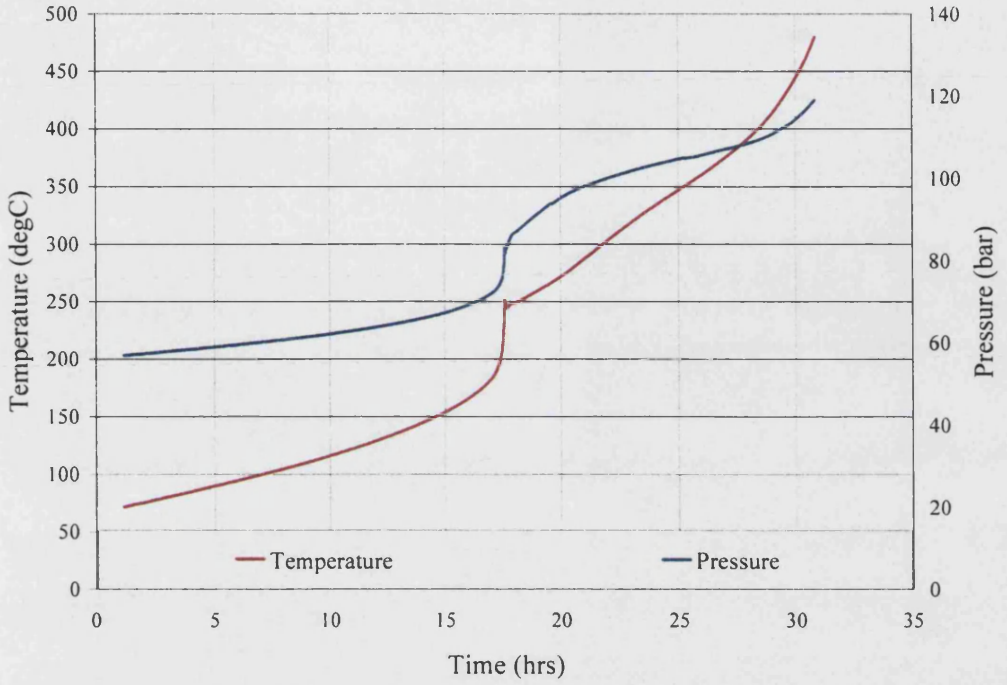

Figure 4.7: Adiabatic Temperature and Pressure Rise over Time, Dr_s1; 0.25ml Oil D, 0.5g Silica, 0.1ml water @ 50 bar

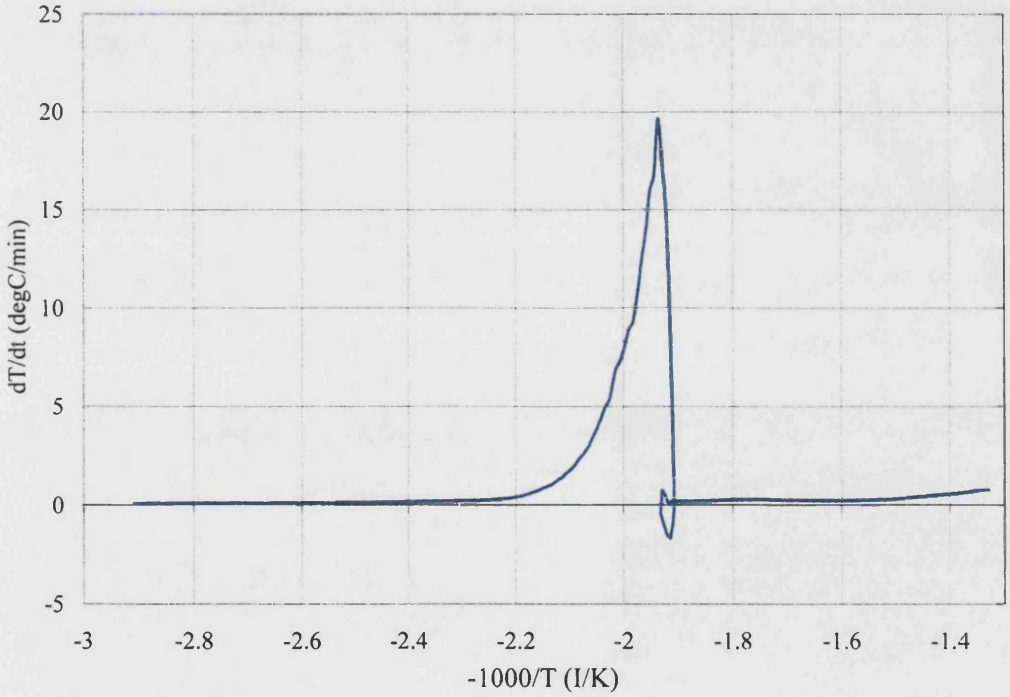

Figure 4.8: Self-Heat Rate against -1000/Temperature, Dr_s1; 0.25ml Oil D, 0.5g Silica, 0.1ml water @ 50 bar

The reaction rate constant (k) values obtained for a reaction with order one is shown in Figure 4.9, and the activation energy and pre-exponential factor is obtained by taking the slope of this line and solving equation 4.4.

The reaction regions are split, using the method detailed below, to show where each of the phenomena described earlier are occurring, and this is shown in figure 4.11 with the reaction regions numbered as follows:

1. LTO Induction Region (LTO k_1)
2. LTO Propagation Region (LTO k_2)
3. LTO Termination Region (LTO k_3)
4. Lower HTO Region (HTO k_1)
5. Upper HTO Region (HTO k_2)

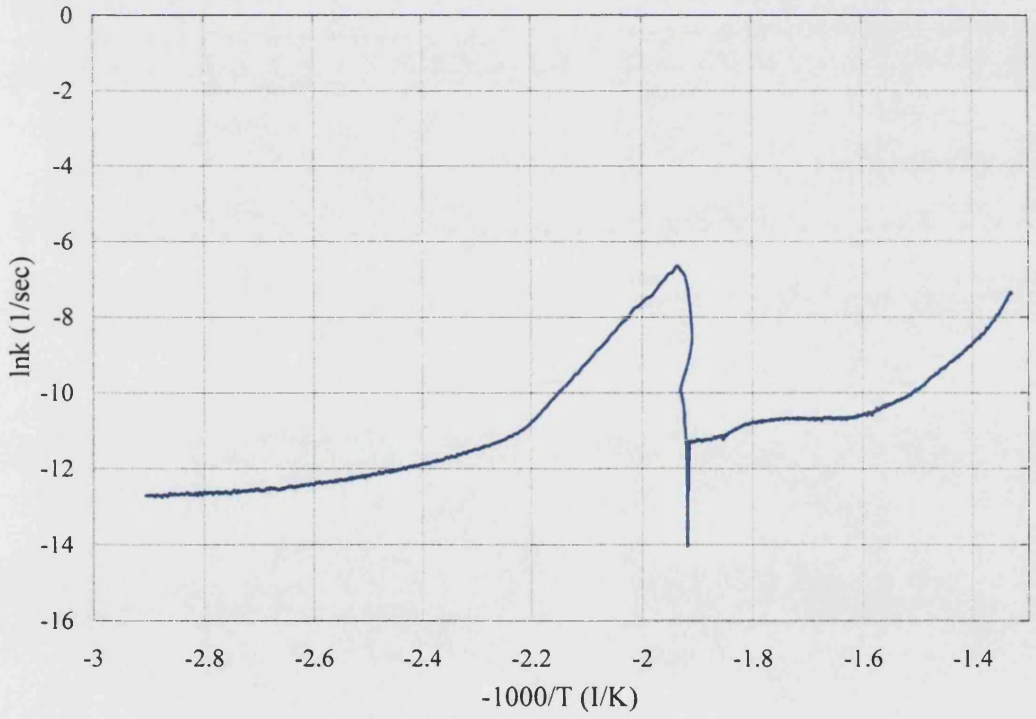

Figure 4.9: Reaction Rate Constant against –1000/T, Dr_s1; 0.25ml Oil D, 0.5g Silica, 0.1ml water @ 50 bar

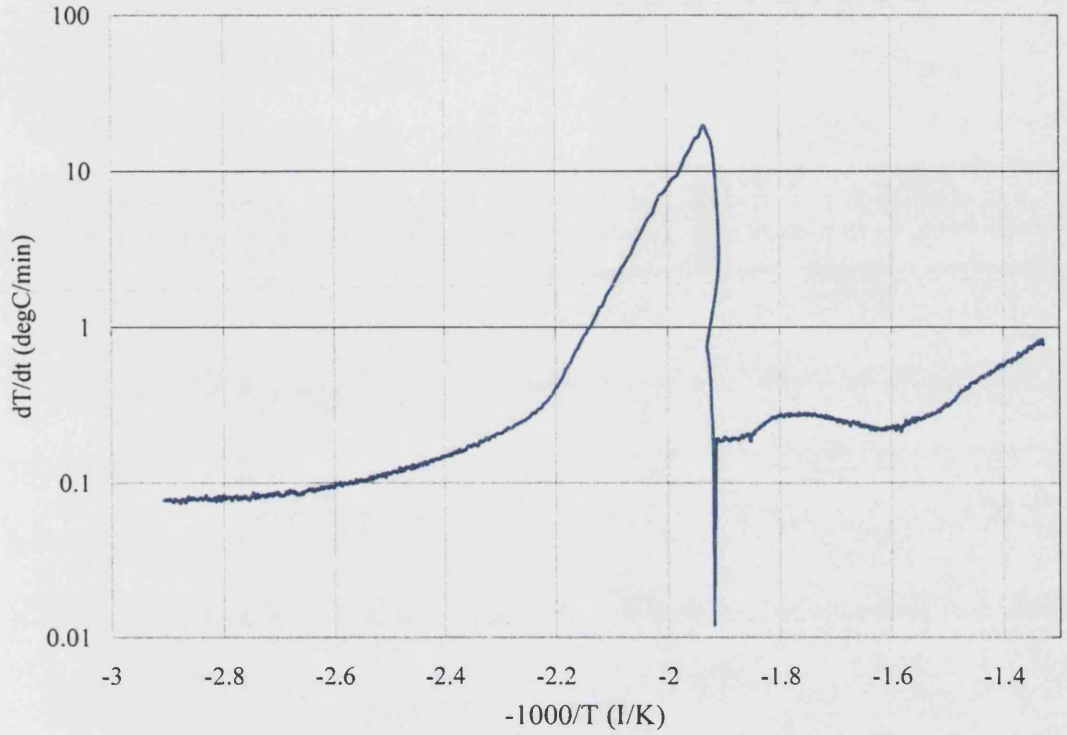

Figure 4.10: Logarithmic Plot of Self-Heat Rate against –1000/T, Dr_s1; 0.25ml Oil D, 0.5g Silica, 0.1ml water @ 50 bar

An analysis of the self-heat rate data shows that the propagation period for most of the experiments starts when the self-heat rate reaches a value of approximately 0.5 degC/min. This is taken as a standard value and is used as a dividing point between induction and commencement of propagation for the subsequent analyses.

The maximum point on the reaction rate constant plot is taken as the end of the propagation region and the start of the LTO termination region while the end of the LTO region is usually very prominent on the plots. The HTO region also shows a dichotomy with the lower part exhibiting a lower heat evolution before the reaction gets properly underway and then accelerates. This lower HTO region which usually ends at about 350 ^{0}C could actually be the MTO region discussed in chapter 2 which has been observed in previous works.

The slope of the reaction rate constant line is taken in each of these regions and the appropriate Arrhenius reaction kinetic parameter is obtained.

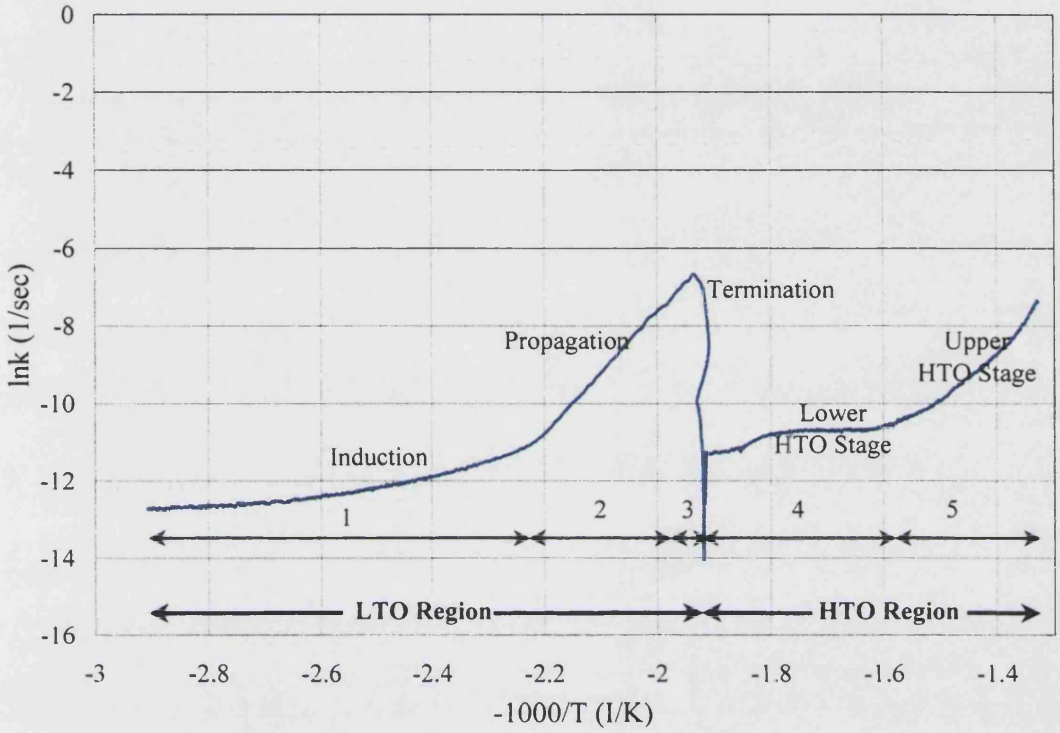

Figure 4.11: Division of Reaction Rate Constant into Regions, Dr_s1; 0.25ml Oil D, 0.5g Silica, 0.1ml water @ 50 bar

The pressure-temperature data is also checked to see if it follows an Antoine – type correlation. The pressure/temperature (P/T) relation is a function of the vapour-liquid equilibrium, and from this plot it can be seen if the reaction in question follows an ideal gas type reaction (straight line) or if a departure from the vapour liquid equilibrium occurs. An examination of the graph in Figure 4.12 illustrates that the LTO stage occurs within the vapour liquid equilibrium area and a departure from equilibrium occurs after the autocatalytic reaction starts, in this experiment at a temperature of 251° C, where the hump in the curve can be seen. Equilibrium is attained again within the HTO stage after a period.

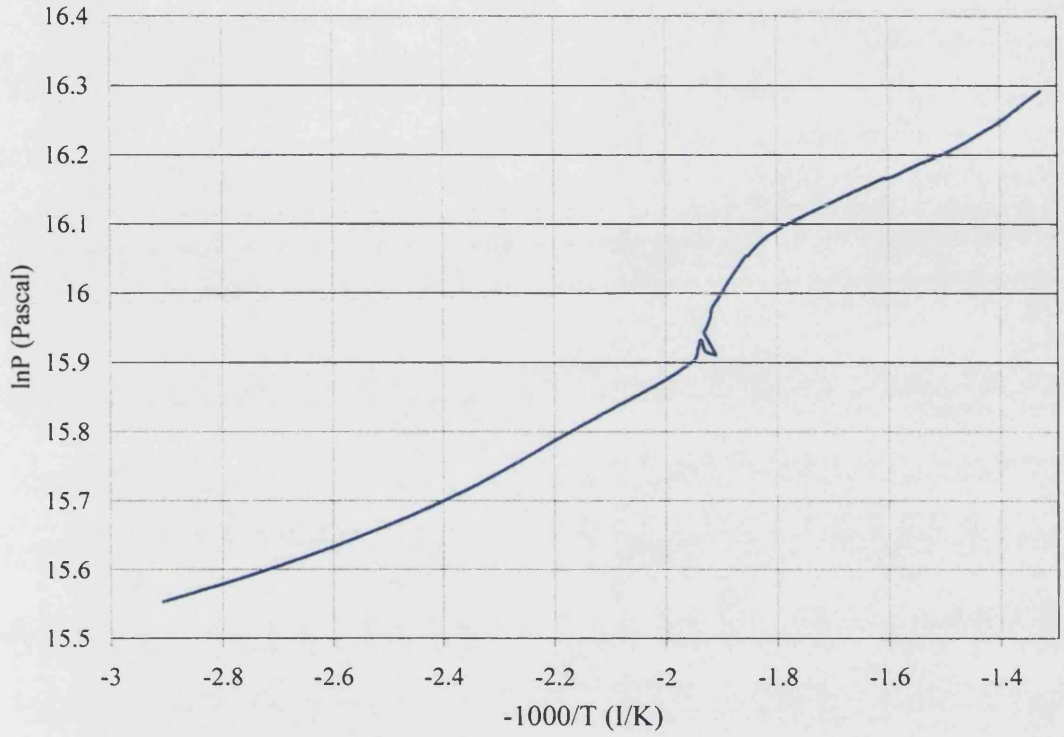

Figure 4.12: Plot of Antoine's Correlation, ln P against –1000/T, Dr_s1; 0.25ml Oil D, 0.5g Silica, 0.1ml water @ 50 bar

It is important to study the two main regions of reaction, i.e. LTO and HTO separately. The possibility of different mechanisms occurring in the two regions could imply that parameters might have diverse effects in the two zones.

The Arrhenius kinetic ratios obtained are the activation energies, as well as the pre-exponential factors from each reaction region, and these are shown in Table 4.1, where E_a is activation energy, and A is Arrhenius pre-exponential factor. For the comparison of different experiments, the focus will be on the exothermic parameters as these are directly obtained from the experiments. The kinetic parameters are a function of the exothermic self-heat rate and therefore should follow similar trends. All the Arrhenius kinetic data obtained for each experiment are shown in Appendix D.

Reported values for the Arrhenius constants have been obtained for temperatures up to 232 ^{0}C by Burger and Sahuquet, and discussed by Fassihi et al 1984. The activation energy is in the range of about 70 kJ/mol. This is roughly comparable with the arrhenius constant values shown below for the upper HTO k2 zone, where full combustion starts.

Table 4.1: Arrhenius Kinetic Parameters, Ds_r1

Reaction Region	E_a (KJ/mol)	A (1/sec)
Overall LTO*, ($k_{Overall\ LTO}$)	33.6	0.18
Induction, (k_1)	19.6	0.002
Propagation, (k_2)	130.1	1.8E+10
Termination, (k_3)	-562.1	2.4E-60
Overall HTO*, (k_1)	44.3	0.21
Lower HTO, (k_2)	17.1	7.3E-04
Upper HTO, (k_3)	97.9	2572.2
Overall*	19.6	2.1E-03

The overall LTO*, HTO* and overall* kinetic parameters are obtained from a line of best fit to the LTO, HTO and the overall kinetic regions respectively, as if it were one reaction taking place. As the line of best fit does not accurately show the variation in the reaction mechanism, these values are an approximation only. The most representative values are from treating the reaction as separated into its different regions. The overall values are for modelling purposes where only a one-step reaction model can be used due to computing or other constraints. The termination region shows

negative kinetic values, which are very strange. However, this value is only for modelling purposes; to signify the end of one reaction mechanism (LTO), visible by the drop in temperature in the reaction exotherm at this point. In a physical sense, it occurs for an extremely short period, as will be seen in the next section.

4.4 Exothermicity of oxidation reactions

The exothermicity parameters obtained from the experiments and used to characterise the energy release or exothermicity of each reaction are listed below:

1. The self-heat rate (dT/dt) during each reaction region
2. Energy evolved during LTO (ELTO)
3. Energy evolved during HTO (EHTO)

4.4.1 *Example of Exothermicity Analysis: Experiment Dr_s1*

Of the various exothermicity parameters listed above, the most important is the self-heat rate, as it is a sign of how vigorous the reaction is. The energy evolved is obtained from the self-heat rate and the reaction time. For the comparative purposes between different experiments, care must be taken when using it as experiments with exceedingly long reaction times would appear to generate a lot of energy. The self-heat rate values calculated for each region region studied for all the different experimental runs is summarised in Appendix A.

The exothermicity parameters for each of the reaction regions are measured. The results for the sample experiment are shown in Table 4.2. The term energy evolved comes from the following equation.

$$\Delta Q = m_s \Phi \int_{T_1}^{T_2} C_p dT \qquad \text{Equation 4.48}$$

where ΔQ is the energy evolved

This value used for the analysis is obtained by multiplying the average dT/dt value for each region with the reaction time and does not include the heat capacity or the phi factor. The values of energy evolved are required only for comparative purposes in this work and where the experiments have the same mass and specific heat capacity values, no adjustment is required. In experiments where the mass of oil changes or other materials including rock or water are included, an inclusion of the mass and specific heat capacity into the equation is made.

An example of this is shown below for illustrative purposes:

The energy evolved for Ds_r1 can be calculated as follows;

Using Equation 4.48, the following parameters are obtained,

C_p for silica is taken as 0.743 J/gK,

mass of silica is 0.5g, mass of water is 0.1ml,

C_p for water is 4.18 J/gK,

Volume of oil is 0.25ml, and the mass of oil is obtained using the density

Oil D is a 39 °API oil,

$$\therefore \rho_{oil} = \frac{141}{131.5+39} = 0.8299 g/ml$$

and the mass of oil is 0.207g

$$\therefore Q = (m_{oil} C_{poil} + m_{water} C_{pwater} + m_{rock} C_{prock}) dT$$

$$= (0.207x2.2 + 0.1x4.18 + 0.5x0.743) dT$$

To obtain more accurate magnitudes for other purposes, the specific heat capacity as it varies with pressure would have to be included in the equation. However

for the purposes of comparison, the use of these heat capacity values is perfectly adequate. An example of this energy evolution calculation is shown in Appendix C.

Other exothermicity parameters that can be read from the data include a maximum self-heat rate (usually in the propagation region), the autocatalytic ignition temperature, and the temperature drop after the end of the LTO region. This latter phenomena was observed in all the reactions and is discussed later in Chapter 8.

Table 4.2: Exothermicity Parameters, Ds_r1

Reaction Region	Average dT/dt (deg C/min)	Reaction Time (min)	Energy Evolved
Overall LTO*	0.49	985.3	262.0
Induction	0.12	947.2	117.2
Propagation	3.40	38.2	
Termination	12.50	0.01	
Propagation + Termination	3.79	38.2	144.8
Overall HTO*	0.33	750.8	239.0
Lower HTO	0.23	456.0	106.1
Upper HTO	0.45	294.9	132.9
Overall	0.41	1736.2	501.0

Where * signifies average values over the whole region

Adding the individual energy evolution values for the different regions and adding them up will give the energy evolved during LTO and HTO. The overall LTO* and HTO* as well as the quoted overall energy evolved values in the table above is

obtained by taking an average over the respective regions and gives slightly different values from actually adding them up. These values are given here for modelling purposes to give a quick approximation of the energy evolved. The most accurate representation is by calculating each region separately rather than using the average.

The ratio of energy evolved over the LTO and HTO (ELTO/EHTO) is obtained by dividing these two values. ELTO/EHTO for experiment Dr_s1 = 1.10, implying more heat evolution in the LTO zone than in the HTO region for this experiment. For subsequent analysis, the energy evolved during the termination region is lumped together with that from the propagation region as the reaction time is so short in this region. Similarly the average "overall" values are not used for comparisons as these are approximate values.

In order to understand the effects of different parameters on the reaction exothermicity, the exothermic data obtained for the two experiments under comparison are analysed to obtain ratios using a similar comparative method as that described earlier in chapter3. The exothermicity data obtained for the two experiments under comparison are divided to obtain ratios in order to see the trend a change in the parameter causes to it.

Some of the exothermicity ratios obtained are the self-heat rates in the various reaction regions, the reaction times and energy evolved from each reaction region.

CHAPTER 5:

Factors Affecting Crude Oil Oxidation Reaction Kinetics

PARAMETERS AFFECTING CRUDE OIL OXIDATION REACTION KINETICS

The effects that result from alterations in the reaction conditions are analysed and discussed in this chapter.

5.1 Amount of Oil Reacted

The amount of oil reacted in the bomb is varied to see what effect this has on the kinetics. This parameter can be directly related to the oil saturation, which is one of the parameters affecting oil recovery processes in a reservoir. It is important to see what impact, if any, it has on the kinetics of oil oxidation.

In the bomb experiments, different oil saturations in the reservoir would imply a different amount of oxygen reacting with unit amounts of oil. Experiments were carried out to investigate this by varying the amounts of crude oil present in the bomb; both with oil alone and in the presence of rock and water. These experiments and the results are compared to observe the effect.

Previous studies have found some effect due to the initial saturation. Alexander et al 1962 found that the fuel deposition decreased when the initial oil saturation reduced. Vossoughi and El-Shoubary 1989 showed that the surface area effect of reservoir matrix was not felt at high oil saturations. The DTG results of saturations higher than 58 wt percentage were similar to those of the crude oil in the absence of any rock.

Table 5.1: Experimental Analysis to Study Effect of Reaction Condition Parameters

Experimental Parameters	Amount of Oil	Amount of water	Pressure	Oil Type
Differences between Experiments	***1 ml / 0.25 ml Oil B*** B7 / B5, B3, B4	***1 ml water / no water*** Drw1 / Dr2	***100 bar / 50 bar*** B1 / B5, B3, B5	***Medium Heavy / Light*** Mr1 / Ar1, Br1, Cr1, Dr1
	0.5 ml / 0.25 ml Oil B B2 / B5, B3, B4	***0.1 ml water / no water*** Dr1 / Dr2, Bw / B0	***100 bar / 50 bar*** D2 / D3	
	1 ml / 0.25ml Oil D Dr4 / Dr1	***0.5 ml water and rock / 0.1 ml water*** Bw1 / Bw	***50 bar / 0 bar*** Dr1 / Dr5	

5.1.1 *Effect of different amounts of oil*

Table 5.1 shows the experimental runs compared to illustrate the effect of the amount of oil on the reaction kinetics.

Graphs showing the data obtained from the experiments and the resulting analysed data, as described in chapter 4, are shown below for experiments B7 (1ml oil) and B5 (0.5ml oil), which are described in Table 3.2.

1 ml Oil B @ 50 bar, B7

Figure 5.1 shows the adiabatic temperature and pressure rise against time for experiment B7 (1ml oil B @ 50 bar). A reaction exotherm is seen to start at a temperature of 100 ° C. This continues until a temperature of 222 ° C, at which point the reaction rate switches into an autocatalytic mode. The exotherm progresses up to a temperature of 332 ° C, at which point it drops to 284 ^{0}C before the temperature starts increasing again. The exotherm persists at a slower rate until a temperature of 500 ° C, which is the maximum allowable temperature for the equipment to reach.

0.25 ml Oil B @ 50 bar, B5

0.25 ml of Oil B is reacted at 50 bar and the temperature and pressure profiles are shown in Figure 5.2. An exotherm starts at a temperature of 83 ^{0}C and continues until it reaches a temperature of 215 ^{0}C, at which point the reaction mode switches. The exotherm then progresses to a temperature of 310 ^{0}C and then drops slightly to a temperature of 301 ^{0}C. The reaction then increases at a slower rate until it reaches a temperature of 480 ^{0}C when it was stopped.

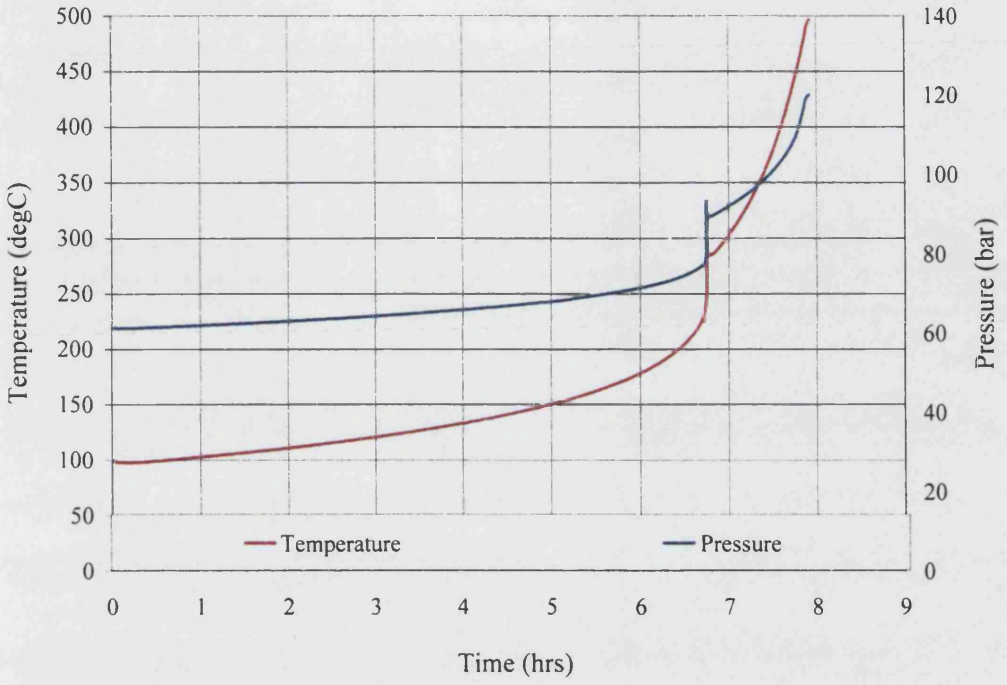

Figure 5.1: Temperature and Pressure Rise against Time, B7 (1ml oil B @ 50 bar)

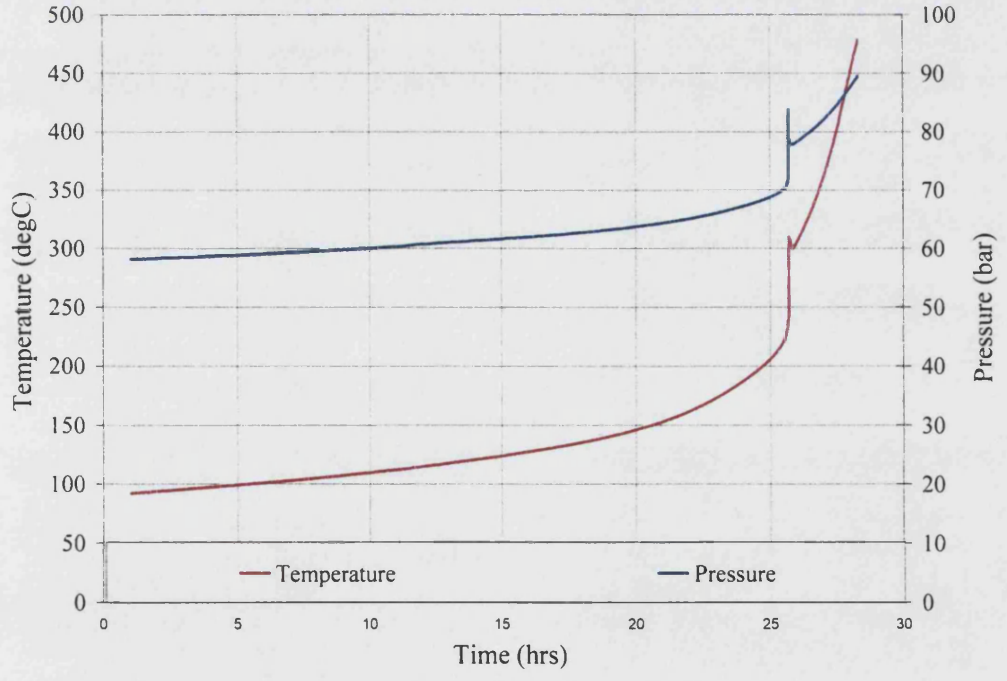

Figure 5.2: Temperature and Pressure Rise against Time, B5 (0.25ml oil B @ 50 bar)

The data was analysed and a plot of the exothermic self-heat rate made. This is shown in Figure 5.3 for two runs with 0.25ml oil and 1ml oil. This plot shows that the self-heating rate is greater over a wider temperature range for the experiment with 1ml of oil.

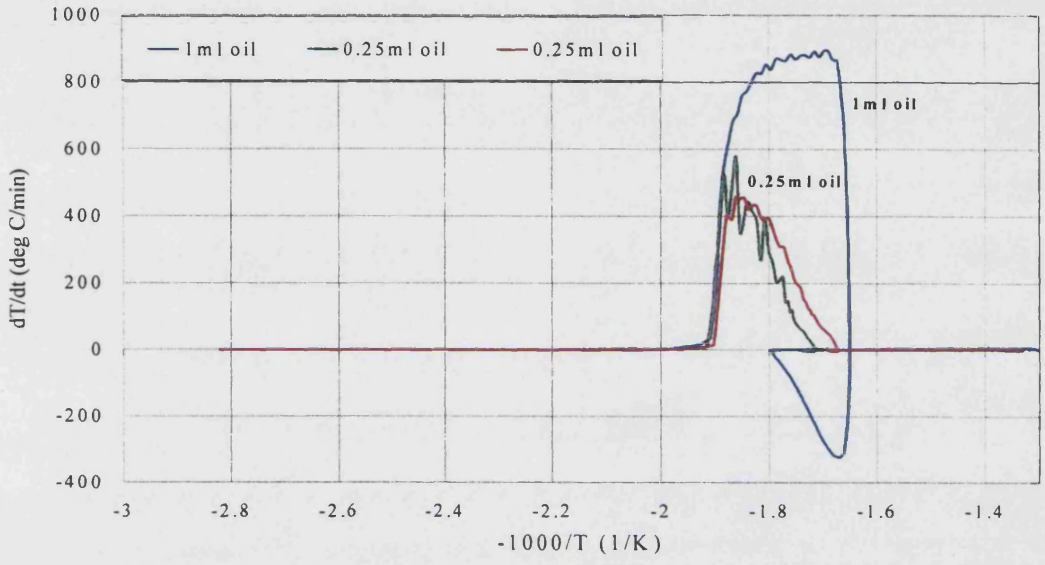

Figure 5.3: Self-Heat Rate against -1000/T, B7 (1ml oil), B5 & B3 (0.25ml oil)

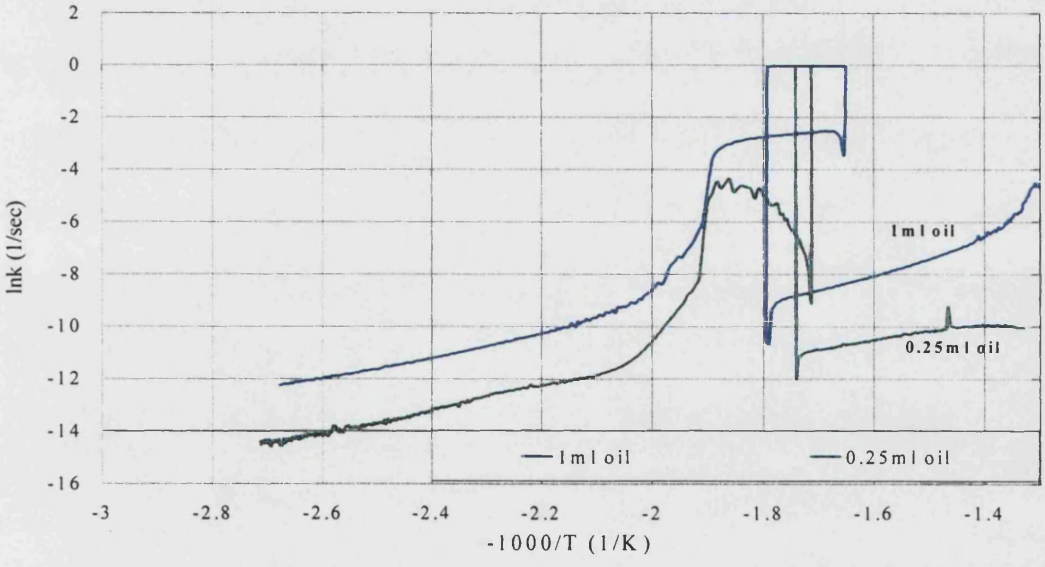

Figure 5.4: Reaction Rate Constant against –1000/T, B7 (1ml oil), B5 (0.25ml oil)

It must be pointed out that the significant negative drop in Figure 5.3 could be due to a temporary failure of the measuring instrument not being fast enough to cope with the rapid increase in temperature at this point.

These reactions are broken down further into the different reacting regions and Arrhenius constant values are obtained for the reactions taking place over both the lower and higher temperature zones as well as one taking the overall composite reaction. The Arrhenius kinetic values are shown in Appendix D.

The Antoine correlation for both experiments is shown in Figure 5.5, showing the very fast nature of the reaction in the propagation stage before it changes from the LTO region. It also shows that similar vapour-pressure processes take place under both experimental conditions. It is hard to believe that there is such a large negative drop in the temperature and pressure of the reaction. One caveat to be kept in mind is that this could be an artifact of the equipment not being able to track the fast nature of the temperature rise and failing at this point.

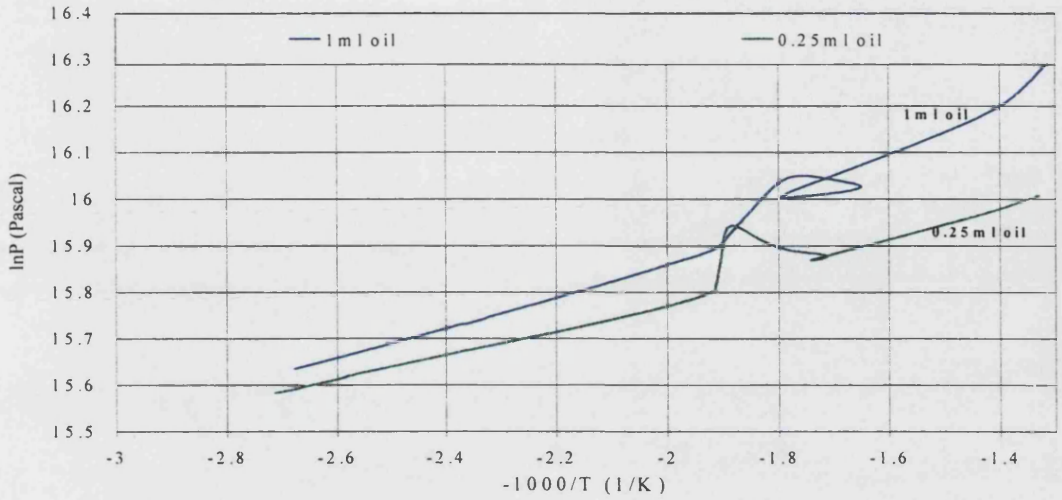

Figure 5.5: Logarithmic Plot of Pressure against –1000/T, B7 (1ml oil), B5 (0.25ml oil)

The various exothermicity parameters as defined in Chapter 4 were obtained, including the self-heat rate ratios, reaction times and energy evolved. These are shown for above mentioned experiments B7 (1ml oil) and B5, B3 and B4 (0.25ml oil) in Figures 5.6-5.8.

The data obtained for each of the reaction regions is compared by dividing the exothermicity value for each region in the 1ml oil experiment (B7) by those obtained in the 0.25 ml oil experiments (B5, B3 and B4).

It can be seen from Figure 5.6 that increasing the amount of oil increases the self-heat rate. For every reaction region in all the different experiments, there is an increase of a factor ranging from 2 to 8.

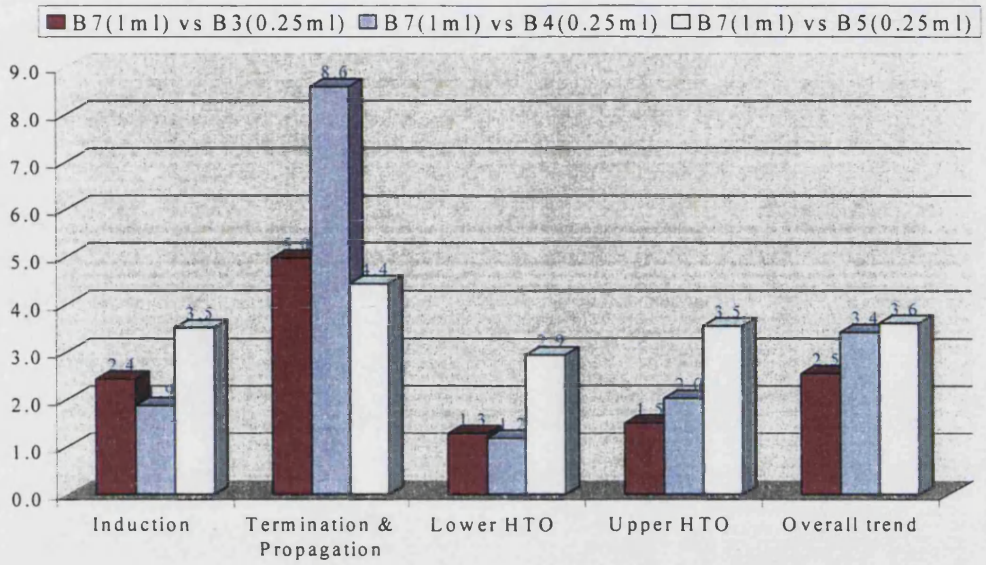

Figure 5.6: Ratio of Exothermic Self-Heat Rates, 1ml Oil B / 0.25ml Oil B

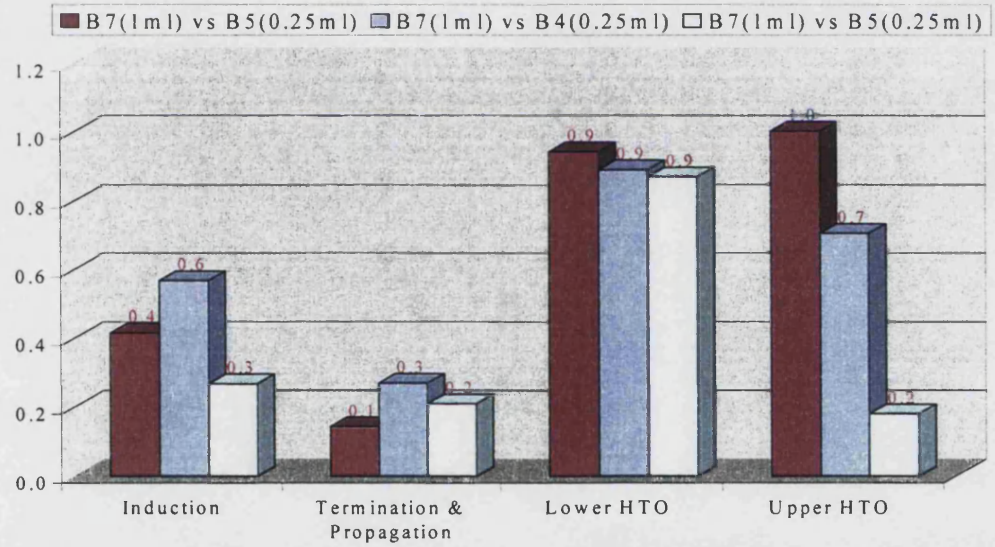

Figure 5.7: Ratio of Reaction Time, 1ml Oil B / 0.25ml Oil B

Concurrently with this increase in the self-heat rate, there was also a reduction in the reaction times for all the regions, as seen in Figure 5.7, implying a faster reaction. This would affect the amount of energy evolved from the reaction, which is a function of both the self-heating rate and the reaction time.

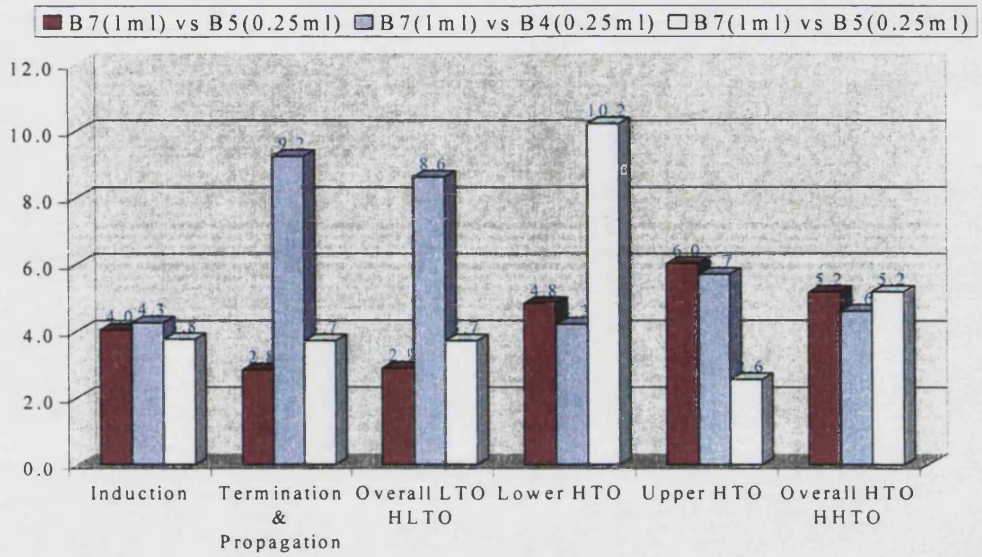

Figure 5.8: Ratio of Energy Released, 1 ml Oil B / 0.25 ml Oil B

As the energy evolved is equal to the mass x specific heat capacity x dT, the values of the ratios obtained from the raw data are multiplied by 4, (1ml/0.25ml). This takes into account the fact that four times the weight of oil in experiments B3, B4 and B5 react in B7. This gives weighted results taking into account the difference in mass of oil reacted.

The amount of energy evolved increases with the increased amount of oil reacted by a factor ranging from 2.5 to 10. This increase in the evolved energy is strongest in the lower HTO and the propagation regions.

Table 5.2 shows the amount of energy evolved overall for the LTO and HTO regions. This shows the increase in the values of each region as the amount of oil is increased. More energy is evolved in the LTO region than in the HTO for all experimental conditions, as the ELTO/EHTO ratio shows. A discrepancy can be seen in experiment B4 due to a pressure leak in the experiment.

Table 5.2: Overall Energy Released, 1 ml Oil B and 0.25 ml Oil B

Energy Evolved	B7 (1 ml)	B5 (0.25 ml)	B3 (0.25 ml)	B4 (0.25 ml)
ELTO	4489	1205	1551	521
EHTO*	389	75	75	85

* up to 500^0 C

The exothermicity behaviour with increasing amount of oil reacted is summarised in Figure 5.9. This involves taking an average of the exothermicity ratios in each region for three experiments. Increasing the amount of oil reduces the reaction time at higher self-heat rates and causes greater energy released than the run with less oil present.

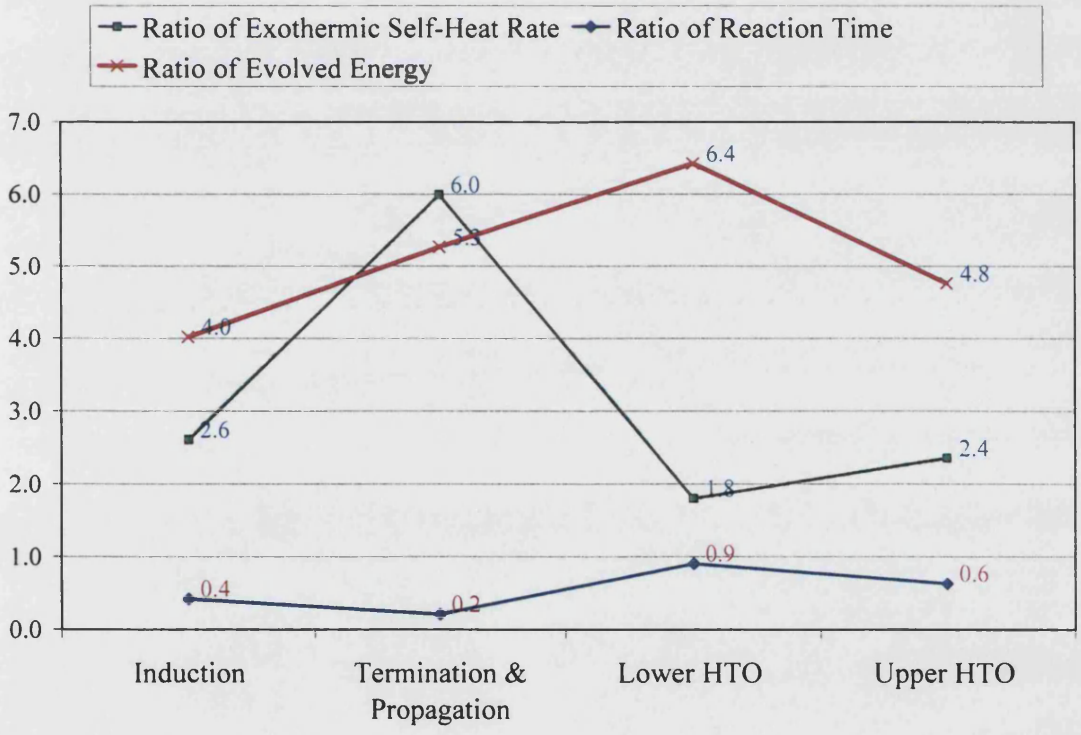

Figure 5.9: Summary of Ratios Showing Effect on Exothermicity of Increasing Amount of oil

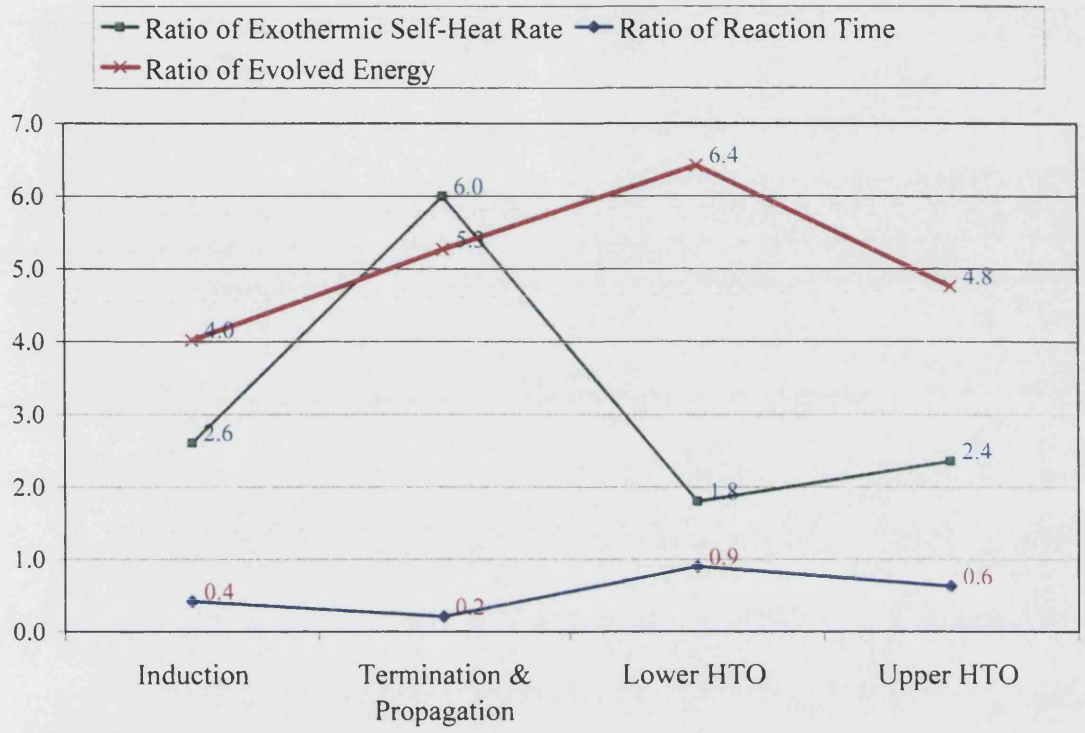

Figure 5.9: Summary of Ratios Showing Effect on Exothermicity of Increasing Amount of oil

Analysis of these results shows the need to know how much air to inject for a unit volume of oil in the reservoir. Injection of too much air will result in less energy released, as is seen by comparison of B7 with B3, B4 and B5 in Table 5.2. This could be unfavourable to the process if the thermal effect of the oxidation is important. Another way to view this parameter is to directly relate it to the concept of minimum and maximum air-oil ratios. The concept of a minimum air flux has been used in previous investigations. Nodwell et al 1997 define this as the minimum flow rate of air per unit cross-sectional area of the reaction zone which will maintain the combustion in the HTO mode, and these parameters can be obtained using this equipment.

Other experiments showing the effect of oil saturation have been carried out as part of this study, and comparisons between 0.5ml oil and 0.25ml oil show the same

trend occurring. The chief exothermicity ratios for these comparisons are shown in Appendix B.

The effects of oil and water saturation have implications for field application, in that the use of air injection might be more successful at the start of a fields' development rather than a mature field with lower oil saturations. Air injection should therefore be part of the Reservoir management program of an oil company from inception, rather than as an afterthought following water flooding, otherwise valuable oil may be lost.

5.2 Amount of Water

Large amounts of water are present in post water-flooded reservoirs, with some reservoirs having very high water saturation. Investigations by Moore et al 1992, Belgrave et al 1994 and Belgrave et al 1997 into in-situ combustion kinetics of heavy oils have noted the importance of water saturation, amongst others, as one of the parameters affecting oxidation kinetics. Moore 1993 speculated that water promotes the decomposition of the oxidised hydrocarbons. Alderman and Osoba, 1971 noted the chief effect of water in their combustion tube experiments was that it efficiently utilised the heat generated from combustion. This increased the oil recovery as heat moved from behind the combustion zone ahead of the combustion zone. The chief question therefore is whether water plays any role in the actual kinetics or if it has a favourable effect solely due to its heat transfer and fluid flow properties.

It was demonstrated by Hyne et al 1984 that H_2 and light saturated hydrocarbons were produced by aquathermolysis (steam/oil) reactions in the 200-300^0 C temperature range. In order to investigate if similar reactions are taking place in light oil oxidation it

would be necessary to analyse the product gases and this can be included in any future work on the water effect.

On the other hand, Hughes et al 1987 report that the initial water saturation had no significant effect on the fuel deposition in DSC experiments. Part of the investigation was therefore to examine the influence of water on the oxidation kinetics.

5.2.1 *Effect of Water Saturation*

The experiments to compare the effect of water are shown in Table 5.1, while the experiments are detailed in Table 3.2 and 3.3.

The adiabatic temperature profile of experiment Bw (0.25 ml oil B with 0.1 ml water @ 50 bar) and Bw1 (0.25 ml oil B with 0.5g rock @ 50 bar) is compared with B0 (no water), and this is shown in Figure 5.10. This clearly shows a retarding effect of water on the reaction in Bw/Bw1 compared to how the reaction occurred in B0, especially in the HTO region.

The adiabatic temperature plots for another set of experiments using a different oil (D) also show a retardation of the HTO reaction. These results for Drw1 (1ml water), Dr1 (0.1ml water) and Dr2 (no water), are shown in Figure 5.11.

Figures 5.12 and 5.13 show the exothermic self-heat rates for oils B and D (with and without water) respectively as a function of temperature. An examination of these plots shows that water has an inhibiting effect on the energy released, with the characteristic spike in the propagation region being greatly reduced for both oils when water is present.

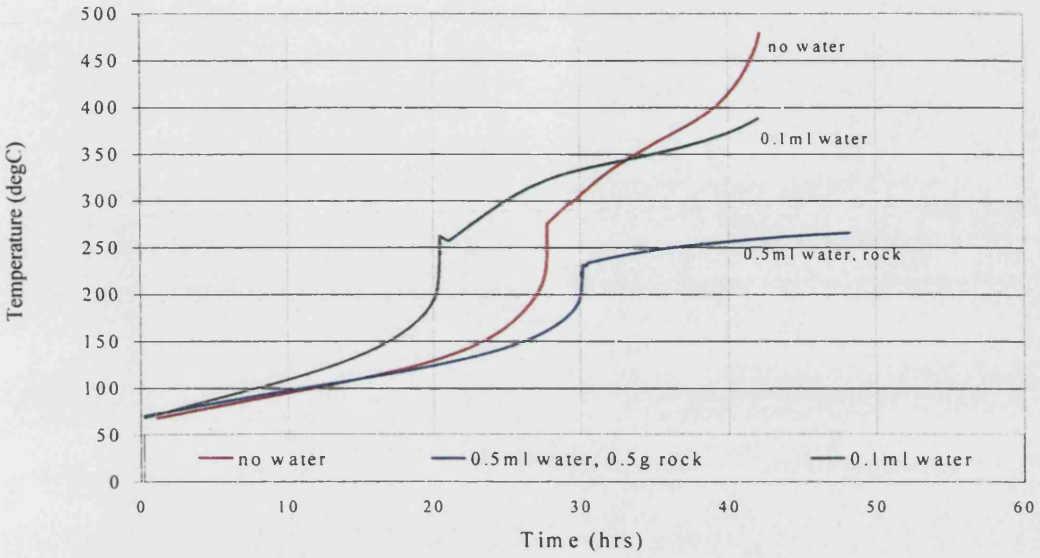

Figure 5.10: Adiabatic Temperature Profile, Bw1 (0.5ml water, 0.5g rock), Bw (0.1ml water) and B0 (no water)

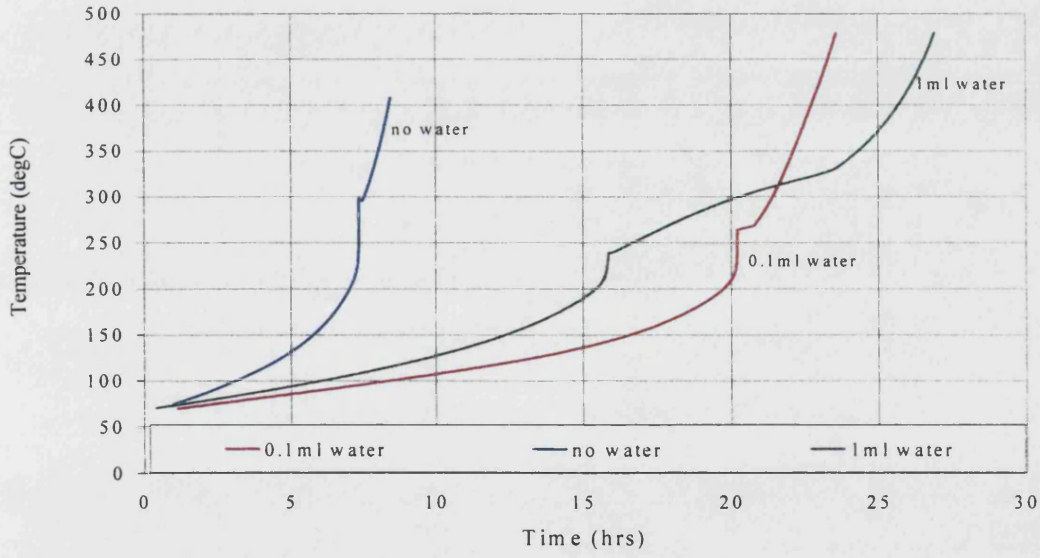

Figure 5.11: Adiabatic Temperature Profile, Drw1 (1ml water), Dr1 (0.1ml water) and Dr2 (no water)

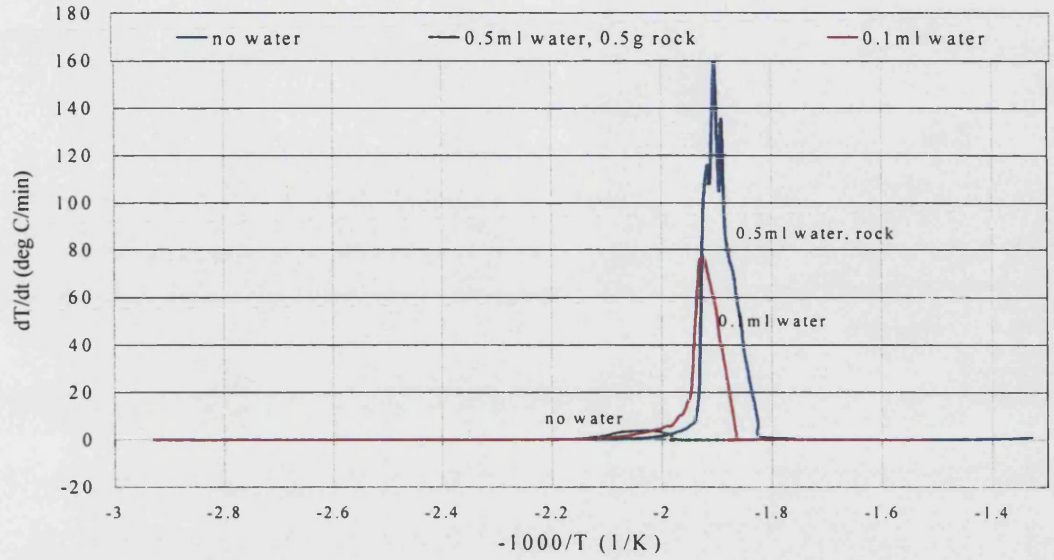

Figure 5.12: Self-Heat Rate against –1000/T, Bw1 (0.5ml water, rock), Bw (0.1ml water) and B0 (no water)

The various exothermicity parameters including the self-heat rate ratios, reaction times and energy evolved are obtained and these are shown in Figures 5.14-16.

It can be seen from Figure 5.14 that an increase in the amount of water results in a reduction in the self-heat rate in every reaction region. This has to be caused either by absorption of the heat formed during reaction or a reduction in reaction with a corresponding reduction in energy. From Figure 5.15, the reaction time is seen to increase in all the regions apart from the propagation and upper HTO region (where they are non-existent). An increase in the reaction time is expected, as a lower self-heat rate in one experiment requires a larger reaction time to reach the same temperature. From the reduced time, autocatalytic reaction in the propagation region appears to be very strongly affected by the presence of water. It could be that the peroxide reactions, which normally cause this spike, are inhibited by the presence of water.

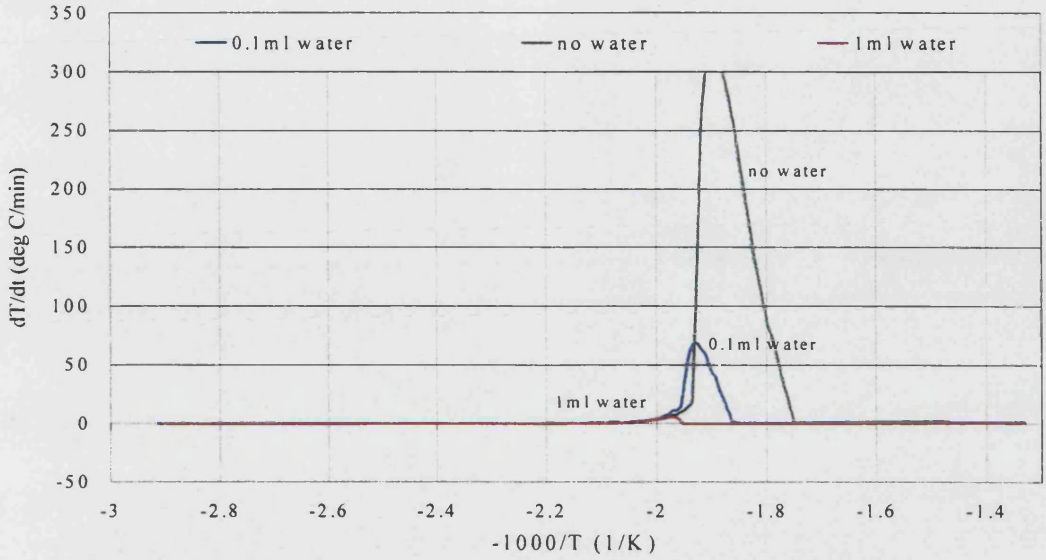

Figure 5.13: Self-Heat Rate against –1000/T, Drw1 (1ml water), Dr1 (0.1ml water) and Dr2 (no water)

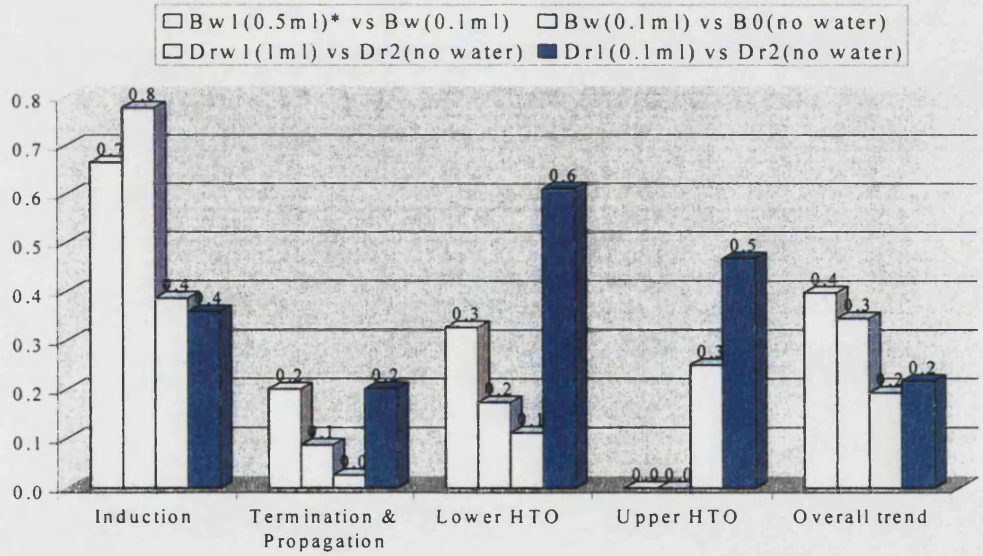

Figure 5.14: Ratio of Self-heat Rates for Comparison of High and Low Amounts of Water

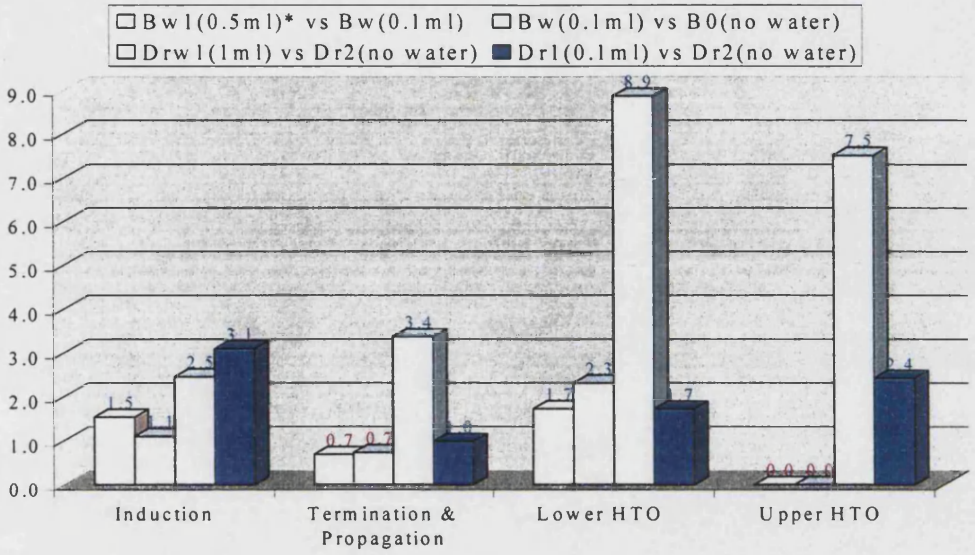

Figure 5.15: Ratio of Reaction Time for Comparison of High and Low Amounts of Water

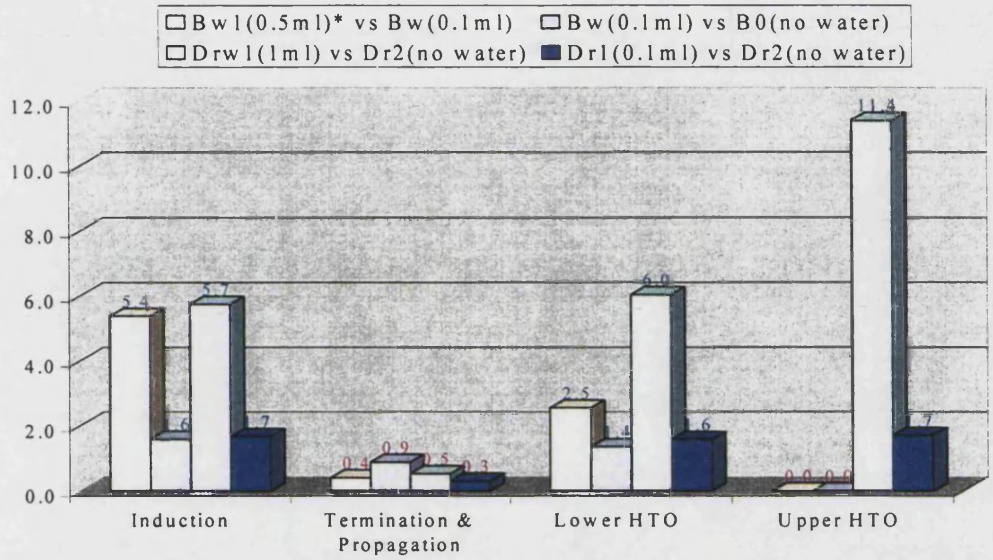

Figure 5.16: Ratio of Energy Released for Comparison of High and Low Amounts of Water

Table 5.3, which is a ratio of the energy released in each region, shows a reduction in the ELTO for Oil D when water is added, which is the same for oil B but occurs over a longer period.

Table 5.3: Overall Energy Evolved, Increasing Amounts of Water for Oils D and B

Energy Evolved	Dr2* (none)	Dr1* (0.1ml)	Drw1* (1ml)	B0 (none)	Bw (0.1 ml)	Bw1* (0.5 ml)
ELTO	1147	508	1238	418	418	522
EHTO	151	248	1357	94	58	109

Where * signifies addition of 0.5grock as well as water.

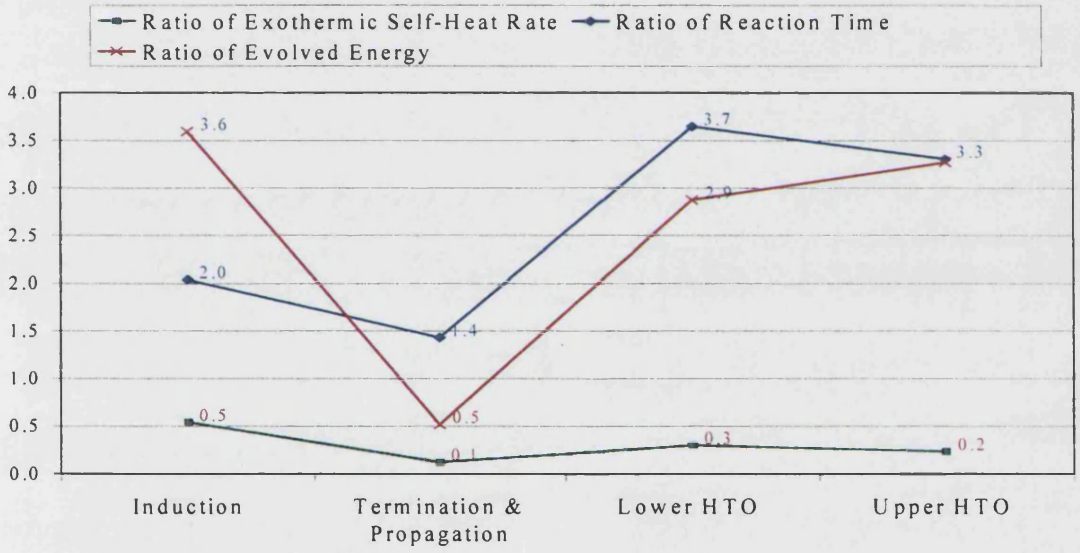

Figure 5.17: Summary of Ratios Showing Effect on Exothermicity of Increasing Amount of Water

The exothermicity behaviour with an increase in the amount of water present is summarised in Figure 5.17. This is done by taking an average of exothermicity ratios in each region for the four experiments with 0.1ml or no water, and comparing with that for 0.5ml and 1ml water. The presence of water is strongly inhibiting in the propagation region, while it has little or no effect on the induction region. For oil B the presence of

water extinguishes the upper HTO reaction entirely. This illustrates the importance of examining each of these regions separately as different effects can occur.

5.3 Effect of Pressure

Exothermicity is also affected by pressure; previous work by Tiffin and Yannimaras, 1997 claim that pressure does indeed have a significant effect on the oxidative kinetics of crude oil. Thomas et al 1979 demonstrated that operating pressure had no effect on activation energy but it did affect the Arrhenius constant. Work by Bae 1977 also showed that oxidation starts at a higher temperature as the pressure is decreased and the low temperature heat generation increased with pressure. Yoshiki and Philips, 1985 studied low and high temperature oxidation rates and found that they increased with pressure, as did their exothermicities. Hughes et al 1998 in unpublished work, carried out high pressure DISC reaction on four light oils. The results indicated a decrease in oxygen consumption as total pressure was increased. Similar results are reported again by Hughes et al 1987. This was attributed to a reduction in the amount of carbon burned at critical pressure, due to a reduction in fuel deposition. Other factors included an increased mobility of the crude oil due to high pressure and a shift in the oxidation being mass controlled and flux dependent, rather than being kinetically controlled.

As was discussed in Chapter 2, investigation of high pressure reservoir effects (Yannimaras et al 1991, Tiffin and Yannimaras, 1997) revealed that air injection is applicable in high pressure light oil reservoirs. It was seen that these processes are more likely to occur, or do so more significantly at higher reservoir temperatures and pressures, partly because the fuel deposition potentially increased at higher pressures.

The major field implication of operating at higher pressures is the need to operate at higher air injection rates to sustain the combustion. It is possible that there may be insufficient fuel at the combustion front as pressure increases since this increased pressure contributes to increasing oil displacement through several mechanisms. Rashidi and Bagci, 1991 also noticed increasing fuel deposition with increasing pressure and attributed it to the effect of pressure on the oil volatility.

Abu-Khamsin et al 1988 found that operating pressure affected the fuel deposition through the influence exerted on distillation, as less material is distilled at higher pressures.

Ren et al 1999 observed from SBR experiments that in the presence of crushed reservoir core, the LTO reaction rate for light oils at low temperatures (100 to 140 ^{0} C) is not significantly affected by the total or oxygen partial pressure when the amount of oil is in excess. It was also found that high pressure does not increase the LTO rate, and would result in a higher required injection rate.

Hughes et al 1987 in DSC experiments at atmospheric pressure noticed that an increase of oxygen partial pressure caused a reduction in the activation energy of the coke oxidation. Belkharchouche et al 1988 and Lukyaa et al 1994 observed, using the same apparatus, that although heat released increased with increasing total pressure and oxygen content, this effect stopped at concentrations greater than 40 %.

Kok et al 1997 found in their DSC cell that an increase in total pressure results in an increase in the heat evolved by the heavy crude oil (18.5 ^{0}API) for liquid combustion. A general trend of decreasing activation energy with increasing pressure was also noticed.

The effect of pressure on fuel deposition is probably the most important effect during the oil oxidation process. Even in the study of in-situ combustion of heavy oils, the conventional model of fuel laydown and oxidation worked well only at lower pressures, < 6 MPa. Moore et al 1990 described the unstable behaviour of some combustion tube experiments run with Athabasca Oil Sands at high pressures.

Air injection into the light oil West Hackberry Field was reported by Gilham et al 1997. Two types of reservoirs were present, a low-pressure (300 to 500 psi) salt dome, and a high pressure reservoir (2500 to 3500 psi). Dramatic production response was obtained in the low pressure reservoir, while the high pressure reservoir had not yielded a production response. Whilst this could have been caused by other factors indigenous to these reservoirs, it does raise the question of whether air injection into light reservoirs can be unfavourable when the reservoir pressure is high.

5.3.1 *Effect of initial pressures*

Graphs showing the data obtained from the experiments and the resulting analysed data are shown below for experiments Dr1 and Dr5. These compare the differences between the results acquired for experiments with 0.25 ml oil D at 50 bar and at 0 bar. In Figure 5.18, the thing most evident about the plot of the experiments at 50 and 0 bar is the similarity between the two profiles. The major difference is in the propagation period of Dr1, which appears to be absent at the low pressure of Dr5. Apart from this, it appears that the major mechanisms still occur even, at the very low pressures.

The exothermicity parameters including the self-heat rate ratios, reaction time, and energy evolved are obtained for the above mentioned experiments Dr1 and Dr5.

Some other experiments are analysed and the results shown, specifically experiments at 100 and 50 bar (B1 and D2 against experimentsB3, B4, B5 and D3 respectively). Figure 5.19 shows the self-heat rate plot for the experiments at 50 and 0 bar, and it can be seen that the exothermicity of the experiment is greatly reduced at the lower pressure. The propagation spike normally seen practically disappears.

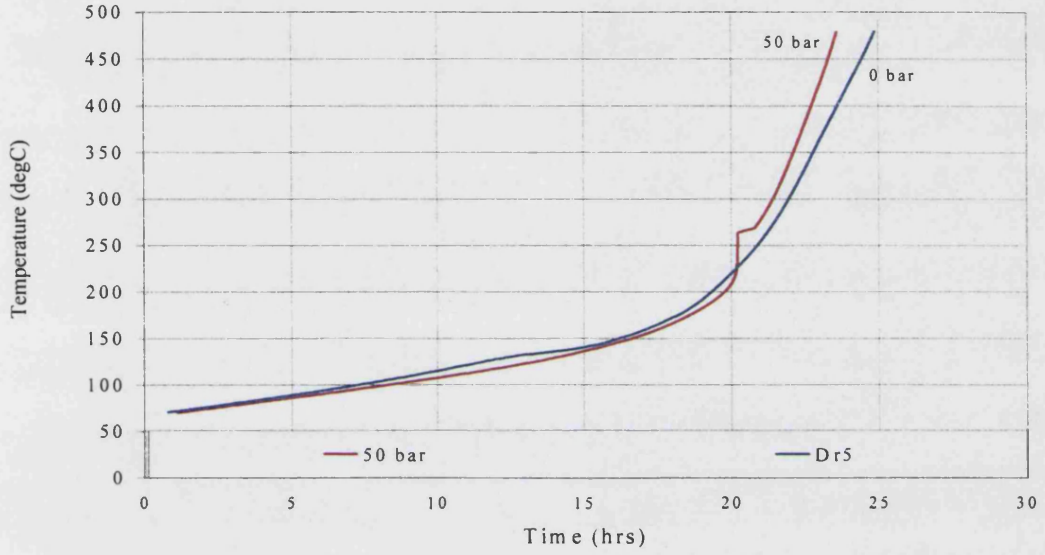

Figure 5.18: Adiabatic Temperature Profile, Dr1 (50 bar) and Dr5 (0 bar)

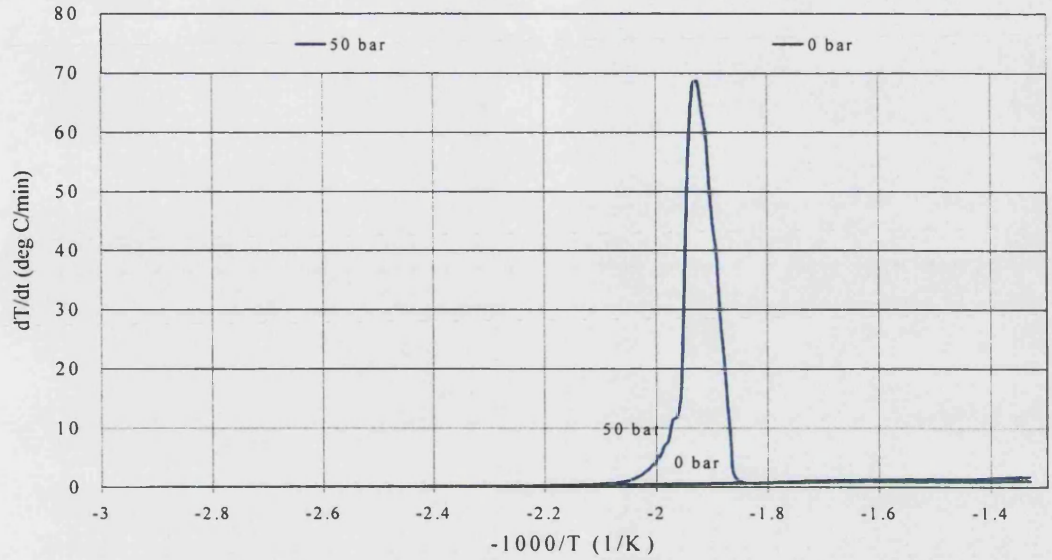

Figure 5.19: Self-Heat Rate vs –1000/T Dr1 (50 bar) and Dr5 (0 bar)

Figure 5.20, which shows the reaction rate constant at 50 and 0 bar, is interesting because the two experiments have exactly the same profile over the induction region, and a similar one over the HTO region. The main difference occurs at the propagation region, but overall it shows a similar mechanism.

Figure 5.21 shows a comparison of results for oil B at higher pressures, 100 and 50 bar. The mechanisms appear to be the same but the times at which they occur changes.

The self-heat rates of the experiments as shown in Figure 5.22, reveal that at 100 bar, autocatalytic ignition starts at an earlier temperature than those at 50 bar but the self-heat rate profiles are similar.

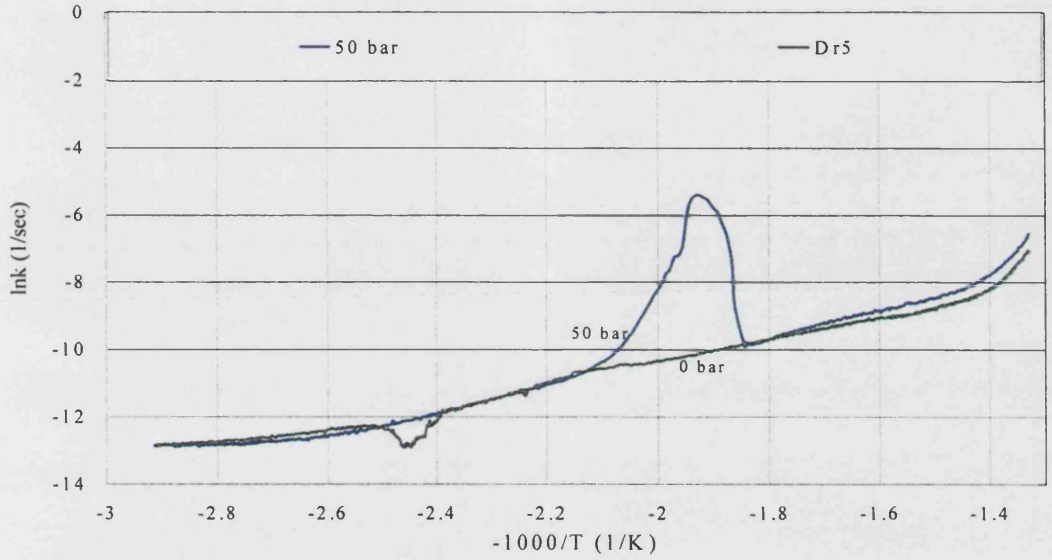

Figure 5.20: Reaction Rate Constant against –1000/T, Dr1 (50 bar) and Dr5 (0 bar)

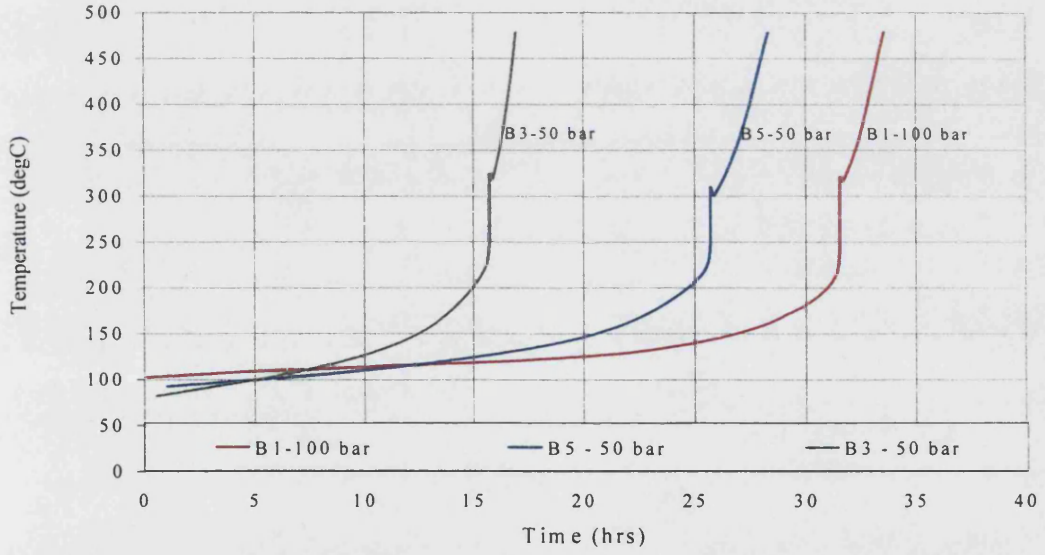

Figure 5.21: Adiabatic Temperature Profile, B1 (100 bar), B5 (50 bar) and B3 (50 bar)

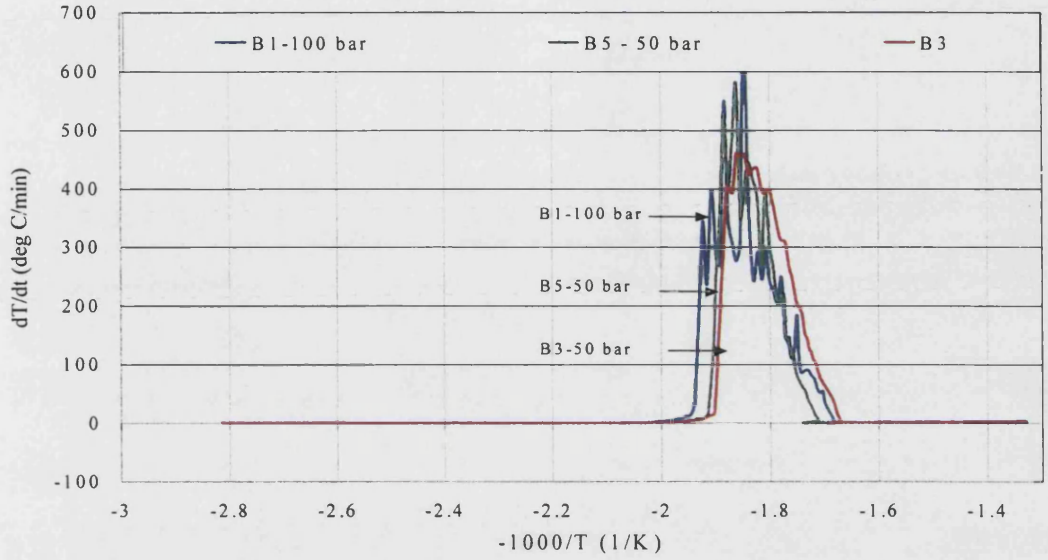

Figure 5.22: Self-Heat Rate vs –1000/T, B1 (100 bar), B5 (50 bar) and B3 (50 bar)

The ratios of the self-heat rate, which are shown in Figure 5.23, do not reveal any overall clear trend of the effect of pressure. The behaviour of Oil D appears to be opposite to that of Oil B.

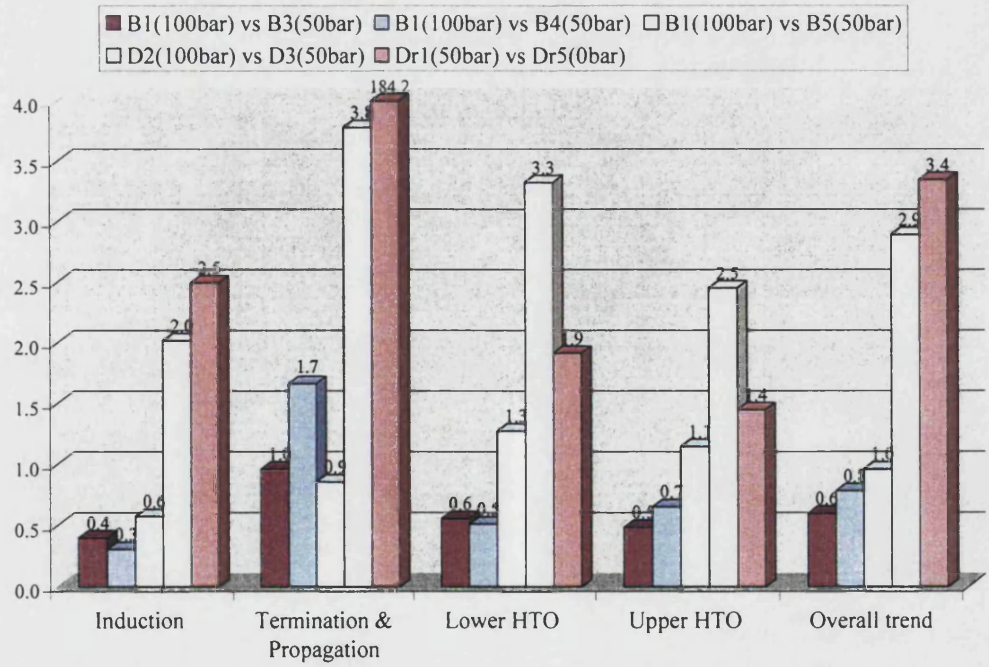

Figure 5.23: Ratio of Self-heat for Comparison of High and Low Pressures

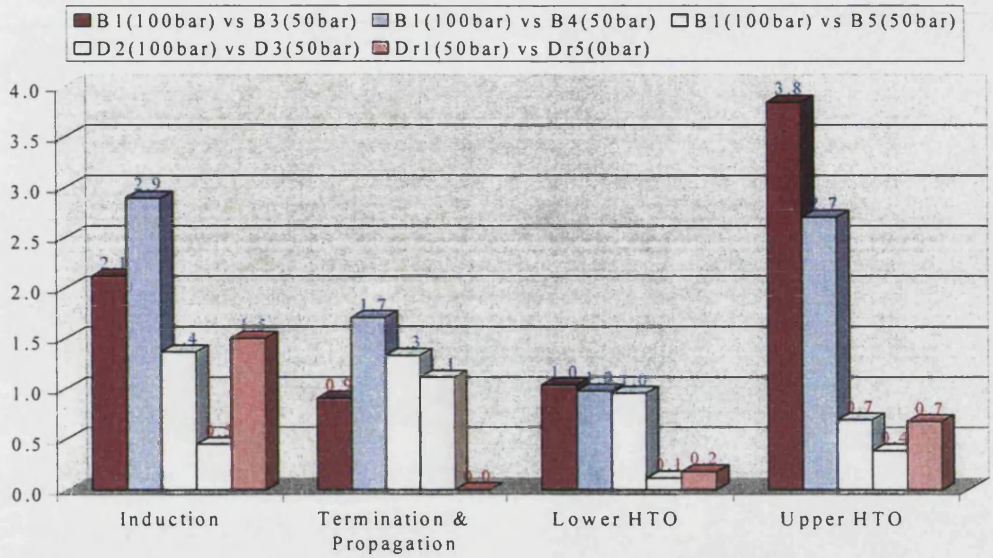

Figure 5.24: Ratio of Reaction Time for Comparison of High and Low Pressures

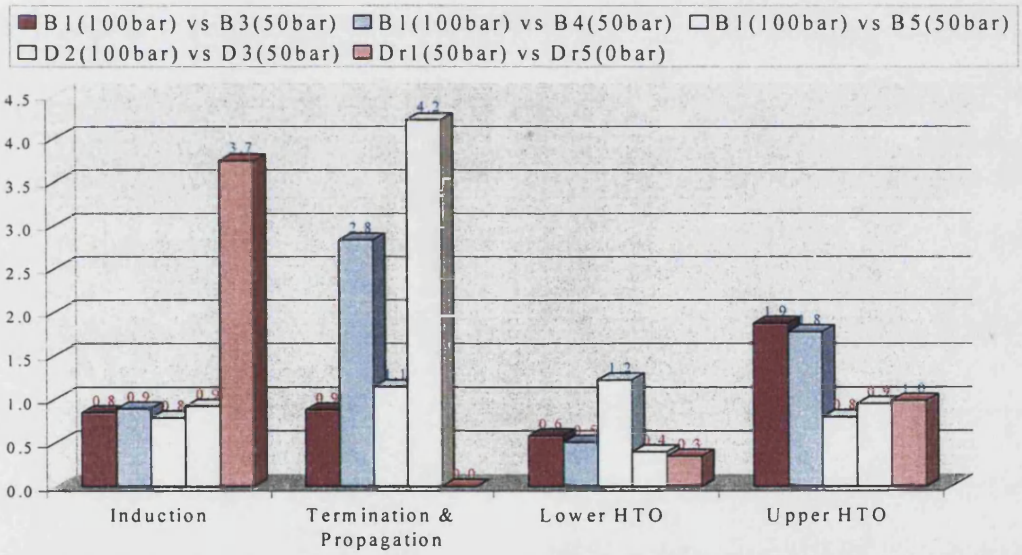

Figure 5.25: Ratios of Energy Evolved for Comparison of High and Low Pressures

Figure 5.25 shows the ratio of energy evolved, indicating a reduction in the induction region for all the 50 to 100 bar experiments, but an increase for the 0 to 50 bar experiment. The propagation region appears similar at both pressures but there is a large increase from 0 to 50 bar. The energy evolved by lower HTO reaction appears to be reduced in all reactions at higher pressures.

Table 5.4: Energy evolved, Runs at Different Pressure (Oil B)

Energy Evolved	B1 (100)	B5 (50)	B3 (50)	B4 (50)
ELTO	1348	1205	1551	521
EHTO	71	75	75	85

Table 5.5: Energy evolved, Runs at Different Pressure (Oil D)

Energy Evolved	D2 (100)	D3 (50)	Dr1 (50)	Dr5 (0)
ELTO	1894	504	508	54
EHTO	48	79	248	456

A summary of the exothermicity effect for increasing pressure for oil B from 50 bar to 100 bar is shown in Figure 5.26. This shows a reduction of the energy evolved in the induction and HTO regions when the pressure is increased. However, these results are the opposite of that obtained with oil D, which could be a function of oil type as opposed to the increasing pressure.

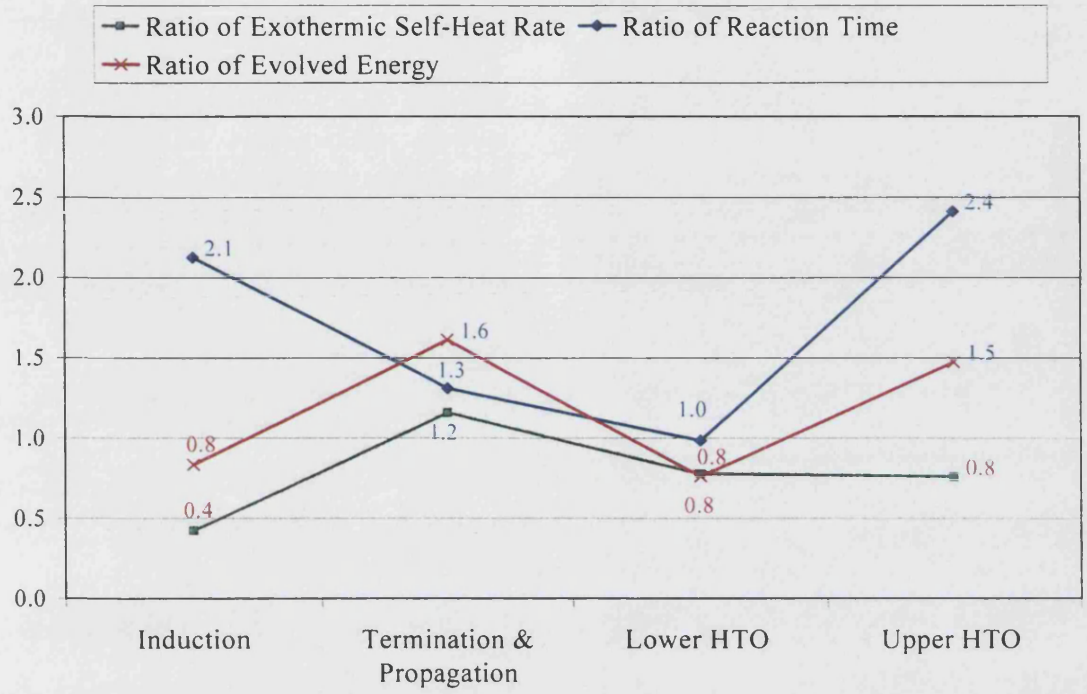

Figure 5.26: Summary of Ratios Showing Effect on Exothermicity of Increased pressure

It is comparatively simple to see the effect of pressure between a very low pressure such as zero bar and a higher one. As the pressure increases however, it becomes more difficult to assess this effect. Judging from the conflicting results obtained by comparing oils B and D with an increase in pressure, it is very likely the effect of pressure is oil specific and should be studied on an individual basis.

5.4 Oil Type

Kisler and Shallcross, 1996 using an EVA method at low pressure found that the oxidation kinetics of a 40.2 ^{0}API crude could be modelled using three competing reactions, as opposed to the usual two used for heavy oils. They also found that LTO in light oils resulted in the production of carbon oxides, which did not happen for heavy oils.

Bae in his study of the thermo-oxidative behaviour of fifteen crude oils could not find any correlation in terms of crude API gravity or crude viscosity. Kok and Okandan, 1997 obtained correlations between the mean activation energy of crude oils and the API gravity or peak temperature. The mean activation energy of the crude oils increased as the API gravity of the crude oil decreased.

The effect of oil saturation and crude oil type, specifically oil viscosity, Conradson residue H/C ratio and ^{0}API gravity on fuel deposition, studied by Alexander et al 1962 has been detailed earlier in chapter 2.2.2.

Pusch and Ranjbar-Hamghawandi, 1991 used a reactor to test the pyrolysis of medium and heavy crude oils. They found that there was a clear dependency of the fuel yield on the composition of oil based specifically on the total colloids content of the oil. The type of oil has also been frequently analysed based on the saturate, resin, aromatic and asphaltene, or colloidal content, and this is detailed in chapter 7.

Kok et al 1997 found that as pressure increased with a light oil (36.1 ^{0}API), there was an enhancement of the oxidation of the liquid hydrocarbon (LTO) as opposed to higher temperature coke combustion (HTO). This was attributed to the light nature of the crude oil, which made it more susceptible to liquid phase oxidation. The increased pressure reduced distillation of the lighter fractions and thereby increased the amount of material available for reaction. The difference noticed between this lighter oil and the heavier ones (18 ^{0}API) was that there was more heat released in the LTO region than there was at the HTO region. The heavier oils had produced more heat in the HTO zone than in the LTO zone. Kok and Karacan, 1998 found that as crude oil becomes heavier the cracking activation energy increased.

Ranjbar 1995 observed a reduction in fuel deposition with light and medium oils compared with heavy oils, attributed to distillation of the lighter fractions.

As has been detailed earlier in Chapter 2, Kok and Karacan (1997) observed a lower LTO starting temperature for the 26 °API medium oil (300 °C) than for the 14.95 °API heavy oil (310 °C). They also noted that more fuel was formed in the MTO region for the heavy oil than was formed with the medium oil. The heavier oil also gave off more heat than the medium light oil during the HTO region in the DSC experiments.

Hughes et al 1987 reported lower activation energies for light oils than for heavy oils with other experimental conditions being the same.

5.4.1 *Effect of different types of oil*

Graphs showing the data obtained from the experiments and the analysed data resulting from this are shown in Figures 5.27 - 5.29, for a medium heavy oil (Maya), in the presence of rock and water, compared with light oils A, B and D.

Other comparisons were made between the exothermicity and reactivity results for the light oils (A-D) using the experiments with 0.25 ml whole oil alone. This analysis was to see if any trends could be observed for the light oils, or if the oils could be assessed on their exothermicity or reactiveness based on viscosity or API gravity. The oils increase in viscosity in the order B, C (same value as B), D, and A, while the API gravity increases in the order A, B, C (again same as B), and D. The exothermicity results for this analysis are shown in Appendix B.

However, no general trends could be observed and the results do not show a specific variation based on these oil parameters. This could be because the oil API

gravity and viscosity are actually very similar (Table 3.1) and more variation in these parameters would be required to observe the trend.

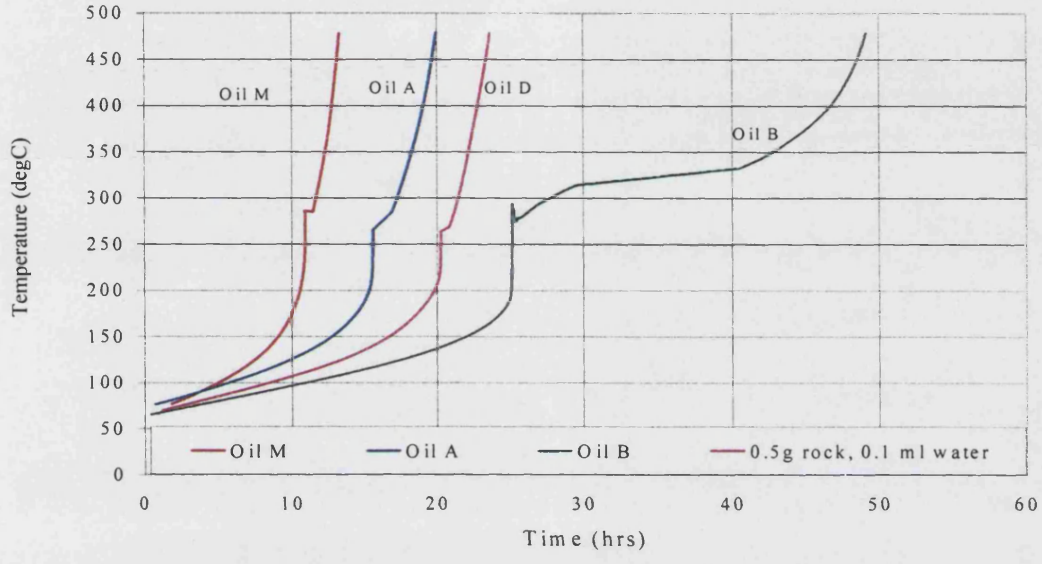

Figure 5.27: Adiabatic Temperature Profile, Medium Heavy Oil (Oil M) and Light Oils (A, B, D)

Figure 5.27 shows the trend in the temperature profile. As the viscosity of the oil increases, the induction period increases. The reaction of oil M which is the heaviest oil occurs in the shortest period, followed by A, D and then B.

The self-heat rate of oils M, A, C and D are shown in Figure 5.28 and clearly shows that the heavier oil M has the highest self-heat rate in the propagation region. The differences between the remaining light oils are not as great.

Figure 5.29 shows the reaction rate constant plot and from this plot it is obvious that the same reaction mechanism takes place for all the oils.

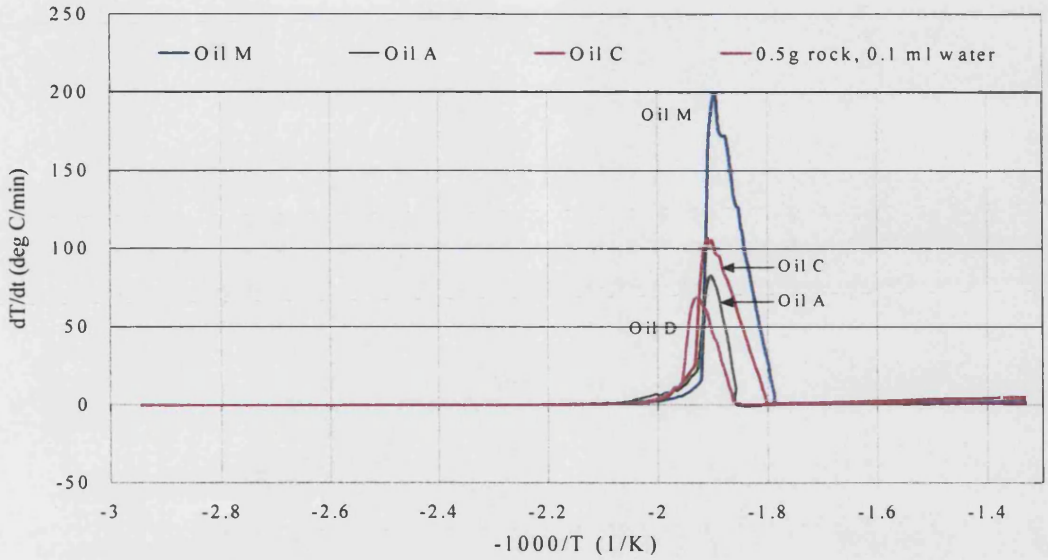

Figure 5.28: Self-Heat Rate against –1000/T, Medium Heavy Oil (Oil M) and Light Oils (A, B, D)

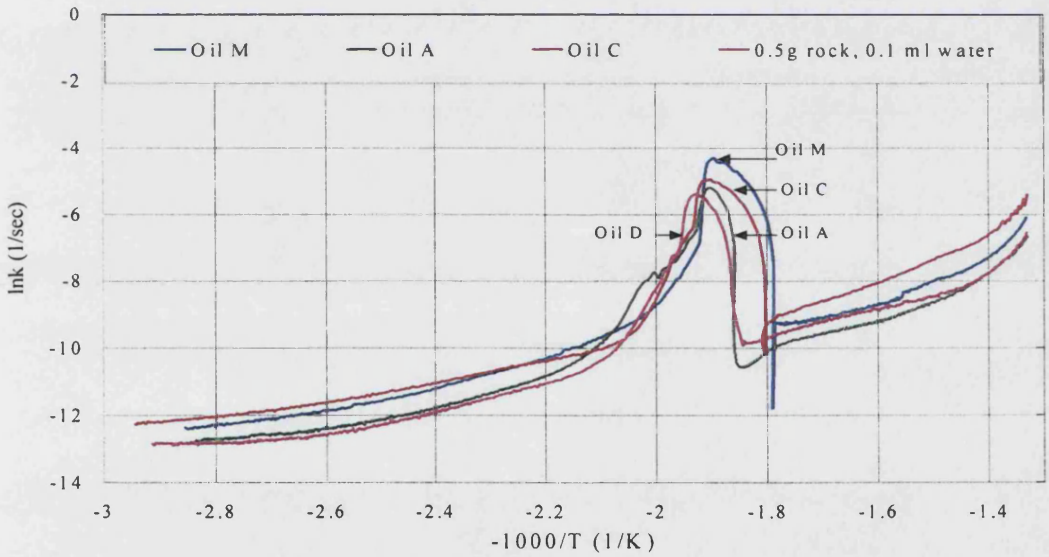

Figure 5.29: Reaction Rate Constant against –1000/T, Medium Heavy Oil (Oil M) and Light Oils (A, B, D)

The exothermicity ratios comparing the medium heavy oil to the light oils are shown in Figures 5.30-5.32. From Figure 5.30, the self-heat rate is higher in virtually every region with the heavier oil M than it is for all the other oils. Figure 5.31 shows the

ratios for the reaction time. An interesting result from this is the reaction time in the propagation region. Examination of the other reaction times for most of the other comparisons made previously in this chapter generally show the same trend. Normally an increase in the self-heat rate ratio is almost always accompanied by a reduction in the reaction time. However, Figure 5.31 shows an increase in the propagation region reaction time ratio. This means that not only is there a higher rate of energy released, but it occurred for a longer period in the heavier oil, implying much higher energy released values.

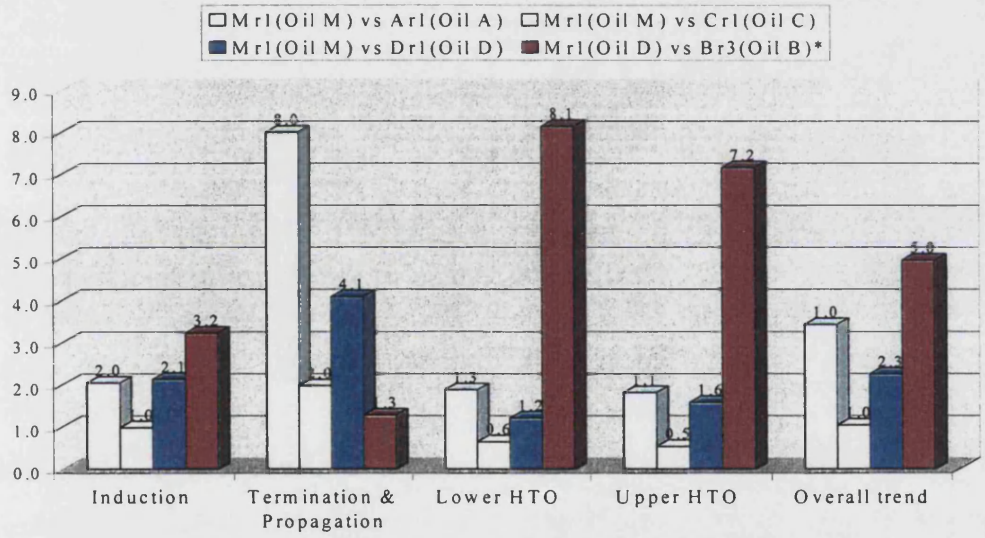

Figure 5.30: Ratio of Self-heat Rates for Comparison of Medium Heavy and Light Oils

This can be verified by inspecting Figure 5.32, which shows a huge increase in the energy released primarily in the propagation region, although the ratio is greater than 1 for every region studied.

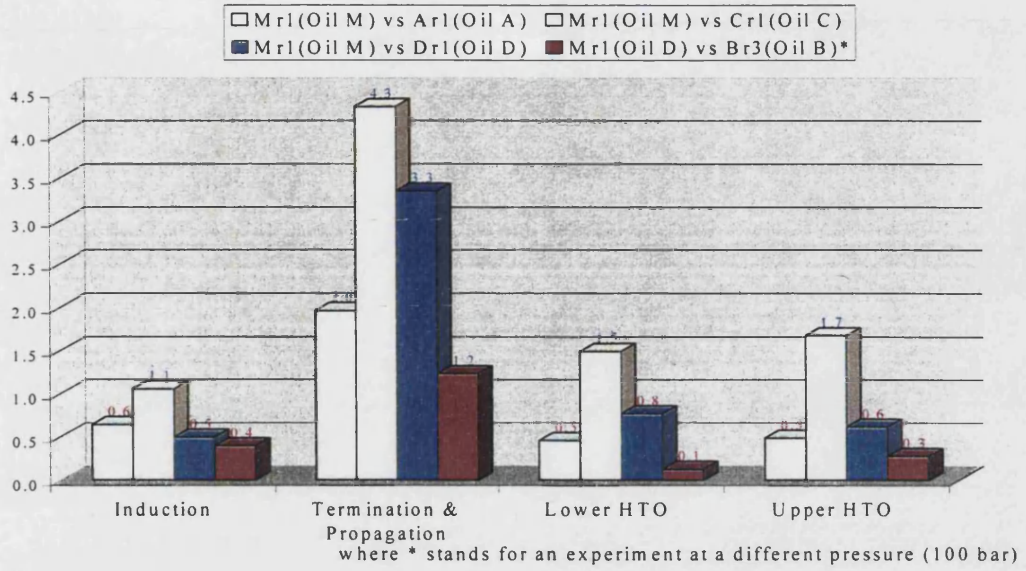

Figure 5.31: Ratio of Reaction Time for Comparison of Medium Heavy and Light Oils

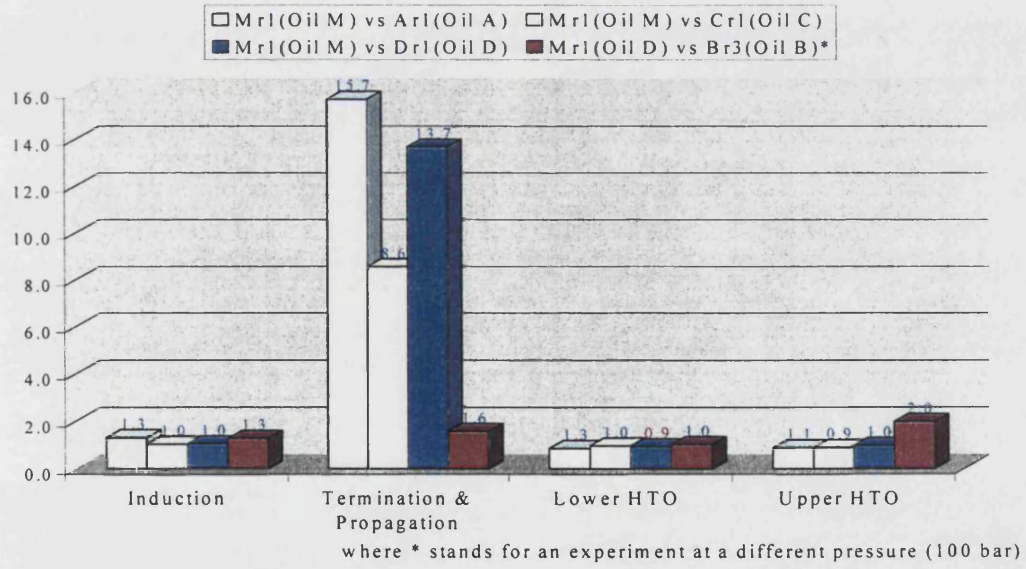

Figure 5.32: Ratio of Energy Released for Comparison of Medium Heavy and Light Oils

An examination of the energy released values in Table 5.6 again confirms this result, with the energy released from oil M in the LTO region being far greater than that for the lighter oils. The medium heavy Maya oil is very susceptible to LTO as well as HTO.

Table 5.6: Energy Released For Medium Heavy and Light Oils

Energy Evolved	Mr1	Ar1	Br3	Cr1	Dr1
ELTO	4489	430	2839	696	508
EHTO	241	271	168	257	248

The exothermic behaviour with increase in oil viscosity and API density is summarised in Figure 5.33 by taking an average of all the exothermicity ratios for oils A, B, C and D compared with M.

This clearly shows the substantial increase in the self-heat rate, reaction time and energy evolved for the heavier oil. It remains to be confirmed if this trend extends to very heavy oils with much lower API gravity. Traditionally, heavy oils are more favourable candidates for in-situ combustion, and it is likely the energy released in the HTO region will be much higher for these types of oils.

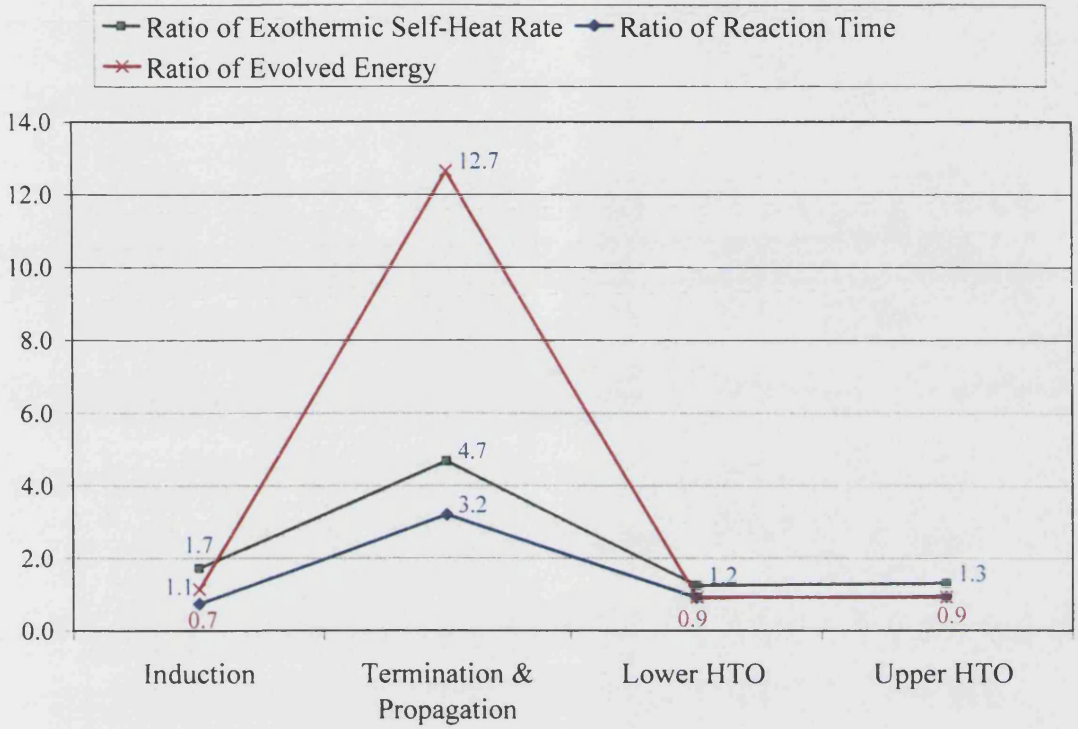

Figure 5.33 Summary of Ratios Showing Effect on Exothermicity of Increasing Oil Viscosity and API Gravity

CHAPTER 6:

Effect of Reservoir Rock on Crude Oil Oxidation Kinetics

EFFECT OF RESERVOIR ROCK ON KINETICS

Aside from the factors discussed in Chapter 5, a very important parameter which was previously thought to affect the oil oxidation, is the presence of reservoir rock. Crude oil reservoirs contain different types of reservoir rock and these may have a significant effect on the oxidation processes. Different types of reservoir rock include sandstone, clay, chalk or limestone. Clay, silica and alumina are classified as solid acid catalysts. Their catalytic activities are related to their acid site density and acid strength. Fassihi et al 1984 and others work have observed different kinetic behaviour between natural reservoir cores and clean sand matrices. This difference was attributed to the presence of metallic additives and clay in the natural reservoir matrix.

Metals are well known for their catalytic potential in both hydrocarbon cracking and oxidation reactions. Fassihi et al 1984 observed a catalytic effect from the addition of metallic additives such as copper, nickel, vanadium and iron. Drici and Vossoughi, 1987 also found that the presence of heavy metal oxides traditionally used as chemical catalysts in the reservoir rock had no significant impact on the oxidation reactions when a large surface area such as silica was used. On the other hand, when sand alone was used, there was a catalytic effect in the HTO region due to greater fuel deposition. The catalysts studied included vanadium, nickel, ferric oxides and titanium oxide. Castanier and Brigham, 1997 studied the effect of metallic additives on the in-situ combustion of two oils of 18.5 and 10.5 ^{0}API respectively. The results indicated increased fuel laydown for iron, tin, zinc and aluminium, while copper, nickel and cadmium salts had little or no effect. Iron and tin appeared to be the additives that best increased fuel deposition.

Table 6.1: Experimental Analysis to Study Effect of Reservoir Rock

	Effect of rock	Clay	Silica	Chalk
Differences between Experiments	***0.5g rock and water / none*** Ar1 / A0, Cr1 / C0, Dr1 / D3	***Clay / Rock D*** Dr_c2 / Dr1	***Silica / rock*** Dr_s1 / Dr1	***Chalk / Rock*** Dr_ch1 / Dr1
	2.0g rock and water / none Dr3 / D3, Br2 / B0	***Clay / Chalk*** Dr_c2 / Dr_ch1	***Silica / Chalk*** Dr_s1 / Dr_ch1	***Chalk / Phillips*** Dr_ch1 / Dr_p1
	2.0g rock / 0.5g rock Dr3 / Dr1	***Clay / Rock A*** Dr_c2 / Dr_p1	***Silica / Rock A*** Dr_s1 / Dr_p1	
		Clay / Silica Dr_c2 / Dr_s1		

Various reservoir rock types used included Sandstone, Chalk, silica (Buckland sand) and crushed reservoir core from two different North Sea Reservoirs. The reservoir cores are sandstones and are primarily a mixture of quartz, silica and clay. The experiments carried out to investigate the effect of rock are shown in Table 6.1.

6.1 Effect of Reservoir Rock on Kinetics

A number of studies have been previously conducted into the effect of different types of reservoir rock on the oxidation of crude oil. In experiments carried out by Chu, 1971, sandstone was found to catalyse the methane oxidation reaction. The question of how the state of the rock affects the reaction has also been addressed. Alexander et al 1962 observed that crushed core material gave the same fuel availability as the original consolidated core, noting that the main difference would arise from the porosity differences and the fluid flow effects. Other investigators have noticed a difference between the oxidation with the crushed rock and that with the original reservoir matrix.

A number of previous studies have stated that the most important factor affecting fuel deposition is the surface area of the rock matrix material. Vossoughi et al 1985 performed combustion tube tests with sandpack rock of different surface area (surface areas of 76, 317, 1120, and 3332 cm^2/g). Sustained combustion in a 19.8 ^{0}API oil was only observed in the run with the greatest surface area.

It is also important to delineate the possibly separate effects in the LTO and HTO regions. Kisler and Shallcross, 1997 found that the LTO region showed no correlation with the grain size. Ren et al observed that the presence of reservoir core increased the LTO reaction rate. Dabbous and Fulton, 1972 studied the LTO of crude oils in porous media and found that the order of reaction was dependent upon the type

of crude but independent of the porous medium properties. The activation energy of the reaction was found to be insensitive to the type of crude or porous medium. Drici and Vossoughi 1985 report a very strong surface area effect on LTO, with an increase in the LTO peak occurring with increasing surface area. Addition of the solid surface to the crude oil causes a shift of a large amount of the heat produced in the HTO to the LTO zone. A reduction in the activation energy is observed after addition of the solid surface area to the crude oil.

Kisler and Shallcross saw an increase in the activation energy and the exponential factor in the HTO region as grain size was reduced.

The fuel deposition and combustion process under in-situ combustion conditions has been studied by several investigators. Fassihi et al 1984 found that the deposition of fuel occurs on the matrix. In the absence of a matrix in the experiments, which is the situation when oil alone is reacted with air, fuel may be deposited on the surface of the bomb, but this should occur only at low rates. However, when reservoir rock is used there should be an appreciable increase in the amount of fuel deposited with a corresponding rise in the vigour of the fuel combustion reaction.

Effect of rock

The kinetic parameters and exotherms obtained with the oil alone in the bomb and that acquired in the presence of reservoir rock and water were compared.

Graphs showing the self-heat rate data obtained from the experiments and the resulting analysis show the difference between the results acquired with 0.5g rock and those with no rock for oils A, C and D. These results are shown in Figures 6.1-6.3. All of the different oils show the same trend, with the self-heat rate reducing during the propagation stage when rock is added. The difference in exothermicities when 2.0g rock

is added instead of the whole oil is also shown for oils B and D in Figures 6.4-6.5. In addition, to investigate the cumulative effect of the rock, the exothermicity difference between addition of 2.0g and 0.5g rock is shown in Figure 6.6. The same trend as described earlier occurs, with a reduction in the propagation self-heat rate with the addition of rock.

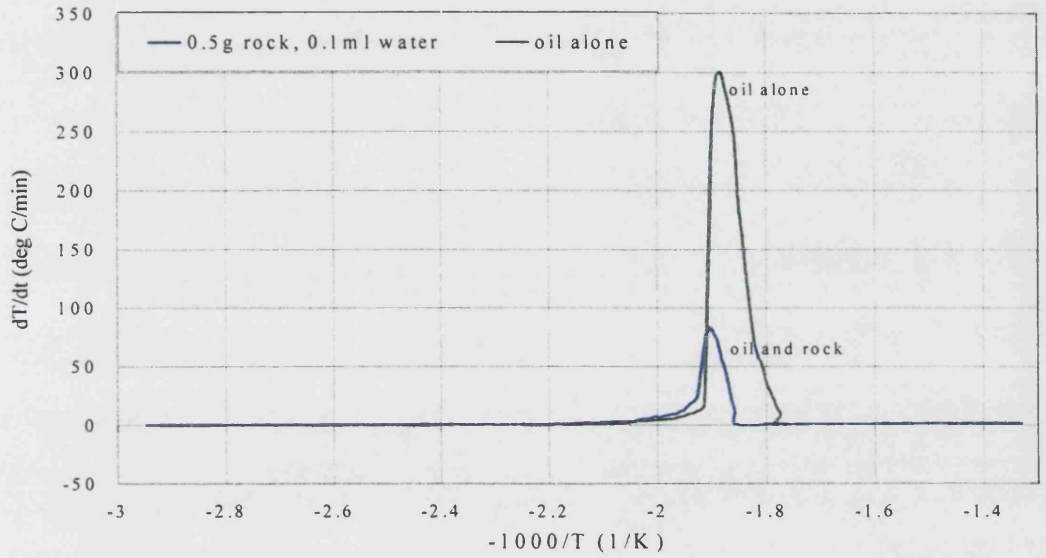

Figure 6.1: Self-Heat Rate against –1000/T, Ar1 (0.5grock, 0.1ml water) and A0 (oil alone)

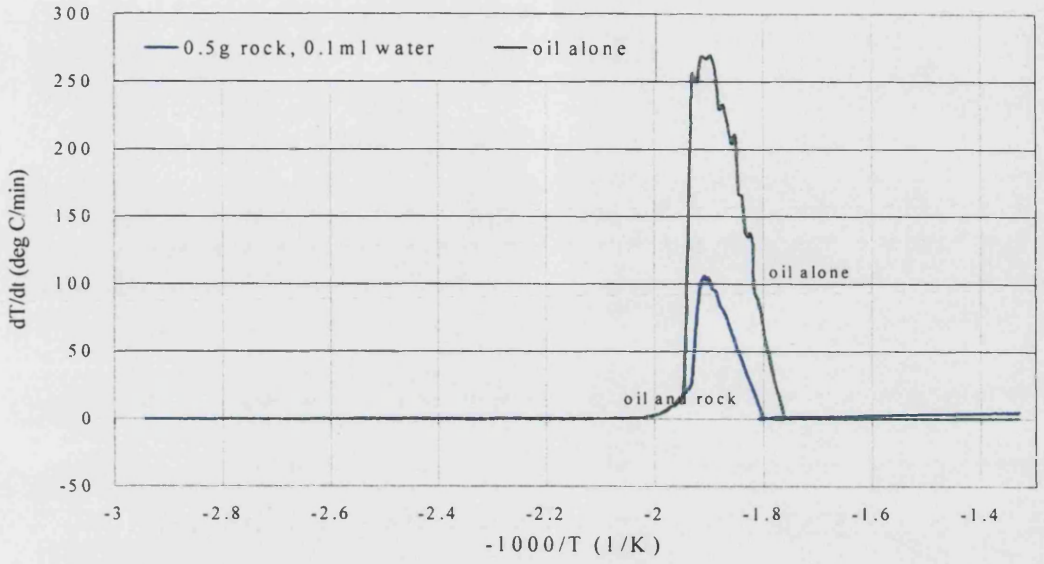

Figure 6.2: Self-Heat Rate against –1000/T, Cr1 (0.5grock, 0.1ml water) and C0 (oil alone)

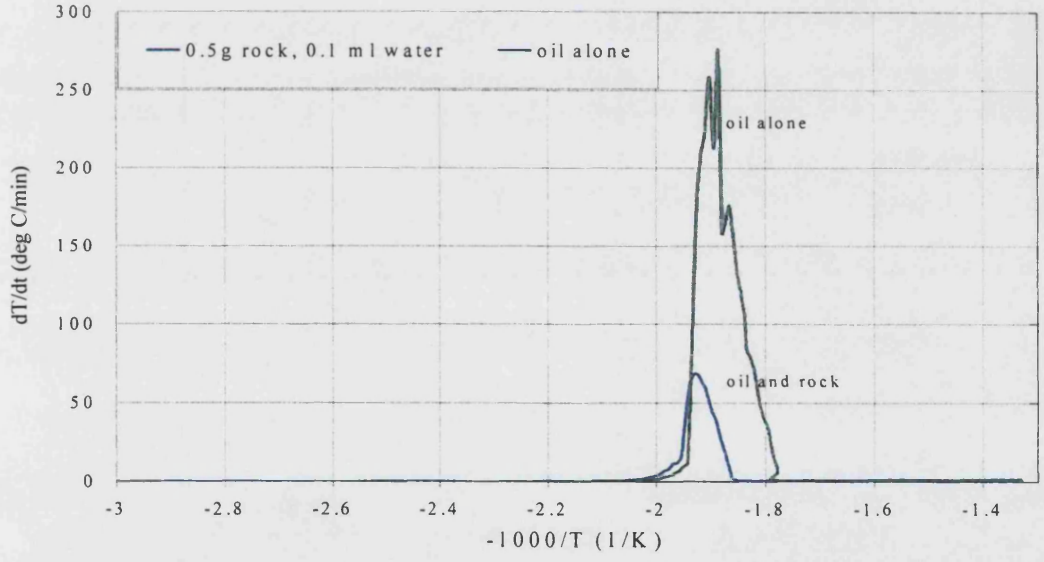

Figure 6.3: Self-Heat Rate against –1000/T, Dr1 (0.5grock, 0.1ml water) and D3 (oil alone)

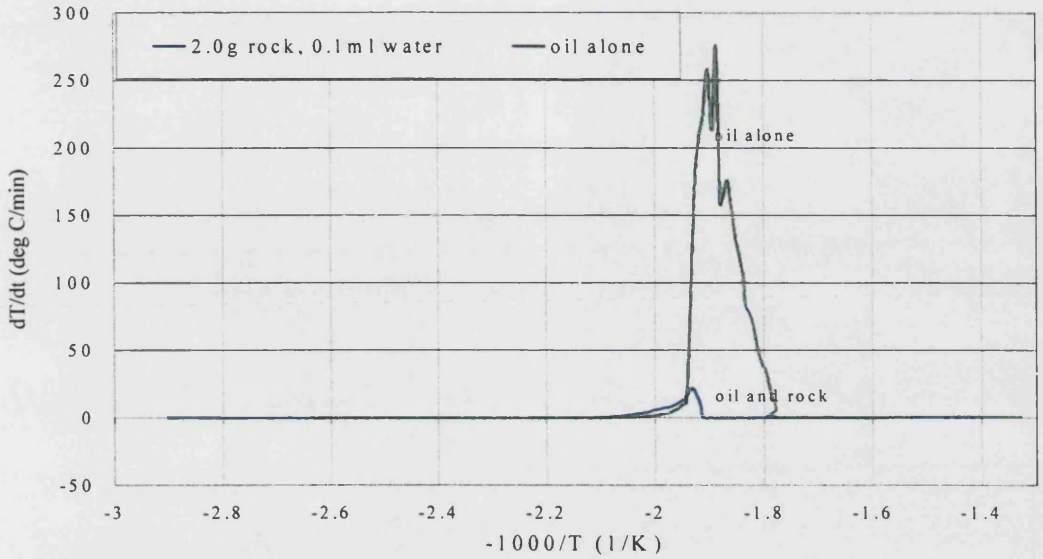

Figure 6.4: Self-Heat Rate against –1000/T, Dr3 (2.0grock, 0.1ml water) and D3 (oil alone)

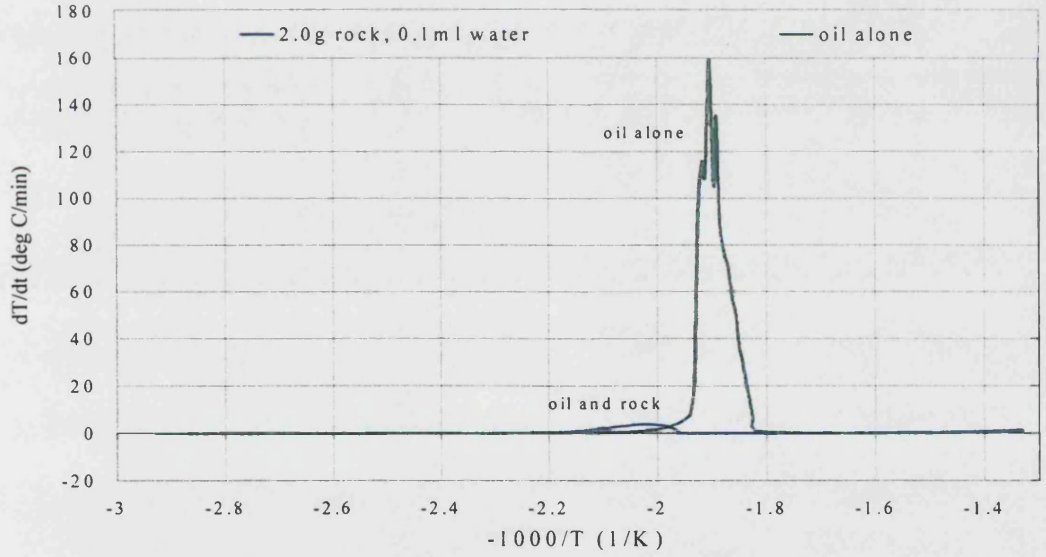

Figure 6.5: Self-Heat Rate against –1000/T, Br2 (2.0g rock, 0.1ml water) and B0 (oil alone)

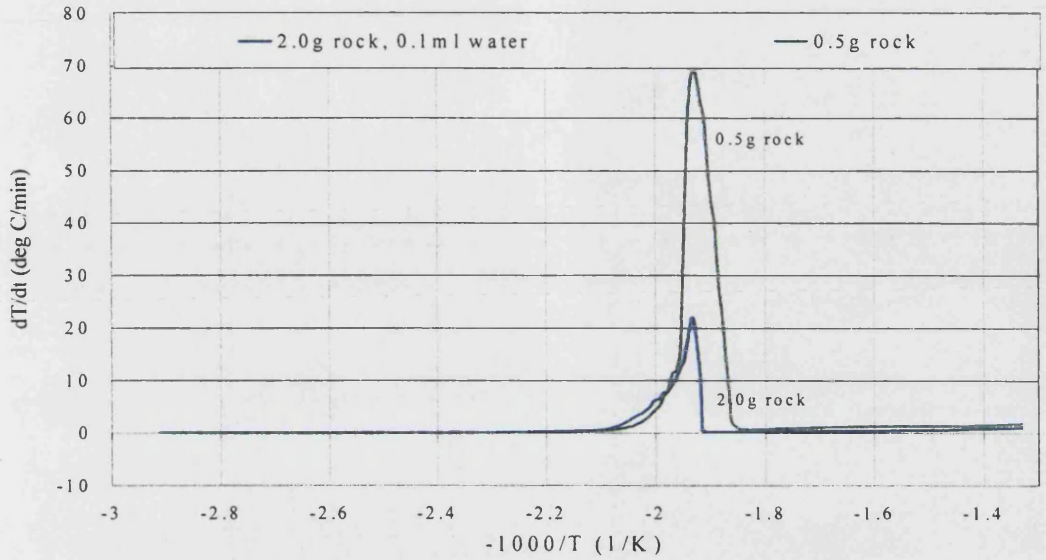

Figure 6.6: Self-Heat Rate against –1000/T, Dr3 (2.0g rock) and Dr1 (0.5g rock)

From Figure 6.6, the same trend in the self-heat rate occurs in the propagation region when 2.0g rock is added. There is also a reduction in the other reaction regions.

The various exothermicity parameters including the self-heat rate ratios, reaction times and energy evolved are shown in Figures 6.7-6.9.

An inspection of Figure 6.7 shows that the self-heat rates are increased with the addition of rock in every region apart from the propagation region. This implies some sort of catalytic contribution by the rock to the reaction, which does not occur in the propagation stage.

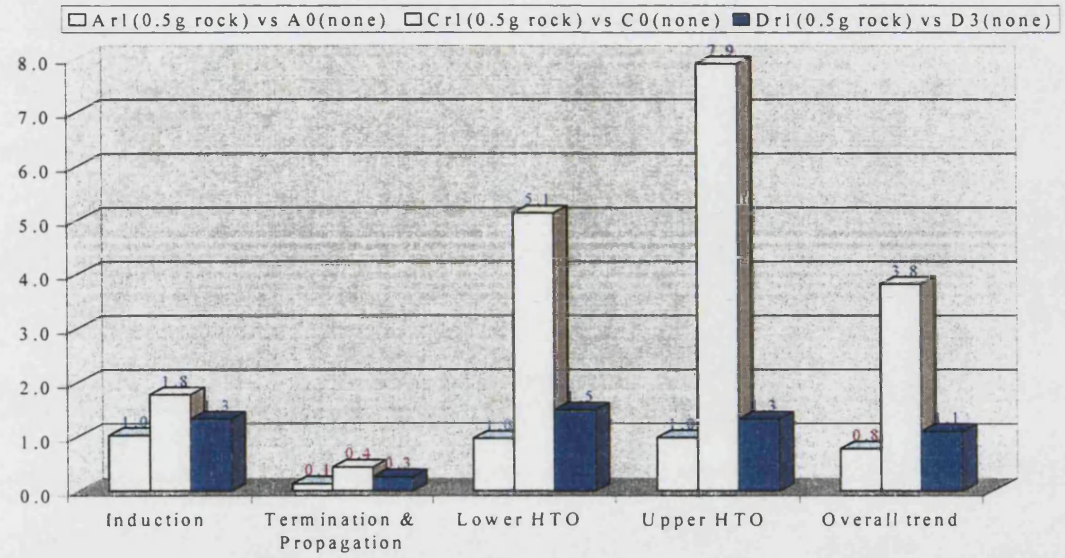

Figure 6.7: Ratio of Self-heat Rates for Comparison of 0.5g Rock with zero Rock

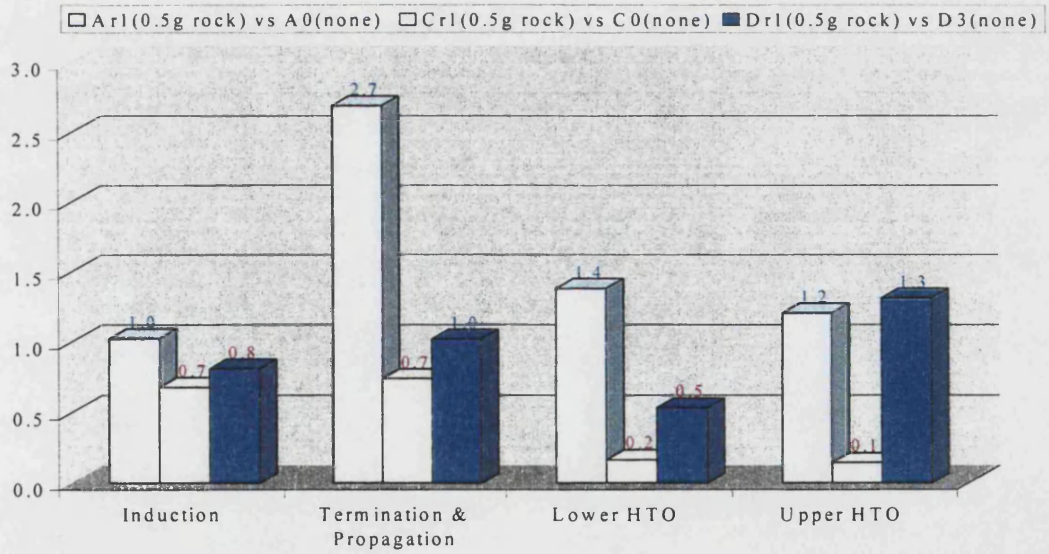

Figure 6.8: Ratio of Reaction Time for Comparison of 0.5g Rock with zero Rock

Figure 6.9 shows a reduction in the reaction time for the induction region when 2.0g rock is added to the oil, compared to the results for 0.5g rock and no rock. All other reactions experience an increase in the reaction times.

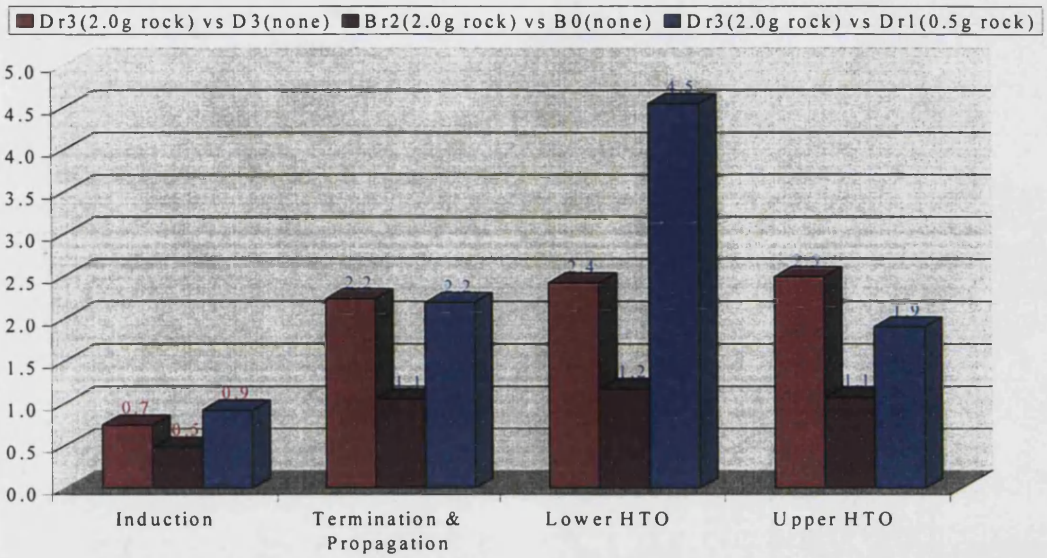

Figure 6.9: Ratio of Reaction Time, Comparison of 2.0g Rock / 0.5g and no Rock

The energy released from the different experiments is compared in Tables 6.2 and 6.3. This shows a reduction in the energy evolved in the LTO region when rock is added. This is due to the reduction in the propagation region exothermicity. There is however an opposite result for the HTO region, with an increase in energy released.

Table 6.2: Energy Released with Reservoir Rock (Oil A and B)

Evolved Energy	A0	Ar1	B0	Br2*
ELTO	348	430	418	359
EHTO	81	271	94	634

Where* signifies 2.0g rock added

Table 6.3: Energy Released with Reservoir Rock (Oil C and D)

Evolved Energy	C0	Cr1	D3	Dr1	Dr3*
ELTO	625	696	504	508	620
EHTO	95	257	79	248	533

Where* signifies 2.0g rock added

The exothermicity behaviour with an increase in the amount of oil reacted is summarised in Figure 6.10-6.11 by taking an average of the exothermicity ratios in each region for the different experiments carried out. These results give an indication of the crude oil oxidation behaviour in a real reservoir. An inspection of Figure 6.10 shows that an increase in the amount of rock in the experiments results in a decrease in the energy evolved during the propagation region. As the amount of rock increases, the results obtained from the PHI-TEC experiments move closer to those obtained for the reservoir.

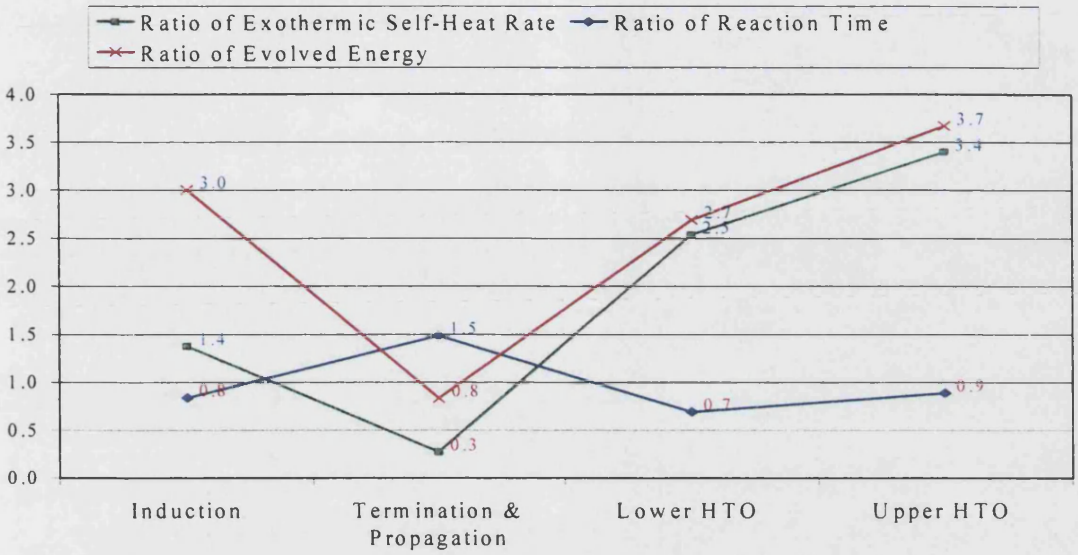

Figure 6.10: Summary of Ratios Showing Effect on Exothermicity of Adding 0.5g rock

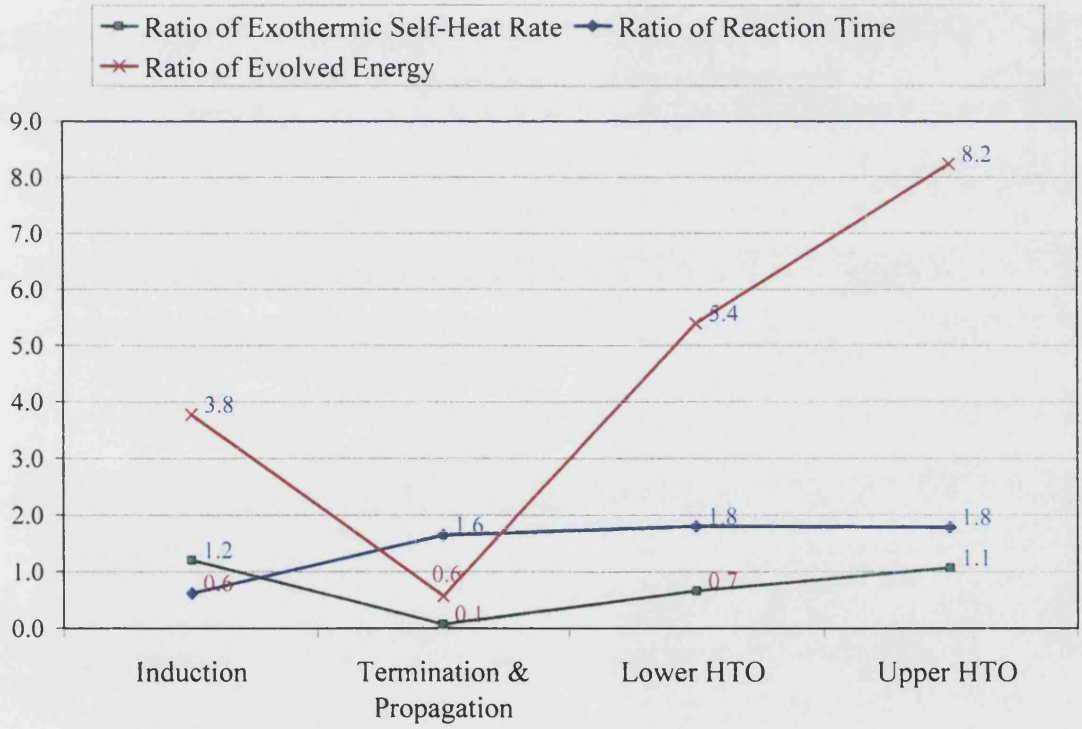

Figure 6.11: Summary of Ratios Showing Effect on Exothermicity of Adding 2.0g rock

This reduction in energy evolved during the propagation region increases when the amount of rock is 2.0g rather than 0.5g. This is shown in Figure 6.12 where the ratio of energy evolved reduces from 0.8 to 0.6 when the amount of rock is increased from 0.5g to 2.0g. If this trend were to continue, it is likely that the propagation region phenomena would disappear at very high rock amounts. In this event the reaction taking place would most likely follow a different mechanism. This reduction in the propagation region probably happens because of heat absorption of the rock. The rock therefore acts as a heat sink and prevents the very vigorous propagation reaction seen with oil alone.

In spite of this reduction in the propagation region, the amount of energy evolved in the HTO region increases with the amount of rock. The rock appears to absorb some of the heat formed in the LTO reactions, hence slowing down the reaction rates till it reached the HTO stage where it actually catalyses the reaction. This trend could also imply higher exothermicity in the HTO regions in the reservoir as the amount of rock increases.

This relationship is best represented using the phi factor described earlier in Chapter 4, and hypothetical phi-factors have to be calculated for the reservoir itself. This involves obtaining values for the average specific heat capacities, and the average oil and water saturations in areas of the reservoir. By building a model of this process, the thermal effect in the reservoir arising from air injection can then be calculated, taking into consideration the thermal conductivity of the particular reservoir rock.

In conclusion, the rock provides a catalytic effect for the reaction in the induction region, as well as the HTO region, while it inhibits the propagation region. A possible explanation for this could be due to the increased surface area provided

through the rock. The oil has accelerated free radical mechanisms in the induction region, as seen by the reduced reaction time in Figure 6.9 and 6.11. However, termination of these reactions on the rock surface is also accelerated, and the free radicals do not reach the critical concentration necessary for the autocatalytic induction to occur. Once the reaction moves to the HTO region, the increased surface area again causes accelerated reaction. This trend is confirmed again in Figure 6.12 which shows the cummulative effect of adding 2.0g rock compared with 0.5g rock.

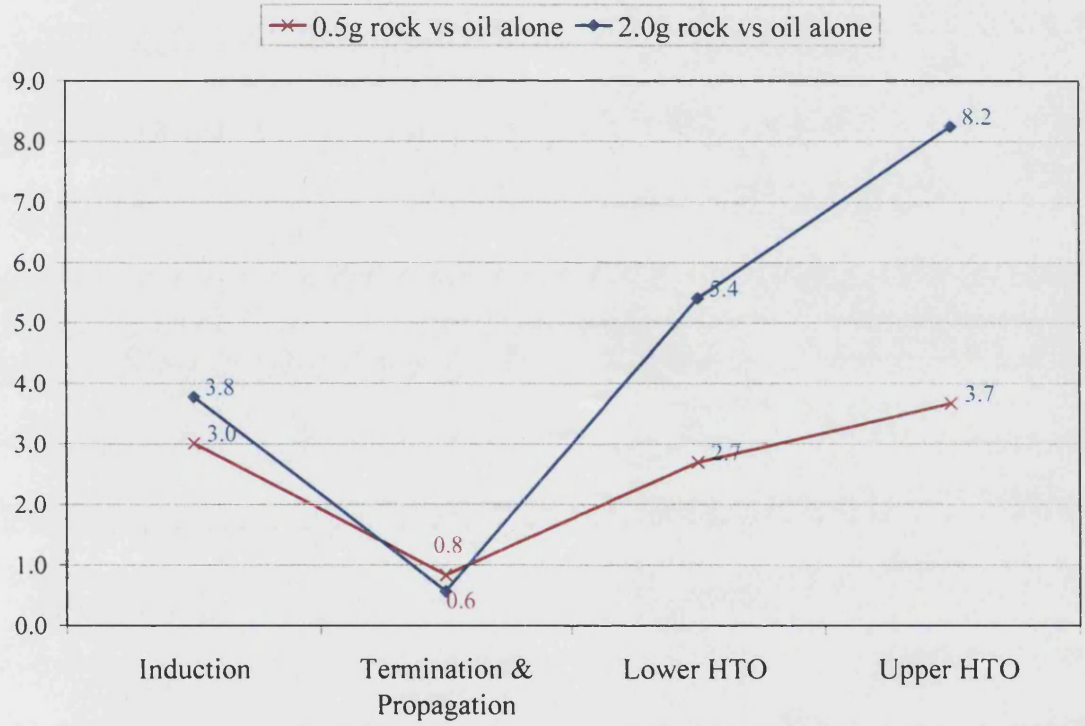

Figure 6.12: Comparison of the Ratio of Energy Evolved for 0.5g and 2.0g of Rock / Oil Alone

6.2 Clay

Clay comprises mostly alumina, silica, and water (Al_2O_3. SiO_2 . $2H_2O$), along with smaller amounts of other materials, such as Fe_2O_3. There are a great number of

different clays in nature, due to the geological conditions of formation of clay beds. They are generally characterised by their fine particle size and chemical stability. Different naturally occurring clay minerals include kaolinite, illite, bentonite and montmorillonite.

It has been shown using differential scanning calorimeter (DSC) and thermogravimetric analysis (TGA) that the presence of clay in the reservoir rock enhances the fuel deposition and the oxidation. Drici and Vossoughi, 1985 attributed this to the high surface area of clay. Vossoughi et al 1985 and Rashidi and Bagci 1991 observed a reduction in the activation energy of the crude oil combustion as a result of adding clay to the crude oil/sand mixture. Fassihi et al 1984 and Ranjbar 1993 report that activation energy and arrhenius constant values decrease with an increase in the clay content, as well as increasing combustion heat released. Numerous studies have been carried out to investigate how the clay fractions present in reservoir rock affect the amount and reactivity of fuel deposited for oxidation, under In-situ combustion and these have been detailed earlier in Chapter 2.2.2. Clay fractions of the matrix tend to have the highest surface area and generally possess catalytic properties towards organic liquids. Ranjbar 1997 in a pyrolysis study of heavy oil fractions of two crude oils found that the higher surface area of clay minerals lead to increasing coke deposition inspite of that particular rock having a lower total specific surface area. This would imply that the catalytic effect of clay is stronger than the surface area effect, at least in the HTO area. All of these studies primarily addressed the HTO region, and few could be found on the LTO effect of clay.

Effect of clay

Graphs showing the data obtained from the experiments and the resulting analysis show the difference between the results acquired with 0.5g rock D and those for experiments with clay, chalk, rock A and silica.

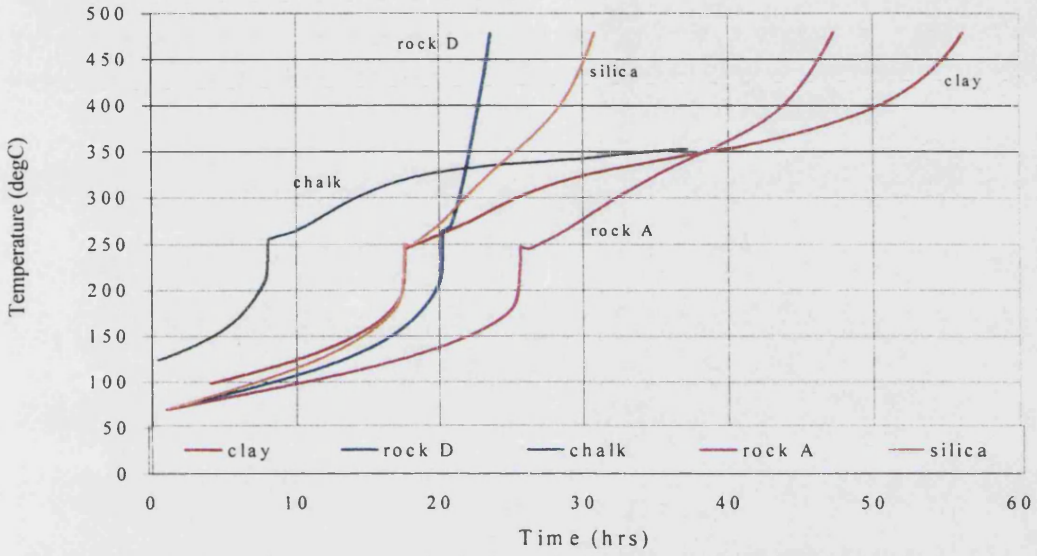

Figure 6.13: Adiabatic Temperature Profile, Dr_c2 (clay), Dr1 (rock D), Dr_ch1 (chalk), Dr_p1 (rock A) and Dr_s1 (silica)

Figure 6.13 shows a difference in the results obtained with the rock D and those from the other rock types, especially in the higher temperature regions. The self-heat rate plot, shown in Figure 6.14 shows that while the different rock types show similar self-heat rate plots, the rate of self-heating in the propagation region is stronger for rock D.

Figure 6.15 shows the reaction rate constant. It appears there is not much difference between the various rock types in the induction period of LTO. After the auto catalytic region though, differences start to appear, and these persist into the HTO region, with a reduction in the reactivity in the order silica, rock A, clay and then chalk.

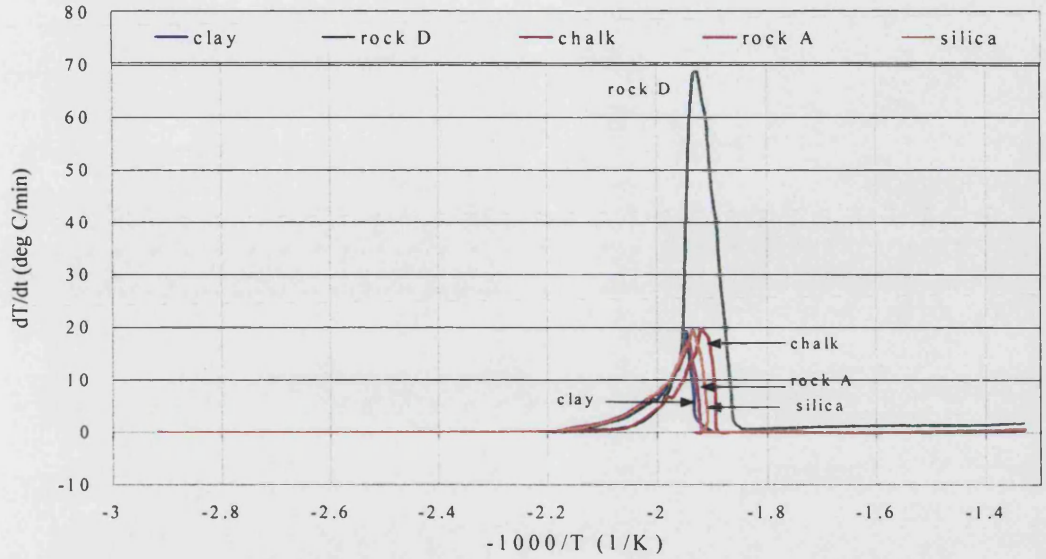

Figure 6.14: Self-Heat Rate against –1000/T, Dr_c2 (clay), Dr1 (rock D), Dr_ch1 (chalk), Dr_p1 (rock A) and Dr_s1 (silica)

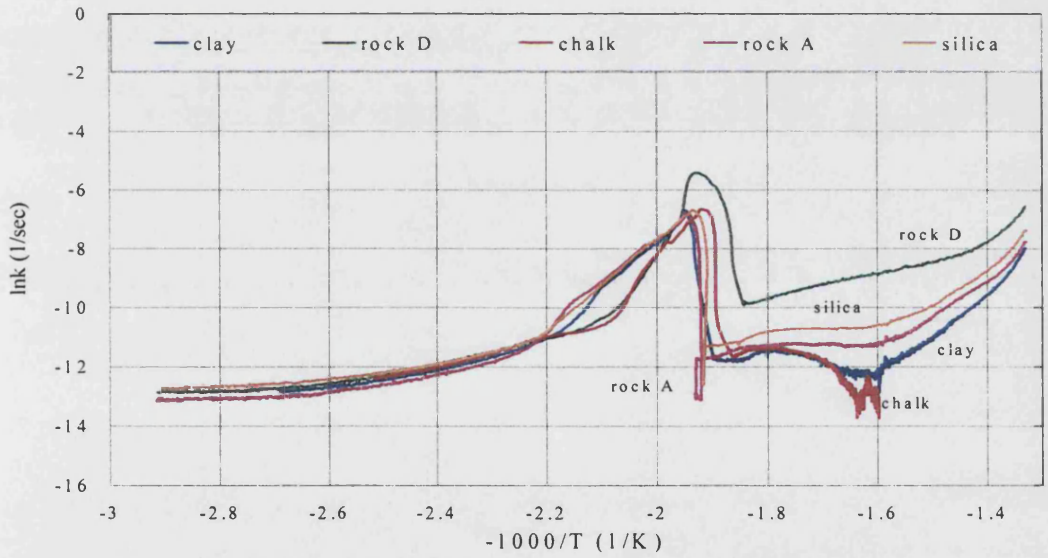

Figure 6.15: Reaction Rate Constant against –1000/T, Dr_c2 (clay), Dr1 (rock D), Dr_ch1 (chalk), Dr_p1 (rock A) and Dr_s1 (silica)

The exothermicity parameters including the self-heat rate ratios, reaction times and energy evolved are shown in Figures 6.16-18.

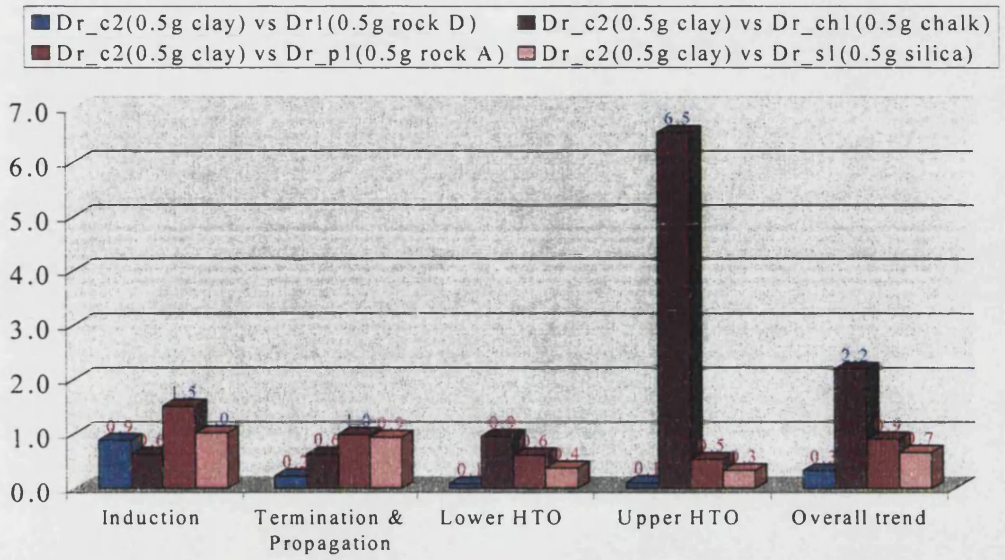

Figure 6.16: Ratio of Self-heat Rates, Comparisons of Different Rocks with Clay

In Figure 6.16, it can be seen that there is a reduction in the self-heat rate in nearly every region when clay is used compared with the other rock types, apart from the chalk experiment.

The reaction time ratios, which are shown in Figure 6.17 show an increase in the HTO region reaction time compared with all the other experiments. In the LTO region, there is an increase when compared with rock D and the chalk, but a reduction compared with rock A and the silica experiment.

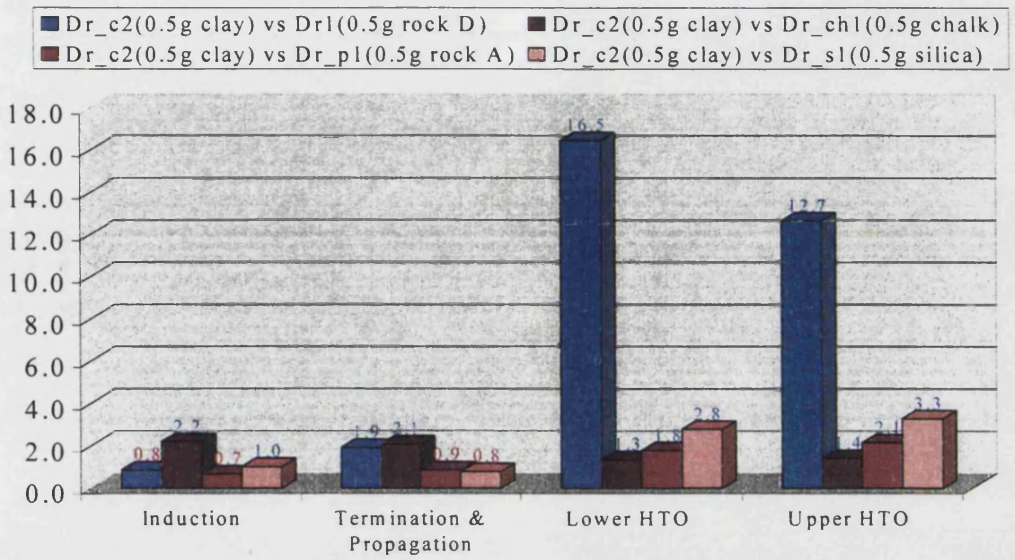

Figure 6.17: Ratio of Reaction Time, Comparisons of Different Rocks with Clay

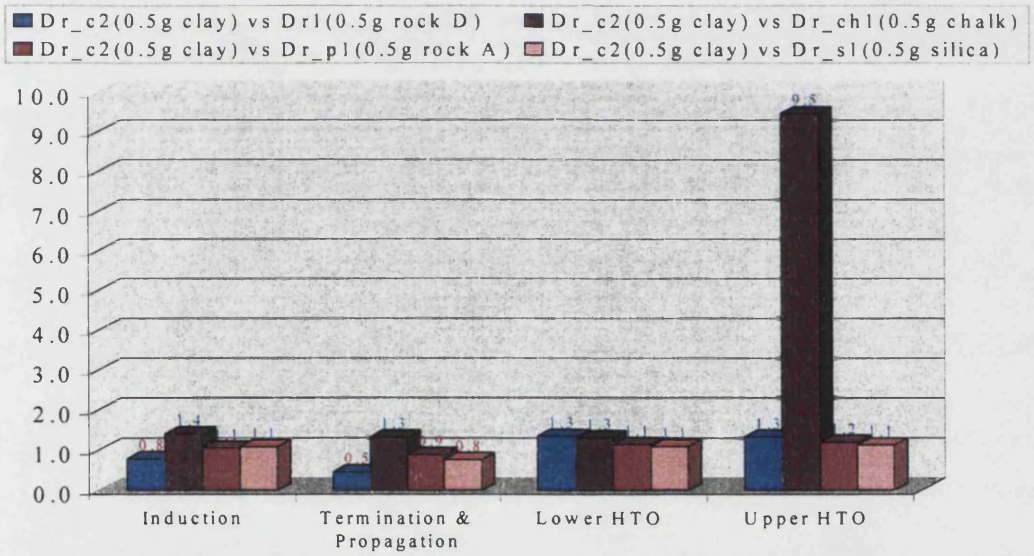

Figure 6.18: Ratios of Energy Evolved, Comparisons of Different Rocks with Clay

Table 6.4, which shows the energy released over each region, shows that while the clay experiment resulted in reduced energy released in the LTO region, more energy is evolved in the HTO region from the clay experiment than all the others. The ELTO/EHTO ratio is also the lowest of any of the experiments, signifying a shift of energy released to the HTO region.

Table 6.4: Energy Released, Experiments to study different rock types

	Dr1	Dr_c2	Dr_ch1	Dr_p1	Dr_s1
ELTO	508	296	216	305	326
EHTO	248	331	130	283	298
ELTO/EHTO	2.0	0.9	1.7	1.1	1.1

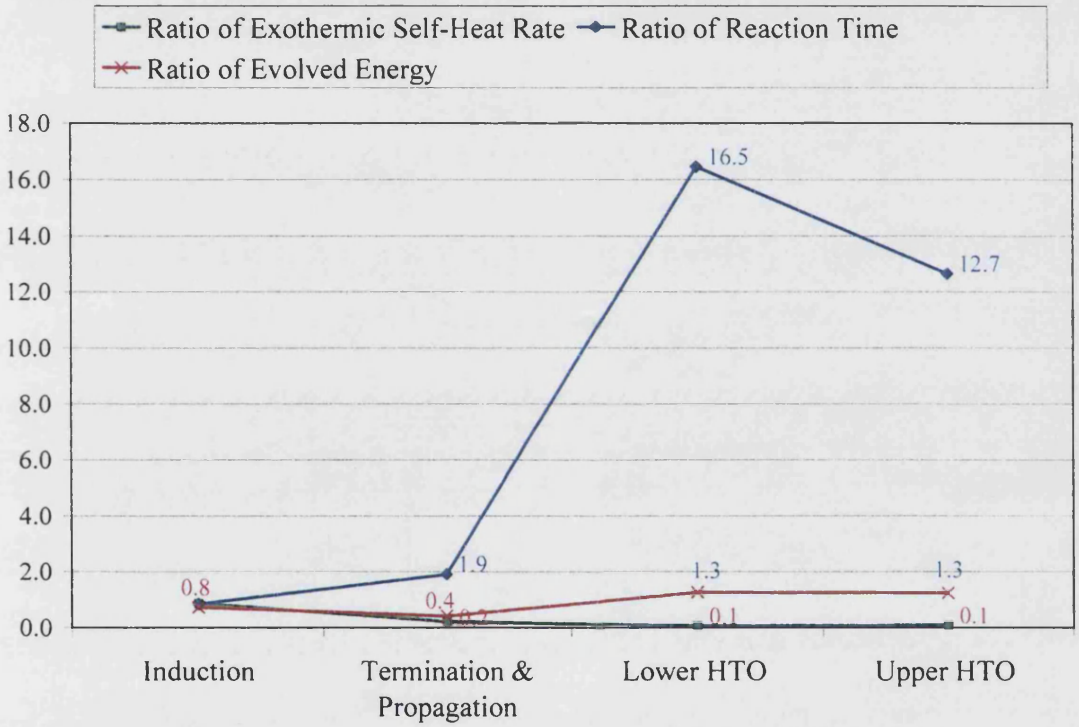

Figure 6.19: Summary of Ratios Showing Effect on Exothermicity of clay vs Rock D

The exothermicity effect of adding clay instead of rock D is summarised in Figure 6.19. The evolved energy is substantially reduced in the propagation region, with a ratio of 0.4 between the two. In the HTO stage, the energy evolved is increased slightly, but at a much slower rate and longer reaction time.

The catalytic effect of clay observed by previous invesigators must primarily be attributed to the increase in energy during the HTO region, although this was usually for heavy oils. However, the self-heat rate for the clay experiments is lower than that for other rock types, which is at odds with its having a catalytic effect. While the clay does not exert any catalytic influence in the LTO region, especially in the propagation reaction, where it appears to be inhibiting, it does influence the HTO region. It is also possible that the type of clay could be the determining factor for a catalytic effect. Pure kaolinite was used in this study, and it is possible that the presence of other minerals and metals contribute to the catalytic effect of natural clays as has been observed in other investigations.

6.3 Buckland Sand/Silica

Washed Buckland sand is used in an experiment for a number of reasons. This industrial grade sand consisted of 97-99% silica, and traces of iron, titanium, chromium, and other metals with a very fine particle size of W150, and a clay content of 0%. It could therefore be used to see if the surface area effect is more important than any catalytic effect arising from the chemical nature of the material. Clays are also made of alumina and silica, so the difference in the Buckland sand and the pure kaolinite used is the presence of alumina as well as the physical characteristics of the two.

The adiabatic temperature profile, self-heat rate plot and reaction rate constant for the experiment with silica is shown in Figures 6.13-15.

In Figure 6.15, silica exhibits a higher reactivity than the clay in all the regions, up to the upper HTO region, where the clay reaction then accelerates. Therefore it appears that the silica is more favourable in LTO and lower HTO reaction than clay is.

The main feature they both have in common, which would come into effect in HTO is a surface area favourable to adsorption. The main factor could therefore be high surface area rather than a catalytic effect due to chemical composition.

The exothermicity parameters obtained including the self-heat rate ratios, reaction times and energy evolved, are shown in Figures 6. 20-6.22.

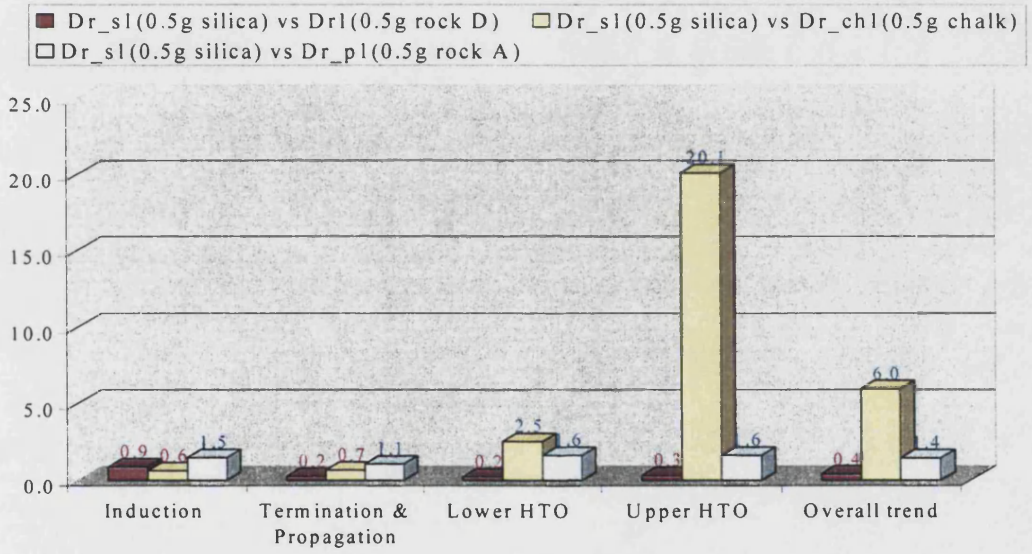

Figure 6.20: Ratio of Self-heat Rate, Comparisons of Different Rocks with Silica

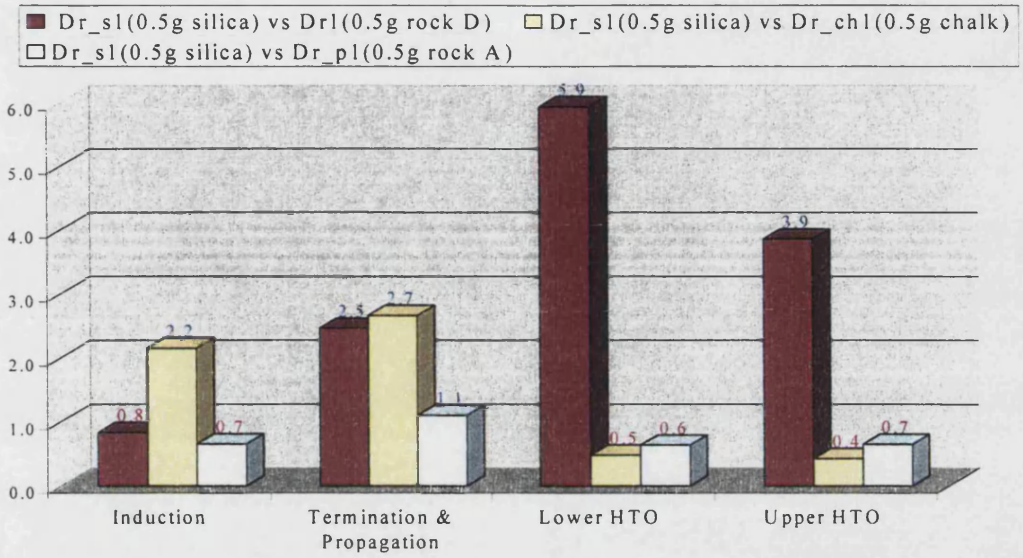

Figure 6.21: Ratio of Reaction Time, Comparisons of Different Rocks with Silica

Figure 6.20 shows that the self-heat rate is greatly reduced with silica relative to rock D in every region, and to chalk in the induction and propagation regions, while it increases relative to rock A in every region and to chalk in the HTO regions. The reaction times show an increase compared to the results with rock D and to the LTO regions of the chalk. However, it is reduced for all the regions relative to rock A and again to the HTO region of the chalk.

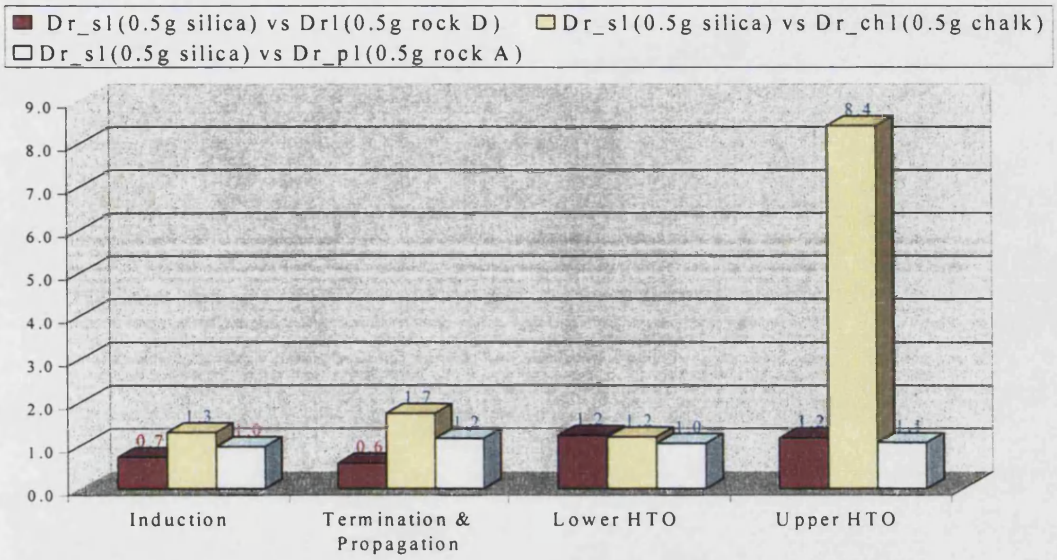

Figure 6.22: Ratios of Energy Evolved, Comparisons of Different Rocks with Silica

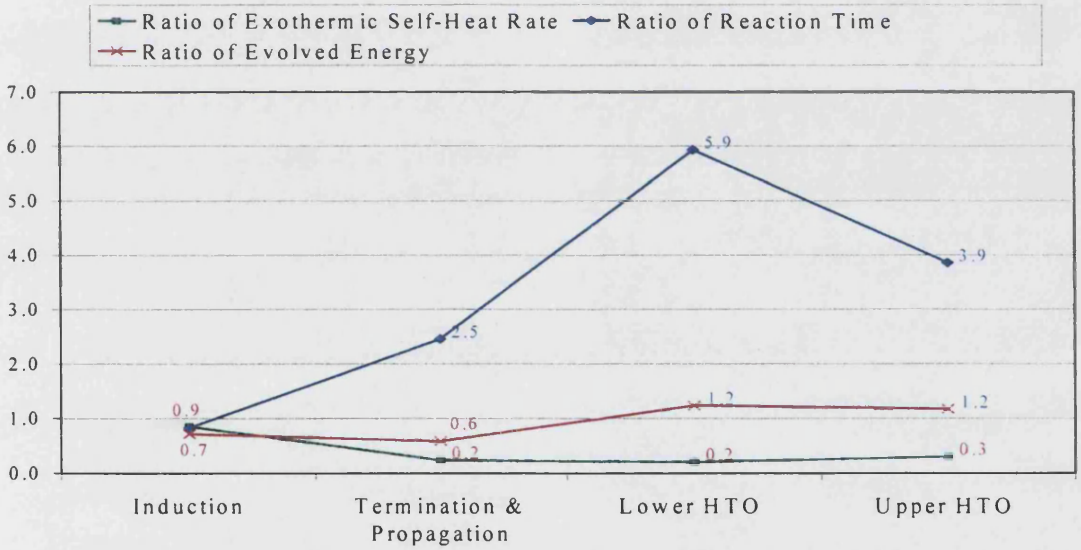

Figure 6.23: Summary of Ratios Showing Effect on Exothermicity of Silica vs Rock D

Figure 6.22 which shows the ratio of energy evolved in all the regions reveals a reduction in the LTO region for rock D but an increase in the HTO regions.

The experiment with silica had a higher energy released than all the other rock types, apart from clay (Figure 6.18), in the HTO region. Figure 6.23 shows a summary

of the exothermic effect when compared with rock D. This shows that silica is favourable to the HTO region with increased energy released. The presence of silica in the other rocks as well as clay could be responsible for a favourable HTO reaction, but this favourable effect is not seen in the LTO region.

6.4 Chalk

Chalk is one form of limestone and was also studied for any effect it had on the exothermicity of the oil oxidation reaction.

Kok et al 1997 observed that limestone significantly enhances the LTO and reduces the overall heat of combustion compared to that of the crude oil on its own. Investigations into the effect of limestone on the oxidation of heavy oils by Bagci et al 1987 showed that the activation energies obtained were not different for LTO and fuel deposition stages run using sandstone. It was however seen that using limestone, the HTO reaction had an activation energy that was twice that obtained using sandstone. Field Applications of air injection into carbonate reservoirs have been reported. The Medicine Pole Hills Unit Air Injection Project, reported by Kumar et al 1995 was carried out into carbonate formations in the Williston basin.

The exothermicity parameters are obtained including the self-heat rate ratios, reaction times and energy evolved and are shown in Figures 6.24-6.26

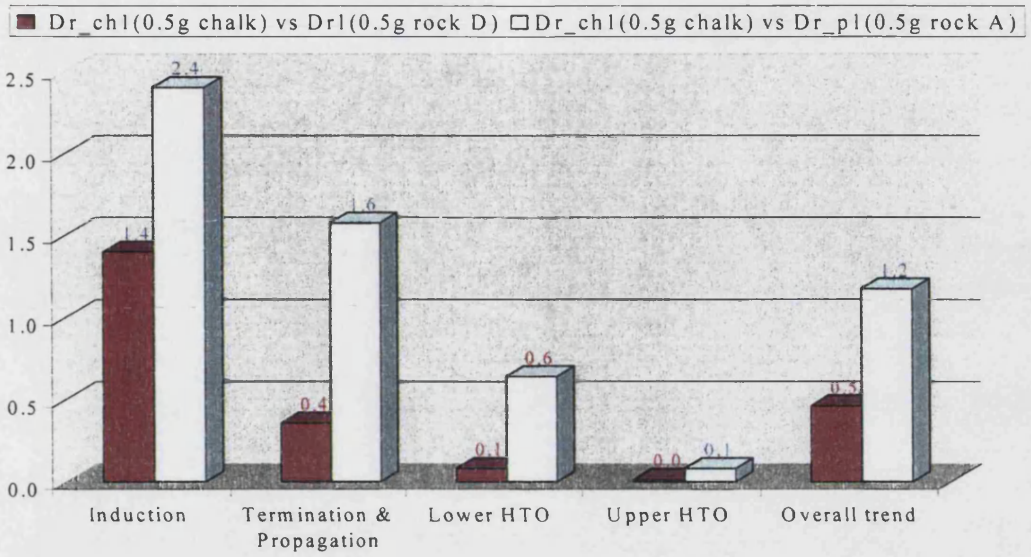

Figure 6.24: Ratio of Self-heat Rate, Comparisons of Different Rocks with Chalk

The self-heat rate ratios can be seen in Figure 6.24 show a reduction in most reaction regions. Looking at the plot of the temperature rise in Figure 6.13, the chalk reaction did not initiate until a higher temperature (125 ^{0}C). The self-heat rates must however be compared over similar temperature ranges for the ratios to be accurate. At higher temperatures, reactions generally have higher self-heat rates, and this would explain the ratios shown in Table 6.24 for the induction region, which are greater than one. From Figure 6.25, the reaction times are seen to have reduced in the LTO region but increase in the HTO region.

An inspection of the energy released ratios in Figure 6.26 reveals a reduction in the energy released of all the regions in the presence of chalk when compared with other rock types. Chalk does not appear to be favourable to any of the reaction regions at all, and is particularly unfavourable in the HTO region with the reaction dying out completely at about 350 ^{0}C.

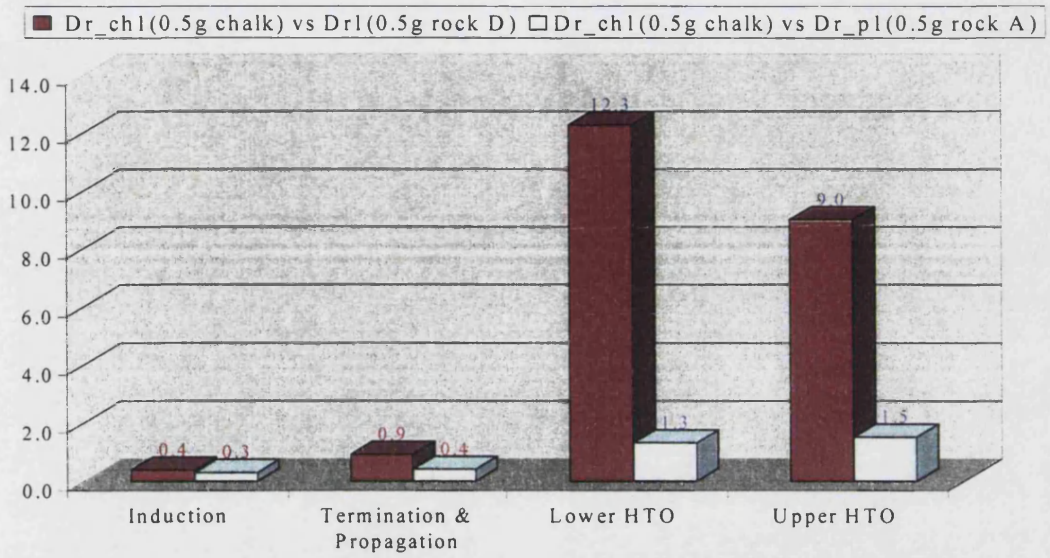

Figure 6.25: Ratio of Reaction Time, Comparisons of Different Rocks with Chalk

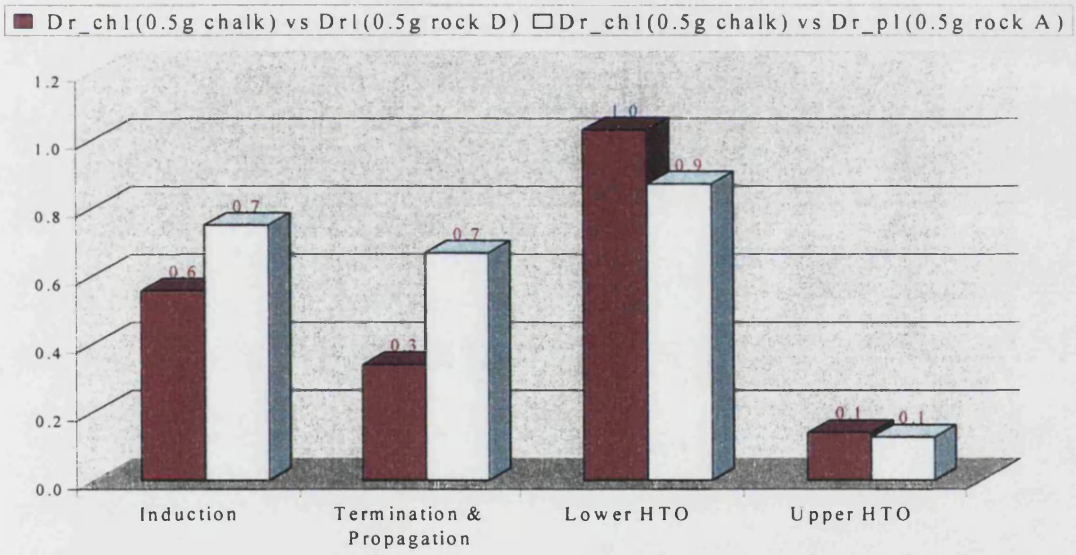

Figure 6.26: Ratio of Energy Evolved, Comparisons of Different Rocks with Chalk

The exothermicity effect of chalk relative to rock D is summarised in Figure 6.27. This shows the unfavourable effect chalk has on practically all the regions but especially in the HTO region. The energy evolved and exothermic self-heat rate are reduced in all regions, with the reactions taking longer. The induction region in Figure 6.27 shows an increase in the self-heat rate relative to rock D but as was explained in

the previous section, due to the late initiation temperatures, this self-heat rate occurs over a different temperature range. This could have implications for a field situation as other parameters affecting the oxidation kinetics would have to be very favourable for air injection into a chalk reservoir to be effective.

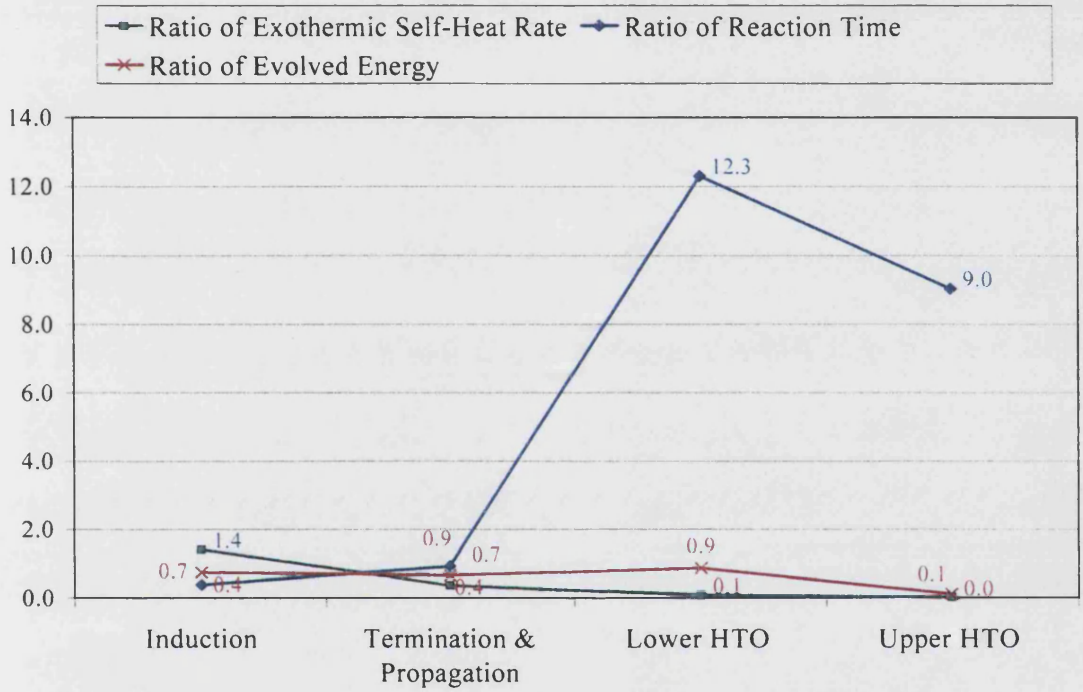

Figure 6.27: Summary of Ratios Showing Effect on Exothermicity of Chalk vs Rock D

A look at the fundamental chemistry behind the oxidation taking place in the presence of limestone can explain the effect they have. Limestones are basic in nature and usually catalyse oxidation processes, however lime would also reduce the amount of polar compounds formed and due to the organic nature of crude oils this could slow down the rate of the fuel deposition and the autocatalytic reaction.

Chalk possesses a high surface area but of a colloidal nature, which would lead to reduced adsorption. In the presence of water, and at the lower temperatures, chalk

provides a poorer adsorption or reaction surface, which would explain the high temperature at which the reaction was initiated (125 ^{0}C, see Figure 6.13).

In conclusion, combustion in chalk reservoirs would require a higher Air-oil-ratio than sand reservoirs in order for it to take off successfully.

CHAPTER 7:

Oxidation Behaviour of Crude Oil

SARA Fractions

USE OF SARA FRACTIONS FOR KINETIC ANALYSIS

Crude oils contain a huge number of complex and chemically diverse mixtures. A typical crude oil can possess thousands of different components and the characterisation of oils is therefore a very difficult task. However some form of characterisation is essential for the computation of thermodynamic properties and phase equilibria. The accuracy of these computations will be enhanced if molecular weight and specific gravity data of fractions containing similar groups, structures or common solubility properties are used. These separate fractions possess critical properties which normally correlate better than that for the whole oil.

The SARA method of separation provides such a characterisation as these fractions have been shown to posess characteristic common properties. It divides the oil up into its saturate, aromatic, resin and asphaltene fractions, which behave in a more similar fashion than the whole oil.

The conventional method of crude oil characterisation involves a separation into boiling point range components. While they are very useful in that they effectively follow the distillation occurring during air injection oxidation, they do not react similarly. SARA fractions on the other hand possess lumped chemical species with the same functional groups displaying similar chemical behaviour.

It is also well known that the ease of oxidation of a compound varies with the functional group, so it is to be expected that the individual SARA fractions will show distinct behaviour with respect to oxidation. It is in turn logical that different SARA fractions should behave differently under heating so they should have some effect on the thermal cracking reactions, although it is likely that distillation cuts would be more

relevant in this case. Any separation according to polarity will group together chemical species with the same functional groups. It is also known that the ease of oxidation of a compound varies with the functional group, so it is to be expected that the individual SARA fractions will show distinct behaviour with respect to oxidation. It is in turn logical that different SARA fractions should behave differently under heating so they should have some effect on the thermal cracking reactions, although it is likely that distillation cuts would be more relevant in this case. Distillation cuts of crude oil will also be investigated, especially with a view to seeing how they would behave under thermal cracking.

The asphaltene and resinous fractions are the heavy fractions of the crude oil and have the highest amounts of polar organic compounds. Asphaltenes are amphiphilic due to the binal presence of both polar and apolar groups. They are associative colloids which form molecular aggregates in solid state. When dissolved, the extent of aggregation may be reduced depending on the composition of the solvent and the temperature. Spectroscopic studies reveal their basic hydrocarbon structure to be large polyaromatic, polycyclic ring substituted with aliphatic, alicyclic and heteroatom (nitrogen, oxygen, sulphur and metals) groups. These characteristics are responsible for their strong interaction with rocks. Other characteristic features of asphaltenes from the available chemistry literature include a lower hydrocarbon-to-carbon ratio relative to other components, generally between 0.9 and 1.2. They also possess higher average molecular weight, and free radical or spin concentration. Mujica et al 2000 in a study of asphaltene molecule caging postulate that free radicals survive in asphaltene molecules due to the shielding provided by other polyaromatic compounds in the aggregates formed by asphaltenes. These free radicals then result in vigorous reactions at later reaction stages, explaining the free-radical role in asphaltene oxidation.

The method by which crude oil is separated into its SARA fractions is carried out is detailed earlier in chapter 3.

7.1 Previous Investigations into SARA Fraction Oxidation Behaviour

A number of studies have been conducted on the behaviour of crude oil SARA fractions in an attempt to achieve a SARA basis for the oxidation chemistry of crude oils.

Few of these studies on SARA fractions under oxidation or on the effect of each of these fractions on the overall oil combustion behaviour have been done on light oils. Considering the fact that light oils generally have little or no asphaltene fractions, there is therefore a lot of scope for examining the oxidation behaviour of light oil SARA fractions.

TGA data from previous tests using heavy oils by Ciajolo and Barbella 1984 indicate that SARA analysis offer a suitable basis for pseudo component selection and indicated that oxidation and cracking behaviour of many oils corresponded to their SARA analysis.

LTO Effect

For a long time it was believed that saturates do not take part in the LTO reaction. It was observed by Babu and Cormack 1984 and Adegbesan, 1987, that the aromatics are significantly more reactive while the saturates appear to be less affected by LTO. Hutchence and Freitag 1991 also report no evidence in the existing literature of LTO taking place in saturates. Studies by Babu and Cormack 1983 on athabasca bitumen showed a stable saturate content, while a decline in aromatic and an increase in asphaltene content was observed.

Ciajolo and Barbella 1984 observed that resins were the most affected during the LTO stage. It is possible that due to the high heating rate of the TGA experiments (40 C/min) LTO reactions were not observable.

Contrary to this result it has been postulated by Kok et al 1997 that due to the heaviness of asphaltene molecules, oxygen does not affect them until very high temperatures and they therefore do not take part in the LTO reaction. There is almost no weight loss due to distillation and LTO reaction while saturates on the other hand take part first and react strongly in LTO reactions followed by resins and then aromatics. They observed a reverse trend for the HTO region with the saturates not contributing to the HTO reaction. The kinetic results for the resin and aromatics appeared to be oil specifiic and varying results were obtained for the oils in the LTO and HTO region.

Verkoczy and Freitag 1997 using autoclave tests observed that asphaltene fractions were the most reactive to LTO, a result which could not be observed using just the TGA tests. It was also observed that saturates displayed the slowest reaction rate at low temperatures and had a variety of products, unlike the other fractions.

Compositionally, Adegbesan observed that the effect of LTO is to increase the asphaltene content of the oil and to decrease its aromatic and resin contents by analysis of the residual oil. It was also found by Ciajolo and Barbella, 1984 that saturates and aromatics produce little or no coke and the majority of coke is produced by the asphaltenes and resins.

Behar et al, 1988 performed experiments on a crude that was predominantly paraffinic and one that was aromatic. They found that higher amounts of coke were produced from the aromatic oil than from the paraffinic oil. The aromatic oil originally

possessed a higher amount of asphaltenes which was suggested as the cause of the higher cracking in form of coke deposition, while the paraffinic oil had a higher amount of saturates. The implication then is that saturates do not undergo much cracking or coke formation during oxidation.

Ranjbar and Pusch, 1991 observed the effect of oil composition, characterised on the basis of light hydrocarbons, resin and asphaltene contents, on the pyrolysis kinetics of the oil. They found that the colloidal composition of the oil had a pronounced effect on fuel formation and composition. Between a temperature range of 350 C and 450 C, a high reduction of fuel concentration, especially for resin rich oils was seen. This implies a thermal instability of resins in this temperature range. They noted a maximum pyrolysis rate of 420 C for resins and 480 C for asphaltenes. This pyrolysis rate was determined using the following equation;

$$r = \left(\frac{dm_c}{dt}\right)\left(\frac{100}{m_c}\right) \qquad \text{Equation 7.1}$$

where r = pyrolysis rate (% fuelmin^{-1}), m_c = instantaneous concentration of fuel (mg), t = time (min). They found that the formation of coke from paraffinic hydrocarbons began only after complete thermal decomposition of the paraffins. Their results confirmed a general pyrolysis scheme which had been determined earlier (Levinter et al 1966). This scheme is shown below.

Verkoczy, 1991 carried out studies on heavy oils and cores, observing a pyrolysis scheme similar to that detailed for the whole oil in Chapter 2. This involves a distillation/evaporation of light components up to about 350 C followed by pyrolysis of a high boiling component from 350 to 500 C. This is similar to the visbreaking described in

Chapter 2. After 50 C a stable coke residue is obtained. Again individual SARA fraction studies showed a major coke contribution by the asphaltene and resin fractions, with small contributions from the aromatic and very little from saturates. The oxidation started earlier in the saturate fraction, with LTO observed from about 130 C.

A combustion peak was observed from about 200 to 260 C, with a second exotherm from about 260 to 380 C. The kinetic behaviour of the aromatic and resin fractions in Verkoczy's studies was similar enough for the two to be lumped together as one.

Ranjbar 1997 carried out low temperature and pyrolysis tests on medium heavy oils with density (at 25 C) of 0.98 and 0.99 Kg/m^3 at 205 C for 50 hrs. The concentration of saturates and aromatics was found to decrease with time, while the concentrations of asphaltenes and coke increased. It was concluded that the LTO reactions of the saturates and aromatics involved formation of asphaltenes and coke with resins as intermediate components. In the presence of clay, higher conversions of resins into sphaltenes was seen to occur due to the catalytic properties of clay. This result concurred with an earlier one by Pusch and Ranjbar-Hamghawandi where it was found that radical polymerisation of alkanes converted them into resins between 300 C and 400 C. It was also found by the same investigators that below 400 C the concentration of resins dominated the reaction rate constant, while above 500 C the amount of asphaltenes dominated. This was postulated to be the mechanism by which light oils low in asphaltene concentration formed fuel for combustion.

A previous study (Huttinger et al 1989) of the thermal cracking of asphaltenes showed no induction period for the formation of coke from asphaltenes, indicating that coke formation occurs directly from asphaltenes and not a series of reactions.

Kok and Karacan, 1997 carried out combustion experiments on SARA fractions of two crude oils (26.12 and 14.95 API) using TGA and DS techniques. It was observed that the saturates underwent LTO, starting at 300 °C and 310 °C for the medium and heavy oil, which was the same temperature at which the whole oil started LTO. The saturates showed a very slow reaction in the MTO (fuel deposition) region and in the HTO region. In addition, the saturates were seen to give off the most heat in the LTO region.

The asphaltenes were reported to have little or no oxidation in the LTO region, and hardly any distillation occurred, presumably due to their weight. The MTO (fuel deposition) started at 380 °C, and resulted in a very vigorous HTO reaction, with the asphaltenes contributing the largest amount of heat to the HTO region.

The observed behaviour of the aromatic fraction was very similar to that of the resins, supporting the hypothesis that resins are formed from oxidation of aromatics. For the resin fraction the LTO region occurred between 320-375 C for the medium and 320-370 C for the heavy oil. The aromatic fraction had an LTO reaction from 320-380 C for the medium and 330-390 for the heavy oil. In the MTO (fuel deposition) and HTO regions, the aromatic and resin fractions had similar temperature interval periods, 380-480 °C MTO; 480-600 °C HTO for the medium oil and 390-475 °C MTO; 475-590 °C HTO for the heavy oil.

It was also suggested that the oxidation of any fraction is independent of the presence of other fractions as the sum effect of each of the fractions equalled the overall behaviour of the crude oils.

This implies that the saturates provide the starting fraction for oxidation in the LTO region, with the resin and aromatic fractions providing a transient heat source in the MTO region and the asphaltene fraction being the strongest contributor to HTO.

Pernyeszi et al 1998 attributed the fuel deposition to the adsorption of asphaltenes on to the rock matrix. One of the most important factor for successful fuel deposition is therefore the adsorption properties of asphaltenes on to a particular type of rock. This is another way of explaining the attractiveness of clay in fuel deposition which has been discussed in chapter 2.2.2.

Ciajolo and Barbella 1984 in their study of four heavy oils found that the saturates were oxidised in the range of 300 to 350 C, the aromatics in the 350 to 400 C range and the resins above 400 C. The asphaltenes seemed not to oxidise at all, and instead pyrolysed at about 500 C to form coke which burned at a higher temperature.

Lin et al 1987 report a study on coke formation by Appleby et al 1962 which showed that aromatics play a strong part in the formation of coke. This process occurs through the dehydrogenation and polymerisation reactions of aromatics to form large aggregates of polynuclear aromatics.

Table 7.1: Experimental Analysis to Study Effect of SARA Fractions

	Saturates	Aromatics	Resins	Asphaltenes
	Saturates / oil	***Aromatics / oil***	***Resins / oil***	***Asphaltenes / oil***
Differences between Experiments	As1 / A0, Ds0 / D3, Bs3 / B0	Aar1 / Ar1, Bar2 / Br2, Dar2 / dr1	Brr1 / Br3	Masr1 / Mr1 Wlasr1 / Mr1
	Lighter / Heavier Saturates			***Lighter / Heavier Asphaltenes***
	Bs3 / As1, Ds0 / As1, As1 / Wls0, Bs3 / Wls0, Ds0 / Wls0			Masr1 / Wlasr1

7.2 Oxidation Behaviour of Saturates

It was observed that during the course of experiments, the saturates change colour. Initially it is generally a clear golden fluid, but became a dark brownish-black fluid, closer to colour of the crude oil.

Verkoczy and Freitag 1997 using TGA tests on saturates observed LTO from about 125 to 300 C followed by a large oxygen uptake akin to NTC between 300 C and 450 C, and then HTO from 400-585 C.

Unpublished work on oxidation of different SARA fractions by Al-Saffar et al show a low LTO peak for resin and aromatic fractions and a pronounced peak in the HTO zone.

7.2.1 *Experimental Results, Saturate v whole oil*

Graphs showing the experimental results and resulting analysed data are shown in Figure 7.1 for "whole" oils (A, D and B), and their corresponding saturate fractions (without rock or water). These were done to illustrate the contribution of saturates to the overall oil oxidation.

The "whole" oil lags the saturate fractions before the autoctalytic ignition occurs. This can be seen in Figure 7.1, where the saturates react faster than the whole oil itself, where the other SARA fractions are present. Oil A is the only whole oil which reacted as fast as other saturate fractions.

Figure 7.2 shows that the reaction mechanisms for the whole oils and their saturate fractions occur in precisely the same manner and at the same temperatures. The saturate fractions also appear to have higher self-heat rates in the propagation region than the whole oil, which seems rather odd. This implies that the reaction in the presence of the other fractions may be inhibited somewhat, resulting in reduced rates.

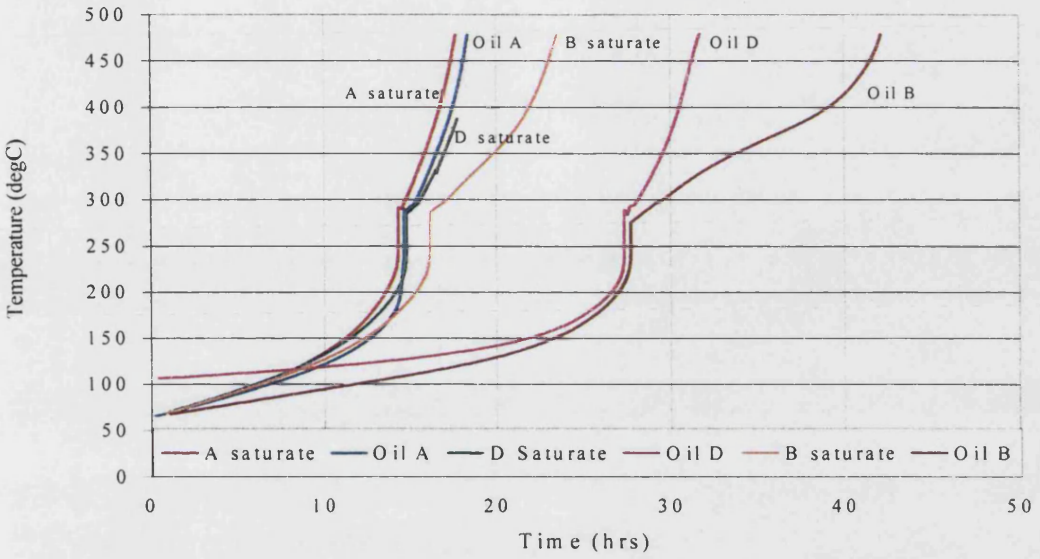

Figure 7.1: Adiabatic Temperature Profile, Oils A, D, B and Saturate Fractions

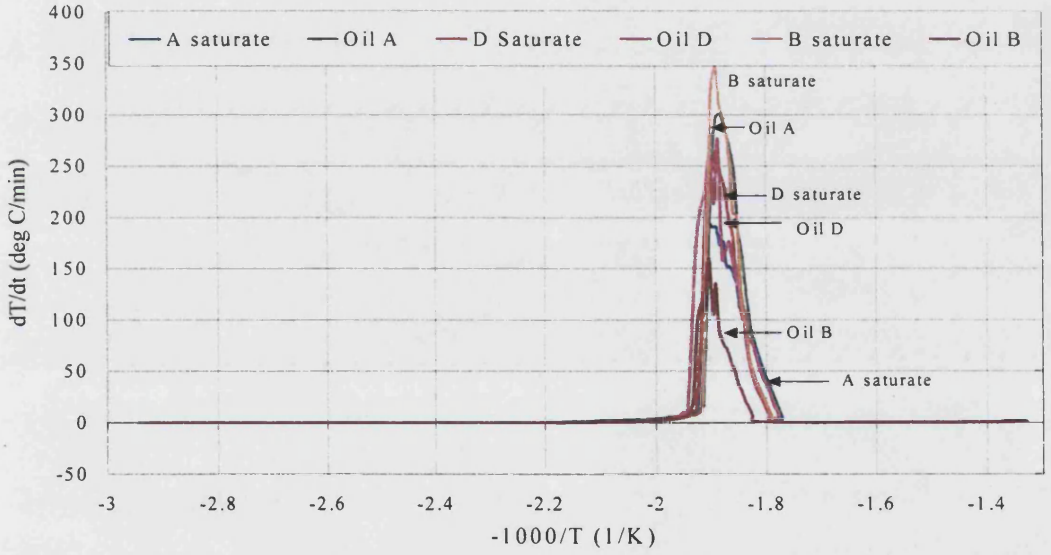

Figure 7.2: Self-Heat Rate against –1000/T, Oils A, D, B and Saturate Fractions

Figure 7.3 and 7.4 showing the reaction rate constant and vapour pressure correlation confirm that the same sort of mechanism takes place both in the saturate and the whole oil. The same trends are seen for both saturate fractions and oils, and more importantly, they occur at the same temperature.

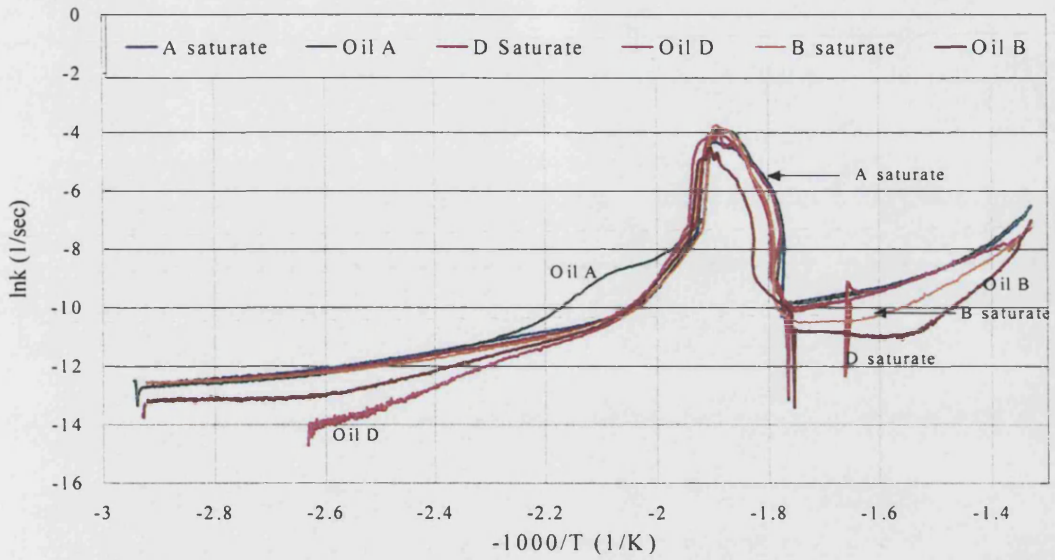

Figure 7.3: Reaction Rate Constant against –1000/T, Oils A, D, B and Saturate Fractions

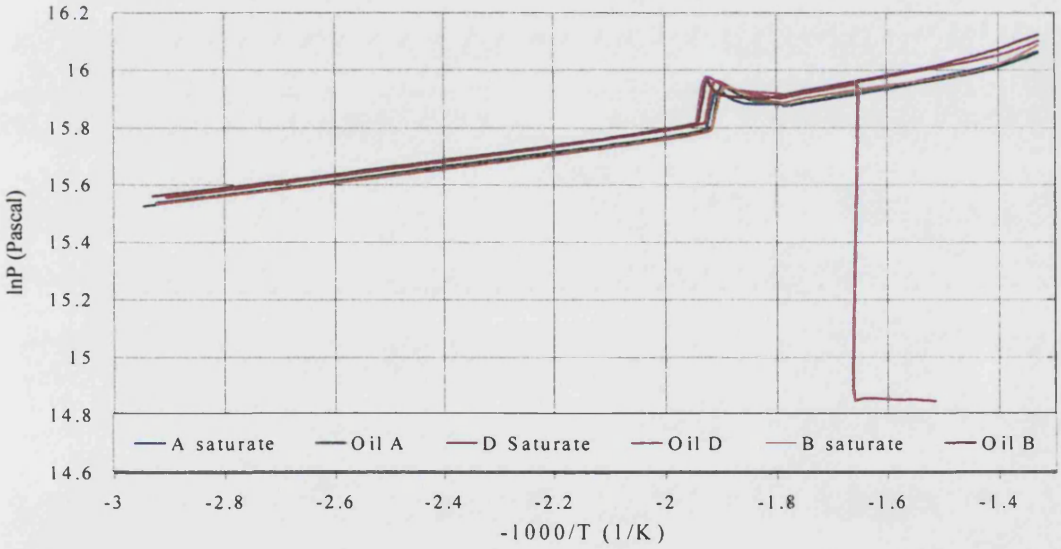

Figure 7.4: Logarithmic Plot of Pressure against –1000/T, Oils A, D, B and Saturate Fractions

The exothermicity parameters are analysed and are shown in Figures 7.5-7.8. The self-heat rate ratios in Figure 7.5 show an increase in the induction and HTO rates of the saturates compared with the whole oil. Oils A and D show a slight reduction in the

propagation region. There may be a contribution to the propagation reaction from one of the other absent SARA fractions.

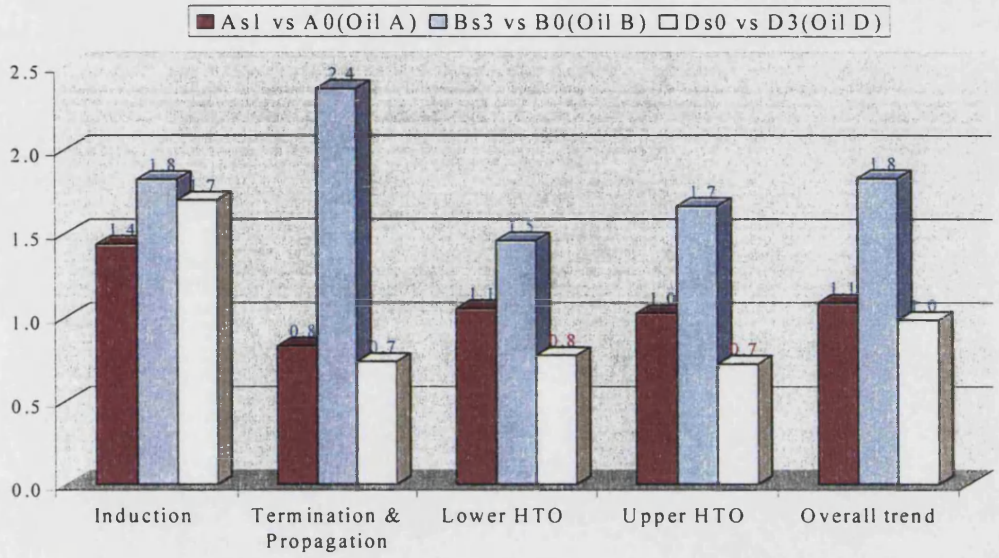

Figure 7.5: Ratio of Self-heat Rate for Saturates Compared to Whole Oil

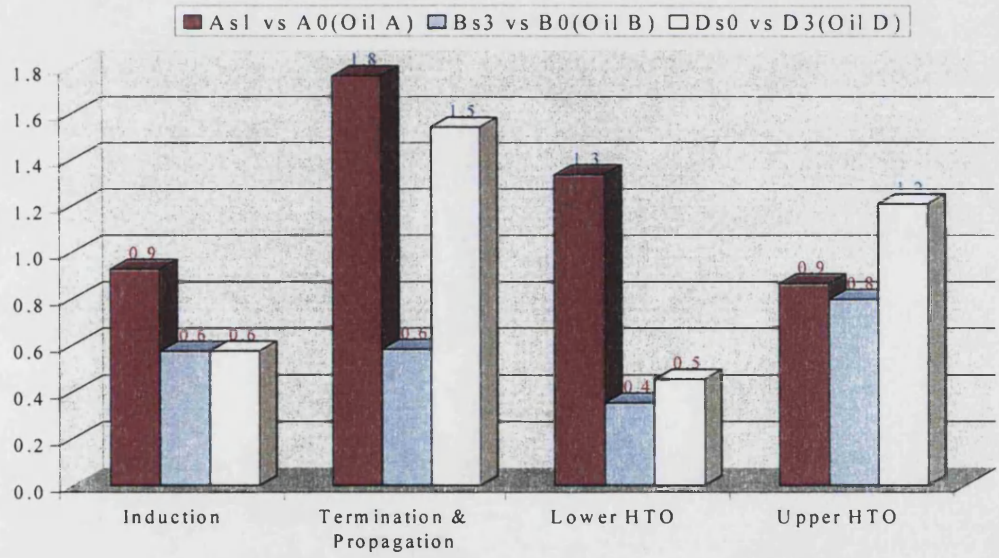

Figure 7.6: Ratio of Reaction Time for Saturates Compared to Whole Oil

Figure 7.6 shows reduced reaction times for the saturates compared with the whole oil. An examination of the energy released ratios in Figure 7.7 shows an increase in the

energy released in the LTO region, while in the upper HTO, the results are slightly reduced. In the lower HTO region though, the reduction is more substantial.

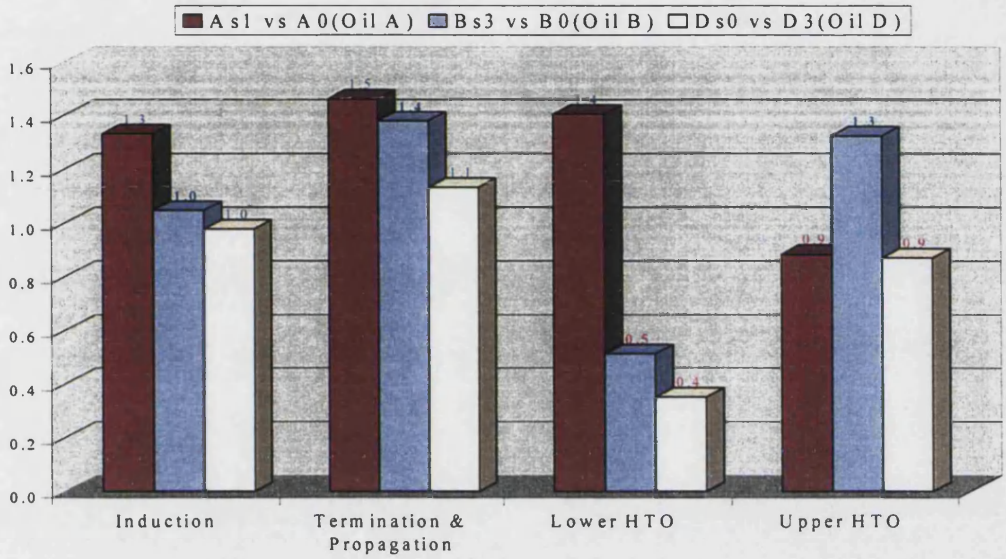

Figure 7.7: Ratio of Energy Released for Saturates Compared to Whole Oil

The energy evolved in the different experiments is compared in Table 7.2 and 7.3. Specific heat capacities of the crude oil were used to calculate the energy evolved for the saturates as there was no publicly available data for these saturates. The energy released values show that the energy evolved in the LTO region increases for the saturates alone while it decreases in the HTO region.

Table 7.2: Energy Released, Saturate and Whole Oil (Oil A and D)

	A0	As1*	D3	Ds0*
ELTO	348	501	504	561
EHTO	81	88	79	43

Where * stands for saturate fraction

Table 7.3: Energy Released, Saturate and Whole Oil (Oil B and W)

	B0	Bs3*	Wls0*
ELTO	418	554	424
EHTO	94	90	107

Where * stands for saturate fraction

An average of the exothermicity ratios for the three different oils and their saturate fractions was taken and used to summarise the effect of saturates, and this is shown in Figure 7.8. This shows the increased energy released values in the induction and propagation regions, confirming the favourable LTO reaction of the saturates.

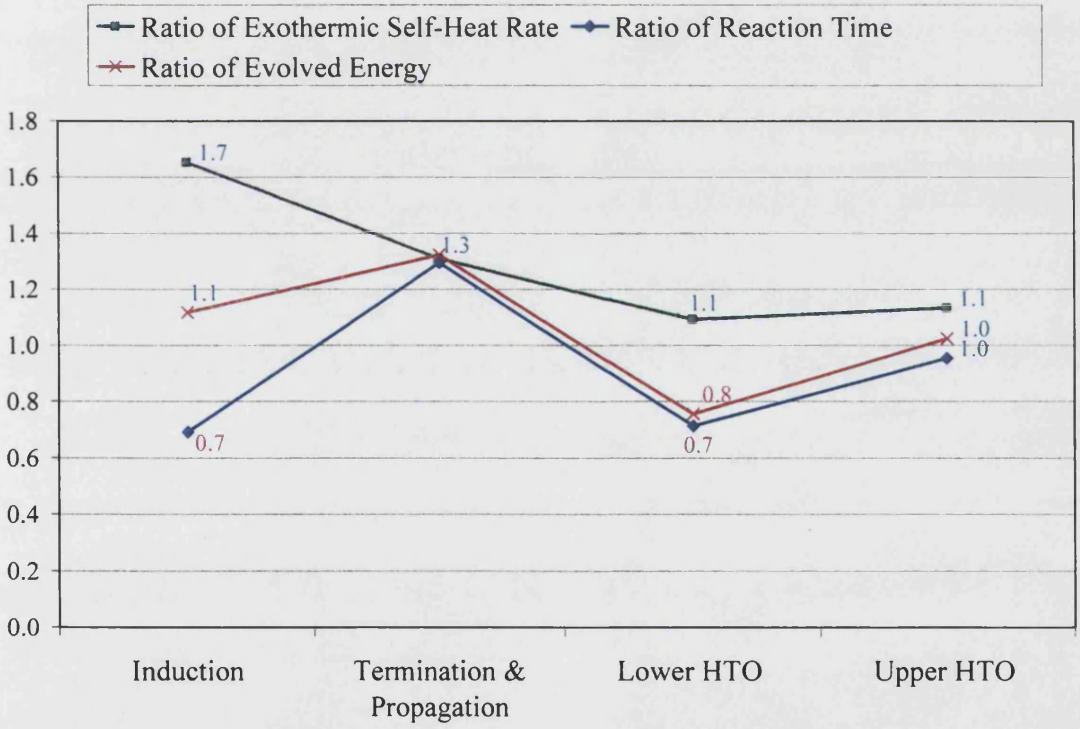

Figure 7.8: Summary of Exothermicity Contribution of Saturates

These results have some implications for the SARA reaction mechanism. The saturates appear to be very reactive in the LTO region, in fact more so than the whole oil itself. This means other fractions leads to inhibition of the saturate free-radical reaction. In addition the behaviour over the lower HTO region, as seen in Figure 7.8 raises some issues. This region is where fuel deposition mainly occurs. The low energy released values seen in this region shown in Figure 7.7 and 7.8 imply that saturates do not contribute greatly to this fuel deposition process.

7.2.2 *Experimental Results, Saturate Type*

Previous kinetic models for the oxidation of crude oils have chosen both light and heavy pseudo-component saturate fractions (Hutchence and Freitag 1991, Verkoczy and Freitag 1997).

In order to investigate the difference between these saturate types, experiments were compared to study the difference between the oxidation of light oil saturate fractions (A, B, D) and that of the heavy oil W. The experimental results are shown in Figures 7.9-7.10.

From Figure 7.9, the heavy Wolflake saturate shows a time lag before the autocatalytic ignition occurs. The self-heat rate plot shown in Figure 7.10 shows a lag for the heavy saturate before the autocatalytic reaction takes off. The lag between the heavy and light fractions is not only in temperature as seen in Figure 7.10 but also in time as is shown in Figure 7.9.

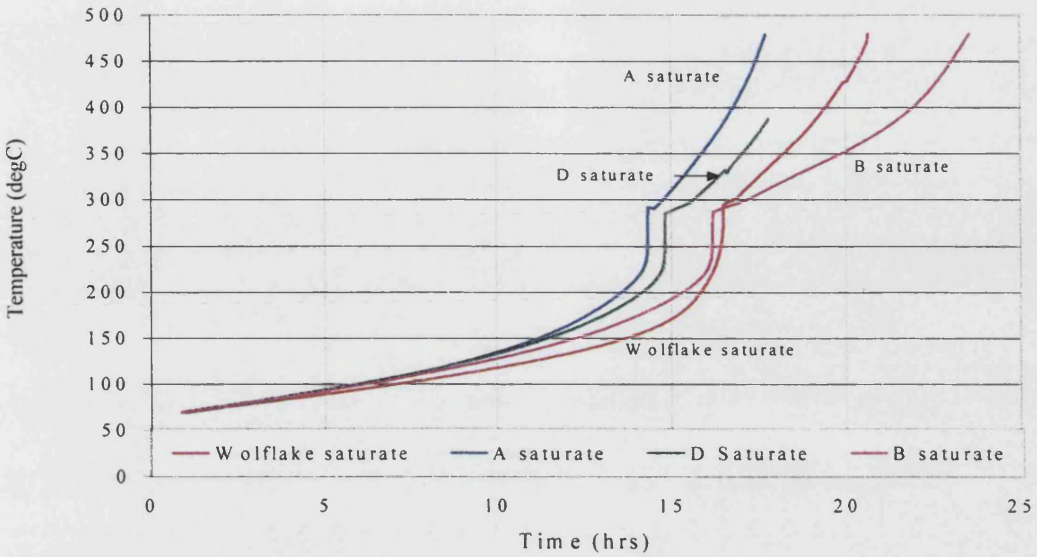

Figure 7.9: Adiabatic Temperature Profile, Oils A, D, B and Saturate Fractions

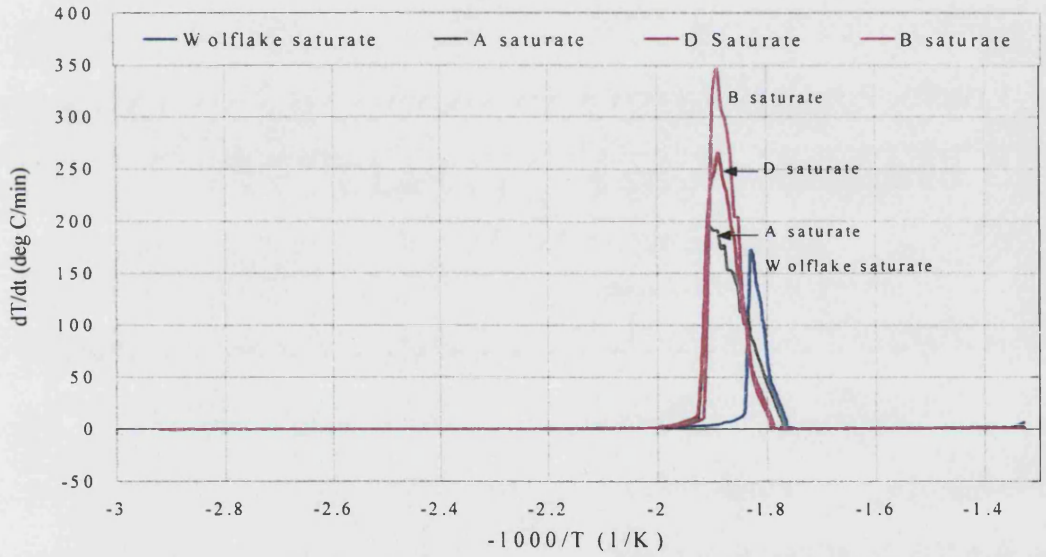

Figure 7.10: Self-Heat Rate against –1000/T, Oils A, D, B and Saturate Fractions

The exothermicity parameters are analysed and are shown in Figures 7.11-7.13.

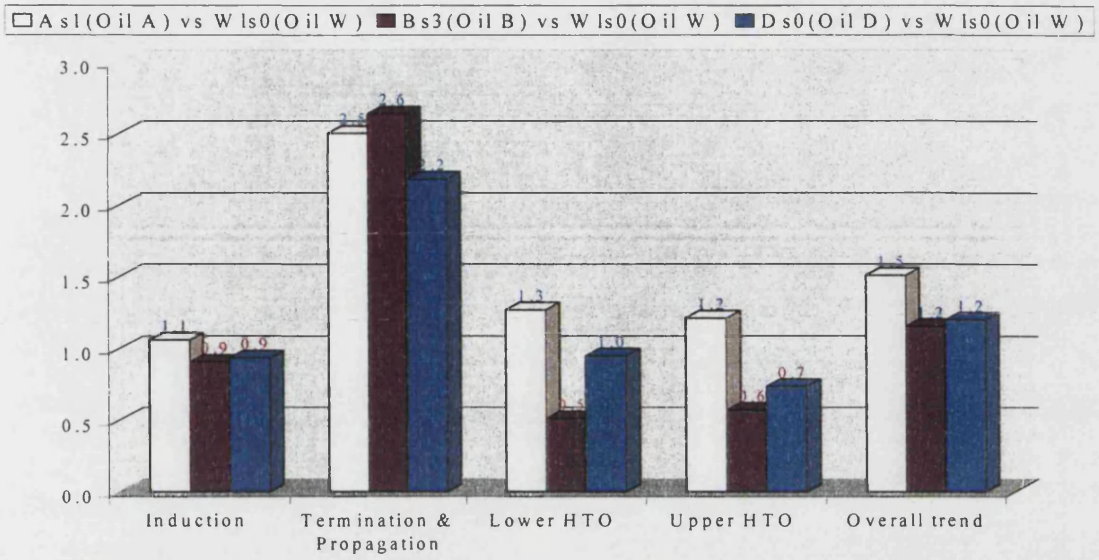

Figure 7.11: Ratio of Self-heat Rate for Light Saturates Compared to Heavy Saturates

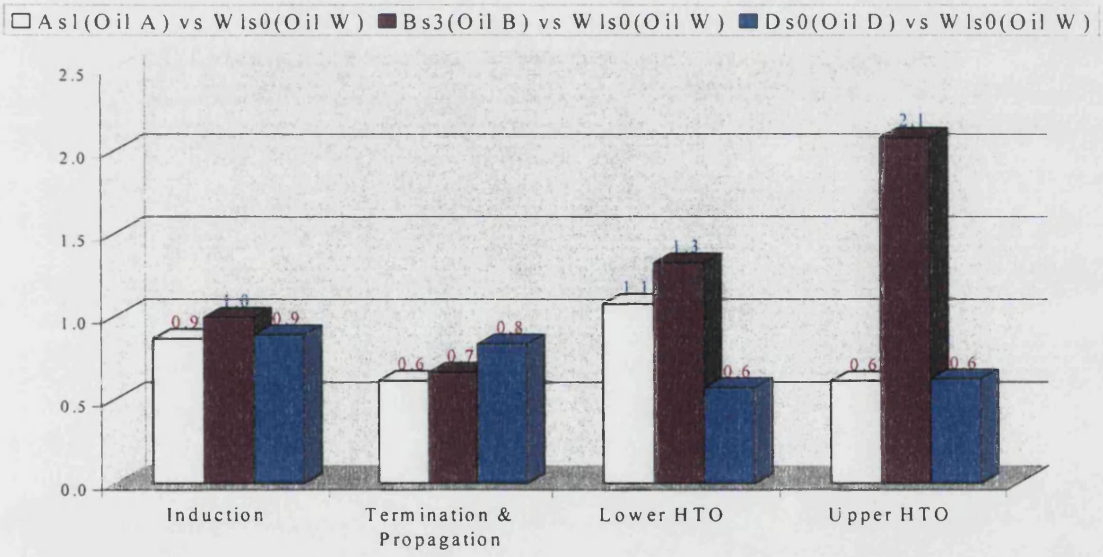

Figure 7.12: Ratio of Reaction Time for Light Saturates Compared to Heavy Saturates

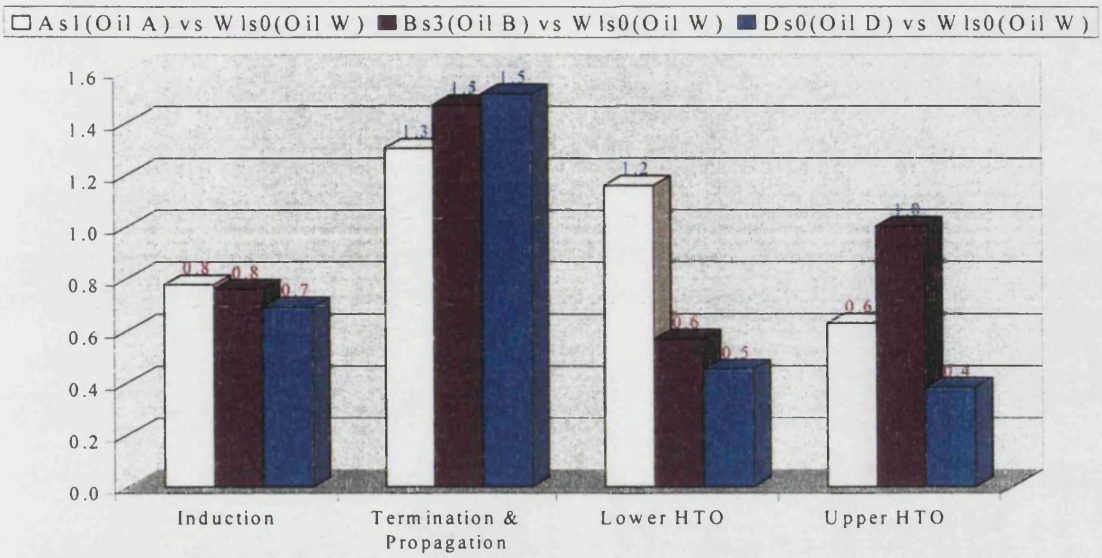

Figure 7.13: Ratio of Energy Released for Light Saturates Compared to Heavy Saturates

Table 7.2 and 7.3 show the energy released value for the heavy saturate type, where an increase of energy evolved in the HTO occurs compared with the lighter saturate fractions.

A summary of the exothermicity difference between the lighter and heavier saturates fractions is shown in Figure 7.14. This shows a reduction in the energy released for all regions apart from the propagation region where it increases slightly. The heavier saturates do not give off as much energy in the propagation region. This can be contrasted with the result obtained earlier in chapter 5 where different oil types were studied. The heavier Maya oil had significantly higher energy released values in the every region including the propagation region.

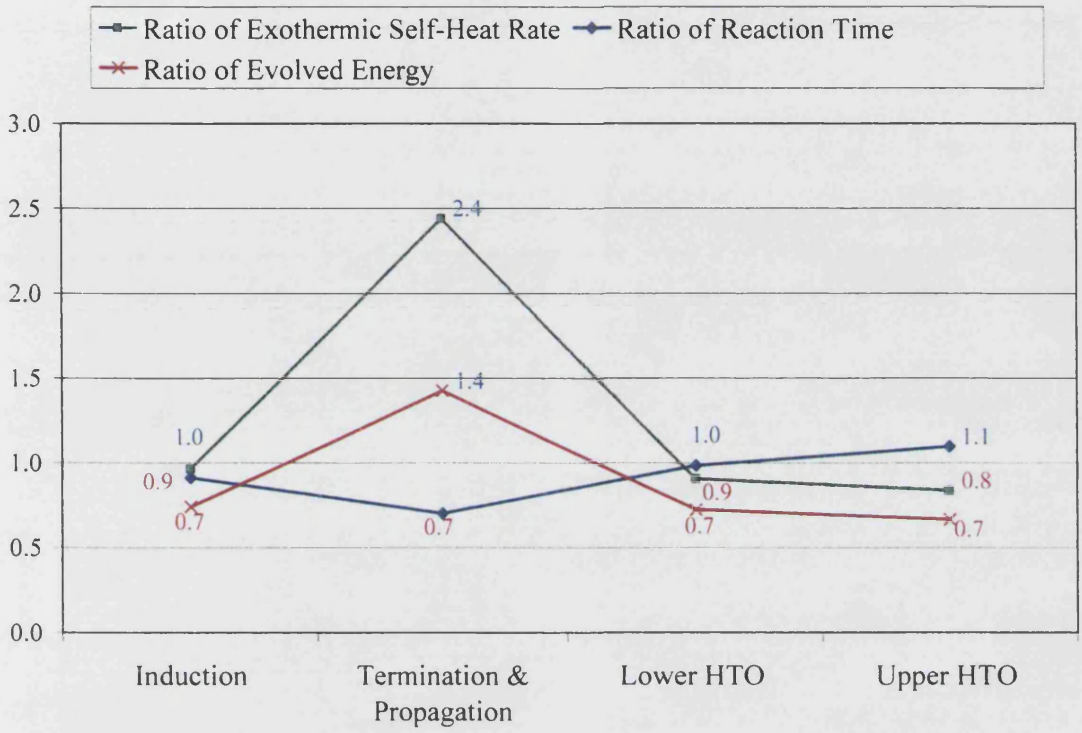

Figure 7.14: Summary of Exothermicity Effect, Lighter / Heavier saturates

7.3 Oxidation Behaviour of Aromatics

7.3.1 *Experimental Results, Aromatic v whole oil*

Graphs showing the experimental results and resulting analysed data are shown in Figure 7.15 - 7.17 for "whole" oils (A, D and B), and their corresponding aromatic fractions, in the presence of rock and water at 50 bar. These were done to illustrate the contribution of saturates to the overall oil oxidation.

From Figure 7.15 it is seen that the aromatic fractions lag the "whole" oil in the induction period before the autocatalytic induction occurs. The self-heat rates are also greatly reduced in the propagation region, as seen from the plot in Figure 7.16.

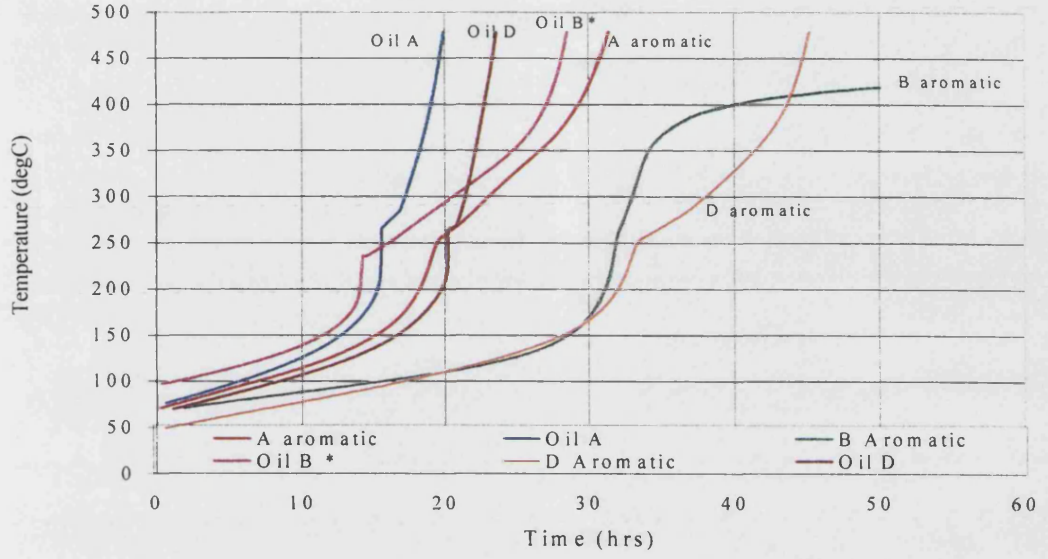

Figure 7.15: Adiabatic Temperature Profile, Oils A, D, B* (100 bar) and Aromatic Fractions

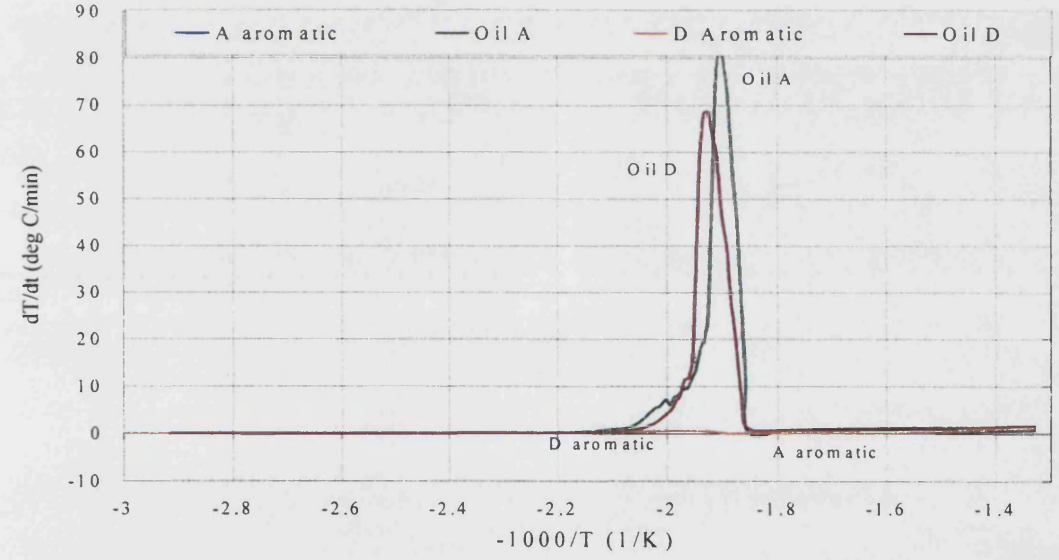

Figure 7.16: Self-Heat Rate against –1000/T Oils A, D, B* (100 bar) and Aromatic Fractions

However, from the plot inFigure 7.17, the reaction mechanisms for the aromatic fractions occur at the same temperatures and in the same manner as the whole oils, albeit at

much lower rates. The aromatic fractions therefore show the same reaction but in an inhibited fashion.

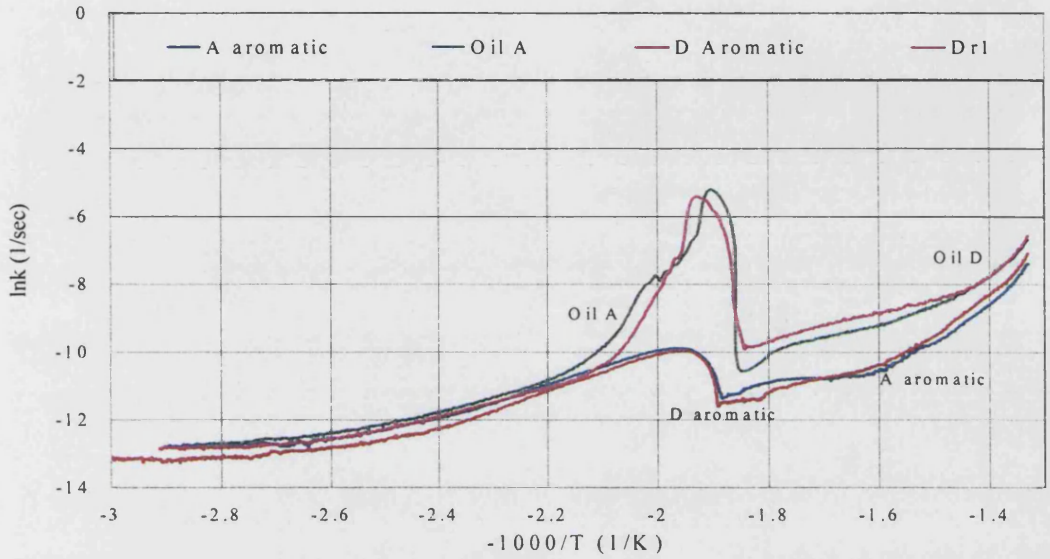

Figure 7.17: Reaction Rate Constant against –1000/T, Oils A, D Aromatic Fractions

The exothermicity ratios comparing aromatic fractions to the whole oils are shown in Figures 7.18-7.20. The self-heat rate ratios in Figure 7.18 show a reduction in virtually every region apart from the lower HTO region of oil B. If this is taken as an aberration, the aromatics clearly have a reducing effect on the self-heat rates in every region.

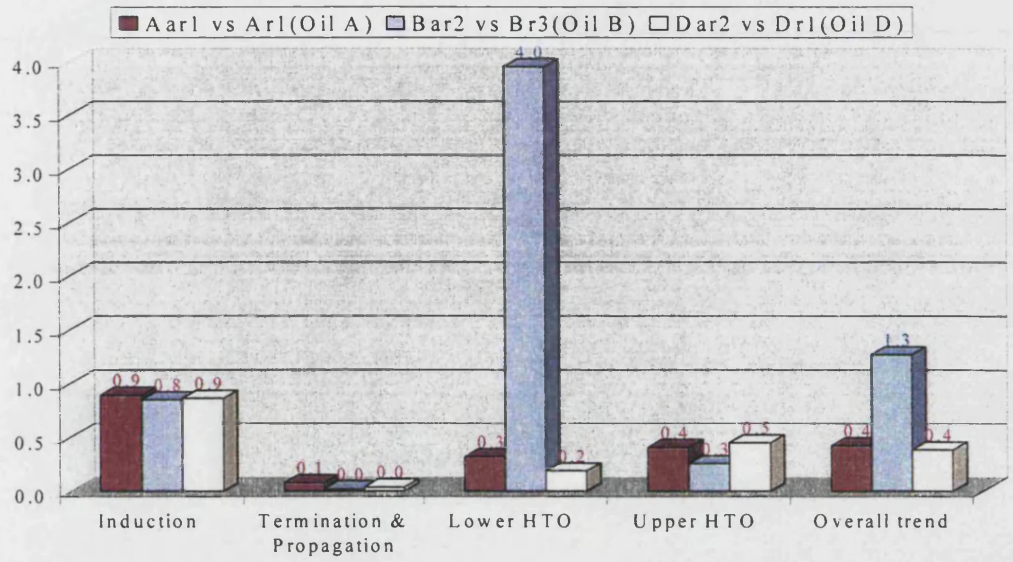

Figure 7.18: Ratio of Self-heat Rate for Aromatics Compared to Whole Oil

Figure 7.19 shows increased reaction times meaning the reactions took longer in every region. The energy released ratios in Figure 7.20 show a big reduction in the propagation region while the other regions are largely unchanged with ratios close to one. The retarding effect of the aromatics is clearly most significant in the propagation region.

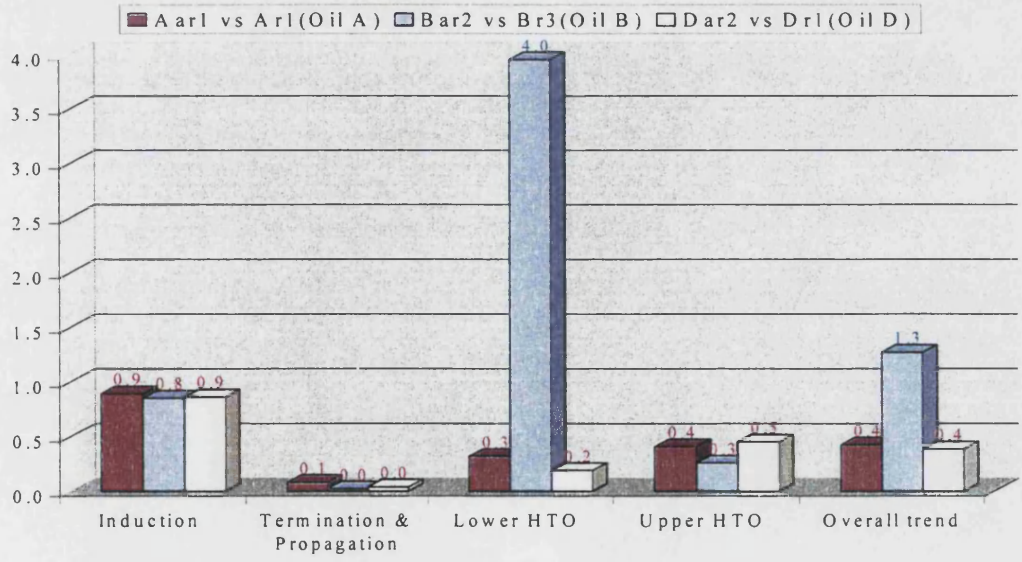

Figure 7.19: Ratio of Reaction Time for Aromatics Compared to Whole Oil

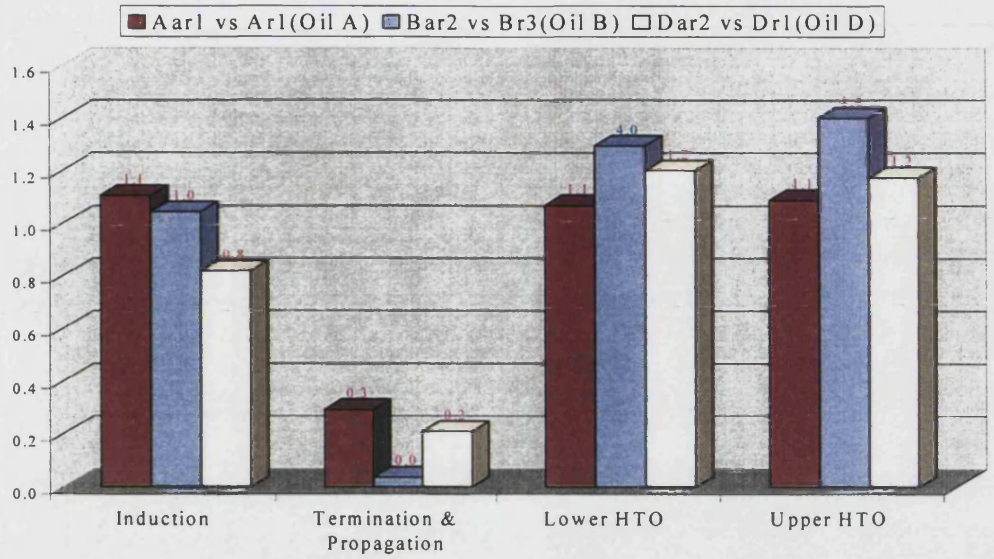

Figure 7.20: Ratio of Energy Released for Aromatics Compared to Whole Oil

The energy evolved in the experiments with different SARA types are compared in Tables 7.3 and 7.4. The specific heat capacity of the crude oil was used to calculate the energy evolved for each SARA fraction due to unavailability of data for each of the fractions. Energy released for the aromatic fraction alone reduces in the LTO region but increases in the HTO region for all the aromatic experiments with the "whole" oil.

Table 7.4: Energy Released, Aromatic, Resin and Asphaltene Oxidation (oil A, B, D)

	Ar1	Aar1	Br3	Bar2	Brr1	Dr1	Dar2
ELTO	430	258	2839	271	260	508	230
EHTO	271	293	168	224	265	248	294

Table 7.5: Energy Released, Aromatic, Resin and Asphaltene Oxidation (oil M, W)

	Mr1	Masr1	Wlar1	Wlrr1	Wlasr1
ELTO	4489	221	239	256	242
EHTO	241	151	347	299	270

The average of the exothermicity ratios for the three oils A, B, D and their aromatic fractions is used to summarise the effect of the aromatics, and is shown in Figure 7.21. This shows the significant reduction in energy released over the propagation region for the aromatic fractions. The aromatics have a stronger contribution to the HTO region.

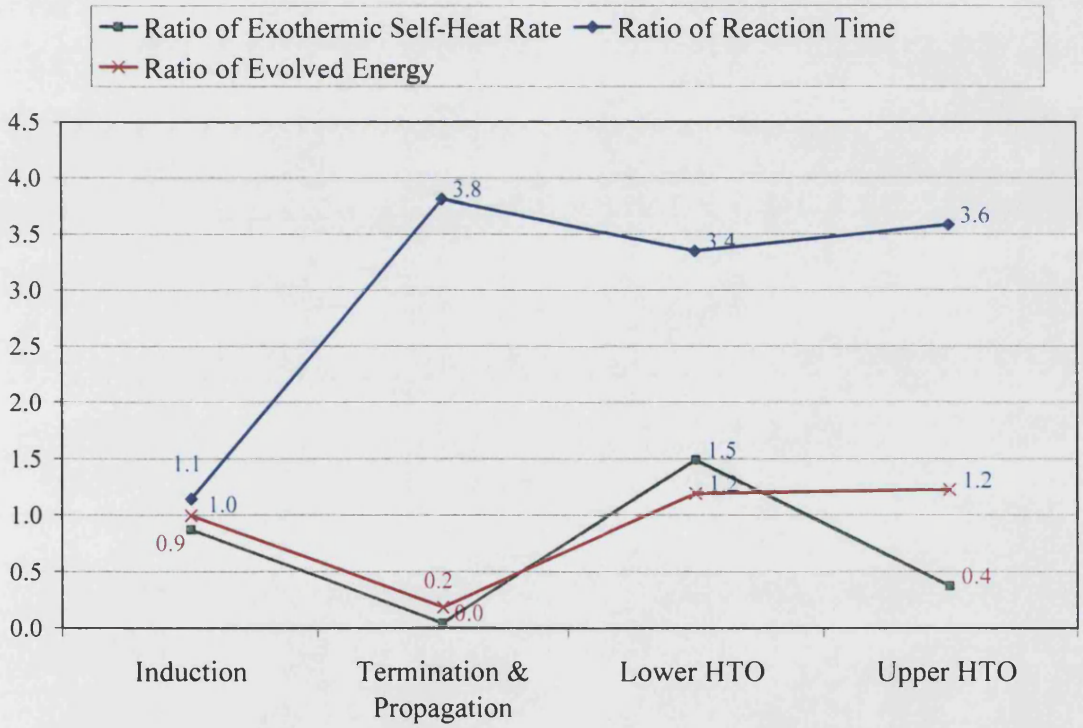

Figure 7.21: Summary of Exothermicity Contribution of Aromatics

Explanation of Aromatic Inhibition Effect

$$C_6H_6 + O_2 \rightarrow C_6H_5^{\bullet} + HO_2^{\bullet}$$ Equation 7.1

$$C_6H_5^{\bullet} + O_2 \rightarrow C_6H_5OO^{\bullet}$$ Equation 7.2

$$C_6H_5OO^{\bullet} + C_6H_6 \rightarrow C_6H_5O^{\bullet} + C_6H_5^{\bullet} + OH$$ Equation 7.3

$$C_6H_5O^{\bullet} + C_6H_6 \rightarrow C_6H_5OH + C_6H_5^{\bullet}$$ Equation 7.4

$$C_6H_5OH \rightarrow C_6H_4(OH)_2$$ Equation 7.5

Phenols are known to be weak inhibitors of alkyl free radicals by reacting with them to form relatively inactive radicals. A reduction in the LTO reactivity of the saturates by the aromatics could arise from the formation of the phenol radical as shown in equation 7.4 above. The mechanism of inhibition by phenols occurs by abstraction of a hydrogen atom from the phenol molecule by the peroxy radical to form a phenoxy radical which is inactive and cannot propagate the chain (Emanuel et al 1967).

$$RO_2^{\bullet} + HOC_6H_5 \rightarrow ROOH + OC_6H_5^{\bullet}$$ Equation 7.6

A similar result would be expected for resins and asphaltenes as well due to their aromatic or napthalenic content.

7.4 Oxidation Behaviour of Resins

7.4.1 *Experimental Results, Resin v whole oil*

Graphs showing the analysed data are shown in Figure 7.22 for experiments Brr1 (0.3g resin, rock and water @ 50 bar) and Br3 (0.25ml oil B, rock and water @ 100 bar).

The "whole" oil lags the saturate fractions with a longer induction period before the autocatalytic induction occurs. The self-heat rate plot of Figure 7.23 shows lower self-heat rates for the resin fraction in the propagation region.

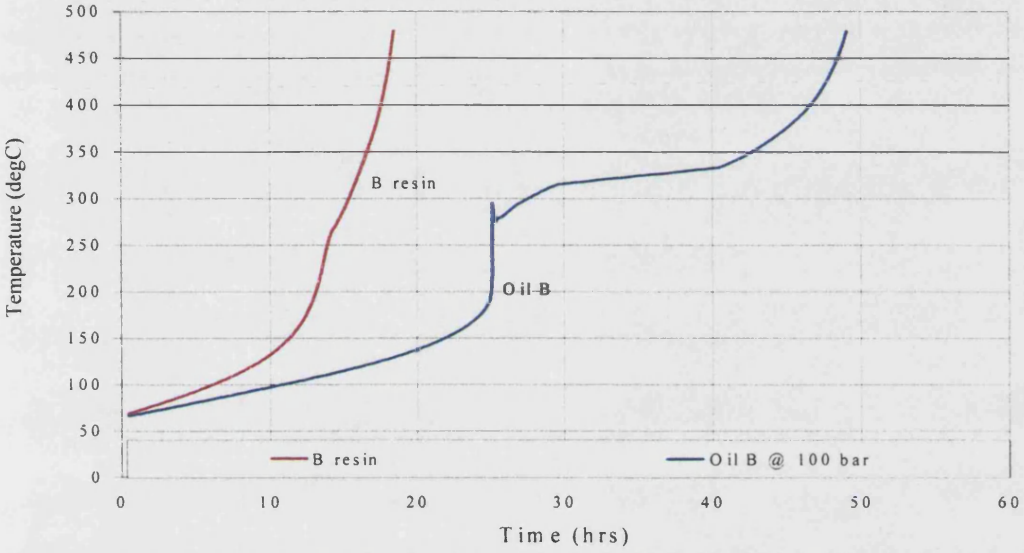

Figure 7.22: Adiabatic Temperature Profile, Oil B and Resin Fraction

Figure 7.23: Self-Heat Rate against –1000/T, Oil B and Resin Fraction

The exothermicity ratios are shown in Figures 7.25-7.27. Figure 7.25 shows an increase in the self-heat rates of the resin fraction for all regions apart from the propagation

region. The reaction times for the resin fraction, shown in Figure 7.26, are reduced for all the regions apart from the propagation region.

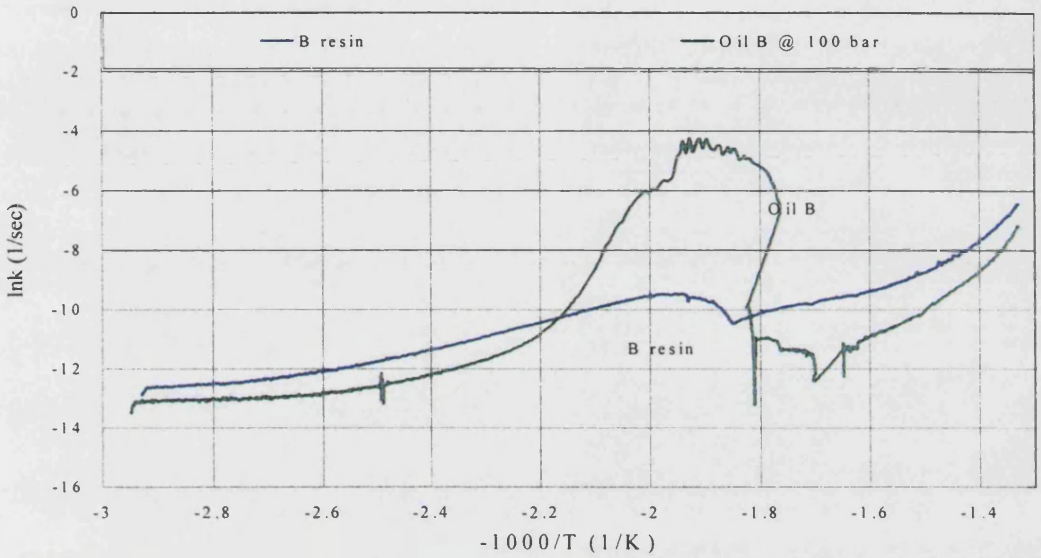

Figure 7.24: Reaction Rate Constant against –1000/T, Oil B and B resin fraction

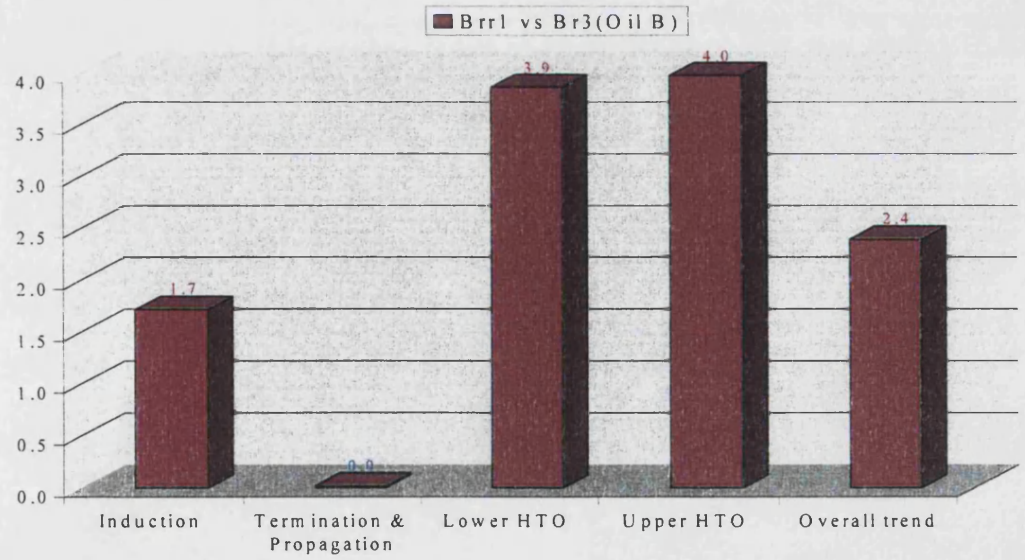

Figure 7.25: Ratio of Self-heat Rate for Resins Compared to Whole Oil

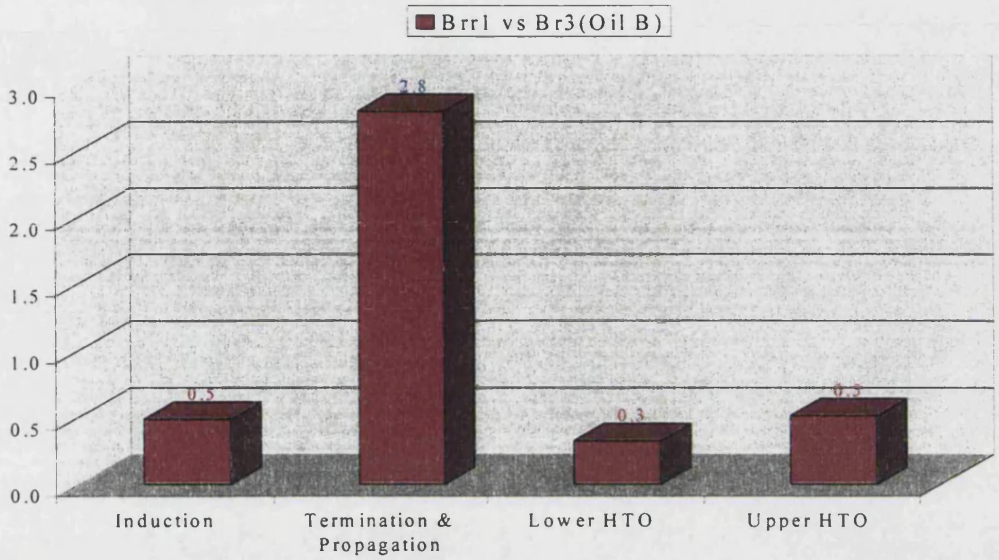

Figure 7.26: Ratio of Reaction Time for Resins Compared to Whole Oil

The energy release ratios for the resin compared with the "whole" oil, which are shown in Figure 7.27 are quite interesting in that they show a reduction for all regions apart from the upper HTO region. This implies a stronger contribution by the resins in this region, and this trend could be expected to continue at higher temperatures.

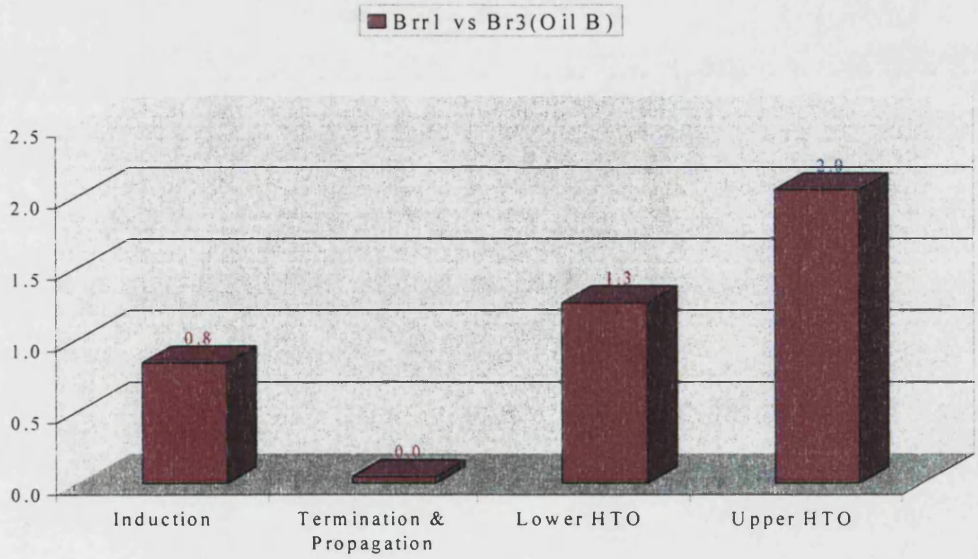

Figure 7.27: Ratio of Energy Released for Resins Compared to Whole Oil

The energy evolved in the experiments with resin fractions is compared with that for the "whole" oil in Tables 7.3. Energy released for the resin fraction alone is similar for the LTO region but increases slightly for the HTO region when compared with the "whole" oil. This confirms a strong contribution to the HTO region by the resin fraction.

The exothermicity effect of the resin compared with the "whole" oil for oil B is summarised in Figure 7.28. This shows the significant reduction in energy released over the propagation region for the resin fraction. However, the resin makes a strong contribution to the HTO region, especially at higher temperatures (upper HTO region).

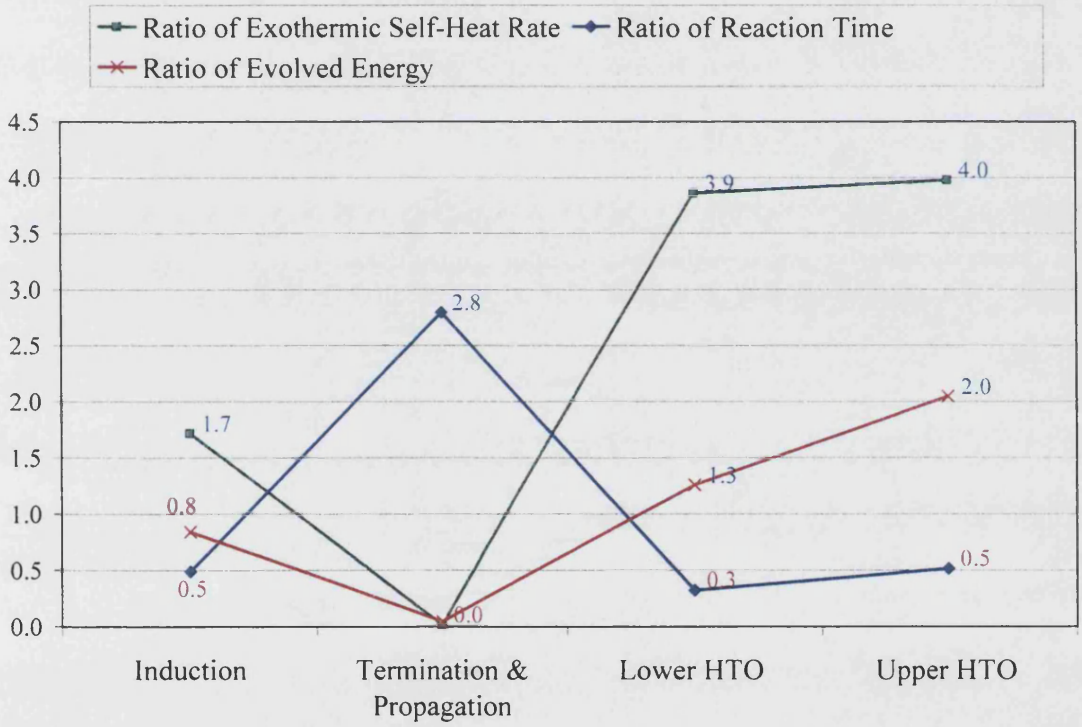

Figure 7.28: Summary of Exothermicity Contribution of Resins

7.5 Oxidation Behaviour of Asphaltenes

7.5.1 *Experimental Results, Asphaltene v whole oil*

Graphs showing the analysed data are shown in Figure 7.29 and 7.30 for experiments with asphaltene fractions (M and Wl asphaltene with rock and water @ 50 bar), and "whole" oil M (0.25ml oil M, rock and water @ 50 bar).

From Figure 7.29, the asphaltene fractions lag the "whole" oil with a much longer induction period before the autocatalytic induction occurs. The exotherm eventually dies out before it reaches the upper HTO region. The reaction rate constant plot of Figure 7.29 shows a different reaction mechanism occurring for the asphaltene fractions.

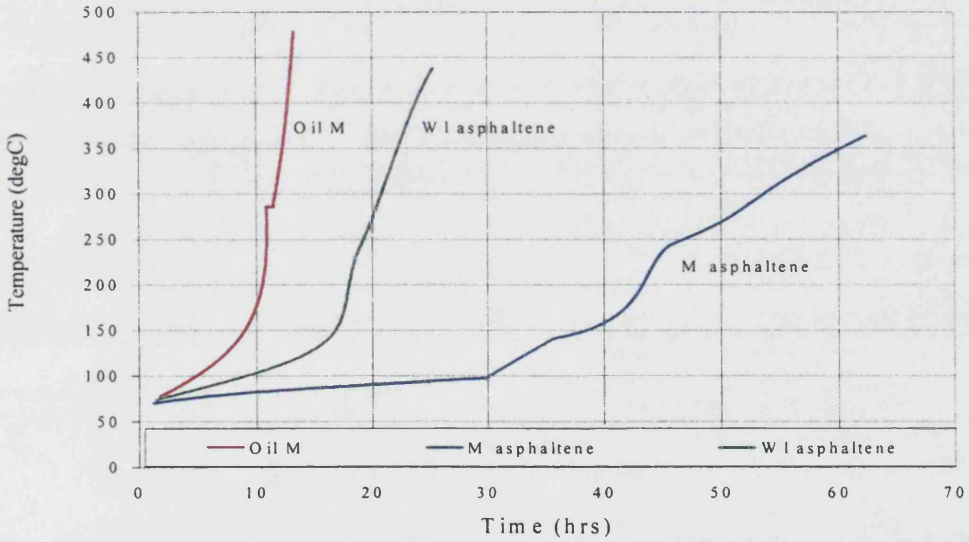

Figure 7.29: Adiabatic Temperature Profile, Oil M and M, Wl Asphaltene Fractions

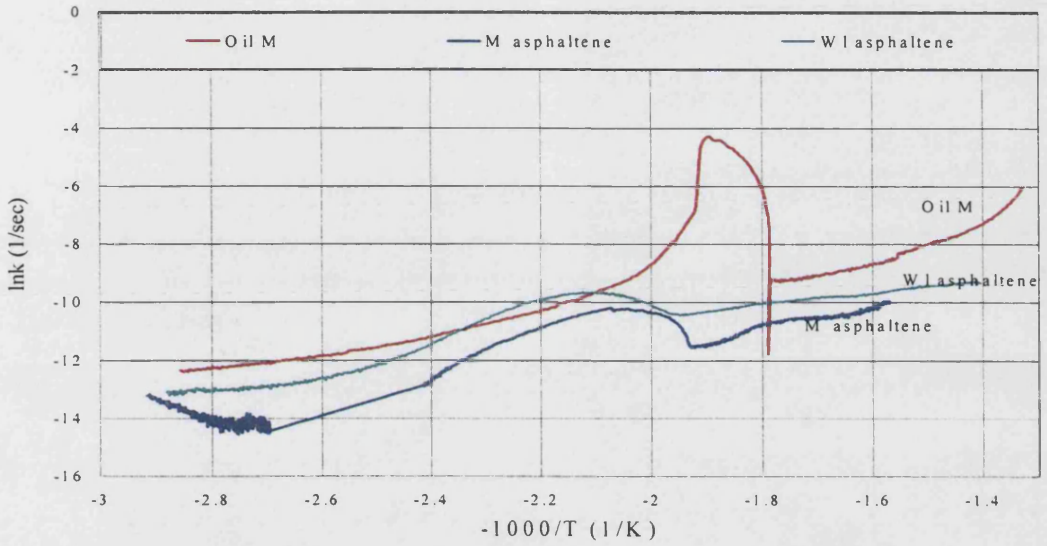

Figure 7.30: Reaction Rate Constant against –1000/T, Oil M and M, Wl Asphaltene Fractions

The exothermicity ratios are shown in Figures 7.31-7.33. Figure 7.31 shows a reduction in the self-heat rates of the asphaltene fractions for all the reaction regions. The reaction times for the resin fraction, shown in Figure 7.32, increases for all regions apart from the upper HTO region where reaction is not sustained.

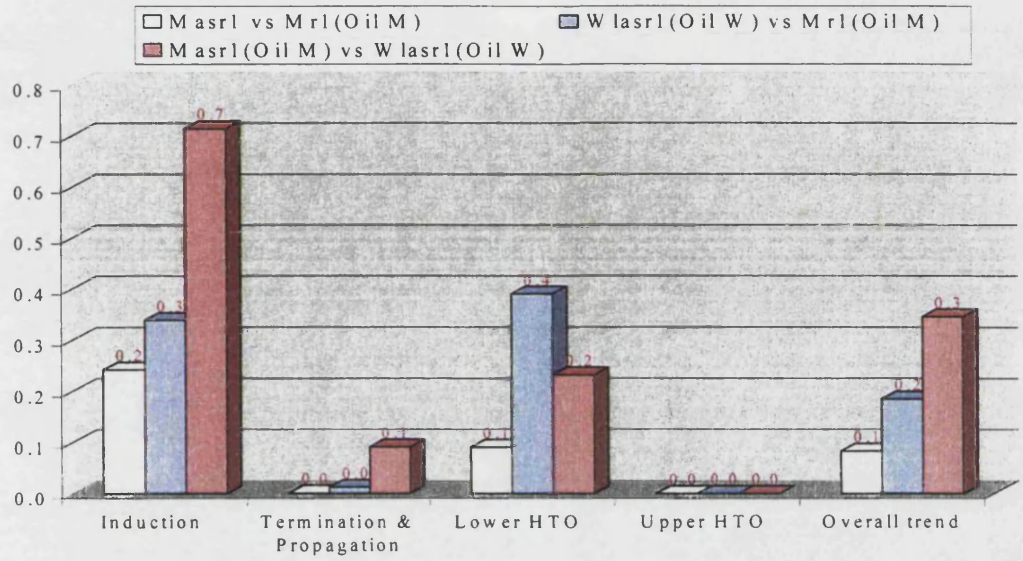

Figure 7.31:Ratio of Self-heat Rate for Asphaltenes Compared to Whole Oil

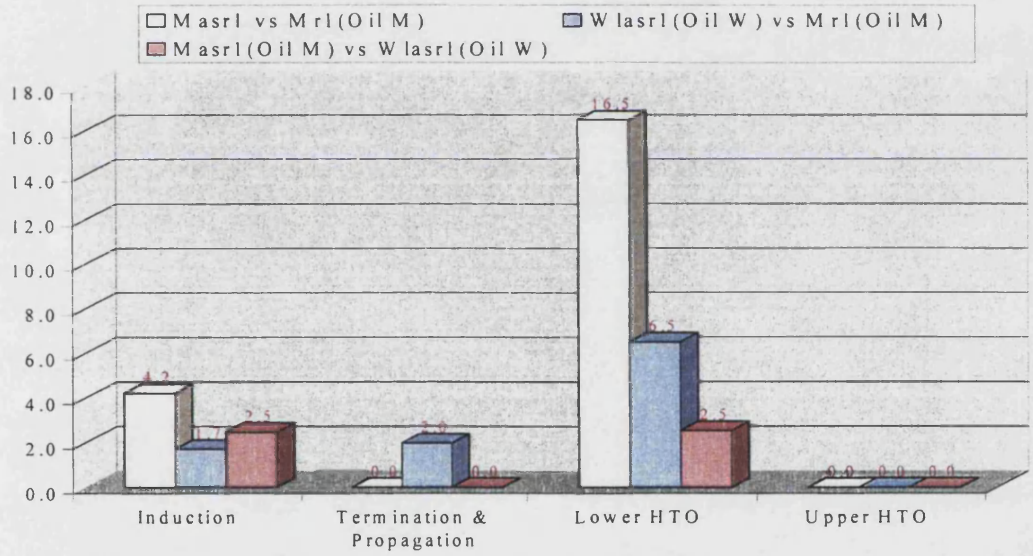

Figure 7.32: Ratio of Reaction Time for Asphaltenes Compared to Whole Oil

The energy released ratios for the asphaltene fraction compared with the "whole" oil, which are shown in Figure 7.32 reflects the absence of the propagation region and the extinguishing of the exotherm before it reaches the upper HTO region. The contribution of the asphaltene fractions to the LTO reaction is quite minimal, and this is confirmed by an

examination of the energy released in Table 7.3. There is a substantial reduction in the ELTO for oil M with the asphaltene fraction alone.

The extinguishing of the exotherm before it reaches the upper HTO region implies that the vigorous HTO reactions which asphaltene fractions partake in did not occur.

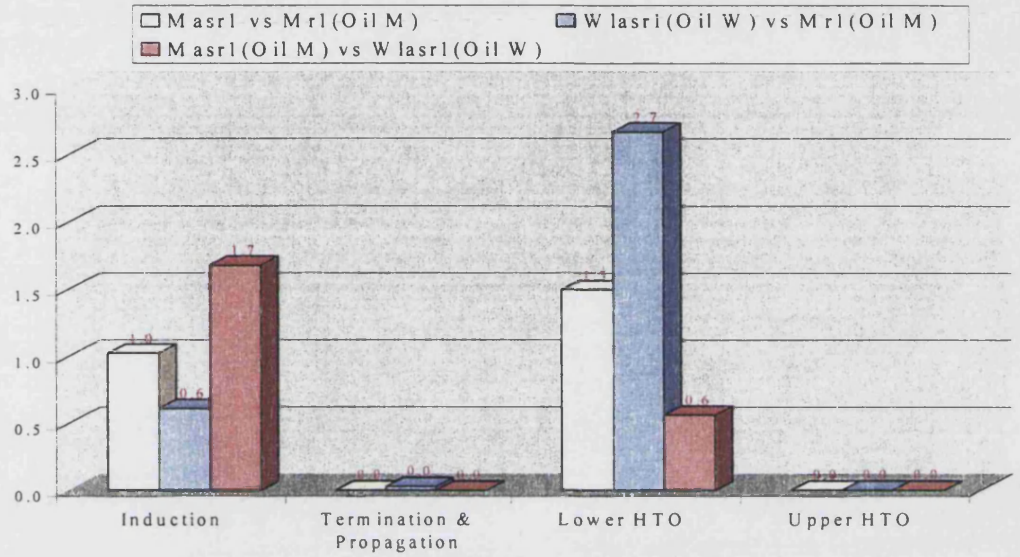

Figure 7.33: Ratio of Energy Released for Asphaltenes Compared to Whole Oil

The exothermicity effect of the asphaltene fractions compared with the "whole" oil is summarised in Figure 7.33. This shows the significant reduction in energy released for all regions apart from the lower HTO region. The expected acceleration in HTO free radical activity due to the asphaltenes was not seen. Based on these results, the asphaltene fractions do not contribute to oxidation reaction in any of the reaction regions studied. This must be because the temperatures under consideration here (80-500 C) are too low for the asphaltene to initiate vigorous reactions.

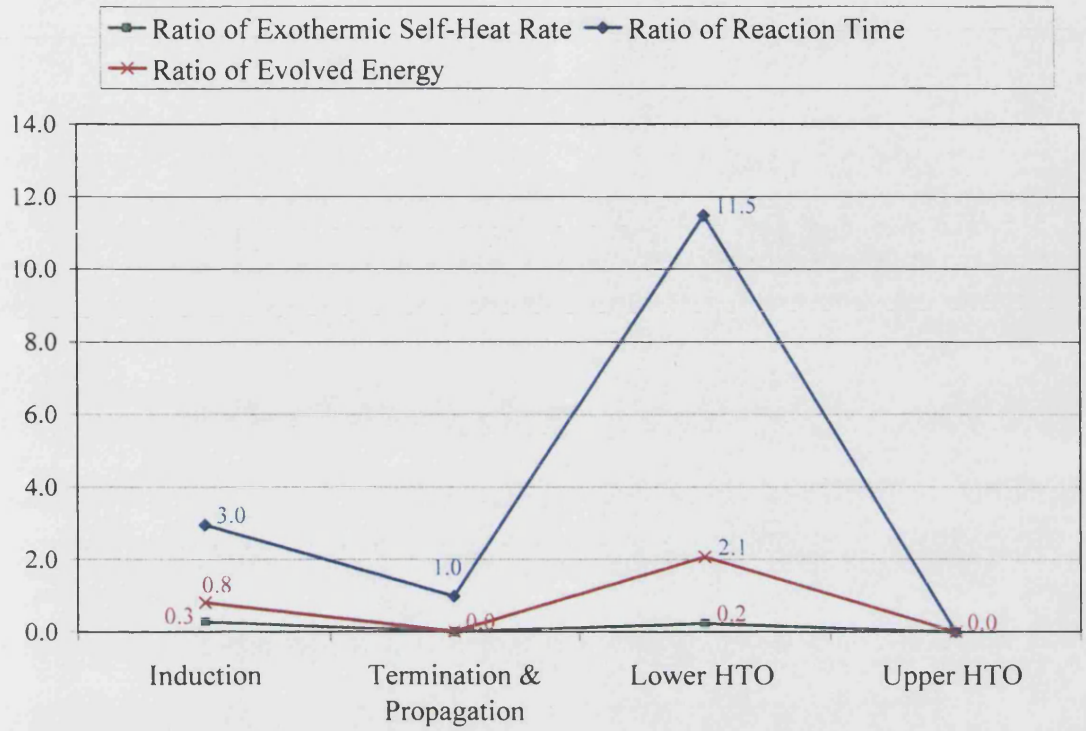

Figure 7.34: Summary of Exothermicity Contribution of Asphaltenes

7.6 Coke Deposition for different SARA fractions

Previous studies by Kok and Karacan, 1998 show that the amount of coke deposited during the pyrolysis of crude oil is greater than the amount of asphaltene in the original crude. This implies that other fractions are responsible for coke deposition as well. As was seen earlier in chapter 3, the light oils have a near zero asphaltene content, therefore, the fact that any coke is deposited at all validates this hypothesis that other mechanisms result in coke deposition.

The fraction most likely to have caused fuel deposition aside from the asphaltenes is the resin fraction, as this is the next heaviest part of the crude oil.

Ciajolo and Barbella, 1984 investigated the pyrolysis and oxidation of four heavy oils and their separate paraffinic (saturate), aromatic, polar (resin) and asphaltene fractions,

and found that the polar (resin) and asphaltene fractions pyrolyse and leave a carbon residue. The resins left a substantially larger coke deposit under air oxidation (23 to 25 wt %) as compared to nitrogen pyrolysis (4 to 5 wt %). This implies that the coke deposition occurs primarily due to oxidation of a material which then formed coke. This could be the conversion of resin to asphaltenes, which in turn pyrolyses to coke. The aromatics and saturates formed little, or no coke, while the asphaltenes formed about 51 to 60 wt % coke, irrespective of whether air or nitrogen was used.

7.7 SARA-Based Oxidation Reaction Mechanism

Belgrave et al 1990 proposed a reaction scheme for pyrolytic fuel deposition based on a classification of crude oil into maltenes and asphaltenes. The maltene fraction includes saturate, aromatic and resin fractions. The reaction scheme used is detailed below.

$$MALTENES \rightarrow ASPHALTENES \qquad \text{Equation 7.7}$$

$$ASPHALTENES \rightarrow COKE \qquad \text{Equation 7.8}$$

$$ASPHALTENES \rightarrow GAS \qquad \text{Equation 7.9}$$

Hutchence and Freitag 1991 proposed a SARA based reaction model, incorporating findings from Ciajolo and Barbella's (1984) studies. The crude oil was divided into pseudo components namely:

1. Light saturates
2. Heavy saturates (the saturate fraction was observed by Ciajolo and Barbella to distill in one or two fractions and due to the wide boiling point range was split into two fractions)

3. Light aromatics
4. Heavy aromatics (for the same reason as given above for saturates. The boiling ranges for the aromatic division into light and heavy fractions is the same for the saturates)
5. Resins and Asphaltenes.

The reactions included in the reaction model included the following reactions

1. An LTO reaction showing heavy aromatics and resins reacting with oxygen (based on findings from Adegbesan 1987 and Ciajolo and Barbella 1984)
2. Pyrolytic reactions involving heavy saturates vis breaking into light saturates and unsaturated compounds
3. Heavy aromatics vis breaking into light aromatics and light saturates
4. Resins forming asphaltenes, heavy aromatics, heavy saturates and light saturates
5. asphaltenes cracking into coke, heavy aromatics, heavy saturates, light saturates, carbon dioxide and water
6. Combustion (oxidation) reactions involving light saturates, light aromatics, heavy saturates, heavy aromatics, and coke reacting with oxygen to form carbon oxides and water.

For light oils, the heavier fractions must be omitted from any proposed model, leaving only the saturates, aromatics, resins.

Verkoczy and Freitag 1997 carried out autoclave tests on SARA fractions. An analysis of the products of the resins pressurised with air at 225 C was mainly asphaltenes (75 %), while the aromatics fraction was 63 % resin. A post mortem of the fraction that was initially saturates, revealed a variety of all of the different fractions were contained in the residue in the autoclave, while the asphaltenes turned into an insoluble fraction like

coke. It should however, be remembered that these reactions might not have gone to completion and many of the observed products could have gone on to further react with oxygen.

Monin and Audibert 1988 carried out autoclave tests on four crude oils (11.1 to 19.7 API), leaving them at 350 C for 200 hours. They noticed an increase in lighter hydrocarbons, mainly saturates while the aromatic content was less affected. The asphaltene and resin fractions deposited an insoluble organic phase "pyrobitumen", possibly coke.

CHAPTER 8:

Other Aspects of Crude Oil Oxidation

OTHER ASPECTS OF CRUDE OIL OXIDATION

There are some aspects of crude oil oxidation which deserve extra attention in order to understand how the oxidation occurs, specifically with light oils, and these are examined in this chapter. These include the pyrolytic effect on the crude oil from the oxidation as well as the behaviour of the light crude oil components. Oxidation phenomena, which are unexplained in the literature, are discussed in this chapter, including the negative coefficient zone.

Table 8.1: Experimental Analysis to Study Other Aspects of Oxidation

	Nitrogen (Pyrolysis Effect)	**Light Pure Components**
Differences between Experiments	***Pyrolysis Effect***	***C16-Component***
	Dn0 / D2, Drn1 / Dr1	C16 / Ar1, C16 / Cr1, C16 / Dr1
	Pyrolysis in the presence of rock	***Heavier / Lighter Component***
	Drn1 / Dn0	C16 / C10

8.1 Pyrolysis of Light Crude oils

Pyrolysis involves a breaking down of long molecules in crude oil into smaller molecules due to thermal effects. It is important to decouple the pyrolytic effect occurring due to temperature increase in a reservoir from kinetic oxidation reaction. Previous investigations have been carried out into the pyrolysis of oil alone and the oil mixed with sand and water, which showed that there was no discrepancy between the two results (Burger et al 1985). This implies that pyrolysis takes place throughout the entire volume of the oil, even in the pores of the reservoir.

Downstream of the oxidation front in a reservoir under air injection, nitrogen moves through a reservoir in a displacement front. As the displacement front moves through the crude oil, some pyrolysis will occur because this nitrogen displacement front will generally be at a higher temperature than the original oil. The displacement front temperature will depend on the thermal conductivity of the reservoir rock and oil, but it is not clear if any thermal effect on the crude oil would result from this. In order to develop a comprehensive reaction mechanism, it is also important to determine if any of the major effects observed during crude oil oxidation are because of the temperature increase throughout reaction, i.e. pyrolysis.

In the context of understanding the reaction mechanism as well as the exothermicity, it is necessary to carry out further investigations into the pyrolysis alone. It appears that a majority of investigations have taken the pyrolysis and reaction process to be the same during in-situ combustion or air injection.

Experiments were carried out using nitrogen as the reacting gas, with other conditions remaining the same, to illustrate the pyrolysis effect on the oil. The adiabatic heat wait search procedure was applied to the oil in the presence of nitrogen only, both with and without rock and water. A slight heat correction was added to the tracking heaters to ensure a slow temperature increase was applied to the experiment. The obtained results are compared with the experiments done with air and are shown in Figure 8.1-8.3.

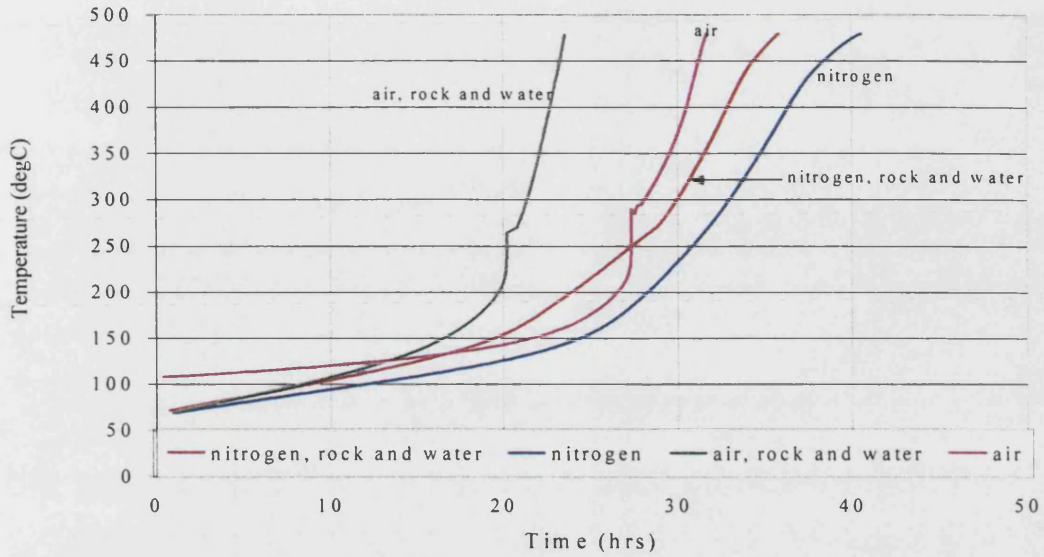

Figure 8.1: Temperature Profile, Drn1 (nitrogen, rock and water), Dn0 (nitrogen), Dr1 (air, rock and water), D3 (air)

The experiments run with nitrogen track the temperature increase over the temperature range, and the temperature profile is shown in Figure 8.1. This shows the four reactions with oil D at 50 bar in the presence of air; air, rock and water; nitrogen; and nitrogen, rock and water. A reduction in the rate at which temperature increases is visible at the higher temperature ranges (>450 C) in the presence of nitrogen, both with and without rock and water. This absorption of heat does not happen in the presence of air and must be due to the cracking some of the heavier oil molecules. This can be seen clearly from Figure 8.2, which shows the self-heat rate of the two experiments run with nitrogen alone. Generally though the thermal effect from the pyrolysis is minimal throughout the temperature range studied.

The exothermicity of the nitrogen runs is compared with that of the air experiments in Figure 8.3, which shows the self-heat rate plots for the four different runs. It is seen that the heat release is higher with the two runs in the presence of air, which is expected.

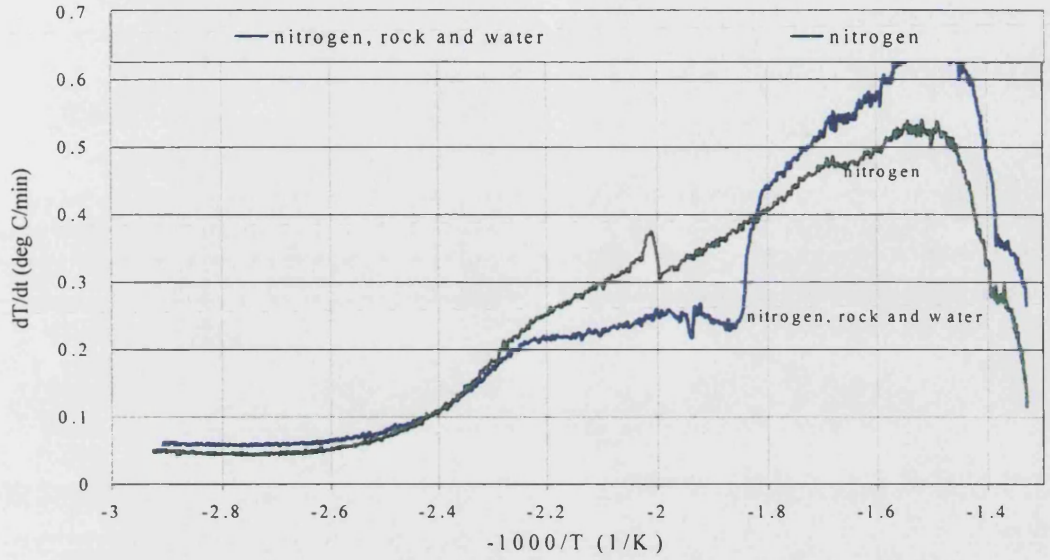

Figure 8.2: Self-Heat Rate against –1000/T, Drn1 (nitrogen, rock and water) and Dn0 (nitrogen)

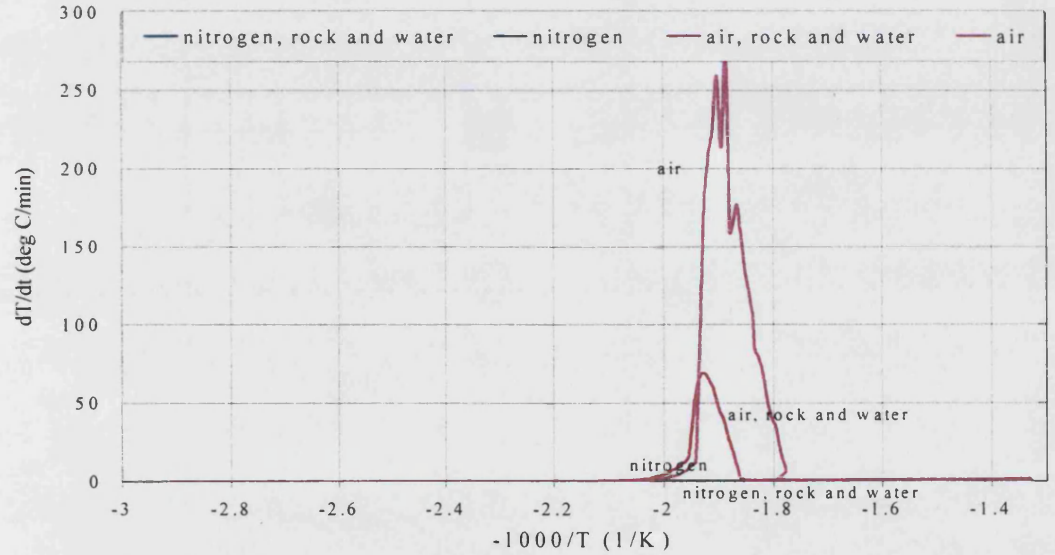

Figure 8.3: Self-Heat Rate against –1000/T, Drn1 (nitrogen, rock and water), Dn0 (nitrogen), Dr1 (air, rock and water), D3 (air)

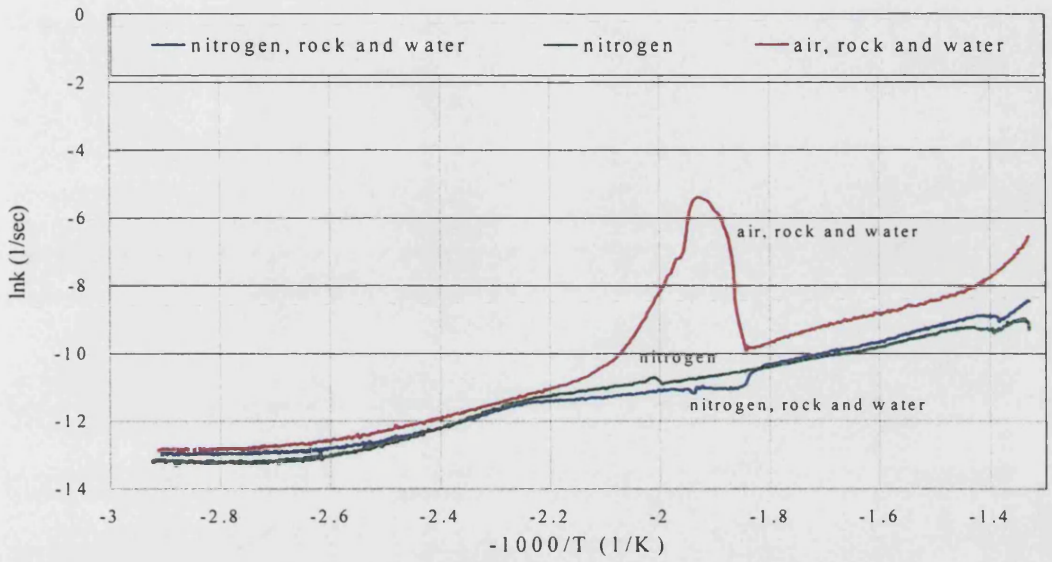

Figure 8.4: Reaction Rate Constant against –1000/T, Drn1 (nitrogen, rock and water), Dn0 (nitrogen), Dr1 (air, rock and water)

The reaction rate constants obtained for three runs are plotted in Figure 8.4 (air, rock and water; nitrogen, rock and water; and nitrogen). This shows that the phenomena occurring in the presence of nitrogen is different from that with air, and this can be ascribed to a pyrolysis effect rather than combustion. In particular, while the induction regions appear similar, there is no autocatalytic reaction occurring in the presence of nitrogen. The blip near the end of the HTO can be taken as the start of the cracking which is expected at these higher temperatures. However, there is also a slight blip at the start of the lower HTO region in the pyrolysis experiment. It is not clear what is occurring here and further experiments, including a sample analysis of the vapour and liquid present in the bomb at this point, are necessary to understand the processes taking place here, which could include visbreaking of some fractions.

Apart from demonstrating the thermal effect of the displacement front as it moves through the crude, this pyrolysis reaction is also representative of what would occur under

air injection with extreme oxygen deficiency. It should be noted that some oxygen would be present in the crude oil and rock, already, and there would possibly be oxygen impurities in the nitrogen gas cylinder.

8.2 Oxidation of Light Oil Components

Another area of uncertainty during light oil air injection is the behaviour of the light components present in these types of reservoirs, usually at high pressures (>1500 psi). At higher pressures, the vapour-liquid equilibrium of crude oil is changed substantially. The lighter fractions of the crude oil would be less susceptible to the distillation that is seen to occur at the lower pressures where thermal analysis investigations are carried out. The distillation effect has been discussed earlier in chapter 2, and the actual fractions of the crude oil that would distill can be calculated using standard distillation correlations.

At the high pressures under which light oil reservoirs are found, the distillation which was noted at lower pressures would be much less upon air injection. It is therefore important when running continuous experiments to run experiments as close to the reservoir pressure as possible.

From classical organic oxidation literature, the reaction rate constant for normal paraffin increases with increasing carbon number while the activation energy decreases with increasing carbon number. A conclusion from this is that oil components get more reactive the heavier they are. However, this mainly details their HTO behaviour, rather than the LTO, which could be quite different. Therefore, examination of the oxidation behaviour of some pure light oil components was performed.

Pure n-decane (C10) and n-hexadecane (C16) were reacted with rock and water at 50bar air, and the experimental runs used to compare the results are shown in Table 8.1.

The adiabatic temperature profile for the two runs with the pure components as well as those with oils A and D is shown in Figure 8.5. The most significant result from this plot is the decrease in the rate of temperature increase at higher temperatures. This implies that the lighter components (C10 and C16) do not react as vigorously at these higher temperatures, and participate more strongly at lower temperatures. This effect is more pronounced in the C10, where the reaction tails off more significantly than the C16 run.

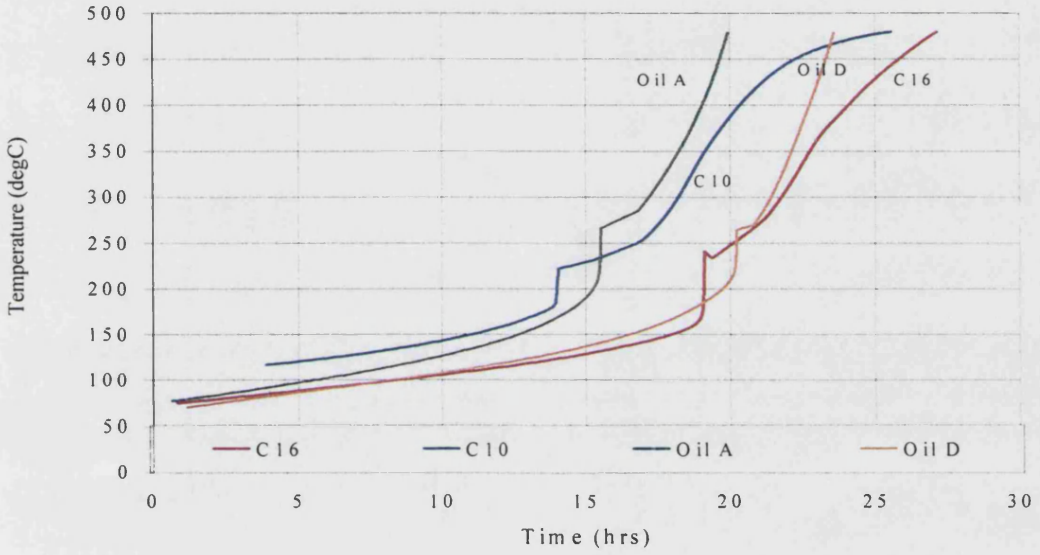

Figure 8.5: Adiabatic Temperature Profile, C10 (n-decane), C16 (n-hexadecane), Oil A and D

The self-heat rate, which is shown in Figure 8.6 displays an interesting trend for the lighter components. The autocatalytic ignition point, with the accompanying increase in self-heat rate, is seen to occur at a much earlier temperature than it does for all the whole oils. The maximum self-heat rate reached is also significantly lower, meaning the lighter fractions participate in less vigorous reactions than the whole oils.

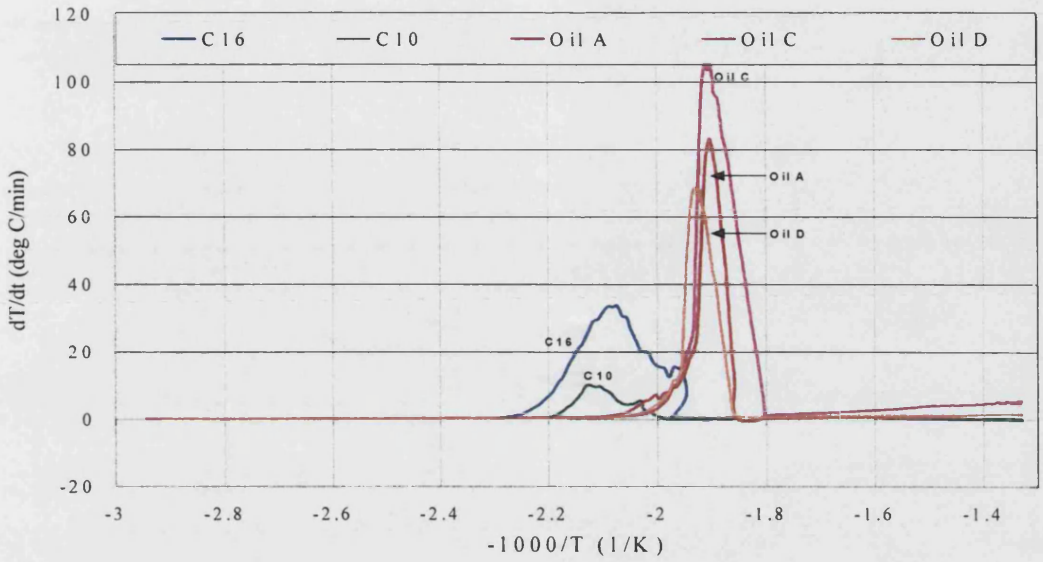

Figure 8.6: Self-Heat Rate against –1000/T, C10 (n-decane), C16 (n-hexadecane), Oil A, C, D

The exothermicity ratios comparing the pure light components to the whole oil are shown in Figures 8.7-8.9.

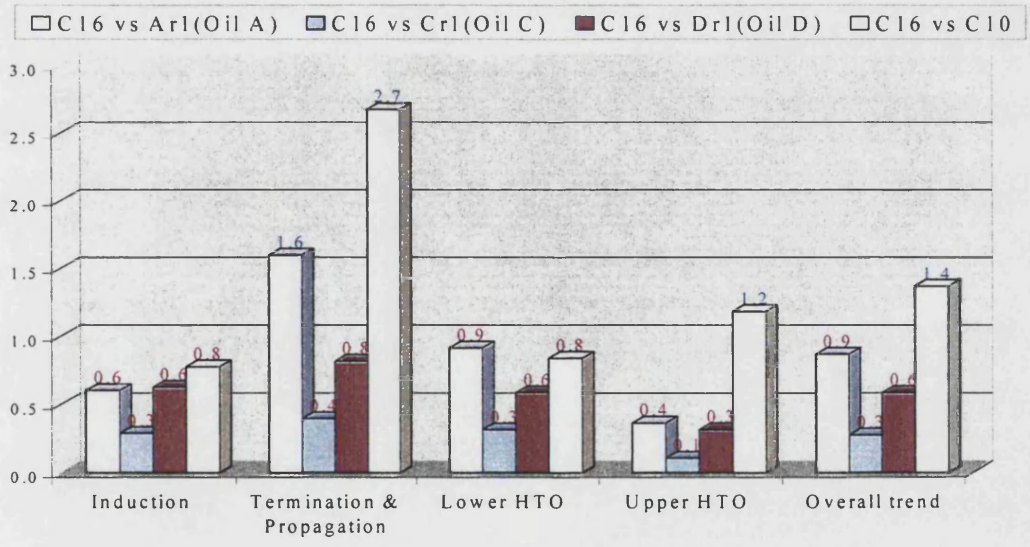

Figure 8.7: Ratio of Self-heat Rate for Light Components Compared to Whole Oil

The self-heat ratios in Figure 8.7 generally show a reduction in the self-heat rate in every region for the light component fractions. The C16 fraction also exhibits a higher self-

heat rate than the C10 fraction in most of the regions. The ratio of reaction time is shown in Figure 8.8, and shows an increase in reaction time of all regions with the light components compared with the whole oil. The reaction generally takes longer periods for completion, implying that other components start the reaction first and cause this acceleration.

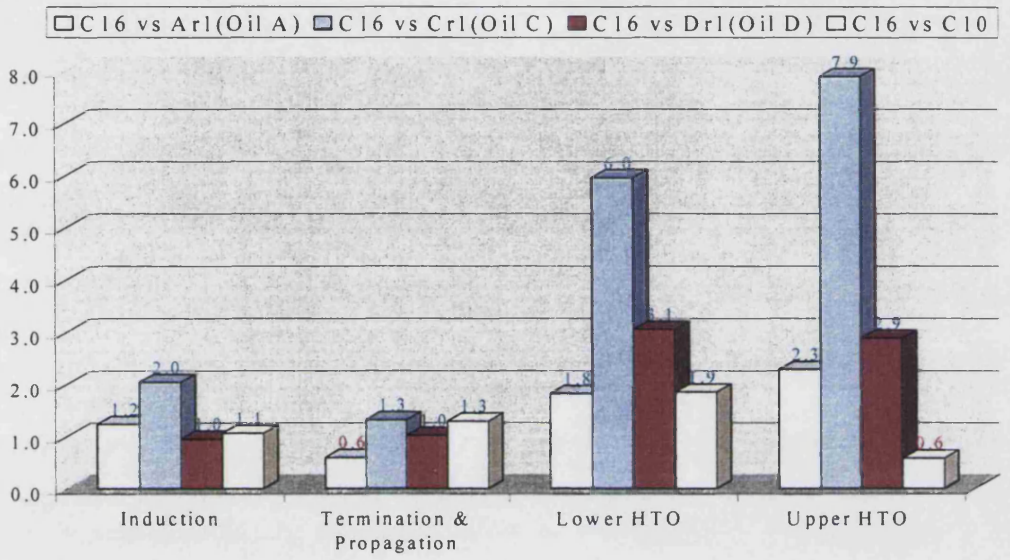

Figure 8.8: Ratio of Reaction Time for Light Components Compared to Whole Oil

The energy released ratios in Figure 8.9 show a reduction in energy released for every region apart from the lower HTO region due to the longer reaction times. The energy evolved in the experiments with the light components as well as the whole oil experiments are compared in Table 8.2. Again the specific heat capacity of crude oil is used to calculate the energy evolved, as this value should be close enough to the actual heat capacities of n-decane and n-hexadecane. Energy released reduces in the LTO region when the light components are reacted.

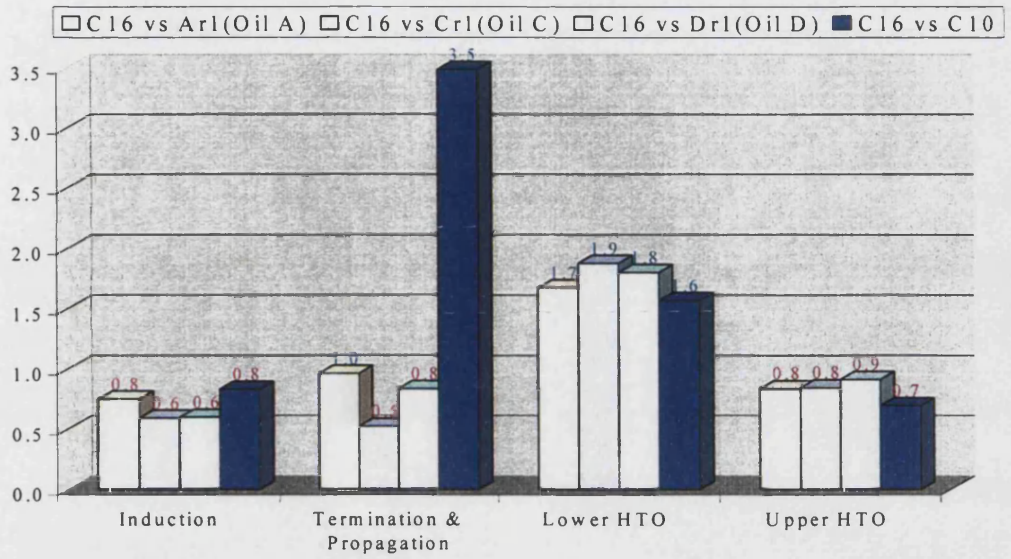

Figure 8.9: Ratio of Energy Released for Light Components Compared to Whole Oil

Table 8.2: Energy released for Light Components

	D3	Arl	Crl	Drl	C10	C16
ELTO	1074	343	555	407	176	303
EHTO	174	216	205	199	247	258

The exothermic behaviour with a reduction in the carbon number of the oil component is summarised in Figure 8.10 by taking an average of the exothermicity ratios for the oils A, C and D compared with the C10 and C16. This confirms the trend of reduced exothermicity in the runs with the light components. The energy released reduces in every region apart from the lower HTO region.

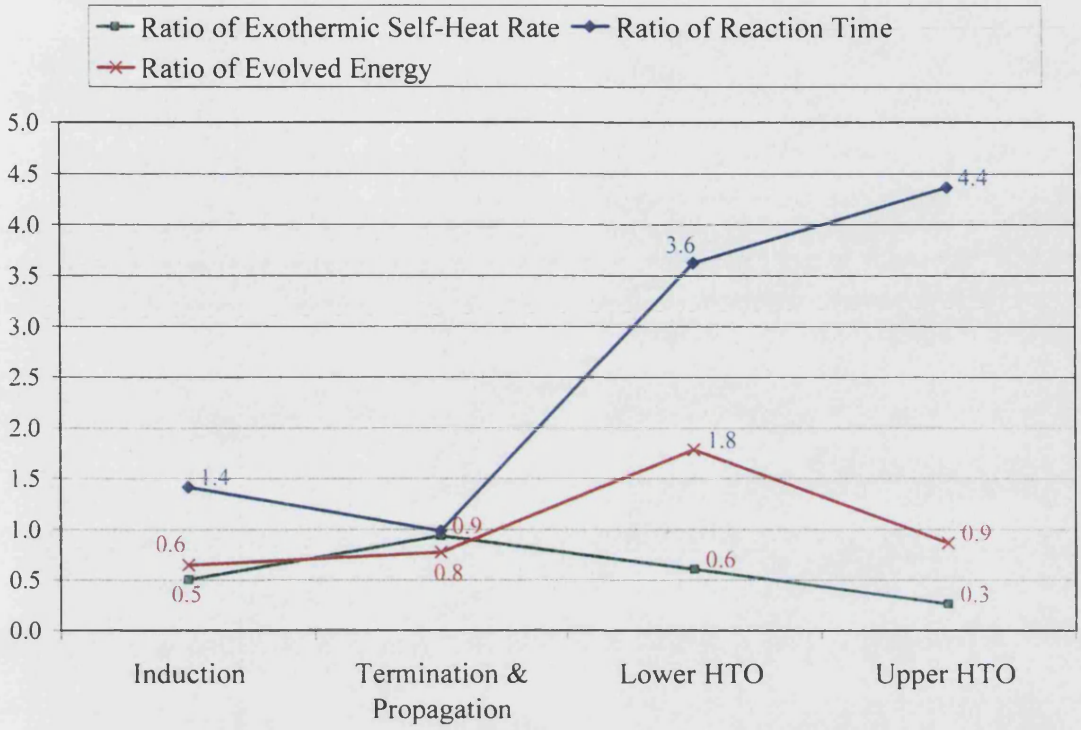

Figure 8.10: Summary of Ratios Showing Effect on Exothermicity of Reducing Carbon number

It can be concluded then that an increase in the carbon number causes an increase in the reactivity and exothermicity, both in the LTO and HTO regions. This trend has been shown by others for other carbon number ranges apart from the lower range (C10, C16) tested in this study. However, the light oil components certainly take part in the LTO oxidation region, and LTO has an impact on HTO. This affects high pressure, light oil air injection processes because the amount of lighter fractions distilled at the high pressures would be much less than in low pressure reservoirs, leaving more oil to serve as fuel. While distillation would still occur, some of the light fractions will react depending on the residence time. Therefore, the percentage of light oil fractions that reacts is a function of residence time and combustion front velocity rate, i.e. rate of displacement versus reaction rate.

8.3 Negative Temperature Coefficient Zone

A number of investigators have drawn attention to a region where the oxygen uptake rates and energy generation rates decrease with increasing temperature. Moore et al 1992 in a study of oxidation of Athabasca Oil Sands reported a lack of data between 370 ^{0}C and 500 ^{0}C. This phenomena was also reported by Zelenko and Solignac, 1997, where oxidation was seen to stop at a temperature of about 197-217 ^{0}C for two crude oils studied. These reactions started again at a temperature of 227 ^{0}C and 247 ^{0}C respectively.

Dechaux, 1971 refers to this as the negative temperature coefficient region, and this sort of behaviour is seen in oxidation profiles from experiments carried out by Burger and Sahuquet, 1972 and Fassihi et al 1984.

This region appears to separate the low temperature oxidation region and the high temperature oxidation regions. As far back as 1959, Tadema observed two isolated temperature peaks, separated by 130 K. Babu and Cormack, 1983, in their study of LTO in Athabasca bitumen found a region where the rate of oxidation dropped to a lower rate. This was explained due to the fact that the more reactive bonds and molecules oxidised first and once these reactants were oxidised the reaction rate declines.

The effect of this NTC zone on the oxidation of any crude oil in the field has also been discussed. Moore et al 1992 stated that this region would determine the possibility of a particular crude oil transitioning from LTO to HTO. This was the basis for the screening method proposed by Yannimaras and Tiffin, 1995.

It is a phenomenon that has been observed classically in the oxidation of organic compounds. From the organic chemistry oxidation literature, the NTC region usually indicates a significant change in the product distribution indicating a shift in the mechanism. Wilk et al 1987 report a NTC zone of between 327-387 ^{0}C for propane and

one of 362-392 ^{0}C for propene oxidation. They reported that following the NTC zone, the net yields of oxygenated hydrocarbon species such as formaldehyde, acetaldehyde and methanol decreased. However the yields of the lower alkenes and alkanes such as ethene and methane increased. Another interesting feature reported by Wilk et al is the fact that the NTC zone in propene, propane and other alkane oxidation reduces in experiments carried out with higher fuel concentrations. In Wilks results at a propene-air equivalence ratio of 0.8, the NTC is much stronger than it is at a ratio of 2.0. This would have field implications for the oxidation kinetics. As the oil saturation would vary in the reservoir, the local kinetics would follow different mechanisms in different areas. This could also explain why the laboratory tests could give different results from actual reservoir runs in terms of a continuity from the LTO to the HTO zone.

Another important implication of this is that there might again be a minimum oil saturation where the NTC zone is strong enough to stop the reaction going from LTO to HTO.

Possible causes of the NTC zone

One reason that may be advanced for a drop in the temperature, as seen in the self-heat rate plots at the end of the LTO, is that the reaction stops. Either the same reaction or another one then starts immediately afterwards. This could be due to four different phenomena, listed below.

1. A change in phase of the reaction, from liquid to gas, and hence a latent heat of vaporization effect could be responsible for the drop in temperature.
2. A natural change in the reaction mechanism indicating the switch from the LTO to HTO reaction predominating.

3. The fall in temperature could be due to cracking of some of the crude oil components, as cracking is predominantly an endothermic reaction. However, cracking is not known to occur at low temperature (<250 C) with the light crude oils being used, hence this can be discounted as the cause, though vis-breaking could be responsible.

The vapour-pressure relationship during the experimental runs can be clearly seen using the plot of pressure versus time. Comparison of this plot under different conditions can be used to test the first hypothesis for the cause of the NTC region, i.e. vaporisation.

The initial departure from the straight P/T line seen below could be a change of the sample from liquid to vapour. The drop in the spike then occurs as the reacting system comes back to equilibrium with the accompanying latent heat of vapourisation being removed from the system. The Antoine plot (P/T) is shown in Figure 8.11 for runs made with oil B at two different pressures, 50 and 100bar.

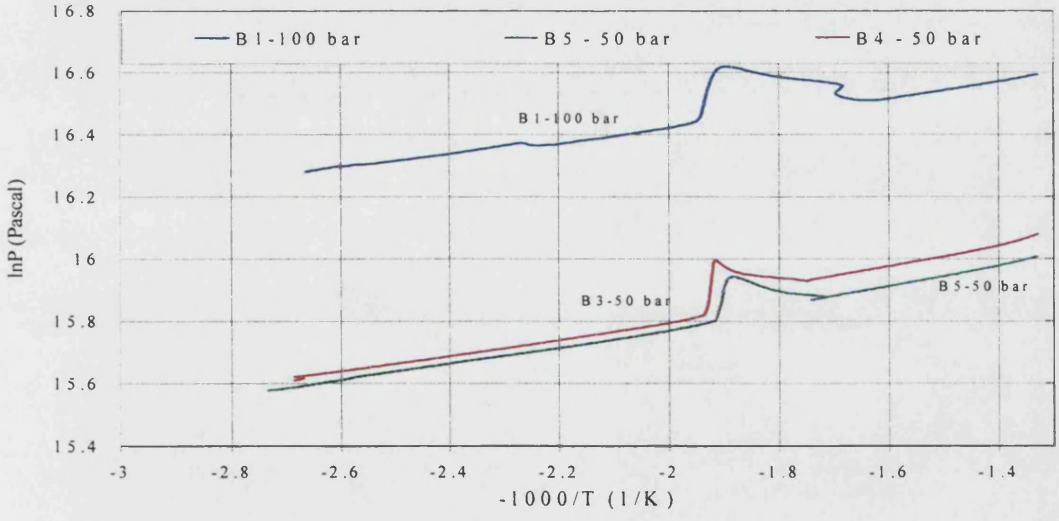

Figure 8.11: Logarithmic Plot of Pressure against –1000/T, B1 (100 bar), B5 (50 bar) and B3 (50 bar)

Pressure is well known for its property of shifting the boiling point of a substance. Lower pressures should reduce the boiling point and vice versa. However, this is not the case, as an examination of Figure 8.11 with different pressure experiments, shows the first spike in pressure occurring at the same temperature for the different pressures. This shows it is probably not a vaporisation effect as doubling the pressure would have a big effect on the vaporisation temperature.

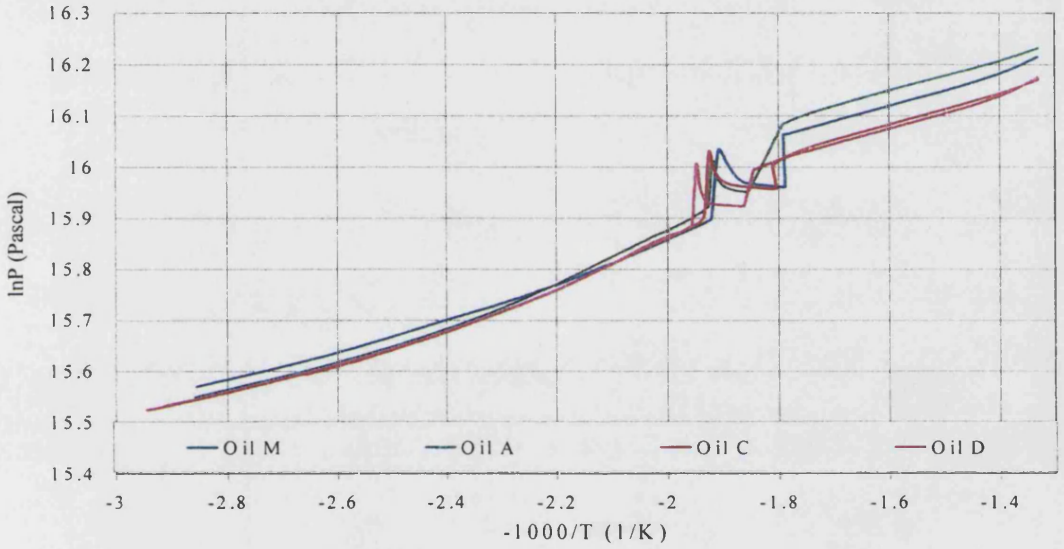

Figure 8.12: Logarithmic Plot of Pressure against –1000/T, Medium Heavy Oil (Oil M) and Light Oils (A, B, D)

The same pressure against temperature plot for various light oils and a medium heavy oil is shown in Figure 8.12. As the different components that make up crude oil have a wide temperature boiling range, vapourisation of the components would occur continuously as temperature changes throughout the reaction, rather than at one temperature. It can be concluded that this phenomena of the NTC is not caused by vaporisation, although vaporisation would happen over the course of the reaction.

Of the possible causes of the NTC zone mentioned earlier, a change in the reaction mechanism is the most probable, though there might be some vaporisation effects as well. This change in the mechanism would arise from the termination stage of the free-radical LTO reactions occurring, as discussed in Chapter 2.

CHAPTER 9:

Conclusions and Recommendations

CONCLUSIONS AND RECOMMENDATIONS

9.1 Conclusions

The main conclusions arising from this study are listed as follows:

1. A relatively quick and easy method has been set up at Bath to assess the oxidation kinetics behaviour of light and medium crude oils under different conditions. The effect of different oil and reservoir parameters on the oxidation kinetics of the crude oils has been studied experimentally by following the adiabatic energy release rate. These effects can be related to reservoir field conditions and used to judge the suitability of air injection.
2. Increasing the amount of oil (oil saturation) reduces the reaction time at higher self-heat rates resulting in a greater energy release than when there is less oil present. This can also be related to the minimum and maximum air-oil ratios used for air injection, but the cause could be due to minimum fuel requirement for combustion. Higher oil recovery may be possible if injected earlier in a fields' development rather than when the field is more mature, i.e. after a long period of waterflooding.
3. Water has a reducing effect on the energy released from crude oil oxidation. There is also heat removal to vaporization when water is present. The presence of water prevents the formation of a critical level of free radicals during the LTO period and also extinguishes the HTO reaction at very high water saturations; consequently air injection may not be very successful in fields possessing very high water saturation.
4. The properties of the reservoir matrix have an important influence on the LTO and HTO reactions:

- Crushed reservoir rock acts as a heat sink preventing vigorous autocatalytic reactions in the LTO region, but at the same time, catalysing HTO reaction, resulting in higher energy evolution.
- Clay (kaolinite) alone exhibited a catalytic effect in the upper HTO region (more vigorous), but its effect in the lower HTO and LTO regions is less vigorous than for reservoir rock.
- Exothermicity is strongly affected by surface area of the solid matrix. Fine silica causes more vigorous exothermic reaction, as opposed to chalk, which inspite of its high surface area, provides a poor adsorption reaction surface because of its colloidal nature.

5. The self-heat rate, reaction time and energy released due to LTO and HTO reaction, are very dependent on the heavy component fractions in the oil. Thus, as the oil density increases (light to medium oil) there is a substantial increase in these quantities.

6. The oil composition provides a useful determinant of the oxidation behaviour of crude oils:

- The saturate components of the oils studied are more reactive in the LTO region than the whole oil itself. Therefore, the other SARA (saturate, asphaltene, resin, aromatic) fractions reduce the LTO free-radical reaction. The aromatics are the most likely candidate for this as they form phenols, which are known to be antioxidants. The retarding effect of the aromatics is most significant in the propagation region, but they do not have any negative retarding effect in the HTO region. The resin fraction is strongly reactive in the HTO region, especially in the upper HTO region. Asphaltenes, however,

did not initiate vigorous reaction in the temperature range studied (80-500 ^{0}C).

- Pure light oil components (n-decane, hexadecane) produced less vigorous reactions than the whole crude oils. Thus, an increase in the carbon number of the oil causes an overall increase in reactivity and exothermicity. These pure light oil components take part in the LTO oxidation region and should therefore be considered in the development of reaction models for high reservoir pressures, because distillation of light fractions will be reduced. The precise effect will be dependent on such factors as residence time, combustion front velocity, etc.

7. The negative temperature coefficient (NTC) region is attributed to a change in the reaction mechanism occurring after the propagation region. It arises because of the termination stage of the free-radical LTO reactions. If an NTC region develops, it may restrict oxidation to the LTO region, without continuity to HTO.
8. Ratio Analysis has been used throughout this study to identify critical trends. Inclusions of all the quantitative aspects of the data proved very unwieldy, so general comprehensive trends have been used for analysis.
9. The reaction mechanism used in the LTO region (Induction, propagation and termination regions) has been widely used for studies of organic chemical combustion. Higher resolution of the PHI-TEC II has made it possible to discriminate in more detail the transitions between these different regions of reaction, both in the LTO and HTO.

9.2 Recommendations

1. In addition to the adiabatic temperature and pressure data obtained during the present experiment, an analysis of the vapour and liquid phases after reaction is essential for the development of a detailed reaction model. The analyses should determine which chemical species participate in the reaction (LTO and HTO), and the precise stoichiometry.
2. Experiments are required where the oxidation reaction is halted at different temperature stages and analysed. In particular, just before autocatalytic induction occurs and also where HTO starts. This would enable a more precise understanding of the particular reactions occurring during LTO. This would allow validations of existing models for LTO, or lead to development of new ones.
3. Continuous flow experiments should be carried out to determine the effect of flow behaviour on the oxidation reactions. Very precise instruments will be needed to carry out these experiments, including an on-line mass spectrometer. The present experiments have been carried out in a batch mode. Under air injection, different parts of the reservoir would encounter greatly varying flow conditions. Close to the injection wellbore, and just downstream of this, the condition would be best represented by continuous flow, while further downstream, the reservoir effect will be closer to the batch experiment.
4. To fully quantify the contribution of each of the SARA fractions to the overall oxidation reaction, experiments need to be carried out on different combinations of SARA fractions.
5. The ideal minimum and maximum air-oil ratios for efficient design and operation of an air injection project. This could be calculated by running several experiments

using different amounts of oil to study the effect on the oxidation rate. This would then need to be scaled to reservoir condition.

References

REFERENCES

Abu-Khamsin S.A., Brigham W.E., Ramey Jr. H.J., 1988, "Reaction Kinetics of Fuel Formation for In-Situ Combustion", SPE Reservoir Engineering, November pp. 1308-1316.

Adegebesan K. O., 1987, "LTO Kinetic Parameters for In-Situ Combustion: Numerical Simulation" SPERE, November, pp. 573-582.

Alderman J.H., Osoba J.S., 1971, "A Study of Oil recovery by In-Situ Combustion with the Addition of Water", SPE Paper 3684, 42nd Annual California Regional Meeting of Society of Petroleum Engineers of AIME, Nov. 4-5.

Alexander J.D., Martin W.L., Dew J.N., 1962, "Factors Affecting Fuel Availability and Combustion During In-Situ Combustion", SPE April 12-13.

Babu D. R., Cormack D. E., 1983, "Low Temperature Oxidation of Athabasca Bitumen" Canadian Journal of Petroleum Technology, Vol. 61, August, pp. 858-861.

Babu D. R., Cormack D. E., 1984, "Effect of LTO on the Composition of Athabasca Bitumen" Fuel, Vol. 63, June, pp. 858-861.

Bae J. H., 1977, "Characterisation of Crude Oil for Fire flooding Using Thermal Analysis Methods" SPE Journal, June, pp. 211-218.

Bagci A.S., Kok, M.V., Okandan, E., 1987, "Combustion Reaction Kinetics in Limestones Containing Heavy Oils", Society of Petroleum Engineers Journal, March, pp. 405-410.

Bastian P.A., Pietsch C.L., Voneiff G.W., 1997, "Solving Engineering Problems With PC-Based Relational Databases", SPE Computer Applications, October.

Behar F., Ungerer P., Audibert A., 1988, "Experimental Study and Kinetics Modelling of Crude Oil Pyrolysis in relation to Thermal Recovery Processes" Fourth UNITAR/UNDP Conference on Heavy Crude and Tar Sands, Edmonton.

Behar F., Vandenbroucke M., 1996, "Experimental determination of the Rate Constants of the n-C_{25} Thermal Cracking at 120, 400 and 800 bar: Implications for High Pressure/High Temperature Prospects", Energy & Fuels, Vol. 10, pp. 932-940.

Belgrave J. D. M., Moore R.G., Ursenbach M.G., 1994, "Gas Evolution From the Aquathermolysis of Heavy Oils", Canadian Journal of Chemical Engineering, Vol. 72, June, pp. 511-516.

Belgrave J. D. M., Moore R.G., Ursenbach M.G., Bennion D.W., 1990, "A Comprehensive Approach to In Situ Combustion Modelling" SPE Advanced Technology Series Vol. 1, No.1, pp. 98-107.

Belkharchouche M., Hughes R., Price D., 1988, " Pressurised DSC Studies of Heavy Oils and their Relevance To In Situ Combustion" 4th Unitar/UNDP Conf. Paper No. 150, pp. 1-22.

Ben-Aim R., Lucquin M., 1959, "La reaction en chaine dans l'oxidation des hydrocarbures satures" Journal de Chimie Physique, 56, 649.

Benson S. W., 1960, "The Foundations of Chemical Kinetics", McGraw-Hill Book Co., New York.

Bousaid I.S., Ramey Jr. H. J., 1968, "Oxidation of Crude Oil in Porous Media", Society of Petroleum Engineers Journal, Trans AIME, 243, June pp. 137-148.

Burger J. G., Sahuquet B. C., 1972, "Chemical Aspects of In-Situ Combustion-Combustion Heat and Kinetics", Society of Petroleum Engineers Journal, October, pp. 410-422.

Burger J., Sourieau P., Combarnous M., 1985, "Thermal Methods of Oil Recovery", Editions Technip, Paris, 1985.

Burger J.G., 1976, "Spontaneous Ignition in Oil Reservoirs" Soc. Pet. Eng. J., April, pp. 73-80.

Burgess A.R., Fernandes C.I., 1996, "A detailed model for the low-temperature oxidation of n-heptane", Joint Meeting of the Portuguese, British, Spanish and Swedish Sections of The Combustion Institute. Funchal (Portugal), pp. 17.4.1-17.4.4.

Castanier L.M., Brigham W.E., 1997, "Modifying In-Situ Combustion With Metallic Additives", In Situ, Vol. 21, pp. 27-45.

Christopher C.A., 1995, "Air Injection for Light and Medium Reservoirs", DTI Share Meeting (1), London, U.K., July 20.

Chu C., 1971, "Kinetics of Methane Oxidation Inside Sandstone Matrices", Society of Petroleum Engineers Journal, June, pp. 145-151.

Ciajolo A., Barbella R., 1984, "Pyrolysis and Oxidation of Heavy Fuel Oils and Their Fractions in a TGA Apparatus", Fuel, 63, pp. 657-661.

Clara C., Durandeau M., Quenault G., Nguyen T., 1999, "Laboratory Studies for Light Oil Air Injection Projects: Potential Application in Handil Field", SPE 54377, 1999 SPE Asia Pacific Oil and Gas Conference and Exhibition, Jakarta, Indonesia, 20-22 April.

Clara C., Zelenko V., Schirmer P., 1998, "Appraisal of the Horse Creek Air Injection Project Performance", SPE 49519, October.

Columbia Scientific Industries Corporation, 1987, "Accelerating Calorimeter Instruction Manual", Austin, TX Sept. 1987.

Dabbous M. K., Fulton P. F., 1972, "Low Temperature Oxidation Reaction Kinetics and Effects on the In Situ Combustion Process" SPE-AIME 47th Annual Fall Meeting San Antonio Texas Oct 8-11. Society of Petroleum Engineering Journal, June 1974, pp. 253-262.

Diaz, D., Bassiouni Z., Kimbrell W., Wolcott J., 1996, "Screening Criteria for Application of Carbon Dioxide Miscible Displacement in Waterflooded Reservoirs Containing Light Oil", SPE Improved Oil Recovery Symposium, Tulsa, Oklahoma, U.S.A., April 21-24, pp. 287-293.

Drici O., Vossoughi S., 1985, "Study of the Surface Area Effect on Crude Oil Combustion by Thermal Analysis Techniques" Journal of Petroleum Technology pp. 731-736.

Drici O., Vossoughi S., 1987, "Catalytic Effect of Heavy Metal Oxides on Crude Oil Combustion", SPE Reservoir Engineering, November pp. 591-595.

Economides M., Oligney R., 2000, "The Color of Oil, The History, the Money and the Politics of the World's Biggest Business", Round Oak Publishing Company, Inc, Texas, USA.

Emmanuel N.M., Denisov E.T., Maizus Z.K., "Liquid-Phase Oxidation of Hydrocarbons", 1967, Plenum Press, New York.

Energy Information Administration, 1999, "International Energy Annual", March, http://www.eia.doe.gov/emeu/iea/wec.html, Washington D.C., USA.

Energy Information Administration, 2000, "International Energy Outlook 2000", Report No. DOE/EIA-0484(2000), http://www.eia.doe.gov/oiaf/ieo/index.html#highlights , Washington D.C., USA.

Erickson A., Legerski J. R., Steece F. V., 1993, "Appraisal of High Pressure Air Injection (HPAI) or In Situ Combustion results from Deep High Temperature High Gravity Oil Reservoirs" 50th Annivesary Field Conference Casper Wyoming August.

Evison B., Niject Services, Gilchrist R.E., Ralph E. Gilchrist Inc., 1992, "New Developments in Nitrogen in the Oil Industry", SPE 24313, SPE Mid-Continet Gas Symposium, Amarillo, Texas, April 13-14, pp. 171-178.

Farouq Ali S.M., Thomas A.S., 1996, "The Promise and Problems of Enhanced Oil Recovery Methods", Journal of Canadian Petroleum Technology, Volume 35, No. 7, September, pp. 57-63.

Fassihi M. R., Brigham W.E., and Ramey H.J, Jr., 1984, "Reaction Kinetics of In-Situ Combustion: Part 2- Modelling," Society of Petroleum Engineers Journal, August, pp. 408-416.

Fassihi M. R., Ramey H.J, Jr., and Brigham W.E., 1980, "The Frontal Behaviour of In-Situ Combustion", SPE 8907, SPE California Regional Meeting, Los Angeles, California, April 9-11.

Fassihi M.R., Brigham W. E., 1980, "Investigation of Reactions Occurring in In-Situ Combustion", Annual Heavy Oil EOR Conference, San Fransisco, California, USA, July 22-24, Koks Khimma, pp. 51-85.

Fassihi M.R., Brigham W. E., Ramey Jr. H.J., 1984, "Reaction Kinetics of In-Situ Combustion: Part 1- Observations" SPE J Vol. 24 No. 4 August, pp. 399-407.

Fassihi M.R., Gillham T.H., Yannimaras D.V., Hassan D., 1996, "Field Tests Assess Novel Air-Injection EOR Processes" Oil And Gas Journal May 20, pp. 69-72.

Fassihi M.R., Meyers K.O., Basile P.F., 1990, "Low-Temperature Oxidation of Viscous Crude Oils" SPE Reservoir Engineering November, pp. 609-615.

Fassihi M.R., Meyers K.O., Welsbrod K.R., 1990, "Thermal Alteration of Viscous Crude Oils", SPE Reservoir Engineering, August, pp. 393-399.

Fassihi M.R., Yannimaras D.V., Kumar V.K., 1997, "Estimation of Recovery Factor in Light Oil Air Injection Projects", SPE Reservoir Engineering, August.

Fraim M. L., Moffitt P. D., Yannimaras D.V., 1997, "Laboratory Testing and Simulation Results for High Pressure Air Injection in a Waterflooded North Sea Oil Reservoir", SPE Annual Technical Conference Exhibition, San Antonio, U.S.A., 5-8 October.

Gaffuri P., Faravelli T., Ranzi E., Cernansky N. P., Miller D., d'Anna A, Ciajolo A., 1997, "Comprehensive Kinetic Model for the Low Temperature Oxidation of Hydrocarbons" AIChE Journal Vol. 43 No.5 May.

Germain P., Geyelin J.L., TOTAL 1997, "Air Injection Into A Light Oil Reservoir: The Horse Creek Project" SPE Paper 37782, Middle East Oil Show Bahrain 15-18 March.

Gilham T.H., Cerveny B.W., Turek E.A., Yannimaras D.V., Amoco Production Company 1997, " Keys to Increasing Production Via Air Injection in Gulf Coast Light Oil Reservoirs" 1997 SPE Annual Technical Conference and Exhibition San Antonio Texas 5-8 October.

Gilham T.H., Fornea M.A., Bassiouni Z., 1997, " A new Economically Viable EOR process for the U.S. Gulf Coast" World Oil November pp. 47-50.

Glassman I., 1977, "Combustion", Academic Press, pp. 18-56.

Goodlett, G.O, Honarpour M.M, Carroll H.B., Sarathi P.S., National Institute for Petroleum and Energy Research, 1986, "Diverse Mechanisms add to Increased Oil Production in Thermal and Gas Projects", Oil & Gas Journal, July 28.

Greaves M., Dudley J.W.O., 1990, "In Situ Combustion Processes: Reaction rate Parameters From Combustion Tube Experiments", Trans IChemE, Vol. 68, Part A, July, pp. 331-341.

Greaves M., Ren S. R., Rathbone R., 1998, "Air-Injection Technique (LTO Process) for IOR From Light-Oil Reservoirs: Oxidation Rates and Displacement Studies", SPE 40062, 1998 SPE/DOE Improved Oil Recovery Symposium, Tulsa, Oklahoma, 19-22 April.

Greaves M., Ren S. R., Xia T.X., 1999, "New Air Injection Technology For IOR Operations in Light and Heavy Oil reservoirs", SPE 57295, SPE Asia Pacific Improved Oil Recovery Conference, Kuala Lumpur, Maylasia, October 25-26.

Greaves M., Ren S.R., Rathbone R.R., Fishlock T., Ireland R., 2000, "Improved residual Light Oil recovery by Air Injection (LTO Process), Journal of Canadian Petroleum Technology, January, Vol. 39, No. 1, pp. 57-61.

Gregory A.T., 1994, "DTI's Improved Oil Recovery Strategy", Transactions of the Institute of Chemical Engineers, Part A, Vol. 72, pp. 137-143.

Hansel J.G., Benning M.A., Fernbacher J.M., 1984, "Oxygen In-Situ Combustion for Oil Recovery: Combustion Tube Tests", Journal of Petroleum Technology, SPE, July pp. 1139-1144.

Hazard Evaluation Laboratory (HEL), 1997, "PHI-TEC Operating Manual Volume 2 Wincalc Software Details" June.

Hazard Evaluation Laboratory (HEL), 1997, "PHI-TEC Operating Manual Volume 1 Hardware Details" June.

Hazard Evaluation Laboratory (HEL), 1997, "WINCONV data re-formatting and reduction software", June.

Henderson J.H., Weber L., 1965, "Physical Upgrading of Heavy Crude Oils by the Application of Heat", Journal of Canadian Petroleum Technology, October-December, 206.

Howard F. A., 1923, "Method of Operating Oil Wells" U.S. Patent No. 1 473 348 (filed Aug. 9 1920; issued Nov. 6).

Hughes R., Kamath V.M., Price D., 1987, "Kinetics of In-Situ Combustion for Oil Recovery", Chem Eng Res Des, Vol. 65, January, pp. 23-28.

Hughes R., Price D., Al-Saffar H., Soufi A., "Air Injection Technique (LTO Process) For IOR For Light Oil Reservoirs", Communication to Author, 1998.

Hutchence K., Freitag N., 1991, " An Alternative Approach To The Selection of Pseudocomponents for the Modelling of In-Situ Combustion" 4th Petroleum Conference South Saskatchewan Section CIM Regina Oct. 7-9.

Hyne J.B., Greidanus J.W., Tyrer J.D., Verona D., Rizek C., Clark P.D., Clark R.A., Koo J.F.K., 1984, "Aquathermolysis of Heavy Oils", Second International Conference, The Future of Heavy Crude and Tar Sands, McGraw Hill, New York, pp. 404-411.

Indrijarso S., Hughes R., Price D., 1991, 5th Unitar/UNDP Conf. pp. 313-319.

Jefferson L.L, Nighswander J.A., Chang-Yen, D.A., 1997, "A Scaleable, database Architecture for Storage of PVT Data", SPE Computer Applications, October, pp. 145-147.

Jha K. N., Verkoczy B., 1986, "The Role of Thermal Analysis Techniques in the In Situ Combustion Process" SPE Reservoir Engineering July, pp. 329-340.

Jordan P. C., 1981, "Chemical Kinetics and Transport", Plenum Press, pp. 98.

Karacan O., Kok M.V., 1997, "Pyrolysis Analysis of Crude Oils and their Fractions", Energy and Fuels, Vol. 11, pp. 385-391.

Kisler J. P., Shallcross D. C., 1995, "Oxidation Kinetics of Very Light Crude Oil" Presented at the IEA Collaborative Project on EOR 16th International Workshop and Symposium Chiba Japan October.

Kisler J. P., Shallcross D. C., 1997, "An Improved Model for the Oxidation Processes of Light Crude Oil", Trans IChemE, Vol 75, Part A, May.

Kodera Y., Kondo T., Saito I., Sato Y., Ukegawa K., 2000, "Continuous-Distribution Kinetic Analysis for Asphaltene Hydrocracking", Energy & Fuels, Vol. 14, pp. 291-296.

Kok M.V., 1997, "High Pressure DSC Applications on Crude Oil Combustion", Energy & Fuels, 11, pp. 1137-1142.

Kok M.V., Karacan C.O., 1997, "Behaviour and Effect of SARA Fractions of Oil During Combustion" SPE International Thermal Operations & Heavy Oil Symposium Bakersfield California 10-12 February, SPE 37559, pp. 421-431.

Kok M.V., Karacan C.O., Pamir R., 1998, "Kinetic Analysis of Oxidation Behaviour of Crude Oil SARA Constituents", Energy & Fuels, 12, 580-588.

Kok M.V., Karacan O., 1998, "Pyrolysis Analysis and Kinetics of Crude Oils", Journal of Thermal Analysis, Vol. 52, pp. 781-788.

Kok M.V., Okandan E., 1997, "Kinetic Analysis of Crude Oils by a Weighted Mean Activation Energy Approach", Journal of Thermal Analysis, Vol. 48, pp. 343-348.

Kok M.V., Pamir R., 1995, "Review of Pyrolysis and combustion studies of fossil fuels by thermal analysis methods", Journal of Analytical and Applied Pyrolysis, Vol. 35, pp. 145-156.

Kossiakoff A., Rice F.O., 1943, "Thermal Decomposition of Hydrocarbons, Resonance Stabilisation and Isomerization of Free Radicals", Journal of the American Chemical Society, Part 1, Vol. 65, January-June, pp. 590-595.

Kumar V.K., Fassihi M.R., Yannimaras D.V., 1995, " Case History and Appraisal of the Medicine Pole Hills Unit Air Injection Project" SPE Reservoir Engineering, August 1995, pp. 198-202.

Kuo K., 1986, "Principles of Combustion", John Wiley & Sons, pp. 93-95.

Lagenberg M.A., Henry D.M., Chlebana M.R., 1994, "Performance and Expansion Plans for the Double displacement process in the Hawkins Field Unit" 69th Annual SPE Technical Conference and Exhibition New Orleans LA U.S.A 25-28 September.

Le Chatelier H., Mallard E., 1883, Ann Mines, 8, 274.

Lerner L., Fleming C., Lara F., 1985, "Dominant Processes in In Situ Combustion of Light Oil Reservoirs" SPE Journal May, pp. 889-900.

Lewis J. O., 1917, "Methods of Increasing the Recovery from Oil Sands" Bull. 148 Petroleum Technology USBM 37.

Lin C. Y., Chen W. H, Culham W.E, 1987, "New Kinetic Models for Thermal Cracking of Crude Oils in In-Situ Combustion Processes" SPE Reservoir Engineering, February Vol. 2, pp. 54-66.

Lin C. Y., Chen W. H., Culham W. E., 1984, "Numerical Simulation of Combustion Tube Experiments and the Associated Kinetics of In-Situ Combustion Processes", SPE AIME December pp. 657-666.

Lukyaa A.B.A., Hughes R., Millington A., Price D., 1994, "Evaluation of a North Sea Oil For Recovery by In Situ Combustion using High Pressure Differential Scanning Calorimetry", Trans IChemE, Vol. Part A, March, pp. 163-167.

Madaoui K., Sakthikumar S., 1993, "Lean Gas Injection in Waterflooded Oil Reservoirs: A systematic Investigation for Field Applications" 7th European EOR Symposium Moscow October.

Mamora D. D., Brigham W. E., 1995, "Effect of Low-Temperature Oxidation on the Fuel and Produced Oil During In-Situ Combustion of a Heavy Oil", In Situ, Volume 19, No. 4, November, pp. 341 - 365.

Mamora, 1993, "Kinetics of In-Situ Combustion", Phd Thesis, Stanford University.

Metwally M., 1990, "Experience with fireflooding in Countess 'B' Pool, Alberta Reservoir aspects", Journal of Canadian Petroleum Technology, March-April, Volume 29, No.2 pp. 87 - 92.

Minkoff C.J., Tipper, C.F.H., 1962, "Chemistry of Combustion Reactions", Butterworths, London.

Moore R.G., 1993, "New Strategies for In Situ Combustion", Journal of Canadian Petroleum Technology, Dec, Vol. 32, No 10, pp. 11-13.

Moore R.G., Belgrave J. D. M., Ursenbach M.G., Bennion D.W., 1992, "Some Insights into the LTO and HTO In Situ Combustion Kinetics", SPE/DOE 8th Symposium on EOR, Tulsa, Oklahoma, April 22-24, pp. 179-190.

Moore R.G., Laurenshen C. J., Mehta S.A, Ursenbach M.G., 1999, "Observations and Design Considerations for In Situ Combustion Projects", Journal of Canadian Petroleum Technology, Special Edition 1999, Vol. 38, No. 13, paper 97-100.

Moore R.G., Laurenshen C. J., Ursenbach M.G., Mehta S.A, Belgrave J. D. M., 1999, "Combustion/Oxidation Behaviour of Athabasca Oil Sands Bitumen", SPE Reservoir Eval. & Eng. 2, Vol. 6, December.

Moritis G. 1994, "EOR dips in U.S. But Remains a Significant Factor" Oil & Gas Journal September 26 pp. 51-74.

Moritis G., 1998, "EOR Production up Slightly", Oil & Gas Journal, April 20, pp. 49-77.

Mujica V., Nieto P., Puerta L., Acevedo S., 2000, "Caging of Molecules by Asphaltenes. A Model for Free Radical Preservation in Crude Oils", Energy & Fuels, Vol. 14, pp. 632-639.

Nace D.M., Voltz S.E., Weekman V.W. Jr., 1971, "Application of a Kinetic Model for Catalytic Cracking", Ind. Eng. Chem., Process Design Dev., Volume 10, No. 2, October, pp. 530-541.

Newitt D. M., Thornes L. S., 1937, Journal of the Chemical Society, pp. 1656-1669.

Nickle S. K., Meyers K. O., Nash L.J., 1987, "Shortcomings in the Use of TGA/DSC Techniques To Evaluate In-Situ Combustion", 62nd Annual Technical Conference and Exhibition SPE Dallas September 27-30, SPE Paper 16867 pp. 323-337.

Nodwell J., Moore R.G., Ursenbach M.G., Laurenshen C.J., Mehta S.A., 1997, "Economic Considerations For the Design of In-Situ Combustion Projects", Paper 97-165, Seventh Petroleum Conference of the South Saskatchewan Section, CIM, regina, Canada, October 19-22.

Oklany J.S., Hughes R., Millington A., Price D., 1994, "Use of Simulation to Predict the Influence of Kinetic Parameters on In-Situ Combustion Performance", In Situ, Vol. 18, No. 2, pp. 123-143.

Pernyeszi T., Patzko A., Berkesi O., Dekany I., 1998, "Asphaltene dsorption on clays and crude oil reservoir rocks", Colloids and Surfaces, A: Physicochemical and Engineering Aspects, 137, pp. 373-384.

Prats, 1986, "Thermal Recovery", Monograph Volume 7, Henry L. Doherty Series, SPE, pp. 1-14.

Pusch G., Ranjbar-Hamghawandi M., 1991, "Thermal Alteration of Medium and Heavy Compounds of Crude Oils by Pyrolysis and Combustion" SPE International Symposium on Oilfield Chemistry Anaheim California Feb. 20-22 pp. 201-208.

Racz D., Kovacs A., Pokol G., Sztatisz J., 1979, Gal Kodaj es Foldgaz S., 12 pp. 1-5

Raemy A., Ottoway M., 1991, "The Use of High Pressure DTA Heat Flow And Adiabatic Calorimetry To Study Exothermic Reactions" Journal of Thermal Analysis, Vol. 37, pp. 1965-1971.

Ranjbar M, 1995, "Improvement of Medium and Light Oil recovery with Thermocatalytic In-Situ Combustion", Journal of Canadian Petroleum Technology, October, Vol. 34, No. 8, pp. 25-30.

Ranjbar M., 1993, "Influence of reservoir rock composition on crude oil pyrolysis and combustion" Journal of Analytical and Applied Pyrolysis, Vol. 27, pp. 87-95.

Ranjbar M., 1997, "Laboratory Simulation of High Pressure Alteration of Crude Oil Compounds During Thermal Oil Recovery", Oil Gas-European Magazine, 4, pp. 26-28.

Ranjbar M., Pusch G., 1991, "Experimental Studies of Crude Oil Pyrolysis, Fuel Formation and Combustion in relation to In-Situ Combustion", 5th UNITAR International Conference on Heavy Crude and Tar Sands, pp. 297-305.

Ranjbar M., Pusch G., 1991, "Pyrolysis and combustion kinetics of crude oils, asphaltenes and resins in relation to thermal recovery processes", Journal of Analytical and Applied Pyrolysis, 20, pp. 185-196.

Ranzi E., Dente M., Faravelli T., Pennati G., 1994, " Prediction of Kinetic Parameters for Hydrogen Abstraction Reactions", Combust. Sci. Tech, 95, 1.

Ranzi E., Faravelli T., Gaffuri P., Sogaro A., 1995, "Low Temperature Combustion: Automatic Generation of Primary Oxidation Reactions and Lumping Procedures", Combustion Flame, Vol. 102, No. 179.

Rao N. S., Roychaudhury S., Sur S., Sapkal A. V., Gupta K. K., Sinha S.K., 1997, "Results of Spontaneous Ignition Test In Balol Heavy Oil Field" SPE Asia Pacific Oil and Gas Conf., Kuala, Lumpur, Malaysia, April 14-16.

Rashidi F., Bagci S., 1991, "Effect of Pressure and Clay content on Combustion Kinetics of Heavy Oil in Limestone Medium", 5th UNITAR IOR Conference on Heavy Crude & Tar Sands, August.

Ren S. R., Greaves M., Rathbone R. R., 1999, "Oxidation Kinetics of North Sea Light Crude Oils At Reservoir Temperature", Trans IChemE Vol. 77, Part A, July.

Sakthikumar S., Madaoui K., Chastang J., TOTAL, 1995 "An Investigation of The Feasibility of Air Injection Into A Waterflooded Light Oil Reservoir" SPE Middle East Oil Show Bahrain 11-14 March.

Schoeppel R. J., Ersoy D., 1968, "Prediction of Spontaneous Ignition in In-Situ Combustion" SPE AIME Oklahoma Oct.25.

Snee T. J., Barcons C., Hernandez H., Zaldivar J.M., 1992, "Characterisation of An Exothermic Reaction Using Adiabatic and Isothermal Calorimetry", Journal of Thermal Analysis, Vol. 38, pp. 2729-2747.

Soodhoo K., Phillips C.R., 1988, "Non-catalytic hydrocracking of asphaltenes", Fuel, Vol. 67, April, pp. 521-529.

Srivadtava R., Huang S., 1997, "Technical Feasibility of CO_2 Flooding in Weyburn Reservoir-A Laboratory Investigation", Journal of Canadian Petroleum Technology, November, Vol. 36, No. 10, pp. 48-55.

Stirling C.J.M., 1965, "Radicals in Organic Chemistry" Oldbourne Chemistry Series, London Press, pp. 61.

Taber J.J., Martin D., Seright R.S., 1996, "EOR Screening Criteria Revisited", SPE/DOE Tenth Symposium on Improved Oil recovery, Tulsa, Oklahoma, U.S.A., April 21-24, pp. 387-394.

Tadema H. J., 1959, "Mechanism of Oil Production of Underground Combustion" Pro. 5th World Pet. Cong. New York Section II, Paper 22, pp. 279-287.

Tadema H. J., Weidjema J., 1970, "Spontaneous Ignition of Oil Sands" Oil and Gas Journal, December 14th, pp. 77-80.

Thomas F.B., Bennion D.B., Zhou X.L., Erian A., Bennion D.W., 1996, "Enhanced Oil Recovery by Gas Injection: Proposed Screening Criteria", Paper 96-119, 47th Annual Technical Meeting of The Petroleum Society, Calgary, Alberta, Canada, June 10-12.

Tiffin D. L, Yannimaras D. V., 1997, "The In-Situ Combustion Performance of Light Oils As a Function of Pressure (1000 to 6000 psig)". In Situ, 21, (1), pp. 47-64.

Tsuzuki N., Takeda N., Suzuki M., Yokoi K., 1999, "The kinetic modeling of oil cracking by hydrothermal pyrolysis experiments", International Journal of Coal Geology, Vol. 39, pp. 227-250.

Turta A., 1994, "In Situ Combustion – From Pilot to Commercial Application", Tulsa In situ Combustion NIDER Forum April.

Turta A.T., Singhai A. K., 1998, " Reservoir Engineering Aspects of Oil Recovery from Low Permeability Reservoirs by Air Injection", SPE 48841, SPE International Conference and Exhibition Beijing China 2-8 November.

Tzanco E.T., Moore R.G., Belgrave J.D.M., Ursenbach M.G., 1990, "Laboratory Combustion Behaviour of Countess B Light Oil", Petroleum Society of CIM/Society of Petroleum Engineers, Paper No. CIM./SPE 90-63, Calgary, June 10-13, Canada. pp. 63-1 – 63-16.

Ungerer P., Behar F., Villalba M., Heum O.R., Audibert A., 1988, "Kinetic Modelling of Oil Cracking", Organic Geochemistry, Vol. 13, Nos 4-6, pp. 857-868.

Verkoczy B., 1991, "Factors Affecting Coking in heavy Oil Cores, Oils and SARA Fractions Under Thermal Stress", CIM/AOSTRA 1991 Technical Conference, Banff, April 21-24 Paper No. CIM/AOSTRA 91-8.

Verkoczy B., Freitag N.P., 1997, "Oxidation of Heavy Oils and Their SARA Fractions – Its Role in Modelling In-Situ Combustion", 7th Petroleum Conference of The South

Saskatchewan Section, The Petroleum Society of CIM, Regina, October 19-22, Paper No. 97-167.

Vossoughi S., Bartlett G. W., Willhite G. P., 1985 "Prediction of In-Situ Combustion Process Variables by use of TGA/DSC Techniques and the Effect of Sand-Grain Specific Surface Area on the Process", April, Society of Petroleum Engineers Journal, pp. 656-664.

Vossoughi S., El-Shoubary Y., 1989, "Kinetics of Crude-Oil Coke Combustion", SPE Reservoir Engineering, May, pp. 201-206.

Vossoughi S., Saim, S., 1992, "A Different Approach in Generating Kinetic Models for Crude Oil Combustion: Application to an In-Situ Combustion Process", AOSTRA Journal of Research, Vol.8, pp. 131-139.

Vossoughi S., Willhite G. P., El-Shoubary Y., and Bartlett G. W., 1985 "Study of the Clay Effect on Crude Oil Combustion by Thermogravimetric and Differential Scanning Calorimetry", April, Society of Petroleum Engineers.

Watts B.C., Hall T.F., Petri D.J., 1997, "The Horse Creek Air Injection Project: An Overview", SPE 38359, SPE Rocky Mountain Regional Meeting, Casper, Wyoming, 18-21 May, pp. 143-154.

White P.D., "In-Situ Combustion Appraisal and Status", SPE Journal of Petroleum Technology, November, pp. 1943-1949.

Wilk R.D., Cernanski N.P., Cohen R.S., 1987, "An Experimental Study of Propene Oxidation at Low and Intermediate Temperatures", Combustion Science and Technology, Vol. 52, pp. 39-58.

Williams F.A., 1965, "Combustion Theory", Addison-Wesley Publishing Co., Reading, Mass.

Wolcott E.R,. 1923, "Method of increasing the Yield of Oil Wells" U.S. Patent No. 1 457 479 (filed Jan.12 1920; issued June 5).

Yannimaras D.V. Sufi A.H. Fassihi M.R. 1991, "The Case for Air Injection into Deep Light Oil Reservoirs" 6th European IOR Symposium Stavanger Norway.

Yannimaras D.V., Tiffin D. L., 1995, "Screening of Oils for In-Situ Combustion at Reservoir Conditions by Accelerating Rate Calorimetry"" SPE Reservoir Engineering, February, pp. 36-38.

Yergin D., 1992, "The Prize: The Epic Quest for Oil, Money & Power", Simon & Schuster.

Yoshiki K. S., Phillips C. R., 1985, "Kinetics of the thermo-oxidative and thermal cracking reactions of Athabasca bitumen", Fuel, pp. 1591-1596.

Zelenko V., Solignac F., 1997, "Use of Accelerating Rate Calorimeter in Reservoir Oil Selection for Air Injection Process", 7th Petroleum Conference, South Saskatchewan Section, Petroleum Society of CIM, Regina, October 19-22.

APPENDIX A:

Reaction Region Self-heat Rates

Average Self-Heat Rate (deg C/min)

Oil alone	Description	Induction Region	Propagation + Termination Region	Lower HTO	Upper HTO
a5	0.25ml A @ 50 bar	0.1	15.1	0.6	1.9
a0	0.25 ml A @ 50 bar	0.1	63.8	0.7	1.3
a1	0.25ml A @ 100 bar	0.2	1.9	1.7	2.6
au1	0.5 ml Au @ 50 bar	0.2	483.0	1.9	3.5
b5	0.25 ml B @ 50 bar	0.1	111.1	1.0	1.5
b0	0.25 ml Oil B @ 50 bar	0.1	23.6	0.2	0.4
b3	0.25 ml B @ 50 bar (2)	0.2	99.1	2.3	3.6
b4	0.25 ml B @ 50 bar (3)	0.2	57.4	2.5	2.7
b2	0.5 ml B @ 50 bar	0.4	455.5	2.5	4.2
b7	1 ml B @ 50 bar	0.4	492.5	3.0	5.4
b1	0.25 ml B @ 100 bar	0.1	95.4	1.3	1.8
c0	0.25ml oil c @ 50 bar	0.2	75.1	0.4	0.6
d1	1ml D @ 30 bar	0.4	1.5	1.1	1.8
d3	0.25 ml D @ 50 bar	0.1	62.7	0.8	1.1
d2	0.25 ml D @ 100 bar	0.2	237.1	2.5	2.8

Water	Description	Induction Period	Propagation + Termination	Lower HTO	Upper HTO
bw	0.25ml Oil B @ 50 bar, 0.1 ml water	0.1	10.2	0.1	0.0
bw1	0.25 ml Oil B @ 50 bar, 0.5g rock, 0.5ml water	0.1	2.1	0.0	0.0
drw	0.25 ml Oil D @ 50 bar, 0.5g rock, 1 ml water	0.2	2.0	0.2	0.8

Average Self-Heat Rate (deg C/min)

Rock	Description	Induction Period	Propagation + Termination	Lower HTO	Upper HTO
ar1	0.25ml oil A @ 50 bar, 0.5g rock, 0.1 ml water	0.1	8.1	0.7	1.3
br2	0.25ml oil B @ 50 bar, 2.0g rock, 0.1 ml water	0.1	1.8	0.2	0.6
br3	0.25ml oil B @ 100 bar, 0.5g rock, 0.1 ml water	0.1	50.7	0.2	0.3
cr1	0.25 ml oil C @ 50 bar, 0.5g rock, 0.1 ml water	0.3	32.7	2.1	4.4
dr2	0.25 ml oil D @ 50 bar, 0.5g rock	0.4	78.1	1.8	3.2
dr1	0.25 ml oil D @ 50 bar, 0.5g rock, 0.1 ml water	0.1	15.8	1.1	1.5
dr3	0.25 ml oil D @ 50 bar, 2.0g rock, 0.1 ml water	0.1	3.8	0.3	0.7
dr4	1 ml Oil D @ 50 bar, 0.5 g rock, 0.1 ml water	0.1	1.6	0.9	3.5
dr5	0.25 ml Oil D @ 0 bar, 0.5 g rock, 0.1 ml water	0.1	0.1	0.6	1.0
dr_c2	0.25ml Oil D @ 50 bar, 0.5g clay, 0.1 ml water	0.1	3.5	0.1	0.1
dr_ch1	0.25ml Oil D @ 50 bar, 0.5g chalk, 0.1 ml water	0.2	5.7	0.1	0.0
dr_p1	0.25ml Oil D @ 50 bar, 0.5g rock A, 0.1 ml water	0.1	3.6	0.1	0.3
dr_s1	0.25ml Oil D @ 50 bar, 0.5g silica, 0.1 ml water	0.1	3.8	0.2	0.5
mr1	0.25 ml oil M @ 50 bar, 0.5g rock, 0.1 ml water	0.3	64.7	1.4	2.3

Average Self-Heat Rate (deg C/min)

Saturates Only	Description	Induction Period	Propagation + Termination	Lower HTO	Upper HTO
as1	0.3 g A sat @ 50 bar	0.2	52.9	0.8	1.3
bs0	0.3 g Oil B sat. @ 50 bar	0.1	16.9	0.0	0.0
bs3	0.3 g B sat @ 50 bar	0.2	55.8	0.3	0.6
cs0a	0.3 g C sat @ 50 bar	0.1	33.3	0.0	0.0
ds0	0.3 g D sat @ 50 bar	0.2	46.1	0.6	0.8
wls0	0.3 g Oil W saturates @ 50 bar	0.2	21.1	0.6	1.1

Saturates + Rock+ water	Description	Induction Period	Propagation + Termination	Lower HTO	Upper HTO
asr1	0.3 g Oil A saturates @ 50 bar, 0.5 g rock, 0.1 ml water	0.1	2.2	0.5	1.1
bsr1	0.3 g Oil B saturates @ 50 bar, 0.5 g rock, 0.1 ml water	0.2	2.3	0.5	1.1
dsr1	0.3 g Oil D saturates @ 50 bar, 0.5 g rock, 0.1 ml water	0.0	1.2	0.0	0.0

Aromatics + Rock+ water	Description	Induction Period	Propagation + Termination	Lower HTO	Upper HTO
aar1	0.3g Oil A aromatics @ 50 bar, 0.5g rock, 0.1 ml water	0.1	0.6	0.2	0.5
bar1	0.3g Oil B aromatics @ 50 bar, 0.5 g rock, 0.1 ml water	0.1	0.8	0.1	0.0
bar2	0.3g Oil B aromatics @ 50 bar, 0.5 g rock, 0.1 ml water	0.1	0.9	0.7	0.1
car1	0.3g Oil C Aromatics @ 50 bar, 0.5g rock, 0.1 ml water	0.1	0.4	0.0	0.0
dar2	0.3g Oil D aromatics @ 50 bar, 0.5g rock, 0.1 ml water	0.1	0.6	0.2	0.7
wlar1	0.3g wolflake aromatic @ 50 bar, 0.5g rock, 0.1 ml water	0.1	0.7	0.2	0.6

Average Self-Heat Rate (deg C/min)

Resins + Rock+ water	Description	Induction Period	Propagation + Termination	Lower HTO	Upper HTO
brr1	0.3g Oil B resins @ 50 bar, 0.5g rock, 0.1ml water	0.2	0.8	0.6	1.3
drr2	0.3g Oil D Resins @ 50 bar, 0.25 ml rock, 0.1 ml water	0.1	0.1	0.0	0.0
wlrr1	0.3g wolflake resin @ 50 bar, 0.5g rock, 0.1 ml water	0.2	0.8	0.7	1.4

Asphaltenes+ Rock+ water	Description	Induction Period	Propagation + Termination	Lower HTO	Upper HTO
aasr1	0.3g Oil A asphaltenes @ 50 bar, 0.5g rock, 0.1 ml water	0.1	0.1	0.0	0.0
masr1	0.3g maya asphaltenes @ 50 bar, 0.5g rock, 0.1 ml water	0.1	0.1	0.1	0.0
wlasr1	0.3g wolflake asphaltenes @ 50 bar, 0.5g rock, 0.1ml water	0.1	0.8	0.5	0.0

Pure Component expts.	Description	Induction Period	Propagation + Termination	Lower HTO	Upper HTO
C10	0.25 ml decane @ 50 bar, 0.5g rock, 0.1 ml water	0.1	4.8	0.8	0.4
C16	0.25 ml hexadecane @ 50 bar, 0.5g rock, 0.1 ml water	0.1	12.9	0.7	0.5

Other expts.	Description	Induction Period	Propagation + Termination	Lower HTO	Upper HTO
dn0	0.25 ml oil D + nitrogen @ 50 bar	0.1	0.1	0.2	0.4
drn1	0.25 ml oil D + nitrogen @ 50 bar, 0.5g rock, 0.1ml water	0.1	0.1	0.3	0.5

APPENDIX B:

Other Comparisons of Average Self-Heat Rate

Ratio of Self-Heat Rate

Oil Saturation

Compared Runs	Induction Region	Propagation + Termination Region	Lower HTO	Upper HTO
0.5ml / 0.25 ml Oil B @ 50 bar				
b2a / b3a	2.2	4.6	1.1	1.1
b2a / b4a	1.7	7.9	1.0	1.5
b2a / b5a	3.2	4.1	2.5	2.7

Oil Viscosity

Compared Runs	Induction Region	Propagation + Termination Region	Lower HTO	Upper HTO
Trends with Increasing Oil Viscosity; Oil a > d > c = b				
a5a / b3a	0.7	0.2	0.2	0.5
a5a / b4a	0.6	0.3	0.2	0.7
a5a / b5a	1.0	0.1	0.6	1.3
a5a / d3	1.4	0.2	0.7	1.7
d3 / b3a	0.5	0.6	0.3	0.3
d2 / b3a	1.3	2.4	1.1	0.8
d3 / b4a	0.4	1.1	0.3	0.4
d2 / b4a	1.0	4.1	1.0	1.0
d3 / b5a	0.8	0.6	0.7	0.7

Ratio of Self-Heat Rate

Oil Viscosity

Compared Runs	Induction Region	Propagation + Termination Region	Lower HTO	Upper HTO

Trends with Increasing Oil Viscosity; Oil a > d > c = b

d2 / b5a	1.9	2.1	2.5	1.8
d2 / b1	3.3	2.5	2.0	1.6
b2 / au1a	2.4	0.9	1.3	1.2
a0 / b0	1.5	2.7	3.5	3.5
a0 / c0	0.8	0.8	1.8	2.4
a0 / d3	1.7	1.0	1.0	1.2
dr1 / cr1	0.5	0.5	0.5	0.3
c0 / b0	1.8	3.2	1.9	1.5
d3 / b0	0.9	2.7	3.5	3.0
a2a / b7a	3.5	0.1	0.0	0.0
a2a / d1a	3.2	31.5	0.1	0.0
ar1 / cr1	0.5	0.2	0.3	0.3
ar1 / dr1	1.0	0.5	0.6	0.9

Ratio of Reaction Time

Oil Saturation

Compared Runs	Induction Region	Propagation + Termination Region	Lower HTO	Upper HTO
0.5ml / 0.25 ml Oil B @ 50 bar				
b2a / b3a	0.3	0.4	0.7	2.3
b2a / b4a	0.5	0.7	0.7	1.6
b2a / b5a	0.2	0.6	0.6	0.4

Oil Viscosity

Compared Runs	Induction Region	Propagation + Termination Region	Lower HTO	Upper HTO
Trends with Increasing Oil /iscosity; Oil a > d > c = b				
a5a / b3a	1.4	0.4	1.5	13.3
a5a / b4a	2.0	0.7	1.4	9.3
a5a / b5a	0.9	0.5	1.4	2.4
a5a / d3	0.9	0.8	0.5	2.9
d3 / b3a	1.6	0.5	2.8	4.6
d3 / b3a	0.7	0.5	0.3	1.8
d3 / b4a	2.2	0.9	2.7	3.3
d3 / b4a	1.0	1.0	0.3	1.3
d3 / b5a	1.0	0.7	2.6	0.8

Ratio of Reaction Time

Oil Viscosity

Compared Runs	Induction Region	Propagation + Termination Region	Lower HTO	Upper HTO
Trends with Increasing Oil /iscosity; Oil a > d > c = b				
d3 / b5a	0.5	0.8	0.3	0.3
d3 / b5a	0.3	0.6	0.3	0.5
b2 / au1a	0.9	1.8	1.3	0.6
a0 / b0	0.5	0.3	0.2	0.3
a0 / c0	1.1	0.6	0.4	0.4
a0 / d3	0.6	0.6	0.6	1.4
dr1 / cr1	2.1	1.3	1.9	2.7
c0 / b0	0.5	0.5	0.6	0.7
d3 / b0	0.9	0.5	0.3	0.2
a2a / b7a	0.1	0.8	9.7	0.0
a2a / d1a	0.5	0.1	8.5	0.0
ar1 / cr1	1.6	2.2	3.3	3.4
ar1 / dr1	0.8	1.7	1.7	1.3

Ratio of Energy Released

Oil Saturation

Compared Runs	Induction Region	Propagation + Termination Region	Lower HTO	Upper HTO
0.5ml / 0.25 ml Oil B @ 50 bar				
b2a / b3a	0.7	1.7	0.7	2.6
b2a / b4a	0.8	5.7	0.6	2.5
b2a / b5a	0.7	2.3	1.6	1.1

Oil Viscosity

Compared Runs	Induction Region	Propagation + Termination Region	Lower HTO	Upper HTO
Trends with Increasing Oil /iscosity; Oil a > d > c = b				
a5a / b3a	1.0	0.1	0.4	7.0
a5a / b4a	1.1	0.2	0.3	6.7
a5a / b5a	1.0	0.1	0.8	3.0
a5a / d3	1.2	0.2	0.4	4.9
d3 / b3a	0.8	0.3	0.9	1.4
d3 / b3a	0.9	1.2	0.4	1.4
d3 / b4a	0.9	1.0	0.8	1.4
d3 / b4a	1.0	4.1	0.3	1.3
d3 / b5a	0.8	0.4	2.0	0.6

Ratio of Energy Released

Oil Viscosity

Compared Runs	Induction Region	Propagation + Termination Region	Lower HTO	Upper HTO
Trends with Increasing Oil /iscosity; Oil a > d > c = b				
d3 / b5a	0.9	1.6	0.8	0.6
d3 / b5a	1.1	1.4	0.6	0.7
b2 / aula	2.1	1.7	1.6	0.7
a0 / b0	0.8	0.8	0.7	0.9
a0 / c0	0.9	0.5	0.7	1.0
a0 / d3	1.0	0.7	0.6	1.6
dr1 / cr1	1.0	0.6	1.0	0.9
c0 / b0	0.9	1.6	1.1	1.0
d3 / b0	0.8	1.3	1.2	0.6
a2a / b7a	0.5	0.1	0.4	0.0
a2a / d1a	1.5	4.2	0.8	0.0
ar1 / cr1	0.8	0.5	1.1	1.0
ar1 / dr1	0.8	0.9	1.1	1.1

APPENDIX C:

Energy Release Calculations

Oil alone	Description	cp (oil), J/gK	mass (oil), g	cp (rock), J/gK	mass (rock), g	cp (water), J/gK	mass (water), g	Mcp (oil) + mcp (rock) + mcp (water)
a5	0.25ml A @ 50 bar	2.2	0.2112	0.745	0	4.18	0	0.46464
a0	0.25 ml A @ 50 bar	2.2	0.2112	0.745	0	4.18	0	0.46464
a1	0.25ml A @ 100 bar	2.2	0.2112	0.745	0	4.18	0	0.46464
au1	0.5 ml Au @ 50 bar	2.2	0.41015	0.745	0	4.18	0	0.90233
b5	0.25 ml B @ 50 bar	2.2	0.20995	0.745	0	4.18	0	0.46189
b0	0.25 ml Oil B @ 50 bar	2.2	0.20995	0.745	0	4.18	0	0.46189
b3	0.25 ml B @ 50 bar (2)	2.2	0.20995	0.745	0	4.18	0	0.46189
b4	0.25 ml B @ 50 bar (3)	2.2	0.20995	0.745	0	4.18	0	0.46189
b2	0.5 ml B @ 50 bar	2.2	0.4199	0.745	0	4.18	0	0.92378
b7	1 ml B @ 50 bar	2.2	0.8398	0.745	0	4.18	0	1.84756
b1	0.25 ml B @ 100 bar	2.2	0.20995	0.745	0	4.18	0	0.46189
c0	0.25ml oil c @ 50 bar	2.2	0.20995	0.745	0	4.18	0	0.46189
d1	1ml D @ 30 bar	2.2	0.8299	0.745	0	4.18	0	1.82578
d3	0.25 ml D @ 50 bar	2.2	0.207475	0.745	0	4.18	0	0.456445
d2	0.25 ml D @ 100 bar	2.2	0.207475	0.745	0	4.18	0	0.456445

Water	Description	cp (oil), J/gK	mass (oil), g	cp (rock), J/gK	mass (rock), g	cp (water), J/gK	mass (water), g	Mcp (oil) + mcp (rock) + mcp (water)
bw	0.25ml Oil B @ 50 bar, 0.1 ml water	2.2	0.20995	0.745	0	4.18	0.1	0.87989
bw1	0.25 ml Oil B @ 50 bar, 0.5g rock, 0.5ml water	2.2	0.20995	0.745	0.5	4.18	0.5	2.92439
drw	0.25 ml Oil D @ 50 bar, 0.5g rock, 1 ml water	2.2	0.207475	0.745	0.5	4.18	1	5.008945

Oil alone	Description	actual Energy evolved during LTO Induction	actual Energy evolved during LTO propagation	actual Energy evolved during LTO ELTO	actual Energy evolved during Lower HTO	actual Energy evolved during Upper HTO	actual Energy evolved during HTO EHTO	actual ELTO/ EHTO
a5	0.25ml A @ 50 bar	70	81	152	20	149	169	0.9
a0	0.25 ml A @ 50 bar	57	290	348	32	49	81	4.3
a1	0.25ml A @ 100 bar	57	29	86	23	78	100	0.9
au1	0.5 ml Au @ 50 bar	48	2920	2968	48	147	195	15.2
b5	0.25 ml B @ 50 bar	73	1132	1205	26	50	75	16.0
b0	0.25 ml Oil B @ 50 bar	71	347	418	43	52	94	4.4
b3	0.25 ml B @ 50 bar (2)	68	1483	1551	54	21	75	20.6
b4	0.25 ml B @ 50 bar (3)	65	456	521	62	22	85	6.2
b2	0.5 ml B @ 50 bar	99	5178	5277	81	110	191	27.6
b7	1 ml B @ 50 bar	275	4214	4489	263	127	389	11.5
b1	0.25 ml B @ 100 bar	57	1291	1348	31	39	71	19.1
c0	0.25ml oil c @ 50 bar	63	562	625	45	50	95	6.6
d1	1ml D @ 30 bar	95	79	174	111	114	226	0.8
d3	0.25 ml D @ 50 bar	69	435	504	50	30	79	6.3
d2	0.25 ml D @ 100 bar	63	1831	1894	19	28	48	39.7

Water	Description	actual Energy evolved during LTO Induction, J	actual Energy evolved during LTO propagation	actual Energy evolved during LTO ELTO	actual Energy evolved during Lower HTO	actual Energy evolved during Upper HTO	actual Energy evolved during HTO EHTO	actual ELTO/ EHTO
bw	0.25ml Oil B @ 50 bar, 0.1 ml water	113	305	418	58	0	58	7.2
bw1	0.25 ml Oil B @ 50 bar, 0.5g rock, 0.5ml water	383	139	522	109	0	109	4.8
drw	0.25 ml Oil D @ 50 bar, 0.5g rock, 1 ml water	696	543	1238	411	947	1357	0.9

Rock	Description	cp (oil), J/gK	mass (oil), g	cp (rock), J/gK	mass (rock), g	cp (water), J/gK	mass (water), g	Mcp (oil) + mcp (rock) + mcp (water)
ar1	0.25ml oil A @ 50 bar, 0.5g rock, 0.1 ml water	2.2	0.2112	0.745	0.5	4.18	0.1	1.25514
br2	0.25ml oil B @ 50 bar, 2.0g rock, 0.1 ml water	2.2	0.20995	0.745	2	4.18	0.1	2.36989
br3	0.25ml oil B @ 100 bar, 0.5g rock, 0.1 ml water	2.2	0.20995	0.745	0.5	4.18	0.1	1.25239
cr1	0.25 ml oil C @ 50 bar, 0.5g rock, 0.1 ml water	2.2	0.20995	0.745	0.5	4.18	0.1	1.25239
dr2	0.25 ml oil D @ 50 bar, 0.5g rock	2.2	0.207475	0.745	0.5	4.18	0	0.828945
dr1	0.25 ml oil D @ 50 bar, 0.5g rock, 0.1 ml water	2.2	0.207475	0.745	0.5	4.18	0.1	1.246945
dr3	0.25 ml oil D @ 50 bar, 2.0g rock, 0.1 ml water	2.2	0.207475	0.745	2	4.18	0.1	2.364445
dr4	1 ml Oil D @ 50 bar, 0.25 ml rock, 0.1 ml water	2.2	0.8299	0.745	0.5	4.18	0.1	2.61628
dr5	0.25 ml Oil D @ 0 bar, 0.25 ml rock, 0.1 ml water	2.2	0.207475	0.745	0.5	4.18	0.1	1.246945
dr_c2	0.25ml Oil D @ 50 bar, 0.5g clay, 0.1 ml water, repeated	2.2	0.207475	0.88	0.5	4.18	0.1	1.314445
dr_ch1	0.25ml Oil D @ 50 bar, 0.5g chalk, 0.1 ml water	2.2	0.207475	0.8	0.5	4.18	0.1	1.274445
dr_p1	0.25ml Oil D @ 50 bar, 0.5g phillips rock, 0.1 ml water	2.2	0.207475	0.745	0.5	4.18	0.1	1.246945
dr_s1	0.25ml Oil D @ 50 bar, 0.5g silica, 0.1 ml water	2.2	0.207475	0.743	0.5	4.18	0.1	1.245945
mr1	0.25 ml oil M @ 50 bar, 0.5g rock, 0.1 ml water	2.2	0.219625	0.745	0.5	4.18	0.1	1.273675

Rock	Description	actual Energy evolved during LTO Induction, J	actual Energy evolved during LTO propagation	actual Energy evolved during LTO ELTO	actual Energy evolved during Lower HTO	actual Energy evolved during Upper HTO	actual Energy evolved during HTO EHTO	actual ELTO/ EHTO
ar1	0.25ml oil A @ 50 bar, 0.5g rock, 0.1 ml water	162	268	430	116	155	271	1.6
br2	0.25ml oil B @ 50 bar, 2.0g rock, 0.1 ml water	213	146	359	220	414	634	0.6
br3	0.25ml oil B @ 100 bar, 0.5g rock, 0.1 ml water	167	2673	2839	98	70	168	16.9
cr1	0.25 ml oil C @ 50 bar, 0.5g rock, 0.1 ml water	205	490	696	103	153	257	2.7
dr2	0.25 ml oil D @ 50 bar, 0.5g rock	121	1026	1147	68	83	151	7.6
dr1	0.25 ml oil D @ 50 bar, 0.5g rock, 0.1 ml water	202	306	508	107	141	248	2.0
dr3	0.25 ml oil D @ 50 bar, 2.0g rock, 0.1 ml water	316	305	620	280	253	533	1.2
dr4	1 ml Oil D @ 50 bar, 0.25 ml rock, 0.1 ml water	411	143	553	317	410	727	0.8
dr5	0.25 ml Oil D @ 0 bar, 0.25 ml rock, 0.1 ml water	#REF!	0	#REF!	312	144	456	#REF!
dr_c2	0.25ml Oil D @ 50 bar, 0.5g clay, 0.1 ml water, repeated	158	138	296	144	186	331	0.9
dr_ch1	0.25ml Oil D @ 50 bar, 0.5g chalk, 0.1 ml water	112	104	216	110	20	130	1.7
dr_p1	0.25ml Oil D @ 50 bar, 0.5g phillips rock, 0.1 ml water	150	155	305	127	156	283	1.1
dr_s1	0.25ml Oil D @ 50 bar, 0.5g silica, 0.1 ml water	146	180	326	132	166	298	1.1
mr1	0.25 ml oil M @ 50 bar, 0.5g rock, 0.1 ml water	217	4272	4489	101	140	241	18.6

Saturates Only	Description	cp (oil), J/gK	mass (oil), g	cp (rock), J/gK	mass (rock), g	cp (water), J/gK	mass (water), g	Mcp (oil) + mcp (rock) + mcp (water)
as1	0.25 ml A sat @ 50 bar	2.2	0.2112	0.745	0	4.18	0	0.46464
bs0	0.25 ml Oil B sat. @ 50 bar	2.2	0.20995	0.745	0	4.18	0	0.46189
bs3	0.25 ml B sat @ 50 bar	2.2	0.20995	0.745	0	4.18	0	0.46189
cs0	0.25 ml C sat @ 50 bar	2.2	0.20995	0.745	0	4.18	0	0.46189
ds0	0.25 ml D sat @ 50 bar	2.2	0.207475	0.745	0	4.18	0	0.456445
wls1	0.25 ml Oil W saturates @ 50 bar	2.2	0.249125	0.745	0	4.18	0	0.548075
Saturates + Rock+ water	**Description**	**cp (oil), J/gK**	**mass (oil), g**	**cp (rock), J/gK**	**mass (rock), g**	**cp (water), J/gK**	**mass (water), g**	**Mcp (oil) + mcp (rock) + mcp (water)**
asr1	0.25 ml Oil A saturates @ 50 bar, 0.5 g rock, 0.1 ml water	2.2	0.2112	0.745	0.5	4.18	0.1	1.25514
bsr1	0.25 ml Oil B saturates @ 50 bar, 0.5 g rock, 0.1 ml water	2.2	0.20995	0.745	0.5	4.18	0.1	1.25239
dsr1	0.25 ml Oil D saturates @ 50 bar, 0.5 g rock, 0.1 ml water	2.2	0.207475	0.745	0.5	4.18	0.1	1.246945
Aromatics + Rock+ water	**Description**	**cp (oil), J/gK**	**mass (oil), g**	**cp (rock), J/gK**	**mass (rock), g**	**cp (water), J/gK**	**mass (water), g**	**Mcp (oil) + mcp (rock) + mcp (water)**
aar1	0.3g Oil A aromatics @ 50 bar, 0.5g rock, 0.1 ml water	2.2	0.2112	0.745	0.5	4.18	0.1	1.25514
bar2	0.3g Oil B aromatics @ 50 bar, 0.5 g rock, 0.1 ml water	2.2	0.20995	0.745	0.5	4.18	0.1	1.25239
car1	0.3g Oil C Aromatics @ 50 bar, 0.5g rock, 0.1 ml water	2.2	0.20995	0.745	0.5	4.18	0.1	1.25239
dar2	0.3g Oil D aromatics @ 50 bar, 0.25 ml rock, 0.1 ml water, repeated	2.2	0.207475	0.745	0.5	4.18	0.1	1.246945
wlar1	0.3g wolflake aromatic @ 50 bar, 0.5g rock, 0.1 ml water	2.2	0.249125	0.745	0.5	4.18	0.1	1.338575

Saturates Only	Description	actual Energy evolved during LTO Induction, J	actual Energy evolved during LTO propagation	actual Energy evolved during LTO ELTO	actual Energy evolved during Lower HTO	actual Energy evolved during Upper HTO	actual Energy evolved during HTO EHTO	actual ELTO/ EHTO
as1	0.25 ml A sat @ 50 bar	76	424	501	45	43	88	5.7
bs0	0.25 ml Oil B sat. @ 50 bar	67	489	556	0	0	0	#DIV/0!
bs3	0.25 ml B sat @ 50 bar	75	479	554	22	69	90	6.1
cs0	0.25 ml C sat @ 50 bar	125	56	182	0	0	0	#DIV/0!
ds0	0.25 ml D sat @ 50 bar	68	493	561	17	26	43	12.9
wls1	0.25 ml Oil W saturates @ 50 bar	98	326	424	39	68	107	4.0
Saturates + Rock+ water	**Description**	**actual Energy evolved during LTO Induction, J**	**actual Energy evolved during LTO propagation**	**actual Energy evolved during LTO ELTO**	**actual Energy evolved during Lower HTO**	**actual Energy evolved during Upper HTO**	**actual Energy evolved during HTO EHTO**	**actual ELTO/ EHTO**
asr1	0.25 ml Oil A saturates @ 50 bar, 0.5 g rock, 0.1 ml water	168	105	273	148	155	303	0.9
bsr1	0.25 ml Oil B saturates @ 50 bar, 0.5 g rock, 0.1 ml water	204	78	282	143	144	287	1.0
dsr1	0.25 ml Oil D saturates @ 50 bar, 0.5 g rock, 0.1 ml water	103	75	178	25	0	25	7.2
Aromatics + Rock+ water	**Description**	**actual Energy evolved during LTO Induction, J**	**actual Energy evolved during LTO propagation**	**actual Energy evolved during LTO ELTO**	**actual Energy evolved during Lower HTO**	**actual Energy evolved during Upper HTO**	**actual Energy evolved during HTO EHTO**	**actual ELTO/ EHTO**
aar1	0.3g Oil A aromatics @ 50 bar, 0.5g rock, 0.1 ml water	180	79	258	124	169	293	0.9
bar2	0.3g Oil B aromatics @ 50 bar, 0.5 g rock, 0.1 ml water	174	97	271	127	97	224	1.2
car1	0.3g Oil C Aromatics @ 50 bar, 0.5g rock, 0.1 ml water	213	60	273	77	0	77	3.6
dar2	0.3g Oil D aromatics @ 50 bar, 0.25 ml rock, 0.1 ml water, repeated	166	65	230	129	166	294	0.8
wlar1	0.3g wolflake aromatic @ 50 bar, 0.5g rock, 0.1 ml water	159	80	239	179	168	347	0.7

Resins + Rock+ water	Description	cp (oil), J/gK	mass (oil), g	cp (rock), J/gK	mass (rock), g	cp (water), J/gK	mass (water), g	Mcp (oil) + mcp (rock) + mcp (water)
brrl	0.3g Oil B resins @ 50 bar, 0.5g rock, 0.1ml water	2.2	0.20995	0.745	0.5	4.18	0.1	1.25239
drrl	0.3g Oil D Resins @ 50 bar, 0.25 ml rock, 0.1 ml water	2.2	0.207475	0.745	0.5	4.18	0.1	1.246945
wlrrl	0.3g wolflake resin @ 50 bar, 0.5g rock, 0.1 ml water	2.2	0.249125	0.745	0.5	4.18	0.1	1.338575

Asphaltenes+ Rock+ water	Description	cp (oil), J/gK	mass (oil), g	cp (rock), J/gK	mass (rock), g	cp (water), J/gK	mass (water), g	Mcp (oil) + mcp (rock) + mcp (water)
aasrl	0.3g Oil A asphaltenes @ 50 bar, 0.5g rock, 0.1 ml water	2.2	0.2112	0.745	0.5	4.18	0.1	1.25514
masrl	0.3g maya asphaltenes @ 50 bar, 0.5g rock, 0.1 ml water	2.2	0.219625	0.745	0.5	4.18	0.1	1.273675
wlasrl	0.3g wolflake asphaltenes @ 50 bar, 0.5g rock, 0.1ml water	2.2	0.249125	0.745	0.5	4.18	0.1	1.338575

Component expts.	Description	cp (oil), J/gK	mass (oil), g	cp (rock), J/gK	mass (rock), g	cp (water), J/gK	mass (water), g	Mcp (oil) + mcp (rock) + mcp (water)
C10	0.25 ml decane @ 50 bar, 0.5g rock, 0.1 ml water	2.2	0.2	0.745	0.5	4.18	0.1	1.2305
C20	0.25 ml n-eicosane @ 50 bar, 0.5g rock, 0.1 ml water	2.2	0.2	0.745	0.5	4.18	0.1	1.2305

Other expts.	Description	cp (oil), J/gK	mass (oil), g	cp (rock), J/gK	mass (rock), g	cp (water), J/gK	mass (water), g	Mcp (oil) + mcp (rock) + mcp (water)
dn0	0.25 ml oil D + nitrogen @ 50 bar	2.2	0.207475	0.745	0	4.18	0.1	0.874445
drnl	0.25 ml oil D + nitrogen @ 50 bar, 0.5g rock, 0.1ml water	2.2	0.207475	0.745	0.5	4.18	0.1	1.246945

Resins + Rock+ water	Description	actual Energy evolved during LTO Induction, J	actual Energy evolved during LTO propagation	actual Energy evolved during LTO ELTO	actual Energy evolved during Lower HTO	actual Energy evolved during Upper HTO	actual Energy evolved during HTO EHTO	actual ELTO/ EHTO
brr1	0.3g Oil B resins @ 50 bar, 0.5g rock, 0.1ml water	140	121	260	123	142	265	1.0
drr1	0.3g Oil D Resins @ 50 bar, 0.25 ml rock, 0.1 ml water	269	0	269	26	0	26	10.2
wlrr1	0.3g wolflake resin @ 50 bar, 0.5g rock, 0.1 ml water	126	129	256	145	153	299	0.9

Asphaltenes+ Rock+ water	Description	actual Energy evolved during LTO Induction, J	actual Energy evolved during LTO propagation	actual Energy evolved during LTO ELTO	actual Energy evolved during Lower HTO	actual Energy evolved during Upper HTO	actual Energy evolved during HTO EHTO	actual ELTO/ EHTO
aasr1	0.3g Oil A asphaltenes @ 50 bar, 0.5g rock, 0.1 ml water	253	0	253	32	0	32	7.8
masr1	0.3g maya asphaltenes @ 50 bar, 0.5g rock, 0.1 ml water	221	0	221	151	0	151	1.5
wlasr1	0.3g wolflake asphaltenes @ 50 bar, 0.5g rock, 0.1ml water	132	111	242	270	0	270	0.9

Component expts.	Description	actual Energy evolved during LTO Induction, J	actual Energy evolved during LTO propagation	actual Energy evolved during LTO ELTO	actual Energy evolved during Lower HTO	actual Energy evolved during Upper HTO	actual Energy evolved during HTO EHTO	actual ELTO/ EHTO
C10	0.25 ml decane @ 50 bar, 0.5g rock, 0.1 ml water	144	73	217	121	183	304	0.7
C20	0.25 ml n-eicosane @ 50 bar, 0.5g rock, 0.1 ml water	120	253	373	190	127	318	1.2

Other expts.	Description	actual Energy evolved during LTO Induction, J	actual Energy evolved during LTO propagation	actual Energy evolved during LTO ELTO	actual Energy evolved during Lower HTO	actual Energy evolved during Upper HTO	actual Energy evolved during HTO EHTO	actual ELTO/ EHTO
dn0	0.25 ml oil D + nitrogen @ 50 bar	165	0	165	136	0	136	1.2
drn1	0.25 ml oil D + nitrogen @ 50 bar, 0.5g rock, 0.1ml water	284	0	284	132	0	132	2.2

APPENDIX D:

Arrhenius Kinetic Parameters

Arrhenius Kinetic Parameters, Oil Alone

		LTO	k1	LTO	k2	LTO	k3
Experimental Run	Description of Experiment	Activation Energy	Pre-exponential Factor	Activation Energy	Pre-exponential Factor	Activation Energy	Pre-exponential Factor
a5	0.25 ml Oil A @ 50 bar	66.08	963.045	214.78	1.09E+19	-450.38	1.38E-47
a0	0.25 ml Oil A @ 50 bar	30.04	0.070	181.82	3.66E+15	-286.28	3.00E-30
a1	0.25 ml Oil A @ 100 bar	27.61	0.034	257.45	7.55E+23	-290.91	2.63E-35
au1	0.5 ml Oil Au @ 50 bar	48.30	6.950	376.39	9.13E+34	-302.71	5.83E-28
b5	0.25 ml Oil B @ 50 bar	37.64	0.101	283.08	1.23E+25	-277.51	6.49E-29
b0	0.25 ml Oil B @ 50 bar	40.55	0.659	230.72	2.69E+20	-391.96	2.32E-41
b3	0.25 ml Oil B @ 50 bar	31.03	0.072	241.71	2.65E+21	-402.11	1.02E-38
b4	0.25 ml Oil B @ 50 bar	42.26	1.778	272.82	5.73E+24	-398.53	2.75E-40
b2	0.5 ml Oil B @ 50 bar	32.45	0.134	278.28	2.07E+25	-402.82	7.26E-36
b7	1 ml Oil B @ 50 bar	38.25	0.937	346.68	2.15E+32	-361.66	2.26E-33
b1	0.25 ml Oil B @ 100 bar	50.66	9.127	235.05	1.12E+21	-389.79	3.72E-38
c0	0.25ml Oil C @ 50 bar	26.74	0.020	292.97	1.27E+27	-382.09	3.29E-39
d1	1 ml Oil D@ 30 bar	45.46	8.477	102.57	1.31E+07	-406.36	3.51E-45
d3	0.25 ml Oil D@ 50 bar	55.93	32.275	280.15	4.21E+25	-277.25	1.15E-29
d2	0.25 ml Oil D@ 100 bar	35.60	2.859	272.01	1.62E+25	-279.43	5.68E-26

Arrhenius Kinetic Parameters, Oil Alone

		HTO	k1	HTO	k2
Experimental Run	Description of Experiment	Activation Energy	Pre-exponential Factor	Activation Energy	Pre-exponential Factor
a5	0.25 ml Oil A @ 50 bar	64.75	80.92	#VALUE!	#VALUE!
a0	0.25 ml Oil A @ 50 bar	33.13	0.05	100.46	1.08E+04
a1	0.25 ml Oil A @ 100 bar	0.00	1.00	0.00	1.00E+00
au1	0.5 ml Oil Au @ 50 bar	45.70	1.73	83.34	1.84E+03
b5	0.25 ml Oil B @ 50 bar	29.42	0.01	0.00	1.00E+00
b0	0.25 ml Oil B @ 50 bar	-6.21	0.00	138.01	1.93E+06
b3	0.25 ml Oil B @ 50 bar	63.44	50.51	333.28	2.27E+21
b4	0.25 ml Oil B @ 50 bar	61.42	44.20	444.48	1.11E+29
b2	0.5 ml Oil B @ 50 bar	#VALUE!	#VALUE!	#VALUE!	#VALUE!
b7	1 ml Oil B @ 50 bar	55.73	15.72	219.86	9.92E+12
b1	0.25 ml Oil B @ 100 bar	62.51	23.27	76.66	2.40E+02
c0	0.25ml Oil C @ 50 bar	1.17	0.00	127.23	3.77E+05
d1	1 ml Oil D@ 30 bar	75.18	3154.55	447.62	5.54E+35
d3	0.25 ml Oil D@ 50 bar	42.79	0.31	68.64	3.70E+01
d2	0.25 ml Oil D@ 100 bar	84.13	1675.22	472.18	9.68E+30

Arrhenius Kinetic Parameters, Oil and water

		LTO	k1	LTO	k2	LTO	k3
Experimental Run	Description of Experiment	Activation Energy	Pre-exponential Factor	Activation Energy	Pre-exponential Factor	Activation Energy	Pre-exponential Factor
bw	0.25ml Oil B @ 50 bar, 0.1 ml water	34.55	0.203	202.26	9.24E+17	-346.69	1.31E-37
bw1	0.25 ml Oil B @ 50 bar, 0.5g rock, 0.5ml water	0.36	1.129	56.59	2.42E+06	-177.70	5.56E-19
drw	0.25 ml Oil D @ 50 bar, 0.5g rock, 1 ml water	20.94	0.004	176.07	6.48E+14	-1511.49	1.49E-159

Arrhenius Kinetic Parameters, Oil rock and water

		LTO	k1	LTO	k2	LTO	k3
Experimental Run	Description of Experiment	Activation Energy	Pre-exponential Factor	Activation Energy	Pre-exponential Factor	Activation Energy	Pre-exponential Factor
ar1	0.25ml oil A @ 50 bar, 0.5g rock, 0.1 ml water	25.52	0.014	170.84	3.03E+14	-326.07	2.84E-35
br2	0.25ml oil B @ 50 bar, 2.0g rock, 0.1 ml water	36.32	0.237	107.56	6.79E+07	-312.72	6.12E-37
br3	0.25ml oil B @ 100 bar, 0.5g rock, 0.1 ml water	19.26	0.001	198.56	1.20E+18	-108.77	2.64E-13
cr1	0.25 ml oil C @ 50 bar, 0.5g rock, 0.1 ml water	22.45	0.011	264.99	1.21E+24	-191.63	8.86E-22
dr2	0.25 ml oil D @ 50 bar, 0.5g rock	23.06	0.016	214.59	9.86E+18	-209.96	9.64E-23
dr1	0.25 ml oil D @ 50 bar, 0.5g rock, 0.1 ml water	25.49	0.012	253.35	1.00E+23	-309.35	5.69E-34
dr3	0.25 ml oil D @ 50 bar, 2.0g rock, 0.1 ml water	20.25	0.002	182.42	3.98E+15	-1467.34	1.95E-151

Arrhenius Kinetic Parameters, Oil and water

		HTO	k1	HTO	k2
Experimental Run	Description of Experiment	Activation Energy	Pre-exponential Factor	Activation Energy	Pre-exponential Factor
bw	0.25ml Oil B @ 50 bar, 0.1 ml water	9.09	0.00	#VALUE!	#VALUE!
bw1	0.25 ml Oil B @ 50 bar, 0.5g rock, 0.5ml water	#VALUE!	#VALUE!	#VALUE!	#VALUE!
drw	0.25 ml Oil D @ 50 bar, 0.5g rock, 1 ml water	-3.00	8.37717E-06	79.29	2.08E+02

Arrhenius Kinetic Parameters, Oil rock and water

		HTO	k1	HTO	k2
Experimental Run	Description of Experiment	Activation Energy	Pre-exponential Factor	Activation Energy	Pre-exponential Factor
ar1	0.25ml oil A @ 50 bar, 0.5g rock, 0.1 ml water	37.14	0.14	76.68	1.92E+02
br2	0.25ml oil B @ 50 bar, 2.0g rock, 0.1 ml water	17.26	0.0006	99.53	5.45E+03
br3	0.25ml oil B @ 100 bar, 0.5g rock, 0.1 ml water	16.62	0.0003	103.41	6.48E+03
cr1	0.25 ml oil C @ 50 bar, 0.5g rock, 0.1 ml water	50.22	5.23	72.66	3.21E+02
dr2	0.25 ml oil D @ 50 bar, 0.5g rock	40.76	0.58	89.19	3.69E+03
dr1	0.25 ml oil D @ 50 bar, 0.5g rock, 0.1 ml water	33.39	0.09	110.69	5.71E+04
dr3	0.25 ml oil D @ 50 bar, 2.0g rock, 0.1 ml water	39.37	0.10	91.90	1.44E+03

Arrhenius Kinetic Parameters, Oil rock and water

		LTO	k1	LTO	k2	LTO	k3
Experimental Run	Description of Experiment	Activation Energy	Pre-exponential Factor	Activation Energy	Pre-exponential Factor	Activation Energy	Pre-exponential Factor
dr4	1 ml Oil D @ 50 bar, 0.5 g rock, 0.1 ml water	26.88	0.013	127.57	2.65E+09	-1363.08	1.92E-141
dr5	0.25 ml Oil D @ 0 bar, 0.5 g rock, 0.1 ml water	13.29	0.000	13.29	2.66E-04	13.29	2.66E-04
dr_c2	0.25ml Oil D @ 50 bar, 0.5g clay, 0.1 ml water	29.84	0.034	145.17	6.62E+11	-835.89	1.31E-88
dr_ch1	0.25ml Oil D @ 50 bar, 0.5g chalk, 0.1 ml water	38.56	0.436	192.43	2.95E+16	-1674.02	3.29E-170
dr_p1	0.25ml Oil D @ 50 bar, 0.5g rock A, 0.1 ml	20.27	0.002	125.77	6.83E+09	-1683.59	3.10E-174
dr_s1	0.25ml Oil D @ 50 bar, 0.5g silica, 0.1 ml water	19.66	0.002	130.06	1.85E+10	-562.10	2.42E-60
mr1	0.25 ml oil M @ 50 bar, 0.5g rock, 0.1 ml water	28.57	0.063	189.20	1.62E+16	-204.44	1.22E-22

Arrhenius Kinetic Parameters, Saturates

		LTO	k1	LTO	k2	LTO	k3
Experimental Run	Description of Experiment	Activation Energy	Pre-exponential Factor	Activation Energy	Pre-exponential Factor	Activation Energy	Pre-exponential Factor
as1	0.3 g A sat @ 50 bar	22.78	0.008	302.41	4.22E+27	-196.06	9.18E-22
bs3	0.3 g B sat @ 50 bar	20.35	0.003	243.40	3.36E+21	-282.92	4.37E-30
ds0	0.3 g D sat @ 50 bar	22.22	0.006	225.87	5.94E+19	-313.92	3.71E-33
wls0	0.3 g Oil W saturates @ 50 bar	28.05	0.034	238.77	1.74E+20	-457.69	4.05E-46

Arrhenius Kinetic Parameters, Oil rock and water

		HTO	k1	HTO	k2
Experimental Run	Description of Experiment	Activation Energy	Pre-exponential Factor	Activation Energy	Pre-exponential Factor
dr4	1 ml Oil D @ 50 bar, 0.5 g rock, 0.1 ml water	39.16	0.26	136.36	1.43E+07
dr5	0.25 ml Oil D @ 0 bar, 0.5 g rock, 0.1 ml water	0.00	1.00	0.00	1.00E+00
dr_c2	0.25ml Oil D @ 50 bar, 0.5g clay, 0.1 ml water	-20.54	9.88166E-08	117.09	2.72E+04
dr_ch1	0.25ml Oil D @ 50 bar, 0.5g chalk, 0.1 ml water	0.00	1.00	0.00	1.00E+00
dr_p1	0.25ml Oil D @ 50 bar, 0.5g phillips rock, 0.1 ml	5.15	3.70961E-05	104.44	5.40E+03
dr_s1	0.25ml Oil D @ 50 bar, 0.5g silica, 0.1 ml water	17.19	0.000736059	97.84	2.57E+03
mr1	0.25 ml oil M @ 50 bar, 0.5g rock, 0.1 ml water	30.03	0.054464836	75.64	2.67E+02

Arrhenius Kinetic Parameters, Saturates

		HTO	k1	HTO	k2
Experimental Run	Description of Experiment	Activation Energy	Pre-exponential Factor	Activation Energy	Pre-exponential Factor
as1	0.3 g A sat @ 50 bar	31.04	0.04	95.53	4.46E+03
bs3	0.3 g B sat @ 50 bar	14.36	0.000542295	94.12	2.01E+03
ds0	0.3 g D sat @ 50 bar	24.61	0.01	50.21	1.30E+00
wls0	0.3 g Oil W saturates @ 50 bar	18.86	0.002560379	93.26	2.44E+03

Arrhenius Kinetic Parameters, Saturates + rock + water

		LTO	k1	LTO	k2	LTO	k3
Experimental Run	Description of Experiment	Activation Energy	Pre-exponential Factor	Activation Energy	Pre-exponential Factor	Activation Energy	Pre-exponential Factor
asr1	0.3 g Oil A saturates @ 50 bar, 0.5 g rock, 0.1 ml water	25.20	0.013	83.30	1.05E+05	-2856.27	3.83E-291
bsr1	0.3 g Oil B saturates @ 50 bar, 0.5 g rock, 0.1 ml water	27.46	0.025	92.57	7.29E+05	-376.84	6.07E-42
dsr1	0.3 g Oil D saturates @ 50 bar, 0.5 g rock, 0.1 ml water	29.55	0.011	60.97	7.12E+02	-312.82	7.86E-39

Arrhenius Kinetic Parameters, Aromatics + rock + water

		LTO	k1	LTO	k2	LTO	k3
Experimental Run	Description of Experiment	Activation Energy	Pre-exponential Factor	Activation Energy	Pre-exponential Factor	Activation Energy	Pre-exponential Factor
aar1	0.3g Oil A aromatics @ 50 bar, 0.5g rock, 0.1 ml water	22.12	0.004	37.71	4.16E-01	-141.90	1.87E-19
bar2	0.3g Oil B aromatics @ 50 bar, 0.5 g rock, 0.1 ml water	33.13	0.083	48.27	8.10E+00	-128.42	1.55E-17
car1	0.3g Oil C Aromatics @ 50 bar, 0.5g rock, 0.1 ml water	26.09	0.008	45.82	2.14E+00	-184.28	5.64E-24
dar2	0.3g Oil D aromatics @ 50 bar, 0.25 ml rock, 0.1	23.85	0.006	39.82	6.24E-01	-212.96	1.31E-26
wlar1	0.3g wolflake aromatic @ 50 bar, 0.5g rock, 0.1 ml water	26.56	0.015	41.64	1.87E+00	-172.29	2.47E-23

Arrhenius Kinetic Parameters, Saturates + rock + water

		HTO	k1	HTO	k2
Experimental Run	Description of Experiment	Activation Energy	Pre-exponential Factor	Activation Energy	Pre-exponential Factor
asr1	0.3 g Oil A saturates @ 50 bar, 0.5 g rock, 0.1 ml water	37.48	0.11	80.47	3.22E+02
bsr1	0.3 g Oil B saturates @ 50 bar, 0.5 g rock, 0.1 ml water	35.94	0.07	87.19	1.02E+03
dsr1	0.3 g Oil D saturates @ 50 bar, 0.5 g rock, 0.1 ml water	0.00	1.00	0.00	1.00E+00

Arrhenius Kinetic Parameters, Aromatics + rock + water

		HTO	k1	HTO	k2
Experimental Run	Description of Experiment	Activation Energy	Pre-exponential Factor	Activation Energy	Pre-exponential Factor
aar1	0.3g Oil A aromatics @ 50 bar, 0.5g rock, 0.1 ml water	17.74	0.000797045	93.22	1.33E+03
bar2	0.3g Oil B aromatics @ 50 bar, 0.5 g rock, 0.1 ml water	23.25	0.01	0.00	1.00E+00
car1	0.3g Oil C Aromatics @ 50 bar, 0.5g rock, 0.1 ml water	0.00	1.00	0.00	1.00E+00
dar2	0.3g Oil D aromatics @ 50 bar, 0.25 ml rock, 0.1	34.40	0.02	99.18	4.78E+03
wlar1	0.3g wolflake aromatic @ 50 bar, 0.5g rock, 0.1 ml water	26.65	0.004716445	104.11	9.19E+03

Arrhenius Kinetic Parameters, Resins + rock + water

		LTO	k1	LTO	k2	LTO	k3
Experimental Run	Description of Experiment	Activation Energy	Pre-exponential Factor	Activation Energy	Pre-exponential Factor	Activation Energy	Pre-exponential Factor
brr1	0.3g Oil B resins @ 50 bar, 0.5g rock, 0.1ml water	24.17	0.012	35.26	3.37E-01	-85.21	2.01E-13
drr2	0.3g Oil D Resins @ 50 bar, 0.25 ml rock, 0.1 ml water	29.16	0.042	29.16	4.20E-02	-144.99	8.91E-20
wlrr1	0.3g wolflake resin @ 50 bar, 0.5g rock, 0.1 ml water	26.01	0.024	35.07	3.82E-01	-70.82	3.57E-12

Arrhenius Kinetic Parameters, Asphaltenes + rock + water

		LTO	k1	LTO	k2	LTO	k3
Experimental Run	Description of Experiment	Activation Energy	Pre-exponential Factor	Activation Energy	Pre-exponential Factor	Activation Energy	Pre-exponential Factor
aasr1	0.3g Oil A asphaltenes @ 50 bar, 0.5g rock, 0.1 ml water	29.10	0.026	29.10	2.58E-02	-191.91	6.25E-26
masr1	0.3g maya asphaltenes @ 50 bar, 0.5g rock, 0.1 ml water	38.22	0.307	38.22	3.07E-01	-88.93	1.49E-14
wlasr1	0.3g wolflake asphaltenes @ 50 bar, 0.5g rock, 0.1ml water	39.26	0.971	39.26	9.71E-01	-43.85	1.05E-09

Arrhenius Kinetic Parameters, Resins + rock + water

		HTO	k1	HTO	k2
Experimental Run	Description of Experiment	Activation Energy	Pre-exponential Factor	Activation Energy	Pre-exponential Factor
brr1	0.3g Oil B resins @ 50 bar, 0.5g rock, 0.1ml water	31.17	0.03	92.51	2.93E+03
drr1	0.3g Oil D Resins @ 50 bar, 0.25 ml rock, 0.1 ml water	0.00	1.00	0.00	1.00E+00
wlrr1	0.3g wolflake resin @ 50 bar, 0.5g rock, 0.1 ml water	31.24	0.04	90.42	2.14E+03

Arrhenius Kinetic Parameters, Asphaltenes + rock + water

		HTO	k1	HTO	k2
Experimental Run	Description of Experiment	Activation Energy	Pre-exponential Factor	Activation Energy	Pre-exponential Factor
aasr1	0.3g Oil A asphaltenes @ 50 bar, 0.5g rock, 0.1 ml water	0.00	1.00	0.00	1.00E+00
masr1	0.3g maya asphaltenes @ 50 bar, 0.5g rock, 0.1 ml water	0.00	1.00	0.00	1.00E+00
wlasr1	0.3g wolflake asphaltenes @ 50 bar, 0.5g rock, 0.1ml water	17.91	0.00	18.38	2.15E-03

Arrhenius Kinetic Parameters, Pure Components + rock + water

		LTO	k1	LTO	k2	LTO	k3
Experimental Run	Description of Experiment	Activation Energy	Pre-exponential Factor	Activation Energy	Pre-exponential Factor	Activation Energy	Pre-exponential Factor
C10	0.25 ml decane @ 50 bar, 0.5g rock, 0.1 ml water	41.58	0.817	295.16	3.65E+29	-275.32	6.12E-34
C16	0.25 ml hexadecane @ 50 bar, 0.5g rock, 0.1 ml water	24.52	0.007	228.56	6.38E+22	-106.29	6.41E-15

Arrhenius Kinetic Parameters, Other Experiments

		LTO	k1	LTO	k2	LTO	k3
Experimental Run	Description of Experiment	Activation Energy	Pre-exponential Factor	Activation Energy	Pre-exponential Factor	Activation Energy	Pre-exponential Factor
dn0	0.25 ml oil D + nitrogen @ 50 bar	25.68	0.009	25.68	9.27E-03	25.68	9.27E-03
drn1	0.25 ml oil D + nitrogen @ 50 bar, 0.5g rock, 0.1ml water	19.90	0.002	19.90	1.73E-03	19.90	1.73E-03

Arrhenius Kinetic Parameters, Pure Components + rock + water

		HTO	k1	HTO	k2
Experimental Run	Description of Experiment	Activation Energy	Pre-exponential Factor	Activation Energy	Pre-exponential Factor
C10	0.25 ml decane @ 50 bar, 0.5g rock, 0.1 ml water	26.19	0.02	29.61	2.65E-02
C16	0.25 ml hexadecane @ 50 bar, 0.5g rock, 0.1 ml water	29.61	0.03	43.36	2.04E-01

Arrhenius Kinetic Parameters, Other Experiments

		HTO	k1	HTO	k2
Experimental Run	Description of Experiment	Activation Energy	Pre-exponential Factor	Activation Energy	Pre-exponential Factor
dn0	0.25 ml oil D + nitrogen @ 50 bar	23.95	0.01	23.95	5.74E-03
drn1	0.25 ml oil D + nitrogen @ 50 bar, 0.5g rock, 0.1ml water	31.19	0.03	31.19	2.74E-02